# Phosphorylation of Filamin A by Cdk1/cyclin B1 Regulates Filamin A Subcellular Localization and is Important for Daughter Cell Separation

**Sandy Gie Yee Szeto**

Thesis submitted to the Faculty of Graduate and Postdoctoral Studies
in partial fulfillment of the requirements
for the Doctorate in Philosophy degree in Biochemistry

Department of Biochemistry, Microbiology and Immunology
Faculty of Medicine
University of Ottawa

# ABSTRACT

In cell culture, entry into mitosis of many adherent mammalian cells is accompanied by substantial changes in cellular architecture. Flat, spread-out interphase cells detach from the extracellular matrix and become more spherical. These changes in cell shape are mediated by rearrangements in the actin cytoskeleton, a dynamic network of actin filaments that are organized by actin-binding proteins. Filamin A (FLNa) is a 280 kD actin-binding protein that crosslinks actin filaments into parallel bundles or three-dimensional orthogonal networks. We previously identified FLNa as an *in vitro* substrate of cyclin-dependent kinase 1 (Cdk1), a kinase that regulates entry into mitosis, and hypothesized that Cdk1 phosphorylation of FLNa regulates mitotic actin remodelling. Using mass spectrometry and a p-FLNa antibody, we show that FLNa is phosphorylated *in vivo* in HeLa cells on multiple Cdk1 sites, including serines 1084, 1459 and 1533. All three sites match the phosphorylation consensus sequence of Cdk1. We further show that p-FLNa is almost fully dephosphorylated by anaphase, consistent with it being a cell cycle-regulated substrate. Using a phospho-specific antibody, we find that p-FLNa has decreased cortical actin localization compared to total FLNa in mitotic cells. To investigate the functional role of mitotic FLNa phosphorylation, we mutated serines 1084, 1459 and 1533 to nonphosphorylatable alanine and expressed this FLNa mutant (FLNa-S1084A, S1459A, S1533A, referred to as "FLNa-AAA GFP") in FLNa-deficient human M2 melanoma cells. FLNa-AAA GFP-expressing cells have enhanced FLNa-AAA GFP localization at sites of contact between daughter cells and this correlates with defects in cell division and impaired cell migration. Therefore, mitotic delocalization of cortical FLNa is critical for successful cell division and interphase cell behaviour.

# ACKNOWLEDGEMENTS

**Materials, protocols, fee-based services and helpful discussions**

I would like to thank Dr. Laura Trinkle-Mulcahy (Department of Cellular and Molecular Medicine, Ottawa Institute of Systems Biology, University of Ottawa, Ottawa, ON) for SILAC protocols, reagents and helpful discussions; Delphine Chamousset (Department of Cellular and Molecular Medicine, Ottawa Institute of Systems Biology) for technical assistance on SILAC protocols and helpful discussions; Dr. Lawrence Puente (Ottawa Hospital Research Institute, Proteomics Core Facility, Ottawa, ON) for LC-MS/MS analysis, technical assistance and helpful discussions, Pamela Zhang (Department of Biochemistry, Microbiology and Immunology, Ottawa Institute of Systems Biology, University of Ottawa, Ottawa, ON) for technical assistance on protein purification, Dr. Heidi McBride (McGill University) for use of her confocal microscope and Raed Hanania (Cell Biology and Image Acquisition Core Facility) for technical assistance on live cell imaging.

**Proofreading and comments on manuscript and thesis**

I would like to thank Dr. Christopher Kennedy (Ottawa Hospital Research Institute, Department of Cellular and Molecular Medicine, Ottawa, ON) for critical reading of my manuscript (submitted), Dr. Nicole Forbes for editing the "Actin Cytoskeleton" and "Filamin A" sections of the Introduction, Elizabeth C. Williams for comments and editing the "Cell Cycle" section of the introduction and Dione Ng for editing the Material and Methods.

**J. Lee lab and TAC members**

I would like to thank my thesis supervisor Dr. Jonathan Lee for taking me on as a grad student in the summer of 2008 and introducing me to the world of actin-binding proteins and

the actin cytoskeleton. His encouragement, never-ending positivity and words of wisdom during the last 6 years have helped shape me into a better researcher. I would like to thank my TAC members, Dr. Adam Rudner and Dr. Chris Kennedy for their invaluable feedback throughout the years. I would like to especially thank Dr. Rudner and his lab for adopting me during Jonathan's sabbatical year. I would like to acknowledge Dr. Rudner and Liz Williams for their contributions and help in the preparation of my manuscript. Also, special thanks to past Lee Lab members (in order of most recent departure), Anne Morrow, Lisa Montgomery, Emily Sheppard, Sahir Shaikh and Dixie Pinke, for their friendship, lab help and of course enthusiasm for Tim's runs at all times of the day!

**Personal acknowledgements**

Lastly, I would like to thank my partner, Dave McVittie, who has supported me since second year undergrad and moved to Ottawa with me when I decided to go to grad school. He always told me he would do whatever it took to help me get my experiments done even if it meant doing the following things: driving me to and from the lab at all hours of the day and night, doing errands with me in between Western blot antibody incubations on the weekends, not getting toooo mad at me for "sandy-time" (a complex equation whereby "I'll be done in 10 min" really does means 10 min, but 1 hr=1.5 hrs and 4 h= "I'll be here all day…sorry"), walking to and meeting me at the "half-way point" to walk me home from the lab at night (halfway between the lab and our apartment ie.the Tim Hortons near Alta Vista Towers)....which at times became the RGN parking lot b/c of "sandy-time", showing me how to use "format painter" in PowerPoint and "section breaks" in Word, and at times staying with me at the lab all day on the weekends just to spend time with me.… ☺.

**TABLE OF CONTENTS**

# LIST OF ABBREVIATIONS

## A

| | |
|---|---|
| ABD | Actin-binding domain |
| ABP | Actin-binding protein |
| ABS | Actin-binding site |
| ADF/cofilin | Actin-depolymerizing factor/cofilin |
| AJ | Adherens junction |
| APC | Anaphase-promoting complex |

## B

| | |
|---|---|
| BSA | Bovine serum albumin |

## C

| | |
|---|---|
| CAK | Cdk-activating kinase |
| CaM-kinase II | $Ca^{2+}$/calmodulin-dependent protein kinase II |
| cAMP-kinase | cAMP-dependent protein kinase |
| $C_c$ | Critical concentration |
| Cdk1 | Cyclin-dependent kinase 1 |
| CEACAM1 | Carcinoembryonic antigen-related cell adhesion molecule 1 |
| CH | Calponin homology |
| Co-IP | Co-immunoprecipitation |
| CRS | Cytoplasmic retention signal |

## D

| | |
|---|---|
| D-box | Destruction box |
| DMEM | Dulbecco's modified eagle medium |
| DMSO | Dimethyl sulfoxide |
| DTT | Dithiothreitol |

## E

| | |
|---|---|
| ECM | Extracellular matrix |
| Ect2 | Epithelial cell transforming 2 |
| EIA | Enzyme immunoassay |
| ERM | Ezrin/radixin/moesin |

## F

| | |
|---|---|
| F-actin | Filamentous actin |
| FAP52 | Focal adhesion-associated phosphoprotein 52 |
| FBS | Fetal bovine serum |
| FH2 | Formin homology 2 |
| FLNa | Filamin A |

| | |
|---|---|
| FLNb | Filamin B |
| FLNc | Filamin C |
| FMD | Frontometaphyseal dysplasia |

## G

| | |
|---|---|
| G-actin | Globular actin |
| GEF | Guanine nucleotide-exchange factor |
| GP | Glycoprotein |

## H

| | |
|---|---|
| H1/H2 | Hinge1/Hinge2 |
| HMW | High molecular weight |

## I

| | |
|---|---|
| ICAM-1 | Intercellular cell adhesion molecule-1 |
| IPTG | Isopropyl β-D-1-thiogalactopyranoside |

## L

| | |
|---|---|
| LB | Luria-Bertaini |
| LC-MS/MS | Liquid chromatography tandem mass spectrometry |
| LPA | Lysophosphatidic acid |

## M

| | |
|---|---|
| MEF | Mouse embryonic fibroblast |
| MEM | Minimal essential medium |
| MNS | Melnick-Needles syndrome |
| mol wt | Molecular weight |
| MRI | Magnetic resonance imaging |
| MS | Mass spectrometry |
| MWCO | Molecular weight cut-off |

## N

| | |
|---|---|
| NEBD | Nuclear envelope breakdown |
| NES | Nuclear export signal |
| NLS | Nuclear localization signal |
| Noc | Nocodazole |

## O

| | |
|---|---|
| OPD | Otopalatodigital |

## P

| | |
|---|---|
| p90 RSK | p90 ribosomal S6 protein kinase |
| Pak1 | p21-activated kinase 1 |

| | |
|---|---|
| PBS | Phosphate-buffered saline |
| PH | Periventricular heterotopia |
| PH | Pleckstrin homology |
| PKA | Protein kinase A |
| PKCα | Protein kinase Cα |
| PLC | Phospholipase C |
| PMSF | Phenylmethanesulfonylfluoride |
| PP1 | Protein phosphatase 1 |
| PP2A | Protein phosphatase 2A |
| PRC | Pre-replicative complex |
| PtdIns(4,5)$P_2$ | Phosphatidylinositol 4,5-bisphosphate |
| PTP-PEST | protein tyrosine phosphatase with a C-terminal PEST motif |
| PVDF | polyvinylidene fluoride |

## R

| | |
|---|---|
| RIPA | Radioimmunoprecipitation assay |
| ROCK | p160-Rho-associated coiled-coil-containing protein kinase |
| RT | Room temperature |

## S

| | |
|---|---|
| S1P | Sphingosine-1-phosphate |
| SAC | Spindle assembly checkpoint |
| SAPK | Stress-activated protein kinase |
| SDS | Sodium dodecyl sulphate |
| SEM | Standard error of the mean |
| SILAC | Stable isotope labeling with amino acids in cell culture |
| Slik | Ste20-like protein kinase |
| SOC | Spindle orientation checkpoint |
| SphK1 | Sphingosine kinase 1 |

## T

| | |
|---|---|
| TBS | Tris-buffered saline |
| TBST | TBS-Tween |
| TF | Tissue factor |
| TNF | Tumour necrosis factor |

## V

| | |
|---|---|
| VE | Vascular endothelial |
| vWF | von Willebrand factor |

## W

| | |
|---|---|
| WASP | Wiskott-Aldrich Syndrome protein |
| WT | Wild-type |

# LIST OF FIGURES

## CHAPTER 4. Filamin A phosphorylation regulates its subcellular localization and is important for cell separation and interphase cell behaviour

## APPENDIX

**Video 1.** Localization of FLNa-WT GFP in M2 cells undergoing mitosis.
**Video 2.** Localization of FLNa-AAA GFP in M2 cells undergoing mitosis.
**Video 3.** FLNa-WT GFP-expressing M2 cells undergoing mitosis.
**Video 4.** FLNa-AAA GFP-expressing M2 cells undergoing mitosis.
**Video 5.** Wound closure assay of FLNa-WT GFP-expressing M2 cells.
**Video 6.** Wound closure assay of GFP EV-expressing M2 cells.
**Video 7.** Wound closure assay of nontransfected M2 cells.
**Video 8.** Wound closure assay of FLNa-AAA GFP-expressing M2 cells.

# LIST OF TABLES

# CHAPTER 1 GENERAL INTRODUCTION

## RATIONALE AND HYPOTHESIS

During cell culture of many adherent mammalian cell types, visually it is quite evident that substantial changes occur in the cell architecture as cells enter mitosis. Flat, spread-out interphase cells detach from the substratum and adopt a rounded morphology. These cell shape changes are mediated by rearrangements in the actin cytoskeleton, a dynamic network of actin filaments that undergo constant polymerization and depolymerization in response to signals to undergo cellular processes such as cell migration and cell division. The organizers of the actin cytoskeleton are actin-binding proteins (ABPs) such as filamin A (FLNa), which can crosslink actin filaments into branched, high-angle orthogonal networks or parallel bundles (reviewed in Popowicz et al. (2006)).

Entry into mitosis is controlled by the activation of cyclin-dependent kinase 1 (Cdk1) in complex with its regulatory subunit, cyclin B1. Cdk1/cyclin B1 phosphorylates many proteins involved in mitotic progression, including proteins involved in chromosome condensation, spindle assembly and nuclear envelope breakdown (NEBD) (reviewed in Nigg (2001)). However, it is unclear how Cdk/cyclin B1 controls actin cytoskeleton rearrangement, a critical, but frequently overlooked event during mitosis. This lack of understanding is primarily due to the fact that few ABPs have been identified as Cdk1/cyclin B1 substrates. There is evidence that Cdk1-phosphorylation of caldesmon, an ABP that inhibits non-muscle cell contractility (Helfman et al., 1999), causes it to dissociate from actin filaments, thereby facilitating actin rearrangement during mitotic cell rounding (Yamashiro

et al., 1990; Yamashiro and Matsumura, 1991; Yamashiro et al., 1991; Hosoya et al., 1993). However, our understanding of mitotic actin remodelling remains incomplete.

Using a yeast two-hybrid screen, we previously identified FLNa as a cyclin B1 binding partner and showed that Cdk1/cyclin B1 could phosphorylate FLNa *in vitro* on three sites-serines 1084, 1533 and 1630 (Cukier et al., 2007). Furthermore, *in vitro* phosphorylation of FLNa with Cdk1/cyclin B1 reduced the ability of FLNa to gelate F-actin (filamentous actin) *in vitro* (Cukier et al., 2007), presumably due to decreased binding of phosphorylated FLNa to F-actin. **Therefore, we hypothesize that *in vivo* phosphorylation of FLNa by Cdk1/cyclin causes FLNa dissociation from actin filaments to facilitate mitotic actin remodelling.**

## 1.1 ACTIN CYTOSKELETON

In eukaryotic cells, the cytoskeleton is a complex network of protein fibres that consist of three main types of cytoskeletal filaments: actin microfilaments, intermediate filaments, and microtubules (Wickstead and Gull, 2011). In terms of diameter, microfilaments are the smallest, with a diameter of 7 nm, followed by intermediate filaments and microtubules with diameters of 10 nm and 24 nm, respectively (Lodish et al., 2000; Heng and Koh, 2010). Together these filaments are crucial for maintaining normal cell processes, among them changes in cell shape, migration, division, vesicular trafficking and cell signaling (Yue et al., 2013).

### 1.1.1 Actin dynamics

The organization of the actin cytoskeleton is based on the polymerization of actin, a 42 kD globular monomeric protein that is one of the most highly conserved and abundant proteins in eukaryotes (Heng and Koh, 2010; Dominguez and Holmes, 2011). There are three main

actin isoforms expressed in vertebrates: α, β and γ. While α-actin isoforms are expressed in muscle cells, β-and γ-actin are expressed in non-muscle and muscle cells (Herman, 1993). Monomeric globular actin (G-actin) subunits polymerize to form actin filaments that under electron microscopy, appear as two protofilaments that turn gradually around each other to form a right-handed, two-chained long helix (Hanson and Lowy, 1963).

F-actin is a polar macromolecule with a barbed end (+) and a pointed end (-), each with different kinetic properties (Figure 1.1) (Revenu et al., 2004; Galkin et al., 2012). "Barbed" and "pointed" refer to the appearance of actin filaments that are decorated with myosin (Pollard and Borisy, 2003). The critical concentration ($C_c$) refers to the concentration of G-actin monomers in equilibrium with actin filaments (Wegner and Isenberg, 1983). Actin monomers assemble much more rapidly at the barbed end compared to the pointed end, thus the $C_c$ of the pointed end is higher than that of the barbed end. When the global $C_c$ is intermediate between those of the two ends separately, F-actin and G-actin are at equilibrium and there is a net loss of molecules at the pointed end and a net gain at the barbed end. This steady-state of actin polymerization and depolymerization is known as actin filament treadmilling (Wegner and Isenberg, 1983; Pollard and Borisy, 2003; Revenu et al., 2004). During treadmilling a given monomer will move gradually from the barbed to the pointed end.

Monomeric G-actin binds either ATP or ADP but ATP monomers assemble at a much higher rate than ADP monomers, therefore ATP-bound G-actin polymerizes to ATP-containing F-actin, a process that is thermodynamically favoured under physiological conditions. F-actin is a slow ATPase, so through time, ATP hydrolyzes to ADP. ADP-bound F-actin is less stable than ADP-bound G-actin so depolymerization occurs at the pointed end

(Figure 1.1) (Revenu et al., 2004). A treadmilling filament therefore contains ATP-bound actin at the barbed end and ADP-bound actin at the pointed end (Wegner and Isenberg, 1983; Pollard and Borisy, 2003; Revenu et al., 2004).

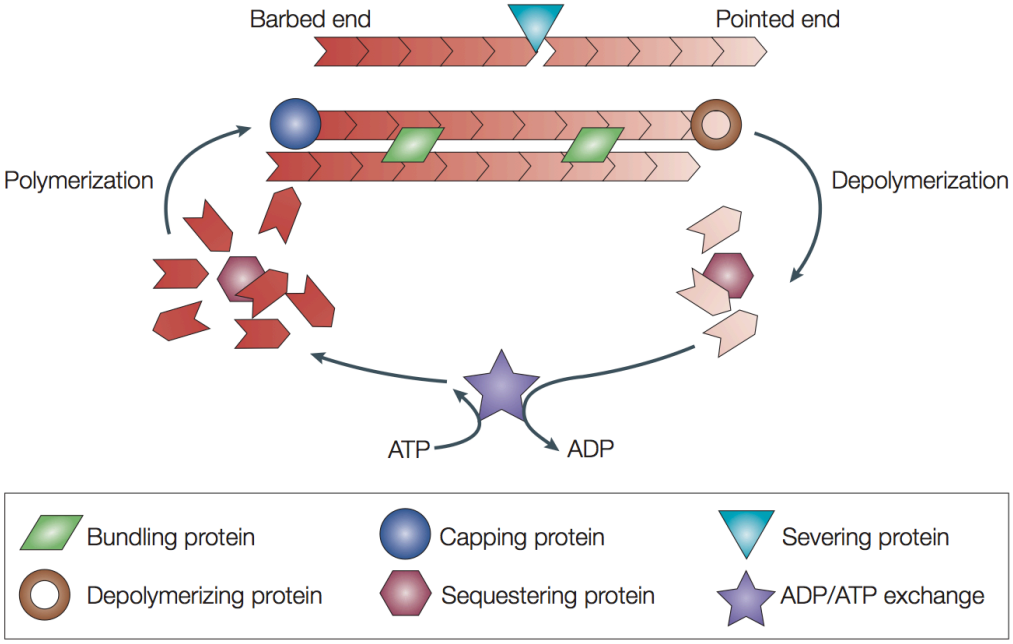
Barbed end
Pointed end
Polymerization
Depolymerization
ATP
ADP
Bundling protein
Capping protein
Severing protein
Depolymerizing protein
Sequestering protein
ADP/ATP exchange

**Figure 1.1. Actin dynamics.** Actin polymerization occurs at the barbed end and actin depolymerization occurs at the pointed end. F-actin treadmilling occurs when there is a net addition of actin monomers at the barbed end and a net loss of actin monomers at the pointed end. The substrate for polymerization is ATP-bound G-actin, which is thermodynamically favoured under physiological conditions. *In vivo*, numerous actin-binding proteins have activities that include bundling, capping, severing, depolymerizing, sequestering and ATPase activities. Figure from (Revenu et al., 2004). *See Appendix, Copyright Permissions for license to republish figure.*

### 1.1.2 Vertebrate actin filament organization

#### 1.1.2.1 Actin filament networks: parallel bundles and orthogonal networks

Actin filament networks are organized into two main types: parallel, unbranched bundles and highly branched, orthogonal networks (Figure 1.2) (Stossel, 1984; Revenu et al., 2004). Parallel bundles are found in various membrane protrusions such as filopodia, stereocilia, microvilli (Mooseker et al., 1984; Tilney and Tilney, 1984), stress fibres (Buckley, 1981; Byers and Fujiwara, 1982; Wong et al., 1983) and pseudopodia (Schollmeyer et al., 1978). Highly branched orthogonal networks are found at the cell cortex and the lamellae and leading edge of spread and migrating cells such as amoebae, macrophages, leukocytes and blood platelets (Stossel, 1984). The physiological function of these two types of actin filament networks is to produce force through the coordinated polymerization of actin filaments against cellular membranes (Tojkander et al., 2012).

Parallel bundles are formed from tightly packed actin filaments that are uniformly polarized. Within membrane protrusions such as microvilli, the barbed ends point toward the membrane to drive membrane protrusion via actin polymerization (Figure 1.2A) (Stossel, 1984; Revenu et al., 2004). Branched, orthogonal actin filament networks, on the other hand, are composed of actin filaments in X-, Y- or T-shaped configurations (Schliwa and van Blerkom, 1981; Flanagan et al., 2001). The barbed ends of actin filaments in the lamellipodia of migrating cells face the leading edge and the pointed ends associate with the side of another filament in a Y-shaped junction (Svitkina et al., 1997). Higher angles result in X-shaped junctions (Mullins et al., 1998). Filopodia, interestingly, are formed from parallel bundles that originate from a pre-existing branched network, such as lamellipodia (Figure 1.2B) (Stossel, 1984; Svitkina et al., 2003).

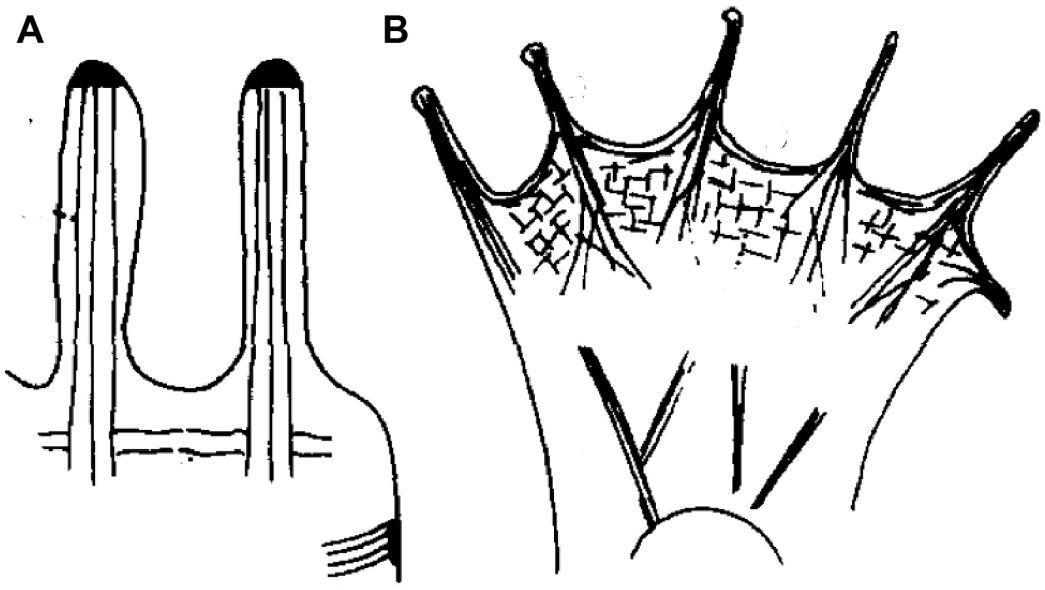
A
B

**Figure 1.2. Schematic of the two main types of actin configurations in cells. (A)** Microvilli showing parallel, unbranched bundles of actin filaments. **(B)** Highly branched, orthogonal networks found in the lamellipodia of motile cells. Filopodia microspikes containing F-actin bundles originate from the lamellae containing orthogonal F-actin networks. Figure adapted from (Stossel, 1984). *See Appendix, Copyright Permissions for Permission Licensing information.*

#### 1.1.2.2 Stress fibres

Actin filaments together with myosin II filaments (actomyosin bundles) form contractile structures that generate force through ATP-driven movement of myosin II motor domains along actin filaments. Contraction occurs when bipolar arrays of actin filaments slide past each other in opposite directions. In non-muscle animal cells, contractile actomyosin structures include the cytokinetic contractile ring, the contractile cortex, and stress fibres, which are major mediators of cell contraction in non-muscle cells (Pellegrin and Mellor, 2007; Tojkander et al., 2012). Stress fibres are composed of bundles of actin filaments crosslinked in a bipolar arrangement by α-actinin (Tojkander et al., 2012) and are often anchored to focal adhesions, which connect the actin cytoskeleton to the extracellular matrix (ECM) (Cramer et al., 1997; Pellegrin and Mellor, 2007; Naumanen et al., 2008). There are four classes of stress fibres that vary in their morphology and association with focal adhesions: dorsal and ventral stress fibres, transverse arcs and the perinuclear actin cap (Figure 1.3) (Heath, 1983; Small et al., 1998; Khatau et al., 2009; Tojkander et al., 2012). Dorsal stress fibres are anchored to focal adhesions at their distal end. Transverse arcs are curved actomyosin bundles near the cell center and are typically connected to focal adhesions through interaction with dorsal stress fibres. Ventral stress fibres are anchored to focal adhesions at both ends and perinuclear actin cap bundles resemble ventral stress fibres but are located above the nucleus (Tojkander et al., 2012).

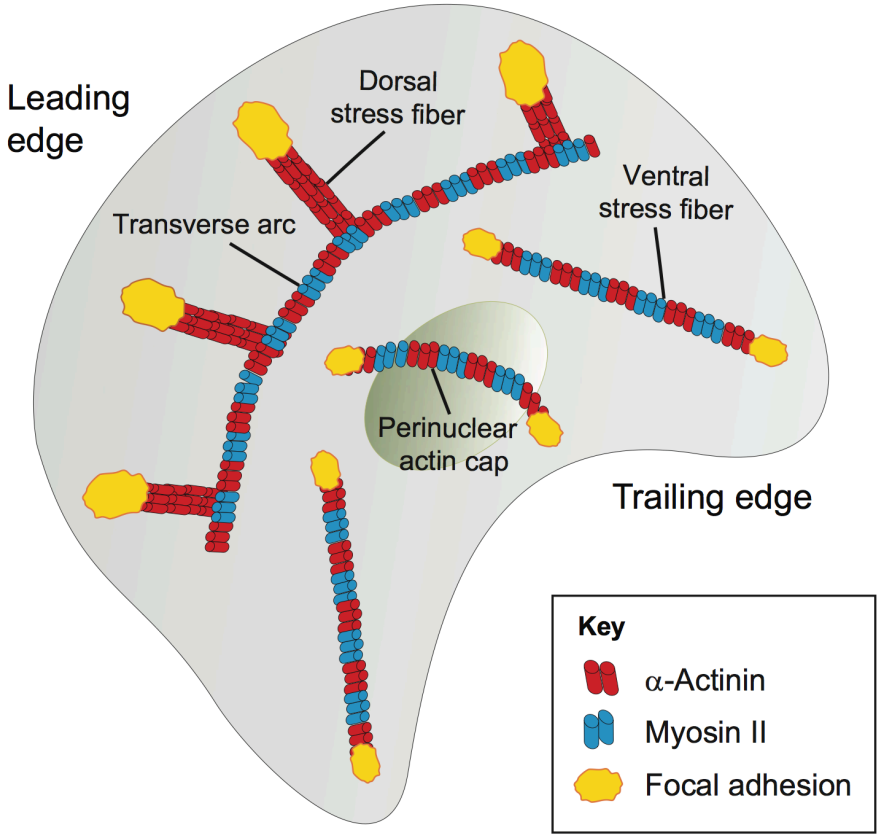
Leading edge
Dorsal stress fiber
Transverse arc
Ventral stress fiber
Perinuclear actin cap
Trailing edge
Key
α-Actinin
Myosin II
Focal adhesion

**Figure 1.3. Different types of stress fibres in cultured motile cells.** Dorsal stress fibres are anchored to focal adhesions at their distal end. Transverse arcs are curved actomyosin bundles near the cell center and typically connected to focal adhesions through interaction with dorsal stress fibres. Ventral stress fibres are anchored to focal adhesions at both ends. Perinuclear actin cap bundles resemble ventral stress fibres but are located above the nucleus. Figure from (Tojkander et al., 2012). *See Appendix, Copyright Permissions for license to republish figure.*

#### 1.1.2.3 Cortex

The cortex is a 50 μm-2 nm thick layer of actomyosin bundles, branched orthogonal actin filaments, and ABPs underlying the plasma membrane of most eukaryotic cells lacking a cell wall (Figure 1.4A) (Bray and White, 1988; Charras et al., 2006; Salbreux et al., 2012). Actomyosin cortex contractions modulate cell surface tension to control cell shape, volume and mechanical strength and rigidity (Stewart et al., 2011). Regulation of these processes is critical for mitotic cell rounding, generation of the cytokinetic contractile ring, morphogenesis and cell migration (Charras et al., 2006; Stewart et al., 2011). Blebs are spherical protrusions of the cell membrane that result from transient detachment of the cell membrane from the actin cortex, resulting in the flow of cytosol into the newly formed bleb (Figure 1.4) (Charras, 2008). Blebs expand for about 30 seconds and then shrink over the course of approximately 2 minutes, reappearing elsewhere on the cell membrane in an asynchronous manner (Charras et al., 2008). Blebbing occurs naturally in animal cells during cytokinesis (Fishkind et al., 1991), apoptosis (Mills et al., 1998) and some types of cell migration (Friedl and Wolf, 2003; Blaser et al., 2006; Yoshida and Soldati, 2006; Fackler and Grosse, 2008).

**A**

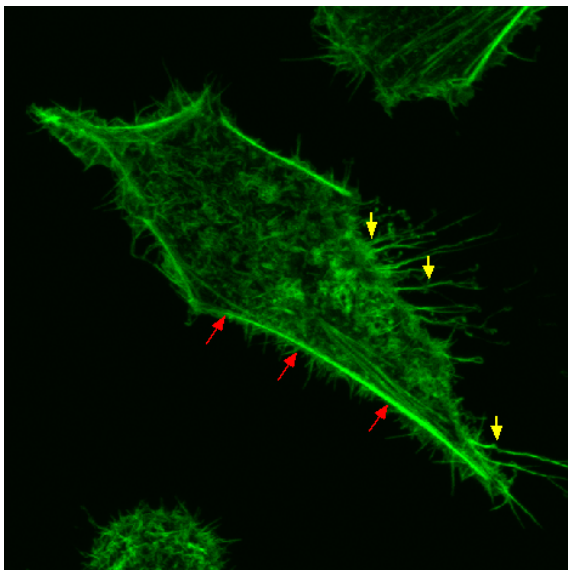

**B**

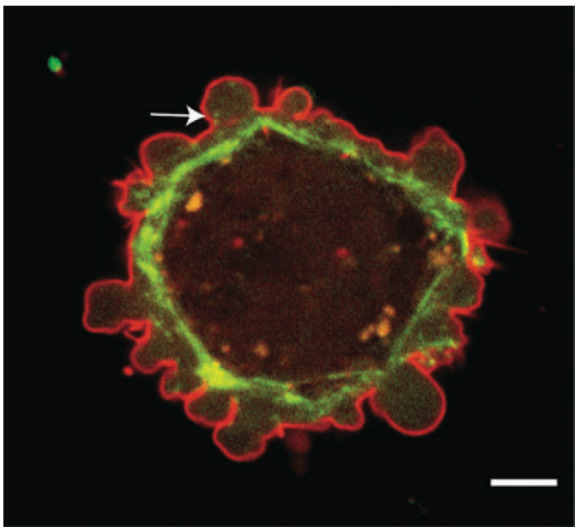

**Figure 1.4. The cell cortex is important for maintenance of plasma membrane integrity.** **(A)** Cell cortex in interphase HeLa cells. The actin cytoskeleton is shown in green. The red arrows point to cortical actin, which form the cell cortex. Red arrows indicate filopodia. **(B)** FLNa-deficient M2 cell undergoing blebbing. Cells were transfected with Myosin regulatory light-chain GFP and with PH- PLCδ-mRFP and imaged with a spinning disk confocal microscope. Myosin regulatory light chain (in green) is localized to the cell cortex and present in distinct foci (arrow) in retracting blebs. The cell membrane is shown in red using the pleckstrin homology (PH) domain of phospholipase C (PLC)δ. Scale bar, 5μm. Panel B from (Charras, 2008). *See Appendix, Copyright Permissions for license to republish panel B.*

#### 1.1.2.4 Lamellipodia

During cell migration, the front of the cell that faces the direction of cell movement is described as the leading edge (Ridley, 2011). At the leading edge, a broad, flat region called the lamellae adheres to the underlying substrate (Ponti et al., 2004). Lamellae are enriched in actomyosin bundles and dorsal and ventral stress fibres and transverse arcs that generate force on the growth substrate to drive cell directed cell movement (Ponti et al., 2004; Hotulainen and Lappalainen, 2006; Hu et al., 2007; Gardel et al., 2008). Structurally, lamellae (or lamellipodia) consist of highly branched, crosslinked actin filaments and filopodia that project from the edge of the lamellipodium (Small, 1994). To migrate, cells attach to substrate at the leading edge and retract at the trailing edge. This is accomplished through the coordinated assembly of small focal contacts at the leading edge of the cell and disassembly of focal adhesions at the rear (Lauffenburger and Horwitz, 1996; Mitchison and Cramer, 1996). When focal contacts mature into larger focal adhesions, they pull the cell forward, generating movement (Kaverina et al., 2002; Wehrle-Haller and Imhof, 2002). Loss of focal contacts at the trailing edge is the result of contact endocytosis (Ezratty et al., 2009).

F-actin is a highly dynamic macromolecule, and can combine to form many types of the aforementioned networks. However, these actin networks cannot be achieved by F-actin alone. The diversity of F-actin networks is due to a variety ABPs that organize actin filaments into different networks and also affect actin dynamics by inducing depolymerization or polymerization.

### 1.1.3 Actin-binding proteins

#### 1.1.3.1 G-actin binding/sequestering proteins

Many non-muscle cells contain large pools of unpolymerized G-actin, which serve as a source for actin filament assembly during cellular processes such as migration, chemotaxis and cell spreading (Safer et al., 1991). In cells, the concentration of actin monomers is generally at least two orders of magnitude above the critical concentration ($C_c$) for polymerization; this suggests the actin monomers are inhibited from polymerizing. Indeed, G-actin monomers are bound by G-actin binding proteins, which inhibit polymerization. Profilin is a G-actin binding protein and is a nucleotide exchange factor that catalyzes the exchange of ADP for ATP in actin (Schlüter et al., 1997). In lower eukaryotes, the main role of profilin is to sequester G-actin and stabilize the G-actin pool. However, in higher eukaryotes, their primary role appears to be the regulation of actin filament dynamics (Sohn and Goldschmidt-Clermont, 1994; Schlüter et al., 1997). Thymosin β4 is another G-actin binding protein that is widely distributed and abundant in many cell types including neutrophils, platelets and fibroblasts (Safer et al., 1991). Compared to profilin, the primary function of thymosin β4 is to sequester actin monomers and inhibit polymerization in higher eukaryotes (Safer et al., 1991).

#### 1.1.3.2 Capping proteins

Capping proteins bind to actin monomers to either nucleate actin polymerization from monomers or control actin filament length by binding to actin filament ends, preventing the addition or loss of actin monomers (Schafer and Cooper, 1995; Ayscough, 1998). Barbed-end capping proteins prevent the addition of actin monomers to the fast growing end. Examples include gelsolin, adseverin, villin and CapG (Schafer and Cooper, 1995). Pointed-

end capping proteins bind to the pointed end, blocking both addition and loss of actin monomers (Weber et al., 1994). Examples of pointed-end capping proteins include tropomodulin and spectrin-B and 4.1 (Schafer and Cooper, 1995). Many of these proteins have multiple activities that include capping. For example gelsolin severs actin filaments and then remains bound to the barbed end, effectively capping it (Schafer and Cooper, 1995; McGough et al., 2003).

#### 1.1.3.3 Actin nucleation proteins

During cell migration, signaling pathways activate the formation of new actin filaments by activating nucleation-promoting factors such as the WASP/Scar family of proteins (Revenu et al., 2004). These proteins stimulate actin nucleation proteins such as the actin-related protein-2/3 (Arp2/3) complex to nucleate actin filaments, which accelerates polymerization. These actin filaments only elongate from their barbed ends (Mullins et al., 1998). The Arp2/3 complex can also initiate the growth of new actin filaments on the sides of pre-existing filaments to drive membrane protrusion at the leading edge (Mullins et al., 1998; Pollard and Borisy, 2003). These new filaments branch at a fixed angle of 70° from the existing filament and form Y-shaped junctions (Mullins et al., 1998).

Formins are another family of actin-nucleating proteins. Formins are defined by the presence of a formin homology 2 (FH2) domain that is necessary and sufficient for *in vitro* actin filament nucleation (Pruyne et al., 2002; Li and Higgs, 2003) through the stabilization of actin dimers (Pring et al., 2002; Kovar et al., 2003; Li and Higgs, 2003). Formins increase F-actin content through their "leaky" capping activity, allowing polymerization to occur even while bound to the barbed end (Pring et al., 2002; Pruyne et al., 2002; Li and Higgs, 2003).

Generally, formin-induced actin filaments function with myosin to support contraction in actomyosin structures such as stress fibres and the contractile ring (Zigmond, 2004).

#### 1.1.3.4 F-actin severing proteins and depolymerizing proteins

Cell motility is a process that requires highly dynamic actin. This is in part accomplished by the severing of actin filaments which increases the number of actin filaments and generates ends for polymerization (Revenu et al., 2004). Examples of F-actin severing/depolymerizing proteins include villin (Northrop et al., 1986), the gelsolin family proteins (Kwiatkowski and Yin, 1987), adseverin (Lueck et al., 1998) and the actin-depolymerizing factor/cofilin (ADF/cofilin) family proteins. Proteins of the gelsolin family have severing and capping activities that are activated by $Ca^{2+}$ binding (Janmey et al., 1985; Lin et al., 2000). After severing, gelsolin caps the barbed end of the actin filament and this prevents the severed filament from re-annealing and elongating. Thus actin filament depolymerization occurs only at the pointed end (McGough et al., 2003). The dissociation of gelsolin from barbed ends is mediated by the binding of phosphatidylinositol 4,5-bisphosphate (PtdIns(4,5)$P_2$), a membrane phospholipid (Janmey and Stossel, 1987; Yamamoto et al., 2001; Xian and Janmey, 2002).

The ADF/cofilin family of proteins, unlike gelsolin, are $Ca^{2+}$-independent (Athman et al., 2002). ADF/cofilin proteins accelerate depolymerization from the pointed ends of actin filaments and weakly sever filaments without capping (Athman et al., 2002). They bind to two actin subunits along an actin filament and sever the interaction by locally modifying the twist of the filament (McGough et al., 1997; Bobkov et al., 2002; Galkin et al., 2003). ADF/cofilin proteins are regulated by the phosphorylation of a single residue (serine 3)

(Agnew et al., 1995), which inactivates their F-actin-depolymerizing/severing activities (Morgan et al., 1993).

#### 1.1.3.5 F-actin crosslinking proteins

F-actin crosslinking proteins can either form parallel F-actin bundles, in which the actin filaments are tightly packed and of the same polarity (Matsudaira, 1991; Bartles, 2000) or high-angle (orthogonal) actin filament structures (Gardel et al., 2004; Gardel et al., 2006; Stossel et al., 2006). To accomplish these activities, actin crosslinking proteins bind two different actin filaments simultaneously and therefore must contain multiple actin-binding sites (ABS) (Figure 1.5) (Bartles, 2000; Revenu et al., 2004). F-actin crosslinking can also be accomplished by homodimerization of two monomers in a parallel or antiparallel fashion (Figure 1.5) (Revenu et al., 2004). Examples of F-actin crosslinking proteins that form bundles are relatively small ABPs such as fascin, forked, fimbrin, espin, villin, members of the formin family, and α-actinin (Figure 1.5) which are localized in bristles, microvilli, sterecilia and filopodia (Revenu et al., 2004; Stossel et al., 2006). F-actin crosslinking proteins that form orthogonal networks include larger, more flexible ABPs such as spectrin and filamin which are localized at the cell cortex (Stossel et al., 2006).

The focus of the next section is the actin-crosslinking protein filamin, specifically, the FLNa isoform, which is ubiquitously expressed and highly abundant in non-muscle cells.

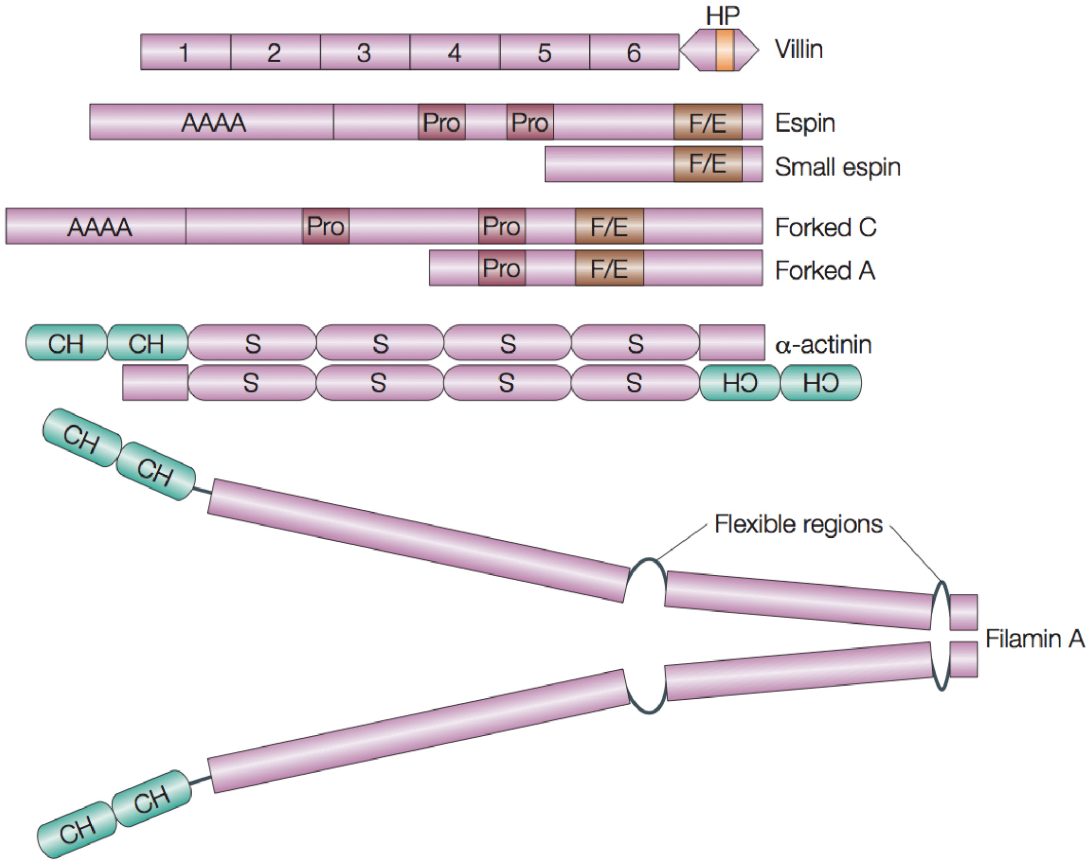
HP
1
2
3
4
5
6
Villin
AAAA
Pro
Pro
F/E
Espin
F/E
Small espin
AAAA
Pro
Pro
F/E
Forked C
Pro
F/E
Forked A
CH
CH
S
S
S
S
α-actinin
S
S
S
S
CH
CH
CH
CH
Flexible regions
Filamin A
CH
CH
CH
CH

**Figure 1.5. Structural organization of actin-crosslinking proteins.** Filamin crosslinks F-actin into high-angle orthogonal networks. Villin binds actin monomers on repeat 1 and 4-6 and actin filaments on repeats 2-3 and the villin headpiece (HP) on the C-terminus. The KKEK motif is essential for filament binding (shown in yellow). The forked/espin homology domain (F/E) contains two actin-binding domains (ABDs) to mediate filament bundling. Pro and AAAA designate proline-rich regions and amino-terminal ankyrin repeats, respectively. In α-actinin and filamin A pairs of calponin-homology (CH) form the ABD. α-actinin forms an anti-parallel homodimer and filamin A forms a parallel homodimer to mediate its crosslinking activities. Figure adapted from (Revenu et al., 2004). *See Appendix, Copyright Permissions for license to republish figure.*

## 1.2 FILAMIN A

### 1.2.1 Discovery of filamin

Filamin was originally identified as a high molecular weight (HMW)-ABP that was an accidental by-product of an attempt to isolate $Ca^{2+}$-sensitive myosin from rabbit alveolar macrophages (Hartwig and Stossel, 1975). Around the same time, a second group purified a HMW protein from chicken gizzard smooth muscle (Wang et al., 1975). Immunofluorescence with an antibody directed against this protein showed localization along actin-rich stress fibres in chick dorsal root ganglion cells, chick fibroblasts and mouse 3T3 fibroblasts. The "filamentous" staining pattern in all these cell types led to the name "filamin" (Wang et al., 1975). Smooth muscle filamin, macrophage HMW-ABP and later a filamin-like protein identified in vertebrate skeletal muscle were shown to be filamin homologs because they were all very similar in subunit molecular weight, amino acid composition, ability to bind actin and immunological properties (Wallach et al., 1978b; Bechtel, 1979).

### 1.2.2 Filamin structure

Human FLNa is a large, 280 kD protein monomer (2647 amino acids) that consists of a high-affinity 275 amino acid ABD at its N-terminus, followed by 24 tandem immunoglobulin G-like domains (also called repeats), each with an average of 96 amino acids (Figure 1.6) (Gorlin et al., 1990; Nakamura et al., 2011). The ABD consists of two calponin homology (CH) domains (CH1 and CH2) separated by a linker (Bañuelos et al., 1998). There are three actin-binding sites (ABS1, ABS2 and ABS3) within the ABD. ABS1 and ABS2 are located within CH1 and ABS2 is located in CH2 (Bresnick et al., 1991). These sites overlap with those of other ABPs including α-actinin, myosin, tropomyosin and caldesmon (McGough,

1998; Van der Flier, 2001). Both F-actin and the ABD undergo structural rearrangements when they interact, implying that the binding of an ABD could affect the shape of F-actin (McGough, 1998; Moores et al., 2000; Van der Flier, 2001). Biologically, FLNa functions as a parallel V-shaped homodimer, and self-association of two FLNa proteins is mediated by repeat 24 (R24) at the C-terminus (Figure 1.6) (Hartwig and Stossel, 1975; Gorlin et al., 1990; Takafuta et al., 1998; Flanagan et al., 2001; Van der Flier, 2001; Nakamura et al., 2011). A segment of FLNa spanning repeats 9-15 is required for high avidity F-actin binding and is referred to as a secondary F-actin-binding segment (Figure 1.6) (Nakamura et al., 2007; Nakamura et al., 2011). Repeats 1-15 and 16-24 are referred to as rod 1 and 2, respectively (Popowicz et al., 2004; Nakamura et al., 2007; Jiang and Campbell, 2008). In addition, two flexible loop regions described as hinges (H1 and H2), each 20-40 amino acids long, are located between repeats 15-16 and 23-24 (Figure 1.6) (Nakamura et al., 2011). These so-called "hinges" are believed to confer conformational flexibility to the FLNa molecule and are sites of proteolytic cleavage (Gorlin et al., 1990; Aguda et al., 2007).

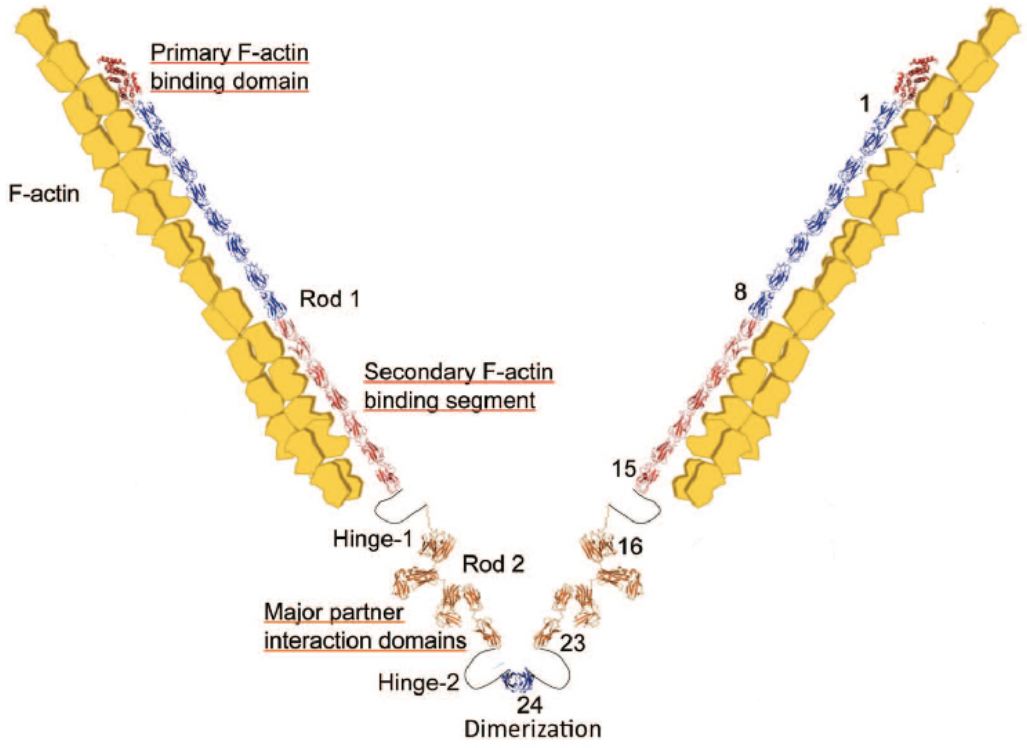
Primary F-actin
binding domain
F-actin
Rod 1
Secondary F-actin
binding segment
Hinge-1
Rod 2
Major partner
interaction domains
Hinge-2
24
Dimerization
23
16
15
8
1

**Figure 1.6. Schematic representation of filamin A molecule and its interaction with actin filaments.** Self-association of two filamin A monomers is mediated by IgFLNa domain 24 at the C-terminus. The primary actin-binding domain (ABD) is located at the N-terminus and a secondary F-actin binding segment is located in IgFLNa domains 8-15. Two flexible hinge regions are located between domains 15 and 16 (H1) and 23 and 24 (H2). Figure adapted from (Nakamura et al., 2011). *See Appendix, Copyright Permissions for license to republish figure.*

### 1.2.3 Mammalian filamin isoforms and their cellular and tissue distribution

The mammalian filamin family has three members, FLNa, filamin B (FLNb) and filamin C (FLNc), that are highly conserved and exhibit about 70% overall amino acid identity (Figure 1.7) (Van der Flier, 2001). The greatest variation is found within the two hinge regions which are 45% homologous (Van der Flier, 2001). Splice-variants of all three filamin isoforms exist and may have specific cellular functions. The human *FLNa* gene is located on the X chromosome and *FLNb* and *FLNc* are located on chromosomes 3 and 7, respectively (Maestrini et al., 1993). Human FLNa and FLNb are expressed ubiquitously, whereas FLNc expression is restricted to skeletal and cardiac muscle (Thompson et al., 2000). Specifically, a FLNc splice variant lacking H1 is dominant in skeletal and cardiac muscle (Thompson et al., 2000). Together, FLNa and FLNb represent about 90% of total filamin (Baldassarre et al., 2009).

In cultured, non-muscle cells, FLNa is localized along actin stress fibres (Pavalko et al., 1989), cortical actin networks (Condeelis et al., 1981) and at the leading edge and membrane ruffles of migrating cells. During cell spreading, FLNa localizes to filopodia, lamellipodia (Kim et al., 2008), and the endoplasm (Lynch et al., 2011). In dividing cells, FLNa is often found concentrated in the cleavage furrow, where it remains associated at the midbody region at the completion of cell division (Nunnally et al., 1980). A small fraction of FLNa has also been found in the nucleus (Yuan and Shen, 2001) where it participates in transcription regulation.

FLNc is the predominant filamin isoform in muscle cells. In skeletal muscle, FLNc is enriched at the Z-lines and myotendinous junctions, but a small amount can be detected at the plasma membrane in association with the cortical actin cytoskeleton (Gomer and Lazarides, 1981, 1983). In cardiac muscle, FLNc localizes to the sarcomeric Z-line complex

and intercalated discs (Thompson et al., 2000; van der Ven et al., 2000) and in chicken smooth muscle, FLNc-like proteins are found in the dense plaques and dense bodies (Tachikawa et al., 1997).

### 1.2.4 Filamins in amoeba, fruit-fly and nematode

Filamin homologs have been found in many organisms including amoeba, fruit flies, and nematodes; however, the number of filamin domains in each varies (Figure 1.7) (Van der Flier, 2001; Razinia et al., 2012). A 120 kD filamin homolog (ABP-120 or gelation factor), is found in amoeba including *Dictyostelium discoideum* (slime mold) (Condeelis et al., 1981; Condeelis et al., 1982) and *Entamoeba histolytica,* which is responsible for dysentery (diarrhea with blood) (Vargas et al., 1996). *D. discoideum* that are genetically depleted of filamin by homologous recombination show substantial reduction in cell growth, pseudopod formation, cell motility, chemotaxis and phagocytosis that are rescued by ABP-120 re-expression (Cox et al., 1992; Cox et al., 1995; Cox et al., 1996).

In the fruitfly *Drosophila melanogaster*, a screen for female sterile mutations identified *cheerio* as the filamin homolog. The *cheerio* locus encodes two filamin transcripts through differential splicing. The larger transcript is involved in ring-canal assembly and follicular cell rearrangements during oogenesis. In *cheerio* mutants, nurse cells fail to grow to wild-type (WT) size and consequently are unable to support the growth of the oocyte, leading to the production of inviable eggs (Li et al., 1999; Sokol and Cooley, 1999, 2003).

Recently, two filamin isoforms have been identified in *Caenorhabditis elegans*, FLN-1 (Kovacevic and Cram, 2010) and FLN-2 (DeMaso et al., 2011). FLN-1 is required for maintenance of actin and calcium signaling in the spermatheca, a tissue that undergoes

dramatic shape changes during the fertilization of oocytes (Kovacevic and Cram, 2010; Kovacevic et al., 2013).

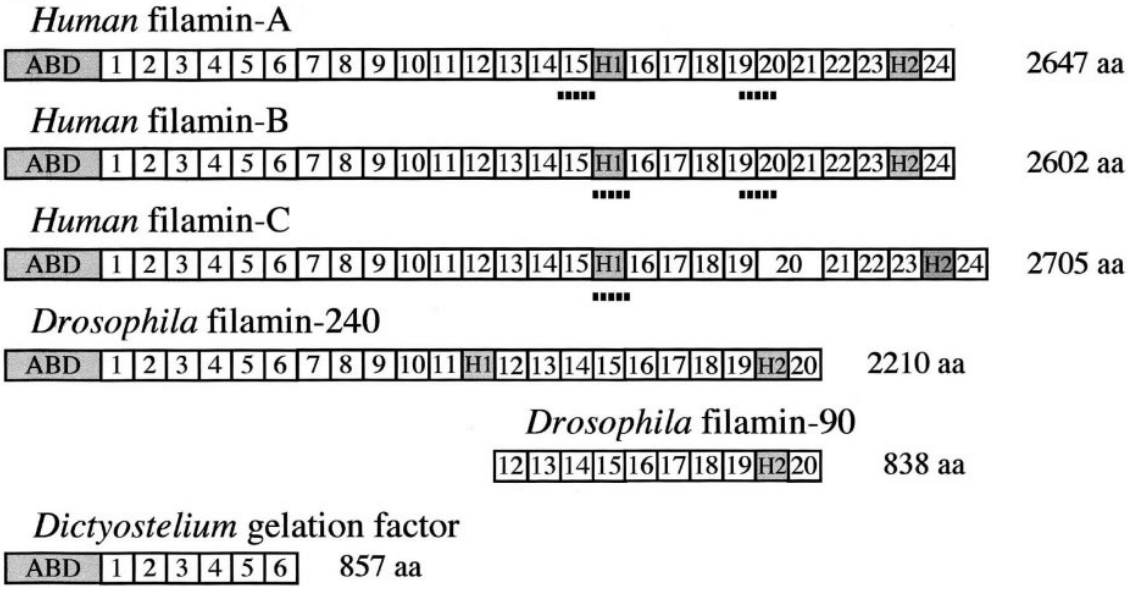
*Human* filamin-A
ABD 1 2 3 4 5 6 7 8 9 10 11 12 13 14 15 H1 16 17 18 19 20 21 22 23 H2 24
2647 aa
*Human* filamin-B
ABD 1 2 3 4 5 6 7 8 9 10 11 12 13 14 15 H1 16 17 18 19 20 21 22 23 H2 24
2602 aa
*Human* filamin-C
ABD 1 2 3 4 5 6 7 8 9 10 11 12 13 14 15 H1 16 17 18 19 20 21 22 23 H2 24
2705 aa
*Drosophila* filamin-240
ABD 1 2 3 4 5 6 7 8 9 10 11 H1 12 13 14 15 16 17 18 19 H2 20
2210 aa
*Drosophila* filamin-90
12 13 14 15 16 17 18 19 H2 20
838 aa
*Dictyostelium* gelation factor
ABD 1 2 3 4 5 6
857 aa

**Figure 1.7. Schematic representation of the domain composition of human, *Drosophila* and *Dictyostelium* filamins.** There are three human filamin isoforms, FLNa, FLNb and FLNc. The actin-binding domain (ABD), hinge 1 (H1) and hinge 2 (H2) are shown in grey. Dotted lines indicate sites of alternative splicing. Figure from (Van der Flier, 2001). *See Appendix, Copyright Permissions for license to republish figure.*

### 1.2.5 Physiological significance of FLNa

Periventricular heterotopia (PH) (OMIM #300049) is the most common human disease linked to mutations in FLNa, an X-linked gene which maps to chromosome Xq28 (Maestrini et al., 1993). PH is a connective tissue disorder clinically characterized by joint hypermobility, arterial dilatation, cardiac valvular defects and cutaneous anomalies (Figure 1.8) (Robertson, 2005; Reinstein et al., 2012). The major manifestations of the disease are neurological and many patients suffer from epileptic seizures, early onset stroke and vascular complications. Most affected individuals with the X-linked form of PH are female, suggesting hemizygous mutation in males is embryonic lethal (Ekşioğlu et al., 1996; Reinstein et al., 2012). FLNa is highly expressed in the developing cortex (Fox et al., 1998) and in PH, a subset of neurons in the brain fail to migrate into the developing cerebral cortex during fetal development and this gives rise to the accumulation of neuronal nodules along the ventricular surface which can be seen by magnetic resonance imaging (MRI) (Figure 1.8A) (Robertson, 2005; Jefferies et al., 2010). These observations suggest a defect in neuronal motility (Ekşioğlu et al., 1996; Fox et al., 1998), consistent with a role for FLNa in cell migration. Abnormal mRNA splicing or nonsense mutations that result in FLNa truncation, leading to loss-of-function, are the most common cause of X-linked PH (Fox et al., 1998; Sheen et al., 2001).

FLNa mutations have also been linked to X-linked chronic idiopathic intestinal pseudo-obstruction (OMIM 300048) (Gargiulo et al., 2007), otopalatodigital (OPD) spectrum disorders (Types I and II, OMIM 311300, OMIM 304120), frontometaphyseal dysplasia (FMD) (OMIM 305620), (Robertson et al., 2006) and Melnick-Needles syndrome (MNS) (OMIM 309350) (Foley, 2010), which typically involve generalized dysplasia involving craniofacial structures, digits and long bones (Figure 1.8) (Robertson et al., 2003;

Robertson, 2005). Dominant-negative or gain-of-function (missense) mutations appear to be the most common cause of these disorders, although the effects of these mutations on FLNa function are currently unknown (Robertson et al., 2003; Robertson, 2005).

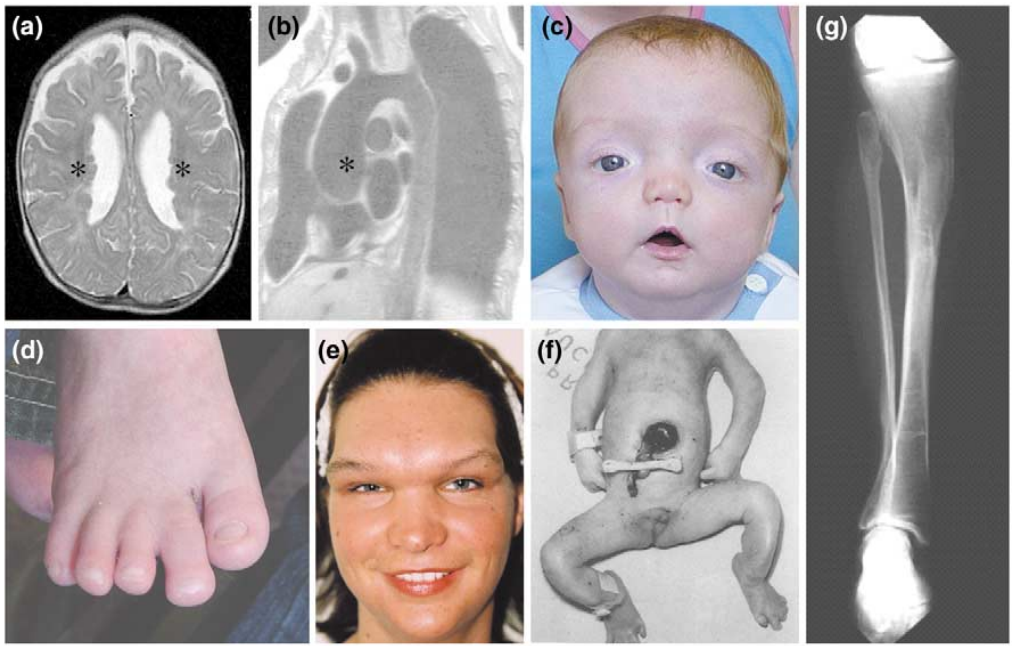
(a)
(b)
(c)
(g)
(d)
(e)
(f)

**Figure 1.8. Phenotypes associated with mutations in FLNA. (A)** Magnetic resonance image (MRI) of the brain of a female with periventricular nodular heterotopia (PH). The asterisks indicate nodules of heterotopic neurons lining the lateral ventricular margins. **(B)** MRI showing aortic dilatation (asterisk) in an individual with PH-Ehlers-Danlos syndrome. **(C)** Facial features of a male infant with otopalatodigital syndrome type 1 (OPD1). Note the widely spaced eyes. **(D)** Foot of the subject pictured in panel C showing partial syndactyly of toes and a foreshortened great toe. **(E)** Female carrier with frontometaphyseal dysplasia (FMD) with marked prominence of the supraorbital region. **(F)** Male with otopalatodigital syndrome type 2 (OPD2) with omphalocoele (sac containing the intestines in the midline) and bowed lower limbs. **(G)** Bowing of the tibia and fibula in a female with Melnick Needles syndrome (MNS). Figure from (Robertson, 2005). *See Appendix, Copyright Permissions for license to republish figure.*

### 1.2.6 Biological filamin A functions

#### 1.2.6.1 Insights gained from FLNa-deficient cells

Insights on the biological function of FLNa were first gained from studies on naturally FLNa-deficient melanoma cells and their FLNa-expressing counterparts. In 1991 Byers et. al. biopsied melanoma tumours from seven different patients and observed their migratory capacity. Seven cell lines were derived from the epidermis (primary melanoma and recurrent primary melanoma) and lymph nodes (metastatic melanoma). Overall, cell lines derived from lymph node metastases had higher migration rates than cell lines derived from primary melanoma (Byers et al., 1991). A year later, another group found that three out of seven of the melanoma cells lines (renamed M1, M2 and M3) had undetectable FLNa protein (Cunningham et al., 1992). All seven cell lines had the FLNa gene but FLNa-deficient cell lines had very low levels of FLNa mRNA and undetectable protein levels, indicating regulation of FLNa gene expression or mRNA degradation causes the lack of FLNa protein (Cunningham et al., 1992). Cells with an intermediate level of FLNa expression had the highest migration rate, wherease very low and high FLNa expression inhibited migration (Cunningham et al., 1992). FLNa-deficient cell lines exhibited extensive blebbing, were more readily deformed by physical stress and had poor pseudopod protrusion (Cunningham et al., 1992). M2 cells (one of the three FLNa-deficient cell lines) stably expressing FLNa resembled that of the native FLNa-expressing lines (Cunningham et al., 1992). This study was the first to demonstrate the importance of FLNa in cellular processes including migration, spreading, membrane integrity and pseudopodia extension.

#### 1.2.6.2 Actin organization

The role of FLNa in the actin filament architecture has been examined extensively using M2 cells (FLNa-deficient) and its FLNa-expressing counterpart, A7, which expresses physiological levels of FLNa (Cunningham et al., 1992). Ultrastructurally, the density of cortical actin filaments in the lamellae of M2 cells is about twice as high as that of FLNa-repleted A7 cells and the average length of actin filaments in the periphery of spread M2 cells is much greater (Flanagan et al., 2001). Consequently, the actin architecture at the cortex of A7 cells is more delicate and porous than M2 cells whose actin filaments are presumably stabilized by other non-FLNa actin crosslinking proteins (Flanagan et al., 2001).

*In vitro*, the type of actin filament organization depends on the filamin to actin ratio, whereby increasing the ratio of filamin to actin leads to tighter networks (Niederman et al., 1983). The formation of parallel bundles is promoted when the molar ratio of filamin to actin is high (1:10-50), while a lower ratio (1:150-740) leads to the formation of orthogonal actin networks, depending on the source of filamin (Brotschi et al., 1978; Dabrowska et al., 1985).

The orthogonal actin networks of macrophage lamellae and the networks of filamin/actin gels generated *in vitro* is surprisingly similar (Hartwig and Shevlin, 1986). However, the actin filament organization *in vivo* is more tightly packed and is not solely dependent on filamin as seen in gels formed *in vitro*. This implies that *in vivo*, orthogonal filament networks and stress fibres are influenced by a combination of different actin-crosslinking proteins. Indeed, a mixture of F-actin, filamin and α-actinin *in vitro*, results in the formation of tight parallel bundles, resembling those found in platelet pseudopodia (Schollmeyer et al., 1978).

#### 1.2.6.3 Cell migration and substrate adhesion

M2 cells have a defect in cell migration, as demonstrated by their inability to migrate across porous filters in response to chemoattractants. Instead, M2 cells exhibit extensive circumferential plasma membrane blebbing, indicative of an unstable cell cortex (Cunningham et al., 1992; Flanagan et al., 2001). A7 cells, on the other hand, have migration rates in the same range as motile cells such as macrophages (Dipasquale, 1975; Cunningham et al., 1992). Other studies that demonstrate the requirement for FLNa in cell migration have been reported (Fox et al., 1998; Baldassarre et al., 2009). For example, periventricular heterotopia, a human disease associated with FLNa mutations, is thought to arise from impaired neuronal migration during development (Fox et al., 1998). Furthermore, Baldassarre et al. (2009) showed that filamins are required for the initiation of cell migration and their general role in migration extends to other cell types including HT-1080 (human fibrosarcoma cell line) and Jurkat (human T lymphocyte cell line) cells. These observations suggest that FLNa has a critical role in cell migration. Indeed, FLNa interacts directly with focal adhesion proteins including the cytoplasmic tail of β-integrin (Sharma et al., 1995; Loo et al., 1998) and FAP52 (focal-adhesion-associated phosphoprotein 52) (Behrendt, 2002; Nikki et al., 2002). However, FLNa is also involved in the inhibition of cell migration. For example, a strong association between integrins and FLNa impairs migration (Calderwood et al., 2001). Both FLNa and talin, a cytoskeletal protein (Burridge and Connell, 1983), bind to the same site on integrin and competition by talin binding to replace FLNa resumes cell migration (Calderwood et al., 2001). Therefore, these contradictory findings suggest that the mechanisms by which FLNa regulates cell migration are complex and dependent on multiple protein interactions.

#### 1.2.6.4 Mechanoprotection and force-sensing

A role for filamin in mechanoprotection was first discovered when Cunningham et al. (1992) observed that M2 cells, which lack FLNa, were more readily deformed by stress than FLNa-expressing A7 cells. Although the cortical actin filaments in M2 cells are still stabilized by non-FLNa crosslinking proteins, these proteins do not confer the same level of elasticity and integrity as FLNa-stabilized crosslinks (Flanagan et al., 2001). Other studies have found that M2 cells are unable to sense external rigidity (Byfield et al., 2009) or control cellular stiffness (Kasza et al., 2009) and are more susceptible to force-induced apoptosis (Glogauer et al., 1998). In FLNa-expressing cells, force application at cell adhesion sites by collagen-coated magnetic beads induces localized changes in the actin network that result in increased local rigidity (Glogauer et al., 1998). This response is mediated by FLNa, which is recruited into cortical areas under increased tension and promotes actin gelation and membrane stabilization to protect against force-induced cell death (Glogauer et al., 1998). Therefore, FLNa has frequently been described as a "force-sensor" due to its involvement in mechanotransduction, the process through which cells sense the external environment and respond to physical and mechanical signals, via integrin adhesion sites, to effect changes in the cell (Razinia et al., 2012).

#### 1.2.6.5 Stabilization of transmembrane proteins

FLNa and/or FLNb interact with several transmembrane proteins including the glycoprotein (GP)-Ibα subunit of the von Willebrand factor (vWF) receptor (Okita et al., 1985), intercellular cell adhesion molecule-1 (ICAM-1) (Kanters et al., 2008), β-integrin (Sharma et al., 1995; Loo et al., 1998), tissue factor (TF) (Ott et al., 1998) and carcinoembryonic antigen-related cell adhesion molecule 1 (CEACAM1) (Figure 1.9) (Klaile et al., 2005).

Many of these interactions occur on the carboxy-terminal region of filamin, thereby allowing filamin to simultaneously bind F-actin through its N-terminal ABD. Expression of filamin has been reported to increase cell surface levels of GP-Ibα and β1-integrin in FLNa-deficient M2 melanoma cells (Meyer et al., 1998). Thus, filamin may have a role in the stabilization of transmembrane receptors at the cell membrane (Van der Flier, 2001).

#### 1.2.6.6 Scaffolding signaling molecules

The Rho family of GTPases are key regulatory molecules that link surface receptors to the organization of the actin cytoskeleton and have been associated with various cellular processes such as cell migration and gene transcription (Hall, 1998). Three members of this family, RhoA, Rac1 and Cdc42, and many factors upstream and downstream of these effectors and other small GTPases have been shown to bind FLNa (Figure 1.9) (Ueda et al., 1992; Ueda et al., 2003; Popowicz et al., 2006). A summary of these FLNa-interactors is provided in the Appendix Table A1 (Nakamura et al., 2011).

Active RhoA induces stress fibre formation by increasing actomyosin contraction and F-actin bundling, whereas active Rac1 and Cdc42 increase lamellipodia/membrane ruffling and filopodia formation, respectively (Ridley and Hall, 1992; Hall, 1998). Most of these interactions occur on repeats 23 and 24 at the carboxy-terminal region of FLNa which is juxtaposed to the plasma membrane when FLNa interacts with to the cytoplasmic tail of integrin (Zhou et al., 2010; Nakamura et al., 2011). RhoA, Cdc42 and Rac1 all bind FLNa constitutively (GTP-independent) (Marti et al., 1997). FLNa also interacts with a member of the Ras family of GTPases, RalA, in a GTP-dependent manner (Ohta et al., 1999). FLNa appears to participate in the formation of filopodia as a downstream target of RalA and it is possible that Cdc42 acts through RalA to induce filopodia formation (Ohta et al., 1999).

Guanine nucleotide-exchange factors (GEFs) activate Rho GTPases by promoting the exchange of GDP for GTP. Trio, a Rho GEF interacts with FLNa through its pleckstrin homology (PH) domain and may function to regulate actin remodelling by switching on RhoA, Cdc42 and Rac1 (Bellanger et al., 2000; Stossel et al., 2001).

FLNa has also been shown to interact *in vitro* and *in situ*, with MKK-4 (SEK-1 or JNKK), a kinase that activates several stress-activated protein kinases (SAPKs). Active SEK-1 coimmunoprecipitates with filamin and is capable of phosphorylating and activating recombinant SAPK *in vitro* (Marti et al., 1997). In FLNa-deficient M2 cells, SAPK activation by lysophosphatidic acid (LPA) is inhibited by 80% and activation by tumour necrosis factor (TNF)-α is essentially abolished. Expression of a FLNa variant lacking the dimerization domain restores SAPK activation by TNF-α but not LPA. This implies that FLNa participates in TNF-α signaling to SAPKs that is independent of its F-actin crosslinking function; instead FLNa acts as a docking site or scaffold for MKK-4 (Marti et al., 1997; Van der Flier, 2001).

Membrane-localized sphingosine-1-phosphate (S1P) is a potent lipid mediator that is a key regulator of cytoskeletal rearrangements and cell movement, by acting through G protein-coupled S1P receptors ($S1P_{1-5}$). S1P formation is catalyzed by activated sphingosine kinase 1 (SphK1) which first needs to translocate from the cytosol to the membrane where its sphingosine substrate resides. S1P is then secreted and activates the appropriate S1P receptor. FLNa has been found to interact with SphK1 and FLNa-dependent translocation of cytosolic SphK1 to lamellipodia allows the enzyme access to its lipid substrate, sphinogosine, resulting in the spatially restricted formation and subsequent secretion of S1P (Maceyka et al., 2008). Spatially restricted S1P secretion is important for oriented cell

movement as extracellular S1P can simultaneously stimulate cell migration through S1P receptors, $S1P_1$ and $S1P_3$ (Liu et al., 2000; Matloubian et al., 2004) and inhibit migration through $S1P_2$ (Sugimoto et al., 2003; Goparaju et al., 2005; Sanchez et al., 2005). Thus FLNa appears to link SphK1 and $S1P_1$ together at the leading edge of migrating cells, ensuring that only $S1P_1$ is activated by the ligand S1P (Maceyka et al., 2008).

Overall, these interactions illustrate the scaffolding function of FLNa in orchestrating complex non-linear signaling processes by virtue of its ability to bind multiple proteins and their upstream and downstream effectors simultaneously. These interactions cause changes in the actin cytoskeleton during cellular processes such as cell migration and cell cycle progression that are not solely dependent on FLNa's actin-binding function.

#### 1.2.6.7 Regulation of transcription

Filamins can have both negative and positive influences on transcriptional activity through their retention or activation of transcription factors in the cytoplasm (Zhou et al., 2010). For example, the binding of FLNa to PEBP2β/CBFβ, a subunit of the transcription factor PEBP2β/CBF (Watanabe et al., 2005; Yoshida et al., 2005), and p73α, a transcription regulator (Kim et al., 2007), causes their retention in the cytoplasm and thus transcriptional repression. On the other hand, interaction of FLNa with transcription factors SMAD2 and SMAD5 positively regulates their receptor-mediated phosphorylation, a process necessary for subsequent nuclear translocation (Sasaki et al., 2001; Zhou et al., 2010).

A small fraction of full-length FLNa has been found in the nucleus of human skin fibroblasts and HeLa cells through immunofluorescence and cell fractionation experiments (Yuan and Shen, 2001). These findings provide support for nuclear FLNa in transcriptional regulation. FLNa has been found to interact with *BRCA2* (Figure 1.9) (Popowicz et al.,

2006), a tumour suppressor that participates in the DNA damage response, *in vivo* in human MCF-7 breast cancer cells (Yuan and Shen, 2001). In light of findings that FLNa also resides in the nucleus, this interaction suggests FLNa is involved in the DNA damage response. Indeed, FLNa-deficient M2 cells are more sensitive to genotoxic agents (γ irradiation, bleomycin and UV-C) than their FLNa-replete counterparts (Yuan and Shen, 2001). FLNa also interacts with FOXC1 (Figure 1.9), a transcription factor that has a key role in the formation of tissues derived from neural crest and mesenchymal mesoderm cell lineages (Kume et al., 2000; Berry et al., 2005; Popowicz et al., 2006). Studies on M2 and A7 cells provide evidence that transcriptional activity of *FOXC1* is inhibited in a FLNa-mediated manner (Berry et al., 2005).

Adding to the complexity of FLNa in transcriptional regulation, proteolytic FLNa fragments have also been found in the nucleus. Cleavage of FLNa by calpain generates a 100 kD C-terminal fragment that interacts with the nucleus-localized androgen receptor (Figure 1.9), a transcription factor that regulates male sexual differentiation (Loy et al., 2003; Popowicz et al., 2006). It is currently unknown how FLNa fragments are imported into the nucleus and whether full-length FLNa modulates the nuclear actin network (Zhou et al., 2010).

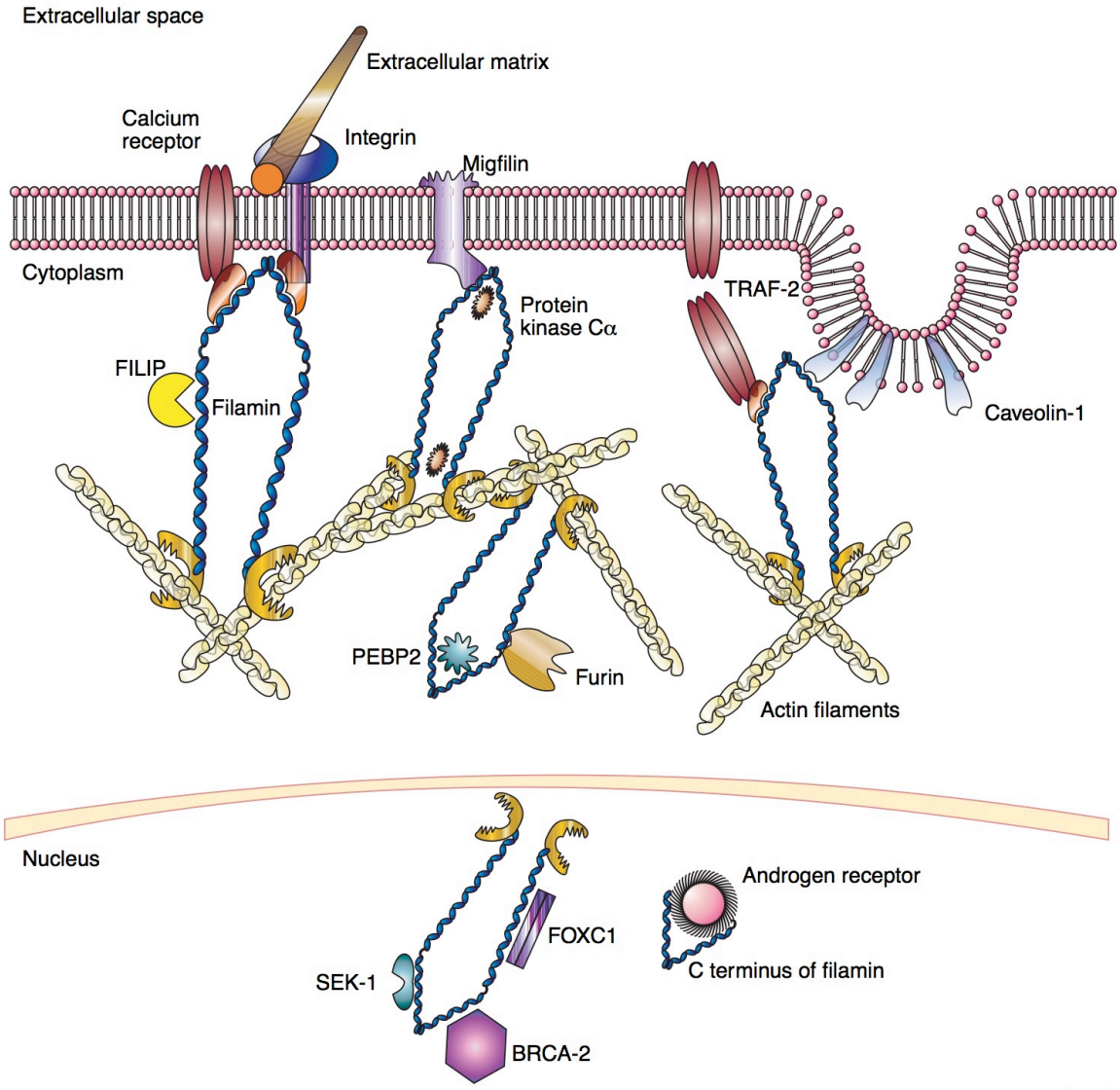
Extracellular space
Extracellular matrix
Calcium receptor
Integrin
Migfilin
Cytoplasm
TRAF-2
Protein kinase Cα
FILIP
Filamin
Caveolin-1
PEBP2
Furin
Actin filaments
Nucleus
Androgen receptor
FOXC1
SEK-1
C terminus of filamin
BRCA-2

**Figure 1.9. Filamin A functions.** In the cytoplasm, filamin A can crosslink F-actin, anchor transmembrane proteins, act as a scaffold for signaling complexes and link membrane receptors to the actin cytoskeleton. In the nucleus, filamin A has been implicated in transcription regulation. Both full-length and a 100 kD calpain-mediated cleavage fragment of filamin A have been found in the nucleus. Figure from (Popowicz et al., 2006). *See Appendix, Copyright Permissions for license to republish figure.*

### 1.2.7 Regulation of filamin A

#### 1.2.7.1 Phosphorylation

Given that FLNa is an ABP, many reports have investigated the effect of phosphorylation on its ability to bind F-actin (Zhuang et al., 1984; Ohta and Hartwig, 1995; Sharma and Goldmann, 2004; Cukier et al., 2007). Many kinases stimulate the phosphorylation of FLNa on serine/threonine residues *in vivo* and *in vitro*. FLNa is phosphorylated *in vivo* by p90 ribosomal S6 protein kinase (p90 RSK) (Ohta and Hartwig, 1996; Woo et al., 2004; Vial and McKeown-Longo, 2012), protein kinase C (PKC) (Tigges et al., 2003) and p21-activated kinase 1 (Pak1) (Vadlamudi et al., 2002) and *in vitro* by cAMP-dependent protein kinase (cAMP-kinase) (Wallach et al., 1978a; Chen and Stracher, 1989; Jay et al., 2000; Jay et al., 2004), Cdk1/cyclin B1 (Cukier et al., 2007) and $Ca^{2+}$/calmodulin-dependent protein kinase II (CaM-kinase II) (Kawamoto and Hidaka, 1984; Ohta and Hartwig, 1995). FLNa is also phosphorylated on tyrosine residue(s) by recombinant p56lck (lymphocyte-specific member of the *src* family of protein tyrosine kinases) *in vitro* (Goldmann, 2002; Sharma and Goldmann, 2004). FLNa and cyclin D1 were found to co-immunoprecipitate by mass spectrometry and decreased cyclin D1 expression correlated with decreased phosphorylation of FLNa at serine 2152 and serine 1459, indicating FLNa may be a substrate for cyclin-dependent kinase-4 (CDK4) (Zhong et al., 2010). Reports have found that FLNa phosphorylation has opposing effects on F-actin binding *in vitro*. Some have reported a decrease in F-actin binding (Ohta and Hartwig, 1995; Cukier et al., 2007) and others have reported an increase (Zhuang et al., 1984; Sharma and Goldmann, 2004). These apparent discrepancies may be due to differences in filamin isoforms, sites of phosphorylation and experimental procedures. Despite these attempts to identify a functional role for FLNa phosphorylation, the physiological relevance has yet to be established.

Reports on the effect of FLNa phosphorylation on its interaction with non-F-actin binding partners are limited. For example, *in vitro* phosphorylation of FLNa by protein kinase A (PKA, cAMP-kinase) was found to decrease its ability to interact with unidentified small GTP-binding protein(s) (Ueda et al., 1992). Furthermore, computational simulation modeling shows that phosphorylation of serine 2152, combined with force application, facilitates integrin adhesion receptor binding (Chen et al., 2009). Platelet activation with thrombin stimulation increased the amount of $^{32}$P-labeled filamin *in vivo* (Carroll et al., 1982) and increased phosphorylation of filamin on serine residues has been observed after force application at cell adhesion sites by collagen-coated magnetic beads (Glogauer et al., 1998).

#### 1.2.7.2 Proteolysis

Filamins are highly susceptible to proteolysis by calpains, $Ca^{2+}$-dependent cysteine-proteases involved in cytoskeleton remodelling and motility (Potter et al., 1998; O'Connell et al., 2009). Calpain cleavage sites are located within H1 and H2 of FLNa and cleavage generates three subfragments: rod 1, rod 2 and the self-association domain (repeat 24) (Gorlin et al., 1990). Cleavage at H1 generates a 100 kD C-terminal fragment corresponding to repeats 16-24 (Loy et al., 2003). The 100 kD fragment translocates to the nucleus, in complex with the androgen receptor, a nuclear transcription factor that mediates male sexual differentiation (Wurtz et al., 1996; Loy et al., 2003). At the nucleus, the FLNa fragment competes with the coactivator TIF2 to modulate androgen receptor activity (Loy et al., 2003). Furthermore, both full-length FLNa and the 100 kD fragment have been found to colocalize with FOXC1 at the nucleus, where its transcriptional activity is impaired in a FLNa-mediated manner (Berry et al., 2005).

There is also evidence that phosphorylation of FLNa modulates its susceptibility to calpain cleavage. Phosphorylation of a conserved cAMP-dependent protein kinase consensus site on FLNa (serine 2152) renders the protein resistant to calpain cleavage at the H1 site (Chen and Stracher, 1989; Jay et al., 2000; Jay et al., 2004). FLNa can also be cleaved by granzyme B, a protease produced by cytotoxic T lymphocytes that are capable of inducing apoptosis in a caspase-dependent and caspase-independent manner (Trapani et al., 1998; Browne et al., 2000). FLNa-deficient M2 cells were significantly protected from granzyme B-mediated cell death compared to FLNa-expressing A7 cells. Therefore cleavage of FLNa by granzyme B may be partly responsible for caspase-independent cell death (Browne et al., 2000).

#### 1.2.7.3 Force-induced conformational change

X-ray crystallography of a FLNa domain containing repeats 19-21 has revealed that repeat 20 is partially unfolded, which brings repeat 21 into close proximity to repeat 19 (Lad et al., 2007). The N-terminus of repeat 20 forms a β-strand that associates with repeat 21 (Lad et al., 2007), a major binding site for the cytoplasmic tail of β-integrin (Loo et al., 1998). This β-strand sterically hinders integrin binding (Lad et al., 2007) and is removed with the application of physiologically relevant forces based on computer simulation models (Chen et al., 2009; Pentikäinen and Ylänne, 2009). Interestingly, computer simulations also showed that phosphorylation on serine 2152 decreases the force and constraints required for auto-inhibition removal of the β-strand (Chen et al., 2009). Repeat 19 also appears to be auto-inhibited by the adjacent repeat 18; therefore the auto-inhibition of ligand binding to FLNa by the preceeding even-numbered repeat may be a more general phenomenon (Lad et al., 2007).

### 1.2.8 Mouse models of FLNa-deficiency

Filamin-null mice for all three filamin isoforms have been generated to understand the molecular function and biological roles of filamins during development (Dalkilic et al., 2006; Feng et al., 2006; Hart et al., 2006; Lu et al., 2007; Zheng et al., 2007; Zhou et al., 2007; Farrington-Rock et al., 2008; Zhou et al., 2010). FLNa-deficient mice have been generated by two groups: Feng et al. (2006) created FLNa-deficient mice using a cre/loxP-mediated conditional gene knockout strategy to delete FLNa exons 3-7, producing a nonsense mutation with early FLNa truncation at amino acid 121. Hart et al. (2006) identified the X-linked, male-lethal, chemical (N-ethyl-N-nitrosurea)-induced mouse mutation *Dilp2* was caused by a T-to-A transversion mutation in the FLNa gene, leading to undetectable FLNa protein in mutant males. Heterozygous females exhibited mild skeletal abnormalities (Hart et al., 2006) and approximately 20% died in the first 3-4 months with multiple anomalies (Feng et al., 2006). FLNa-deficiency was embryonic-lethal in males and lethality resulted from incomplete septation of the heart accompanied by other cardiac, skeletal and palate defects (Hart et al., 2006). These phenotypes are similar to the clinical manifestations of the OPD spectrum of disorders that arise from missense mutations (Zhou et al., 2010). FLNa-deficient mice also displayed a disorganized vasculature and defective blood vessels, suggesting a role for FLNa in angiogenesis (Feng et al., 2006). Given that periventricular heterotopia (PH) is defined as a disorder resulting from impaired neuronal migration, various cell types were isolated from FLNa-deficient mice and examined for cytoskeletal and migratory defects. FLNa-deficient mouse embryonic fibroblasts (MEFS), neurons and vascular endothelial cells did not exhibit defects in cytoskeletal structures, F-actin distribution or migratory capacity, compared to WT (Feng et al., 2006; Hart et al., 2006). The lack of defects in cytoskeletal structures in these FLNa-deficient cells was surprising given FLNa's known role in F-actin

binding. The lack of cytoskeletal defects in FLNa-null neurons contrast previous findings that dominant expression of a FLNa variant lacking the ABD dramatically inhibits neuronal migration in rats (Nagano et al., 2004). Interestingly, the most striking cellular defects observed in FLNa-deficient vascular endothelial cells were structural defects in adherens junctions (AJ) and reduced expression of vascular endothelial (VE)-cadherin, an AJ protein (Feng et al., 2006). AJ are intercellular junctions found in epithelial and endothelial cells and are critical for regulating endothelial cell growth, contact inhibition, paracellular permeability and cell-cell adhesions (Bazzoni and Dejana, 2004; Niessen, 2007). These mouse models of FLNa-deficiency suggest FLNa has a critical role in AJ function and the motility-dependent functions of FLNa are not solely responsible for the diverse developmental abnormalities observed in patients with FLNa mutations (Feng et al., 2006; Hart et al., 2006; Zhou et al., 2010).

In other reports, FLNa-null monocytes isolated from FLNa-null mice had motility defects that were rescued by constitutively active Rac1 and Cdc42 (Leung et al., 2009). Furthermore, MEFs isolated from FLNb-null mice displayed impaired migration associated with reduced RhoA activity (Zhou et al., 2007). Overall, these mouse models indicate FLNa's role as a scaffolding protein, in particular for small GTPases, has critical involvement in organ development and cell locomotion (Zhou et al., 2010).

## 1.3 CELL CYCLE

### 1.3.1 Stages of cell cycle

In embryos there are only two stages to the cell cycle, M-phase (mitosis) and S-phase (DNA synthesis), and a full cell cycle takes only 30 minutes to complete (Massague, 2004). In adult tissues, the cell cycle includes a gap period (G1), which is controlled by metabolic, stress and environmental cues that either signal entry into S-phase or a quiescent state (Figure 1.10) (Massague, 2004). At this stage cells have multiple fates: they can undergo self-renewal, differentiation or apoptosis. The signals for these events come from neighbouring cells, the circulatory system or the cell itself (Massague, 2004). During S-phase, DNA replication occurs. Another gap phase (G2) follows S-phase and is devoted to correcting replication errors that may have occurred during DNA replication (Figure 1.10) (Massague, 2004). Interphase comprises G1, S and G2 phase. The final stage of the cell cycle is M-phase, which comprises mitosis and cytokinesis (Figure 1.10) (Nigg, 2001; Massague, 2004) and is visually the most striking stage of the cell cycle.

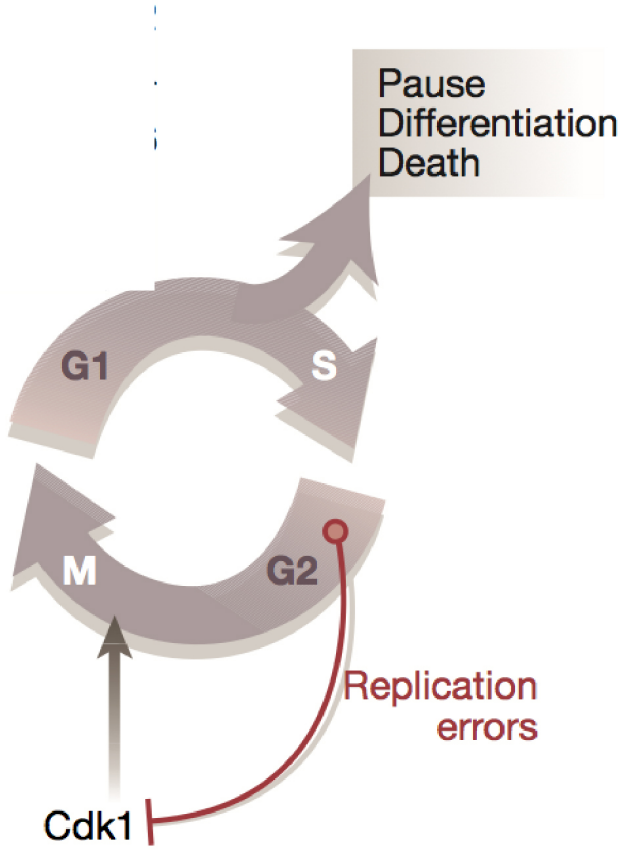
Pause
Differentiation
Death
G1
S
M
G2
Replication
errors
Cdk1

**Figure 1.10. Cell cycle and assignment of Cdk activity to particular cell transitions.** The cell cycle includes a gap period (G1 phase) during which the activity of various Cdks is controlled by positive (growth, survival and mitogenic) and negative (apoptotic and cytostatic; genotoxic, metabolic, oncogenic and oxidative stress) signals. During S-phase DNA replication occurs. Another gap period (G2 phase) is devoted to mending replication errors, which if present, inhibit Cdk1 and thus mitotic entry. Figure adapted from (Massague, 2004)**.** *See Appendix, Copyright Permissions for license to republish figure.*

### 1.3.2 Mitosis

The main purpose of mitosis is to segregate sister chromatids into two daughter cells and divide the cytoplasm. This is primarily accomplished by the assembly of the mitotic spindle, a dynamic bipolar array of microtubules that forms during mitosis to move sister chromatids apart (Nigg, 2001). There are five distinct stages in mitosis: prophase, prometaphase, metaphase, anaphase and telophase (Figure 1.11) (Nigg, 2001; O'Connor, 2008). During prophase, chromatin begins to condense into chromosomes and this continues until metaphase. Meanwhile, nuclear envelope breakdown (NEBD) allows cytoplasmic centrosomes access to the nucleus where they begin to nucleate microtubules. In prometaphase, microtubules are captured by kinetochores, specialized proteinaceous structures that associate with centromeric DNA. Metaphase is characterized by the alignment of chromosomes at the "metaphase plate". When all the chromosomes establish bipolar attachment, the anaphase-promoting complex (APC), an E3 ubiquitin ligase, targets securin (Pds1 in budding yeast) for proteasomal degradation (Manchado et al., 2010). Securin degradation activates separase (Esp1 in budding yeast), the protease that triggers sister chromatid separation through the cleavage of cohesion (Manchado et al., 2010). This sudden loss of sister chromatid cohesion triggers anaphase and sister chromatids are pulled towards the poles. This pulling force is mediated by both the shortening of kinetochore microtubules (anaphase A) and the separation of spindle poles as they move toward the cortex (anaphase B). Telophase marks the end of mitosis when sister chromatids reach the poles. At this stage, chromosomes begin to decondense and the nuclear membrane reassembles. The final step, cytokinesis, is mediated by the formation of an actomyosin-based contractile ring which "pinches off" the membrane to generate two daughter cells (Nigg, 2001; O'Connor, 2008).

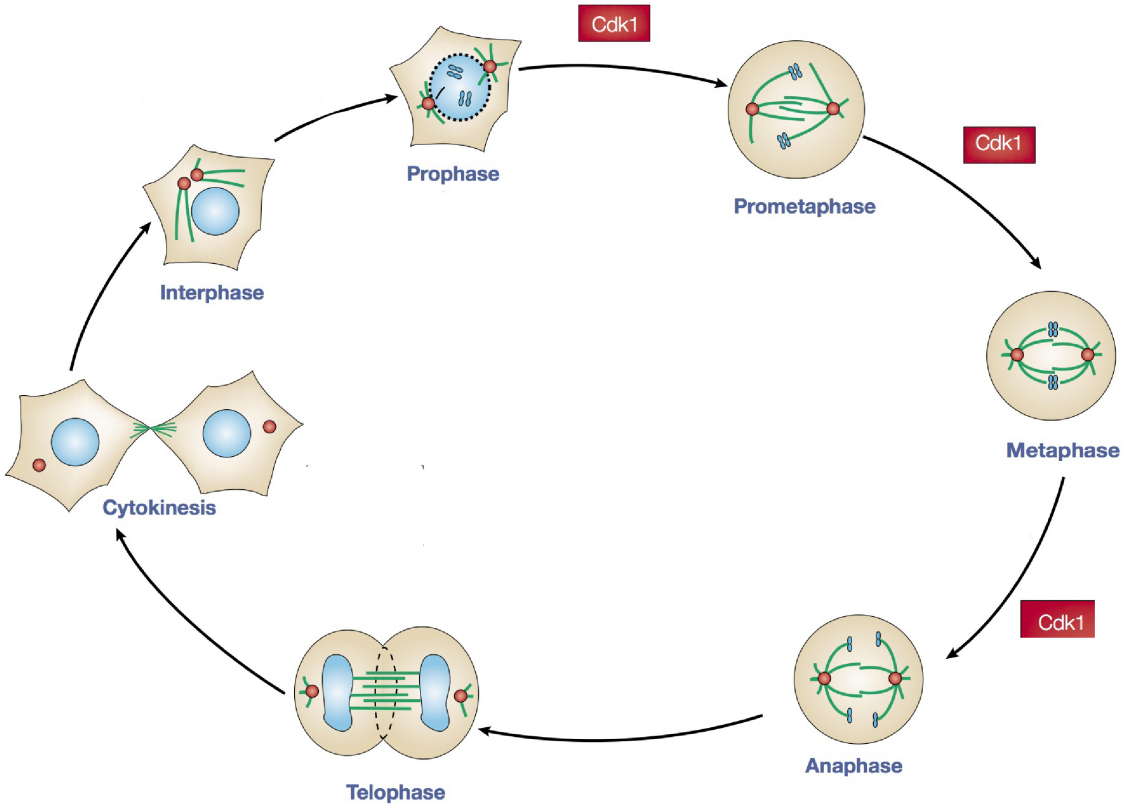
Cdk1
Prophase
Prometaphase
Cdk1
Metaphase
Cdk1
Anaphase
Telophase
Cytokinesis
Interphase

**Figure 1.11. Stages of mitosis.** ***Prophase:*** chromosome condensation and nuclear envelope breakdown occur. ***Prometaphase:*** microtubules are captured by kinetochores. ***Metaphase:*** chromosomes align at the "metaphase plate". ***Anaphase:*** a loss of sister chromatid cohesion allows sister chromatids to be pulled towards the poles. This is mediated by both the shortening of kinetochore microtubules (anaphase A) and the separation of spindle poles as they move toward the cortex (anaphase B). ***Telophase:*** sister chromatids reach the poles, chromosomes begin to decondense and the nuclear membrane reassembles. ***Cytokinesis:*** formation of an actomyosin-based contractile ring "pinches off" the membrane to generate two daughter cells. Legend: Blue: nucleus, chromatin and chromosomes; Green: microtubules; Red: centrosome, mitotic spindle. Figure adapted from (Nigg, 2001). *See Appendix, Copyright Permissions for license to republish figure.*

### 1.3.3 Cyclin-dependent kinases

The orderly progression from one cell cycle stage to another is mediated by timed activation of distinct Cdks and their binding to regulatory proteins called cyclins (Smits and Medema, 2001). The progressive accumulation of cyclins A and B during the cell cycle and their abrupt degradation at the onset of anaphase, mediates entry and exit from mitosis, respectively. During G1 in higher eukaryotes, Cdk2 combines with cyclin E and cyclin A (Morgan, 1997; Murray, 2004). When Cdk2 is activated, pre-replicative complexes (PRCs) recruit DNA helicase, primases and polymerases to DNA to begin unwinding and synthesizing new DNA during S-phase (Kelly and Brown, 2000; Prasanth et al., 2004). However, Cdk2 substrates that directly trigger DNA replication are still unknown (Massague, 2004). Mitosis cannot proceed until DNA replication is complete. Conversely, newly replicated origins cannot assemble new PRCs until the end of mitosis. These events ensure that DNA replication occurs only once per cell cycle (Kelly and Brown, 2000; Prasanth et al., 2004). Entry into mitosis is controlled by the B-type cyclins, which accumulate prior to mitotic onset and associate with the mitotic kinase Cdk1 (Nigg, 1995; Pines, 1995). The activation of Cdk1/cyclin B1 leads to the phosphorylation of multiple substrates involved in mitotic progression.

### 1.3.4 Regulation of Cdk1

#### 1.3.4.1 Cyclin B1

Activation of Cdk1 requires binding to its regulatory subunit, cyclin B1 (Clb1 and Clb2 in budding yeast, cdc13 in fission yeast). Cdk1 levels are generally abundant throughout the cell cycle; therefore their activity is primarily regulated by the timed synthesis and destruction of cyclin B1 (Smits and Medema, 2001). In human cells, B-type cyclins are

actively transcribed at the end of S-phase and accumulate in mitosis (Pines and Hunter, 1989; Piaggio et al., 1995). Cyclin B1 localizes in the cytoplasm during S-phase and G2-phase and is translocated to the nucleus at the beginning of mitosis (Pines and Hunter, 1991). The cytoplasmic retention signal (CRS) of cyclin B1 is inactivated by phosphorylation at the beginning of mitosis to allow nuclear import (Li et al., 1995). Nuclear export of cyclin B1 is mediated by a nuclear export signal (NES) within the cytoplasmic retention signal (CRS), which is blocked by leptomycin B, an inhibitor of the nuclear export factor exportin 1 (Hagting et al., 1998; Toyoshima et al., 1998). Interestingly, phosphorylation of cyclin B1 to promote nuclear import also functions to inhibit nuclear export (Hagting et al., 1998). How cyclin B1 gets imported into the nucleus is unclear, as it does not contain a classical nuclear localization signal (NLS) whose function is well characterized (Moore et al., 1999).

In anaphase, cyclin B1 degradation is mediated by the APC, which is activated at the metaphase to anaphase transition (Glotzer et al., 1991; Clute and Pines, 1999; Manchado et al., 2010).

#### 1.3.4.2 Phosphorylation

During G2-phase, Cdk1 (Cdc28 in budding yeast, cdc2 in fission yeast) is phosphorylated on tyrosine 15 and threonine 14, two inhibitory residues located within the ATP-binding site (Nigg, 2001). Phosphorylation of tyrosine 15 in cdc2 (fission yeast) interferes with the transfer of phosphate to the substrate (Atherton-Fessler et al., 1993). Threonine 14 phosphorylation inhibits ATP binding (Endicott et al., 1994). Phosphorylation on these sites is mediated by Wee1 kinase (Swe1 in budding yeast) and function to delay mitotic entry until proper growth conditions are met in G2 (Nigg, 1995; Harvey et al., 2005). At the G2/M transition, Cdk1/cyclin B1 activation occurs with the dephosphorylation of these inhibitory

residues on Cdk1 by Cdc25 phosphatase (Mih1 in budding yeast, also Cdc25 in fission yeast), followed by the translocation of the Cdk1/cyclin B1 complex into the nucleus (Morgan, 1995; Nigg, 2001; Smits and Medema, 2001; Rupeš, 2002; Harvey and Kellogg, 2003; Harvey et al., 2005). In the nucleus, phosphorylation of threonine 161 by a cdk-activating kinase (CAK) is absolutely required for Cdk1 activity. This residue is located within a T-loop domain that controls the access of substrate to the catalytic site (Morgan and De Bondt, 1994; Nigg, 1995). The phosphorylation status of threonine 161 parallels that of cyclin B1 binding (Smits and Medema, 2001).

### 1.3.5 Cdk1/cyclin B1 substrates

Active Cdk1/cyclin B1 phosphorylates many proteins including those involved in centrosome separation, microtubule dynamics, NEBD, chromosome condensation, and actin cytoskeleton rearrangement (Nigg, 2001).

#### 1.3.5.1 Spindle assembly and centrosome separation

Human Eg5, a kinesin-related motor protein required for centrosome migration and spindle morphogenesis *in vivo*, is a likely Cdk1 substrate. Phosphorylation of Eg5 on serine/threonine residues is strongly increased in mitosis compared to S-phase (Blangy et al., 1995). Furthermore, Eg5 can be phosphorylated *in vitro* by recombinant Cdk1/cyclin B1. Expression of nonphosphorylatable Eg5 in HeLa cells abolishes its ability to associate with the spindle apparatus and microinjection of Eg5+ antibodies leads to mitotic arrest and defects in centrosome migration. These results suggest Eg5 is required for centrosome separation and subsequent bipolar spindle formation (Blangy et al., 1995).

#### 1.3.5.2 Microtubule dynamics

Microtubules are non-covalent cytoskeletal polymers that undergo cycles of rapid growth and disassembly, a phenomenon known as dynamic instability, a property that allows microtubules to probe the intercellular environment for interacting partners (Burbank and Mitchison, 2006; Wojnacki et al., 2014). Dynamic microtubules are short-lived and have half-lives ranging between 5-10 minutes, whereas a small subset of microtubules have half-lives of up to 20 hours (Wojnacki et al., 2014). Microtubule dynamics are regulated by microtubule-associated proteins and microtubule-destabilizing proteins (Nigg, 2001). Stathmin (oncoprotein 18) is an example of a microtubule-destabilizing protein that is also a Cdk1 substrate *in vivo*. Phosphorylation by Cdk1 and an unidentified kinase downregulates its microtubule-destabilizing activity during mitosis (Larsson et al., 1997). However, the dynamics of microtubules in mitotic cells is about 10-fold more rapid than in interphase cells; this is due to an increase in the frequency of catastrophes, the sudden switch of a growing microtubule into a rapidly shortening state (Belmont et al., 1990; Gardner et al., 2013). This observation is inconsistent with the observation that mitotic phosphorylation of stathmin inhibits its microtubule-destabilizing activity. This suggests the primary physiological function of stathmin might be to regulate microtubule dynamics in interphase rather than in mitosis. Therefore, in mitosis, interphase microtubule activities mediated by stathmin would need to be turned off in order for mitotic microtubule dynamics to occur (Larsson et al., 1997).

#### 1.3.5.3 Nuclear envelope breakdown

The nuclear envelope is stabilized by nuclear lamina, an intermediate filament-type network underlying the inner nuclear membrane (Peter et al., 1990; Nigg, 2001). Peter et al. (1990)

showed that the nuclear lamina is disassembled at the onset of mitosis due to lamin hyperphosphorylation. Cdc2 kinase (budding yeast Cdk1 homolog) can phosphorylate chicken lamins *in vitro* on sites that are phosphorylated during mitosis *in vivo*. Lamina disassembly reduces nuclear envelope stability but is not in itself sufficient to cause NEBD, suggesting the involvement of additional Cdk1 targets in NEBD (Nigg 2001).

#### 1.3.5.4 Chromosome condensation

Chromosome condensation occurs from prophase to metaphase and is accompanied by extensive phosphorylation of both histones and non-histone proteins. However, it is still unknown how this process is regulated as few nucleosome proteins have been identified as *in vivo* Cdk1 substrates. The linker histone H1 is a well-known Cdk1 substrate and is the quintessential substrate used to measure Cdk1 activity *in vitro*. Ironically, the functional significance of H1 phosphorylation *in vivo* is still largely unknown (Nigg, 2001).

#### 1.3.5.5 Actin cytoskeleton rearrangement

Non-muscle caldesmon is an actin and calmodulin-binding protein that decreases cell contractility through inhibition of actomyosin ATPase (Helfman et al., 1999) and is involved in the control of cell motility (Bretscher, 1986; Horiuchi et al., 1986). Furthermore, caldesmon, coupled with tropomyosin, can inhibit both severing and capping activities of the ABP gelsolin (Ishikawa et al., 1989b, a); therefore caldesmon appears to play a role in the stabilization of actin filaments (Yamashiro and Matsumura, 1991). A series of reports from a group led by Matsumura in the early 1990s suggest Cdk1-phosphorylation of caldesmon causes mitotic actin filament reorganization during mitosis (Yamashiro et al., 1990; Yamashiro and Matsumura, 1991; Yamashiro et al., 1991; Hosoya et al., 1993; Yamashiro et al., 1994; Yamashiro et al., 2001). Antibody-induced aggregation of "intact" actin filaments

from mitotic and non-mitotic rat fibroblast cells showed almost a complete absence of caldesmon from mitotic actin filament aggregates compared to non-mitotic aggregates (Yamashiro et al., 1990). This correlated with an increase in caldesmon phosphorylation in mitotic cells (Yamashiro et al., 1990) and the kinase was later identified to be Cdk1 (Yamashiro et al., 1991). Therefore, mitotic phosphorylation of caldesmon may weaken its interaction with F-actin and contribute to the reorganization of actin filaments during mitotic cell rounding (Yamashiro and Matsumura, 1991; Yamashiro et al., 1994).

### 1.3.6 Cytokinesis

Cytokinesis occurs after the completion of mitosis and is the physical partition of one cell into two daughter cells. In eukaryotic cells, cytokinesis involves positioning and assembly of an actomyosin contractile ring at the equatorial cortex of the cell, activation of the actomyosin contractile ring to drive furrow ingression, membrane deposition at the cleavage furrow to close the junction between daughter cells (Li, 2007) and finally abscission of the midbody connecting the two daughter cells (Agromayor and Martin-Serrano, 2013). Cytokinesis is complex and more than 100 regulatory proteins (Pollard, 2010) were identified in genome-wide localization studies in budding yeast (Huh et al., 2003) as well as high-throughput RNAi screens in *C. elegans*, *Drosophila* and mammalian cells (Echard et al., 2004; Eggert et al., 2004; Skop et al., 2004; Sonnichsen et al., 2005; Zhu et al., 2005).

Assembly of the contractile ring depends on the accumulation and activation of the Rho GTPase RhoA (the main Rho isoform in mammalian cells) around the equatorial cortex, the future site of the cleavage furrow (Figure 1.12) (Li, 2007). This process is called cleavage plane specification (Glotzer, 2009). RhoA is localized and activated to RhoA-GTP at the equatorial region by Ect2 (epithelial cell transforming 2)/pebble, a Rho GEF (Yüce et

al., 2005; Kamijo et al., 2006; Nishimura and Yonemura, 2006; Birkenfeld et al., 2007). Ect2 is found in a complex with the Rho GAP MgcRacGAP (Cyk-4) and the kinesin MKLP1/ZEN-4, a microtubule plus end-directed motor protein. This complex is called the 'central spindlin complex' and the recruitment of additional proteins forms the central spindle (Piekny et al., 2005; Glotzer, 2009). MgcRacGAP, when phosphorylated by Aurora B in mitosis, can also activate RhoA (Minoshima et al., 2003). The presence of kinesin in this complex raises the possibility that microtubules can direct RhoA activation through kinesin-mediated transport of the central spindle complex to the equatorial region where RhoA is concentrated (Somers and Saint, 2003).

Two downstream effectors of RhoA are Rho-activated kinase (ROCK) and mDia2, a member of the formin family of F-actin nucleating proteins (Zigmond, 2004; Matsumura, 2005; Piekny et al., 2005). mDia2 activation by RhoA leads to the *de novo* nucleation of actin filaments that form the contractile ring (Pelham and Chang, 2002; Tolliday et al., 2002; Großhans et al., 2005). However, it has also been proposed that recruitment of existing actin filaments through cortical flow may also contribute to contractile ring formation (Cao and Wang, 1990; Murthy and Wadsworth, 2005). The lost of cortical actin is possibly replaced by bleb-induced cortical actin formation at the cell poles (Charras, 2008). Formins are also likely involved in anchoring actin filaments to the plasma membrane (Pollard, 2010). RhoA-mediated activation of ROCK leads to the activation of non-muscle myosin II through ROCK phosphorylation of the myosin II regulatory light chain (Kimura et al., 1996; Totsukawa et al., 2000). Together, the nucleation of F-actin and activation of myosin II form the basis of actomyosin contractile ring formation (Figure 1.12) (Li, 2007).

Once the contractile ring is assembled, furrow ingression is mediated by constriction and disassembly of the contractile ring; however, little is known about the mechanisms that coordinate these events (Pollard, 2010). The simplest model is that bipolar myosin II filaments generate force by sliding actin filaments that are attached to the cortex (Schroeder, 1990). A finding that mDia2 is degraded by proteasomes at the conclusion of mitosis may shed light on the mechanism of contractile ring disassembly (DeWard and Alberts, 2009).

As furrow ingression progresses, new plasma membrane is formed at the cleavage furrow in animal cells (Li, 2007). Endocytosis, exocytosis and membrane fusion are required for membrane deposition, but the mechanism is unknown (Figure 1.12) (Finger and White, 2002; Gromley et al., 2005; Matheson et al., 2005; Baluška et al., 2006; Li, 2007). After completion of furrowing, the daughter cells remain connected by an intracellular bridge or midbody, a remnant of the central spindle (Schiel and Prekeris, 2010). The severing of the midbody is called abscission and marks the final step of cytokinesis.

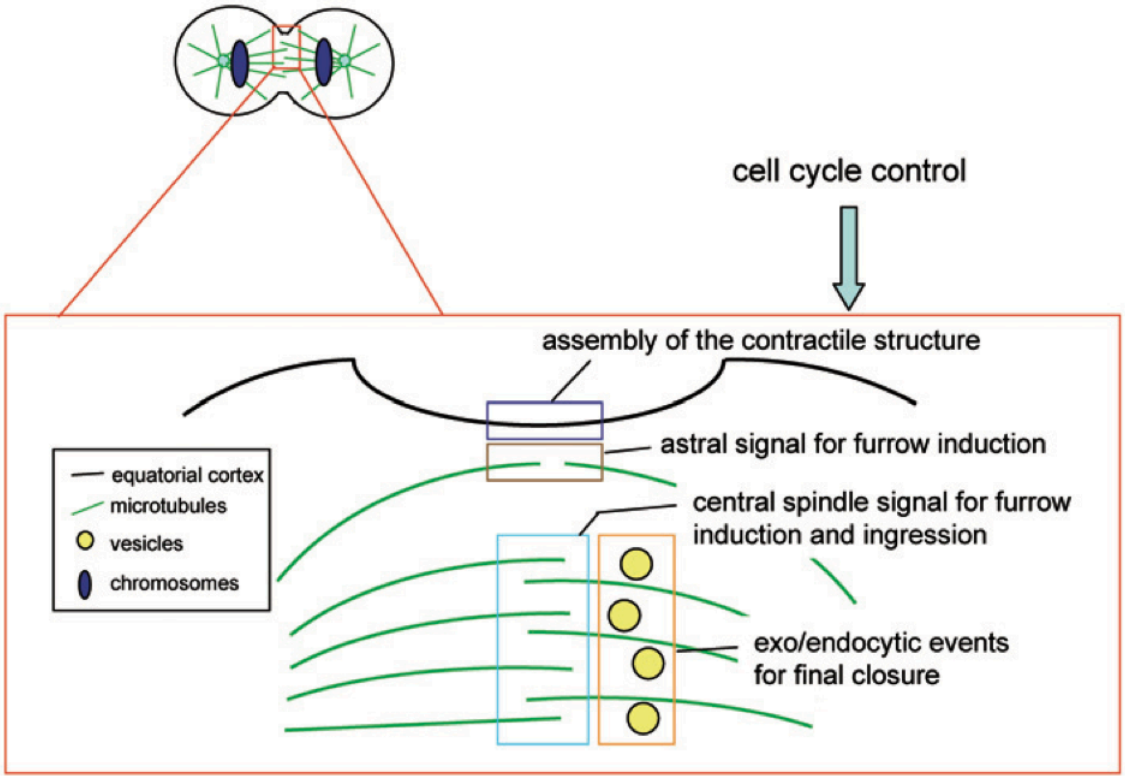
cell cycle control
assembly of the contractile structure
astral signal for furrow induction
central spindle signal for furrow induction and ingression
exo/endocytic events for final closure
equatorial cortex
microtubules
vesicles
chromosomes

**Figure 1.12. Key events in animal cell cytokinesis.** Cytokinesis requires highly coordinated events at the equatorial region of the cell (red box), including spatial positioning of the cleavage furrow by astral microtubules (brown box) and central spindle (light blue box) associated complexes, assembly and activation of the actomysoin contractile ring (dark blue box) to drive furrow ingression, and targeted exocytosis and endocytosis (orange box) to deposit membrane and complete final closure. Many of these events are directly controlled by cell cycle regulators to ensure temporal coordination with chromosome segregation. Figure from (Li, 2007). *See Appendix, Copyright Permissions for license to republish figure.*

### 1.3.7 Actin cytoskeleton and mitotic cell rounding

Mitotic cell rounding is the process in which a flat interphase cell undergoes cell shape changes to become more spherical in mitosis (Maddox and Burridge, 2003). This process is accompanied by increased cortical actin rigidity (Mitchison and Swann, 1955; Yoneda and Dan, 1972; Matzke et al., 2001), de-adhesion from substrate (Sanger et al., 1987; Hock et al., 1989; Burton and Taylor, 1997; Yamakita et al., 1999) and actin cytoskeleton rearrangement (Cortese et al., 1989; Cramer and Mitchison, 1997); however, little is known regarding the mechanism surrounding mitotic cell rounding (Maddox and Burridge, 2003).

Evidence that actin structures can affect cell morphology during mitosis came from a study of moesin, a member of the ezrin/radixin/moesin (ERM) family of ABPs which, when activated, crosslink actin filaments to the cytoplasmic tails of plasma membrane proteins in a signal-dependent manner and participate in the regulation of cortical cohesion in interphase (Bretscher et al., 2002; Polesello et al., 2002; Carreno et al., 2008). Recently, a role for moesin phosphorylation in mitotic cell rounding has emerged (Carreno et al., 2008; Kunda et al., 2008). In *Drosophila* S2 cells, mitotic onset is characterized by activation of moesin through Slik (Ste20-like protein kinase) phosphorylation. Phosphorylated moesin localizes at the cortex in prometaphase and becomes increasingly concentrated at the equator as mitosis progresses (Carreno et al., 2008). Inhibition of moesin phosphorylation and moesin knockdown results in severe cortical deformations, impaired microtubule organization, and defects in mitotic spindle positioning (Carreno et al., 2008). Moesin appears to function independently of myosin II because cells expressing phospho-mimetic moesin, but lacking myosin light chain, are still able to undergo mitotic cell rounding with a corresponding increase in cortical actin rigidity (Kunda et al., 2008). However, the activities of both moesin

and myosin are likely required to establish the rounded cell shape and cortical rigidity that is required for subsequent spindle assembly and positioning (Heng and Koh, 2010).

### 1.3.8 Actin-regulated cell cycle checkpoints

The significance of the actin cytoskeleton in cell cycle progression and checkpoint control is evident from experiments that use drugs or chemicals to interfere with actin polymerization. In *Saccharomyces cerevisiae*, a morphogenesis checkpoint monitors actin organization and triggers a G2 arrest in response to actin perturbation by latrunculin A (McMillan et al., 1998). However, the ability of cells to undergo G2 arrest in response to latrunculin A is limited to a critical early phase of bud formation, when the checkpoint effector Swe1p, a Cdc28 kinase, is most abundant (McMillan et al., 1998; McMillan et al., 2002; Lew, 2003).

A spindle orientation checkpoint (SOC) in fission yeast monitors the integrity of the actin cytoskeleton and delays sister chromatid separation, spindle elongation and cytokinesis until spindle poles are properly oriented (Gachet et al., 2001). This mitotic delay was observed in cells treated with actin depolymerizing drugs latrunculin A/B and cytochalasin D, and in the temperature-sensitive actin mutant *cps8* (Ishiguro and Kobayashi, 1996; Gachet et al., 2001). Mechanistically, activation of the SOC likely involves disruption of the interaction between astral microtubules and cortical actin filaments, which is critical for proper mitotic spindle orientation (Segal and Bloom, 2001; Gadde and Heald, 2004; Lee and Song, 2007).

Although similar actin-regulated checkpoints have not been established in mammalian cells (Heng and Koh, 2010), disruption of the actin cytoskeleton via actin or myosin inhibitors has been reported to delay progression of mitosis in primary and non-

transformed mammalian cells, suggesting the presence of an actin checkpoint at the G2/M transition (Gachet et al., 2001; Lee and Song, 2007).

Apart from causing a delay in mitosis, disruption of actin filaments also leads to G1 arrest (Reshetnikova et al., 2000). In a study in which disruption of the actin cytoskeleton was induced by the over-expression of cofilin, an actin-depolymerizing protein, more than 90% of H1299 lung carcinoma cells arrested at G1 (Lee and Keng, 2005). Conversely, excessive F-actin polymerization by expression of a mutant WASP (Wiskott-Aldrich Syndrome protein) or treatment with the drug jasplakinolide, which interferes with F-actin depolymerization, caused an increase in multinucleated cells, suggesting a possible defect in cytokinesis (Moulding et al., 2007). These observations demonstrate actin's involvement in cell cycle progression and checkpoint control.

## OBJECTIVES

We hypothesize that *in vivo* phosphorylation of FLNa by Cdk1/cyclin causes FLNa dissociation from actin filaments to facilitate mitotic actin remodelling. Having already established that FLNa is phosphorylated by Cdk1/cyclin B1 *in vitro* (Cukier et al., 2007), **my first objective was to determine whether or not FLNa is phosphorylated *in vivo* by Cdk1/cyclin B1 and my second objective was to identify *in vivo* FLNa phosphorylation sites by quantitative mass spectrometry.** These two objectives are the focus of Chapter 3. **My third objective is to determine the functional relevance of FLNa phosphorylation by Cdk1/cyclin B1.** The third objective is the focus of Chapter 4.

# CHAPTER 2 MATERIALS AND METHODS

## 2.1 CELL CULTURE, DRUG TREATMENTS AND TRANSFECTION

HeLa cells (CCL-2, ATCC, Manassas, VA) were maintained in Dulbecco's Modified Eagle Medium (DMEM) (Invitrogen Life Technologies, Burlington, ON) supplemented with 10% fetal bovine serum (FBS) (Invitrogen). M2 cells were a gift from Thomas P. Stossel (Brigham and Women's Hospital, Harvard Medical School, Boston, MA) (Cunningham et al., 1992). M2 cells were maintained in Minimum Essential Medium (MEM) (Invitrogen) supplemented with 10% FBS (Invitrogen), 1% sodium pyruvate (Invitrogen) and 10 mM HEPES, pH 7.0. All cell lines were maintained in a humidified incubator at 37°C and 5% $CO_2$. HeLa and M2 cells were treated with 100 ng/mL nocodazole for 14-18 h for mitotic arrest. Flow cytometry was used to verify the arrest of HeLa cells in G2 phase (Figure 2.1). Mitotic cells were selectively harvested using the mitotic shake-off method (Terasima and Tolmach, 1963). To release cells from mitotic arrest, cells were gently washed with phosphate buffered saline (PBS) followed by the addition of fresh media with 1 μM okadaic acid or dimethyl sulfoxide (DMSO). M2 and HeLa cells were transfected using Lipofectamine LTX and PLUS reagents (Invitrogen) in a 6-well format according to manufacturer's instructions. M2 colonies were picked and maintained in MEM complete media containing 0.5 mg/mL G418 (Sigma-Aldrich, Saint Louis, MO) to generate monoclonal stable cell lines.

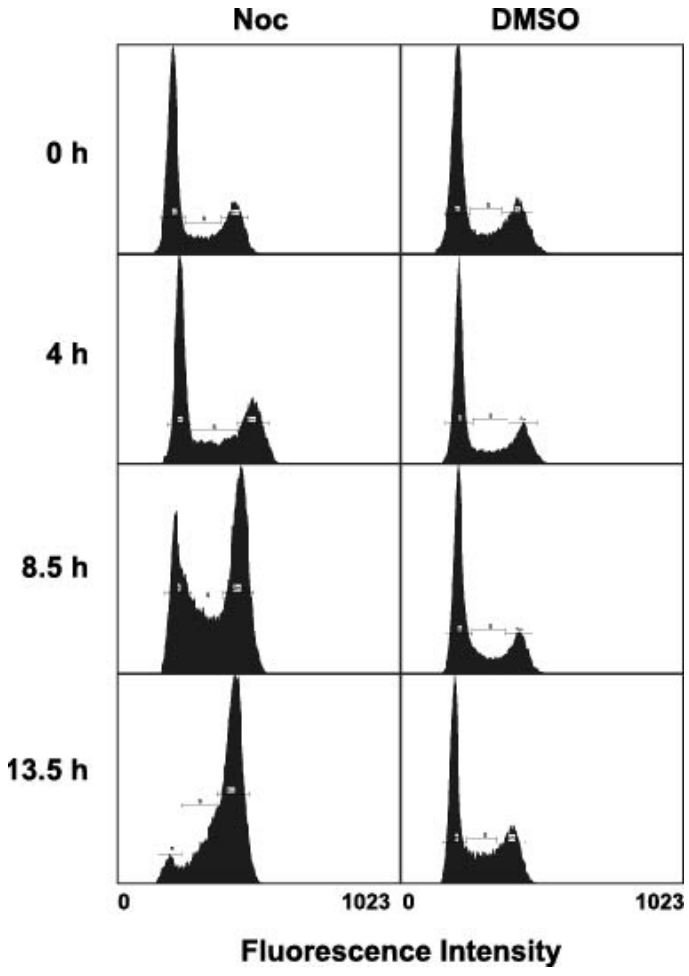
Noc
DMSO
0 h
4 h
8.5 h
13.5 h
0
1023
0
1023
Fluorescence Intensity

**Figure 2.1. Nocodazole arrests HeLa cells in mitosis.** Nocodazole (100 ng/mL) shifts HeLa cells from having a mainly 2n DNA content to a 4n DNA content. Cells were treated with DMSO as a control. Fixed cells were treated with 10 μg/mL propidium iodide and 0.25 mg/mL RNase A and analyzed by flow cytometry.

## 2.2 FLOW CYTOMETRY

HeLa cells were grown in 10 cm plates and treated with nocodazole as described above. Cells were harvested and washed with PBS. For fixation, cells were resuspended in 300 µL PBS and then 700 µL of 100% ethanol was added dropwise. The cells were inverted 3x and then rotated end-over-end at 4°C for 30 min. Cells were stored at -20°C until all time points were prepared and ready to be analyzed. Prior to flow cytometry, cells were centrifuged at 2,000 rpm and washed 2x with 1 mL PBS. The cell pellet was re-suspended in 500 µL PBS containing 0.25 mg/mL RNase A (Invitrogen) and incubated at room temperature (RT) for 1 h. Propidium iodide (Sigma-Aldrich) was added to a final concentration of 10 µg/mL. Samples were analyzed on a Cytomics FC 500 flow cytometer (Beckman Coulter, Mississauga, ON) with CXP software.

## 2.3 PLASMIDS, SITE-DIRECTED MUTAGENESIS AND CLONING

pcDNA3-EGFP vector containing full-length WT FLNa or FLNa lacking the actin-binding domain (ABD) (FLNa ΔABD) with a C-terminal GFP tag was a gift from David A. Calderwood (Department of Pharmacology, Yale University School of Medicine, New Haven, CT) (Lad et al., 2007). S1084A, S1459A and S1533A mutations were introduced using a Stratagene QuikChange Lightning Multi Site-Directed Mutagenesis kit (Agilent Technologies, La Jolla, CA) according to manufacturer's instructions. The following forward mutagenic primers were used:

**S1084A:** G CAG GGA GGC AGT ***GCC*** GGC **GCC** CCC GC
**S1459A:** GGG CCC GGC CTG **GCC** CCA GGC ATG GT
**S1533A:** GAA GAG GTA CCC CGG **GCC** CCC TTC AAG GTC AAG

The alanine codon is underlined and in bold; a GCC (bold and italics) silent mutation was introduced into the S1084A mutagenic primer to incorporate a Cfr10l restriction site for diagnostic purposes. pET-His-FLNa, referred to as recombinant His-FLNa throughout this thesis (see Figure 3.1A in Chapter 3 for schematic,) was a gift from Fumihiko Nakamura (Brigham and Women's Hospital, Harvard Medical School, Boston, MA). It consists of the ABD, followed by FLNa repeats 8-15, followed by Hinge 2 and R24 (+ABD, IgFLNa8-15, +R24) (Nakamura et al., 2007). The ABD and R24 were deleted using a homologous recombination strategy (Hansson et al., 2008). The following forward and reverse primers were used to delete R24 and ABD:

**R24** *FOR:* GTG ACG GCT CCC TGA GCG GCC GCA CTC GAG
*REV:* C TCA GGG AGC CGT CAC TTG GAA GGG GCT GTT G

**ABD** *FOR:* GAA TTC CTG GAC CTC AGC AAG ATC AAG GTG
*REV:* GAG GTC CAG GAA TTC CGG ATC CAT GGC G

The underlined regions for each primer pair are homologous. Note that FLNa Hinge 2 (as shown in Figure 3.1A) was also deleted along with R24. All plasmids were sequenced using capillary-based Sanger DNA sequencing (StemCore Laboratories, The Sprott Centre for Stem Cell Research, Ottawa Hospital Research Institute, Ottawa, ON).

## 2.4 Preparation of lysate, SDS-PAGE and Western blot

Cells were lysed in 10 volumes lysis buffer A (50 mM Tris pH 7.4, 5 mM EDTA, 150 mM NaCl, 1% NP-40) containing Complete Protease Inhibitor (Roche Diagnostics Canada, Laval, QC), PhosSTOP Phosphatase Inhibitor (Roche), 1 mM phenylmethanesulfonylfluoride (PMSF), 1 μM aprotinin and 10 μM calpain inhibitor for 30 min on ice and then centrifuged at 14,000 rpm for 15 min. Soluble protein concentrations were determined using bovine serum albumin (BSA) standards and Bio-Rad Protein Assay

Dye Reagent (BioRad, Mississauga, ON) according to the Bradford method (Bradford, 1976). Samples were treated with 4x sample buffer (500 mM Tris-HCl, pH 6.8, 20% glycerol, 1% sodium dodecyl sulfate (SDS), 0.03% bromophenol blue, 1 mM dithiothreitol (DTT), 8 M urea, 0.71 M β-mercaptoethanol) and incubated for 30 min at 42°C. Proteins were separated by SDS-PAGE and transferred to polyvinylidene fluoride (PVDF) membranes using a Bio-Rad semi-dry transfer apparatus. Blots were blocked with 5% skim milk in Tris-buffered saline (TBS, 20 mM Tris pH 7.5, 150 mM NaCl) with 0.1% Tween-20 (TBS-T). Primary and secondary antibodies were diluted in TBS-T and incubated for 1 h at RT. Blots were washed 3x for 10 min with TBS-T between steps. Immunoreactive bands were detected using Immobilon Western Chemiluminescence reagents (HRP Substrate peroxide solution and HRP substrate-Luminol reagent) (EMD Millipore, Billerica, MA) and exposed to X-ray film or imaged on a GE Image Quant LAS4010 imaging system (GE Healthcare Life Sciences). Densitometry of Western blot bands were performed using ImageJ (1.43u and 1.47v).

## 2.5 ANTIBODIES

Commercial antibodies used for Western blots were mouse α-FLNa, MAB1678, clone PM6/317 (Chemicon, Temecula, CA: 1:10 000 dilution), rabbit α-C-terminal FLNa, clone ab76289 **(**Abcam: 1:300 000), mouse α-cyclin B1, Ab-3, clone GNS1 (Thermo Fisher Scientific: 1:10 000 dilution), rabbit α-cyclin B1, H-20 (Santa Cruz Biotechnology, Santa Cruz, CA: 1:10 000 dilution), rabbit α-pan-actin, 4968 (Cell Signaling Technology: 1:1000), mouse α-β-actin (Sigma-Aldrich: 1:10 000 dilution), rabbit α-GFP N-terminal (Sigma-Aldrich: 1:5 000 dilution), α-mouse-HRP (Cell Signaling Technology, Beverly, MA: 1:20 000 dilution) and α-rabbit HRP (Cell Signaling Technology: 1:5 000 dilution). For the

generation of rabbit p-FLNa antibody, rabbits were injected with HQVPG-pS-PFKVPVHDVTDASKVKC peptide (containing S1436) (Princeton BioMolecules, Langhorne, PA) derived from amino acids 1431-1453 of human FLNa (Uniprot P21333). Immunization of rabbits and production of antisera was performed by Covance (Princeton, NJ). The p-FLNa antibody was used at a dilution of 1:100 000.

Commercial primary antibodies used for the verification of mass spectrometry co-immunoprecipitation (Co-IP) results were α-gelsolin, Ab2966 (Millipore: 1:1 000), α-14-3-3τ, Ab9744 (Millipore, 1:3000), α-14-3-3γ, 05-639 (Upstate Biotechnology, 1:1 500), α-14-3-3ε, Ab9732 (Millipore, 1:15 00), α-14-3-3 ζ, Ab 9746 (Millipore, 1:1 500), and α-P16, 04-239 (Millipore, 1:250).

## 2.6 His-FLNa expression and purification

FLNa constructs in a pET23 vector with N-terminal His tag (ABD-IgFLNa8-15+24, IgFLNa8-15+24, ABD-IgFLNa8-15, IgFLNa8-15 WT and IgFLNa8-15 AAA) were transformed into One Shot BL21 (DE3) chemically competent *E. coli* (Life Technologies, Burlington, ON) for protein expression. Induction with isopropyl β-D-1-thiogalactopyranoside (IPTG) was found to be unnecessary for protein expression. 250 mL Luria-Bertani (LB) media with 100 μg/μL ampicillin was directly inoculated with cells from a fresh transformation plate and grown at 37°C and 225 rpm until the $OD_{600}$ reached 1.4-1.6 (~18 h). Cells were pelleted at 6,000 x g for 15 min and resuspended in 25 mL lysis buffer B (20 mM sodium phosphate, pH 8.0, 300 mM NaCl, 1 mM β-mercaptoethanol) containing Complete Protease Inhibitor, EDTA-free (Roche), 2 mM PMSF and 10 μM calpain inhibitor XI. Following sonication, the soluble supernatant was filtered (0.20 μm pore size) and incubated with 1.25 mL TALON Metal Affinity Resin (Clontech Laboratories, Mountain

View, CA) for 1 h at 4°C. The resin was washed 3x for 15 min with 10 volumes lysis buffer B. Bound His-tagged proteins were eluted sequentially with 10 volumes lysis buffer B supplemented with 500 mM imidazole, pH 8.0. Proteins were concentrated using Amicon Ultra centrifugal devices (Millipore) with molecular weight cut-offs (MWCO) of 10 and 100 kD. Protein concentration and purity was assessed by SDS-PAGE and SimplyBlue SafeStain (Life Technologies). The purification process was monitored by SDS-PAGE and SimplyBlue SafeStain staining.

## 2.7 IMMUNOPRECIPITATION

### 2.7.1 Immunoprecipitation of Cdk1/cyclin B1

Cdk1/cyclin B1 was immunopurified from nocodazole-treated HeLa cells. Mitotic HeLa cells were harvested from 5 confluent 15 cm plates, resuspended in 3 mL lysis buffer A and incubated on ice for 30 min. Following a 15 min spin at 14,000 rpm, the soluble supernatant was incubated with 10 µL of mouse α-cyclin B1 antibody (Ab-3, clone GNS1) (Thermo Fisher Scientific) for 2 h at 4°C. The lysate was transferred to 200 µL washed protein G sepharose 4 Fast Flow (Amersham Biosciences, Piscataway, NJ) and incubated overnight at 4°C. Beads were washed 2x with 10 volumes lysis buffer A, 2x with 10 volumes enzyme immunoassay (EIA) buffer (50 mM Tris-HCl, pH 7.4, 250 mM NaCl, 1 mM EDTA, 0.5% NP-40) and 3x with 10 volumes kinase buffer (50 mM HEPES, pH 7.0, 5 mM $MnCl_2$, 10 mM $MgCl_2$, 0.8 mM EGTA). Cdk1/cyclin B1 beads were suspended in 10 volumes kinase buffer supplemented with 0.1% sodium azide and stored at 4°C.

### 2.7.2 Immunoprecipitation of FLNa

Interphase and mitotic FLNa were immunoprecipitated from untreated and nocodazole-treated HeLa cells, respectively. 5 µL mouse α-FLNa and 50 µL rabbit α-p-FLNa were

incubated with 1 mg whole cell lysate for 1 h at 4°C. The lysate was added to 50-100 µL washed protein G sepharose 4 Fast Flow (Amersham Biosciences) and incubated overnight at 4°C. The beads were pelleted with a low speed spin (3,000 rpm for 1 min) and washed 3x with lysis buffer A. Immunoprecipitated proteins were dissociated with 4x sample buffer and heated to 42°C for 30 min. Proteins were separated by SDS-PAGE and analyzed by Western blot.

To obtain functional FLNa for use in assays, FLNa was immunoprecipitated from untreated HeLa cells as described above and washed 2x with 10 volumes lysis buffer A, 2x with 10 volumes EIA buffer and 3x with 10 volumes kinase buffer. FLNa-beads were suspended in 10 volumes kinase buffer supplemented with 0.1% sodium azide and stored at 4°C.

### 2.7.3 Co-immunoprecipitation to validate FLNa-interactors identified from mass spectrometry

Nocodazole and DMSO-treated cells from 5-15 cm confluent plates were harvested, flash frozen in liquid nitrogen and stored at -80°C until use. Whole cell lysate was prepared as described in Material and Methods section 2.3, except 2.5 mL ice-cold radioimmunoprecipitation assay (RIPA) buffer (50 mM Tris, pH 7.5, 150 mM NaCl, 1% NP-40, 0.5% deoxycholate) with protease inhibitors was used for lysis. For immunoprecipitation, 2 mg whole cell lysate from nocodazole and DMSO-treated cells was incubated with 50 µL Normal mouse IgG-sepharose 4B, 50 µL FLNa-sepharose 4B and 50 µL FLNa-sepharose 4B, respectively, in a total volume of 500 µL RIPA buffer for 1.5 h at 4°C, rotating end-over-end. Immunoprecipitated proteins were washed 3x with 500 µL RIPA. One bead volume of 1% SDS was added to the combined beads and heated to 42°C for 1 h followed by the addition of 4 bead volumes of water. The beads were vortexed and returned to 42°C for 2 h

to maximize recovery of dissociated proteins. The supernatant was removed and vacuum centrifuged (Thermo Savant Speedvac) at 65°C to reduce the volume. Proteins were reduced with 10 mM DTT for 1 h at 42°C and alkylated with 50 mM iodoacetamide for 30 min in the dark at RT. The sample was heated to 42°C with 4x NuPAGE LDS sample buffer (Invitrogen) for 30 min and electrophoresed on a NuPAGE 10% Bis-Tris gel (Invitrogen) using NuPAGE MOPS SDS running buffer (Invitrogen). Protein bands were stained with SimplyBlue Safestain (Invitrogen).

## 2.8 QUANTIFICATION OF TOTAL P-FLNA FROM MITOTIC HELA CELLS

For quantification of p-FLNa levels in mitotic HeLa cells, p-FLNa was depleted from mitotic cell lysate using α-p-FLNa-bound protein G beads. The p-FLNa depleted lysate was then probed for total FLNa and p-FLNa via Western blot. Briefly, 20 μg of nocodazole-arrested HeLa cell lysate (1 μg/μL) was incubated with 10 μL of α-p-FLNa-bound protein G sepharose beads (an excess of α-p-FLNa was incubated with protein G beads first) overnight at 4°C. Bead and supernatant (unbound lysate) samples were denatured with 4x SDS-PAGE sample buffer and analyzed by SDS-PAGE/Western blot.

## 2.9 IN VITRO PHOSPHORYLATION OF FLNA WITH CDK1

### 2.9.1 Detection of phosphorylated HeLa FLNa, recombinant His-FLNa and FLAG-FLNa with p-FLNa antibody

To phosphorylate endogenous HeLa FLNa, previously immunopurified FLNa-beads (from untreated HeLa cells) were mixed with increasing amounts of immunopurified cyclin B1/cdk1 in kinase buffer supplemented with 0.05 mM ATP. The reactions were placed on ice for 30 min and then transferred to 37°C for 1 h.

For recombinant His-FLNa (IgFLNa8-15 WT/AAA) phosphorylation timecourse experiments, approximately10 µg protein was incubated with 5 µL cyclin B1/cdk1 beads in 50 µL kinase buffer with 0.05 mM ATP. Reactions were incubated at 37°C and stopped with the addition of 4x sample buffer.

To obtain phosphorylated recombinant His-FLNa (ABD-IgFLNa8-15+24, IgFLNa8-15+24, ABD-IgFLNa8-15, IgFLNa8-15) for use in F-actin cosedimentation assays, 100 µg protein was incubated with 10 µL Cdk1/cyclin B1 beads at 37°C for 1 h and then overnight at 4°C. Reactions were performed in 100 µL kinase buffer in the presence and absence of 0.05 mM ATP (to obtain phosphorylated and nonphosphorylated protein respectively).

Phosphorylation of FLAG-FLNa was performed by incubating 1 µg FLAG-FLNa protein with 20 µL Cdk1/cyclin B1 beads in 200 µL kinase buffer with 0.05 mM ATP for 1 h at 4°C, then 1 h at 37°C.

### 2.9.2 Detection of phosphorylated recombinant His-FLNa with radioactive ATP

Cdk1/cyclin B1-bound beads were incubated with recombinant FLNa constructs in kinase buffer with 0.6 mM DTT, 0.01 mM cold ATP, and γ [$^{32}$P]ATP. Reactions were incubated for 45 min at 37°C, and stopped by the addition of an equal volume of 2X sample buffer, and heated 10 min at 65°C. Reactions were run on a 10% SDS-PAGE gel, dried, exposed to a phosphorimager screen, and visualized using Typhoon Trio Phosphorimager.

## 2.10 In vitro dephosphorylation assay

For *in vitro* FLNa dephosphorylation assays, 20 µg HeLa whole cell lysate (from DMSO and nocodazole-treated cells) were treated with 2.5 µL lambda phosphatase (New England Biolabs, Whitby, ON) in a reaction volume of 90 µL, according to manufacturer's

instructions. Samples were incubated at 30°C for 45 min and then prepared for SDS-PAGE/Western blot.

## 2.11 F-ACTIN COSEDIMENTATION ASSAYS

F-actin cosedimentation assays were performed according to manufacturer's instructions (Actin binding protein biochem kit BK001 with muscle actin, Cytoskeleton, Denver, CO) with the following changes: 5 μM F-actin was used per assay and samples were centrifuged at 63,000 rpm in a TL-100 ultracentrifuge (Beckman Coulter, Mississauga, ON) with TLA 100.3 rotor (Beckman Coulter). The pellet fractions were resuspended in 50 μL water, pipetted up and down for 2 min and subjected to one cycle of freeze-thaw (-20°C for 2 h and then RT until thawed). Supernatant and pellet fractions were analyzed by SDS-PAGE/SimplyBlue SafeStain (Life Technologies). BSA was added to some aliquots of 30 μM F-actin for long-term storage at -80°C. BSA and α-actinin were used as negative and positive controls for F-actin cosedimentation as described in the Actin-binding protein biochem kit BK001 (Cytoskeleton).

## 2.12 PREPARATION OF FIXED CELLS FOR IMMUNOFLUORESCENCE

Cells were plated in 6-well plates or 4-well Lab TekII Chamber Slides (Nalge Nunc International). Cells were counted using a coulter counter. Primary antibodies were used at a dilution of 1:200 or 1:100 in PBS; the α-p-FLNa antibody was diluted 1:1 000. AlexaFluor488 α-mouse, AlexaFluor546 α-mouse and AlexaFluor647 α-rabbit antibodies (Invitrogen) were used at a dilution of 1:200. Phalloidin488 and Phalloidin594 (Invitrogen) were diluted 1:200 and 1:50, respectively. The nucleus was stained with Hoechst 33258 (Invitrogen) at a concentration of 20 μg/mL. To prepare cells for immunofluorescence

microscopy, cells were plated on glass cover slips at a confluency of 50-80% in a 6-well plate and allowed to adhere overnight. The next day, cells were fixed with 3.7% paraformaldehyde in PBS for 30 min, permeabilized with 0.5% Triton X-100 in PBS for 15 min and blocked in immunofluorescence blocking buffer (130 mM NaCl, 7 mM $Na_2HPO_4$, 3.5 mM $NaH_2PO_4$, 7 mM $NaN_3$, 0.2% Triton X-100, 0.05% Tween-20, 0.1% BSA) for 1 h at RT or 4°C overnight. Primary and secondary antibodies were incubated for 1 h. Phallodin and Hoechst were both incubated for 45 min. All incubations were performed in the dark to minimize light exposure and washed 3x with PBS (10-15 min each) between incubations. The prepared cover slips were mounted onto glass slides with Dako fluorescence mounting media (Invitrogen) and sealed with nail polish.

## 2.13 IMMUNOFLUORESCENCE CONFOCAL MICROSCOPY

Confocal images of fixed cells were acquired on an Olympus Fluoview FV1000 laser-scanning confocal microscope (Olympus Canada, Markham, ON) with a 100X NA 1.4 oil immersion objective (Olympus Canada, Mississauga, ON) operated on FV1000 software (version 1.4a). Images comparing p-FLNa levels at different stages of mitosis were acquired with the same microscope settings. Each z-slice was set at 0.2 μm, with approximately 50-100 z-slices taken per cell. Compiled Z-stack images combine all z-slices into a single image. Post-acquisition, images were analyzed using Olympus Fluoview FV1000 software (versions 1.4a and 2.0). Confocal images of fixed cells shown in Chapter 5 were acquired on a Zeiss LSM 510 META microscope and analyzed with the associated Zen 2009 program.

## 2.14 PHASE CONTRAST MICROSCOPY

For quantification of M2 phenotypes, 35 000 cells of each cell line were plated on 35 mm dishes and imaged after 1 and 5 days. Cell culture dishes were placed on a stage heated to 37°C. Phase contrast images were taken on a Leica DMIRB inverted stage microscope with a 10X objective, operated on Open Lab software (Improvision, Lexington, MA).

## 2.15 TIME-LAPSE IMAGING

For wound healing assays, 50 000 M2 cells were plated into Ibidi inserts (Ibidi, Martinsried, Germany) placed into a 35 mm glass-bottom uncoated μ-Dish (Ibidi) and allowed to adhere overnight. The following morning, Ibidi inserts were removed and fresh, pre-warmed M2 media was added. Videos of wound healing assays were acquired on a Zeiss LSM 5 Pascal/AxioVert 200 inverted confocal microscope. Cells were maintained in a humidified incubator set to 37°C and 5% $CO_2$. Phase contrast images were acquired every 15 min for approximately 48 h with a 10X EC Plan-Neofluar Ph1 objective (0.3 numerical aperture) on five different positions along the wound. Movies were compiled using AxioVision software. ImageJ (1.43u) was used to quantify wound surface areas at 0 h and 37.5 h.

For time-lapse imaging of FLNa-WT GFP, FLNa-AAA GFP and GFP EV-expressing M2 cells undergoing mitosis, cells were plated on a 35 mm MatTek uncoated glass bottom dishes (MatTek Corporation, Ashland, MA) and imaged on an Olympus VivaView FL incubator microscope (Olympus) equipped with an ORCA-R2 Hammamatsu CCD camera and operated on MetaMorph software. (Molecular Devices, Sunnyvale, CA). Differential interference contrast and fluorescent images were acquired with a 20X objective. Cells were maintained in a humidified 37°C chamber containing 5% $CO_2$. Frames were acquired approximately every three minutes for up to 48 h.

## 2.16 COVALENTLY COUPLING ANTIBODIES TO SEPHAROSE BEADS

To covalently couple antibodies to sepharose beads, 100 µL of mouse α-FLNa antibody and 200 µL Normal mouse IgG antibody (Abcam, Toronto, ON) was dialyzed against coupling buffer (0.1 M $NaHC0_3$, 0.5 M NaCl, pH 8.4) at 4°C for 1 h using equilibrated Slide-A-Lyzer MINI Dialysis Devices with a MWCO of 10 000 kD (Thermo Scientific). CNBr-activated sepharose 4B beads (Sigma-Aldrich) were prepared according to manufacturer's instructions. α-FLNa and Normal mouse IgG were covalently coupled to sepharose 4B at a ratio of ~1 mg antibody/mL swollen beads according to manufacturer's instructions. The antibody-sepharose 4B beads (FLNa-sepharose 4B and Normal mouse IgG-sepharose 4B) were stored in 5 bead volumes of 1.0 M NaCl (0.22 µm filtered) with 0.03% sodium azide. These antibody-bound beads were used for immunoprecipitation of FLNa for liquid-chromatography tandem-mass spectrometry (LC MS/MS).

## 2.17 STABLE ISOTOPE LABELING WITH AMINO ACIDS IN CELL CULTURE (SILAC)

HeLa cells were triple-labeled as described in (Figure 2.2) (Trinkle-Mulcahy et al., 2008). HeLa cells were expanded in "light", "medium" and "heavy" SILAC (Stable Isotope Labeling with Amino Acids in Cell Culture) media for six doublings (to ensure complete incorporation of the isotopic amino acids). "Light", "medium" and "heavy" SILAC media was kindly provided by Laura Trinkle-Mulcahy (Department of Cellular and Molecular Medicine and Ottawa Institute of Systems Biology, Faculty of Medicine, University of Ottawa) in exchange for cell culture supplies. 5-15 cm confluent plates of cells were used for three separate immunoprecipitations (one for each label). Briefly, "light" and "medium" cells were treated with 100 ng/mL nocodazole for 16 h and "heavy" cells were treated with

DMSO. Cells from 5-15 cm confluent plates were harvested, flash frozen in liquid nitrogen and stored at -80°C until use. Whole cell lysate was prepared as described in Material and Methods, section 2.3, except 2.5 mL ice-cold RIPA buffer with protease inhibitors was used for lysis. For immunoprecipitation, 2 mg whole cell lysate from "light", "medium" and "heavy" labeled cells was used in three separate immunoprecipitations. Light, medium and heavy cell lysate was incubated with 50 µL Normal mouse IgG-sepharose 4B, 50 µL FLNa-sepharose 4B and 50 µL FLNa-sepharose 4B, respectively, in a total volume of 500 µL RIPA buffer for 1.5 h at 4°C, rotating end-over-end. Immunoprecipitated proteins were washed 3x with 500 µL RIPA. Beads from all three immunoprecipitations were then combined into one microfuge tube. One bead volume of 1% SDS was added to the combined beads and heated to 42°C for 1 h followed by the addition of 4 bead volumes of water. The beads were vortexed and returned to 42°C for 2 h to maximize recovery of dissociated proteins. The supernatant was removed and vacuum centrifuged (Thermo Savant Speedvac) at 65°C to reduce the volume. Proteins were reduced with 10 mM DTT for 1 h at 42°C and alkylated with 50 mM iodoacetamide for 30 min in the dark at RT. The sample was heated to 42°C with 4x NuPAGE LDS sample buffer (Invitrogen) for 30 min and electrophoresed on a NuPAGE 10% Bis-Tris gel (Invitrogen) using NuPAGE MOPS SDS running buffer (Invitrogen). Protein bands were stained with SimplyBlue Safestain (Invitrogen). See Figure 2.2 for SILAC workflow (Trinkle-Mulcahy et al., 2008). Some Invitrogen SDS-PAGE supplies and reagents were kindly supplied by the Trinkle-Mulcahy lab.

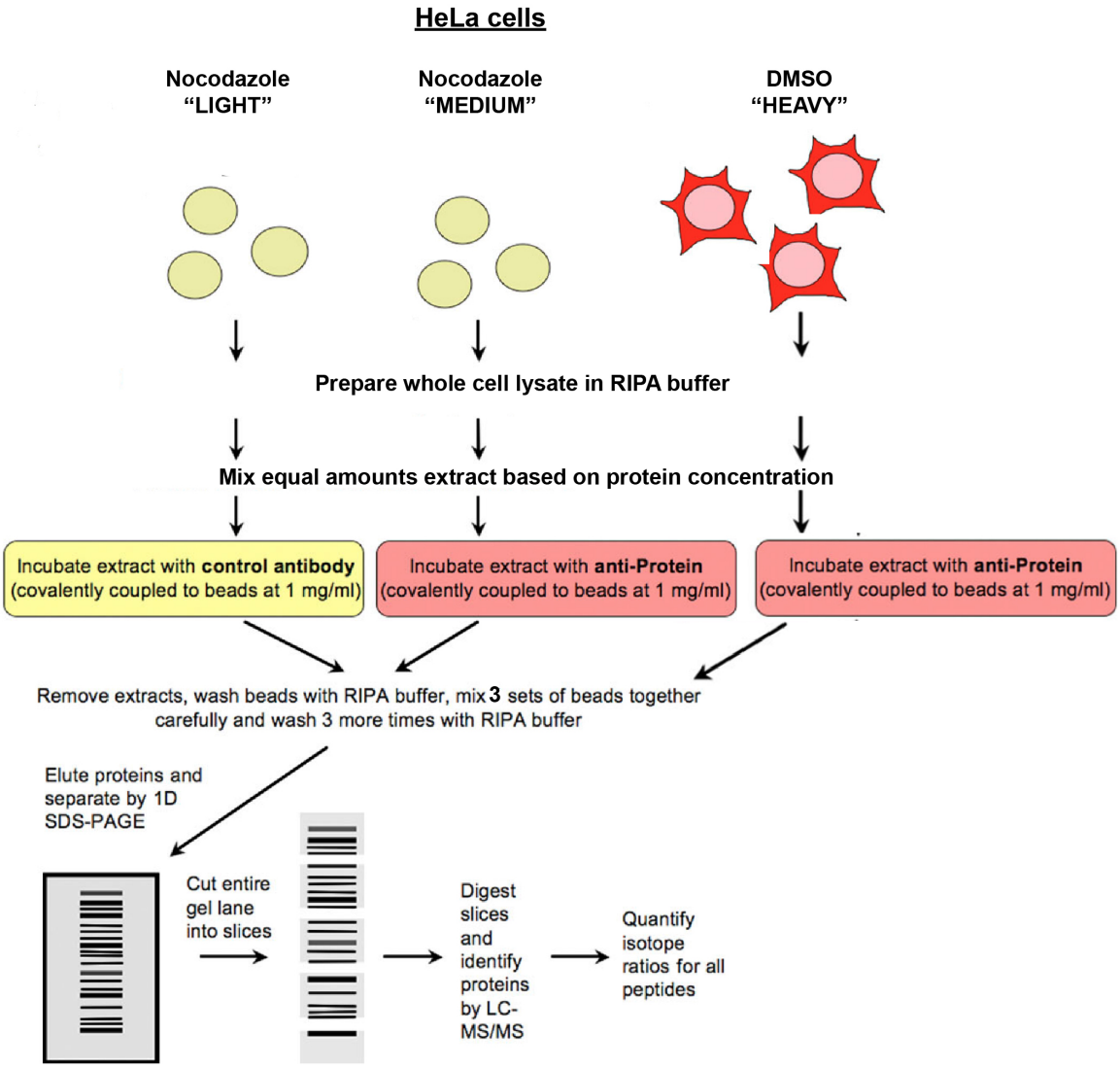
HeLa cells
Nocodazole "LIGHT"
Nocodazole "MEDIUM"
DMSO "HEAVY"
Prepare whole cell lysate in RIPA buffer
Mix equal amounts extract based on protein concentration
Incubate extract with control antibody (covalently coupled to beads at 1 mg/ml)
Incubate extract with anti-Protein (covalently coupled to beads at 1 mg/ml)
Incubate extract with anti-Protein (covalently coupled to beads at 1 mg/ml)
Remove extracts, wash beads with RIPA buffer, mix 3 sets of beads together carefully and wash 3 more times with RIPA buffer
Elute proteins and separate by 1D SDS-PAGE
Cut entire gel lane into slices
Digest slices and identify proteins by LC-MS/MS
Quantify isotope ratios for all peptides

**Figure 2.2. Workflow for SILAC LC-MS/MS based analysis of mitotic and interphase-specific FLNa interactors in HeLa cells.** HeLa cells are grown in light, medium and heavy SILAC media for 5-6 passages. Light and medium cells are treated with nocodazole and immunoprecipitated with Normal mouse IgG beads and anti-FLNa-beads, respectively. Heavy cells are immunoprecipitated with anti-FLNa-beads. Beads are mixed, eluted and separated by SDS-PAGE. Proteins are digested and analyzed by LC-MS/MS. SILAC analysis is performed. Figure adapted from (Trinkle-Mulcahy et al., 2008). *See Appendix, Copyright Permissions for Permission Licensing information.*

## 2.18 In-gel digestion, extraction of peptides and phosphopeptide enrichment

The band corresponding to FLNa (280 kD) was excised from a SDS-PAGE gel, destained and in-gel digested with 100 µL of 0.01 µg/µL sequencing grade modified trypsin (Promega, Madison, WI). After digestion, peptides were extracted with two rounds of 1% formic acid and stored at -20°C. FLNa phosphopeptides were enriched using a Pierce $TiO_2$ Phosphopeptide Enrichment and Clean-up Kit (Thermo Scientific) according to manufacturer's instructions. The flow-through (containing nonphosphorylated peptides) was retained and purified using Pierce C18 Spin Columns (Thermo Scientific) according to manufacturer's instructions.

## 2.19 Liquid chromatography tandem mass spectrometry

Samples were analyzed using mass spectrometry (MS) by Lawrence Puente at the Ottawa Hospital Research Institute (OHRI) Proteomics Core Facility (Ottawa, ON). The following methods were provided. LC-MS/MS was performed on an LTQ Orbitrap XL hybrid mass spectrometer (Thermo Scientific) with nanospray ion source. MS/MS spectra were matched against all sequences in a custom database (human sequences from the 2011_07 version of uniprot_sprot.fasta.gz downloaded from ftp.uniprot.org concatenated with the Contaminants database downloaded from maxquant.org, June 9th 2011) using MASCOT 2.3.01 software (Matrix Science, UK) with MS tolerance of ±5 ppm and MS/MS tolerance of 0.6 Da. Carbamidomethylation of cysteine, oxidation of methionine, protein N-terminal acetylation, deamidation, conversion of Glu or Gln to Pyro-Glu, and SILAC labeling were allowed as potential modifications. In a separate set of Mascot analyses, phosphorylation of serine, threonine or tyrosine were also allowed as potential modifications. Samples were loaded onto

a peptide trap column (Agilent Technologies) using a Dionex UltiMate 3000 RSLC nano HPLC system. Samples were loaded for 5 min at 15 μL/min in 3% acetonitrile with 0.1% formic acid. Peptides were eluted over a 60 min gradient of 3% - 45% acetonitrile with 0.1% formic acid at 0.3 μL per min through a 10-cm analytical column (New Objective Picofrit self-packed with Zorbax C18) and sprayed directly into the LTQ Orbitrap XL using a nanospray source (Thermo Scientific). Mass spectra were acquired using a data-dependent method. $MS^2$ scans were acquired using the Orbitrap module while MS scans were acquired in the ion trap module.

## 2.20 CELL PROLIFERATION ASSAY

Proliferation of monoclonal M2 cell lines was determined using a CyQUANT Cell Proliferation Assay kit (Invitrogen Life Technologies, Burlington, ON, CA). Briefly, cells were plated at varying densities (50, 100 and 250 cells) in a 96-well plate in triplicate and incubated in a humidified incubator at 37°C and 5% $CO_2$. At 12, 24, 48 and 72 hours after plating, the media was removed, adherent cells were washed with PBS and the 96-well plate was stored at -80°C until all samples were ready to be assayed. The cells were quantitated according to manufacturer's instructions.

# CHAPTER 3 FILAMIN A IS PHOSPHORYLATED BY CDK1 *IN VIVO*

## 3.1 ABSTRACT

Filamin A (FLNa) is a 280 kD protein that crosslinks actin filaments into parallel bundles or three-dimensional orthogonal networks. Using a yeast two-hybrid screen we previously identified FLNa as a cyclin B1 interacting partner and later showed that FLNa is a cyclin-dependent kinase 1 (Cdk1) substrate *in vitro*. Serines 1436, 1533 and 1630 were identified as *in vitro* phosphorylation sites. Using a p-FLNa antibody raised against p-S1436 we find that FLNa is phosphorylated *in vivo* on multiple Cdk1 sites, including serines 1084, 1459 and 1533, which were identified by mass spectrometry as mitosis-enriched phosphorylation sites in HeLa cells. All three sites match the phosphorylation consensus sequence of Cdk1. When the p-FLNa antibody is used in immunofluorescence, only mitotic cells are stained, consistent with the activation of Cdk1/cyclin B1 during mitosis. Furthermore, p-FLNa intensity is greatest during prophase and is noticeably decreased at anaphase. Overall, we show that FLNa is phosphorylated *in vivo* by Cdk1/cyclin B1 on serines 1084, 1459, 1533, and likely other sites.

## 3.2 INTRODUCTION

Using a yeast two-hybrid screen, a previous member of our lab identified FLNa as a cyclin B1 binding partner and showed that Cdk1/cyclin B1 could phosphorylate FLNa *in vitro* (Cukier et al., 2007). When activated, Cdk1/cyclin B1 phosphorylates many substrates that are required for mitotic progression, including proteins involved in chromosome condensation, mitotic spindle assembly and nuclear envelope breakdown (NEBD) (Nurse, 1990; Nigg, 1993; Jackman et al., 2003; Bentley et al., 2007; Vagnarelli, 2012; Lianga et al., 2013). Cdk1/cyclin B1 substrates also include actin-binding proteins (ABPs) such as caldesmon, an ABP that inhibits actin-activated ATPase activity (Yamashiro and Matsumura, 1991) and cortactin, a cortical ABP that recruits the Arp2/3 complex to existing actin filaments (Blethrow et al., 2008). *In vitro*, Cdk1-phosphorylated caldesmon has reduced actin-binding ability (Yamashiro et al., 1990). However, the physiological significance of caldesmon and cortactin phosphorylation by Cdk1/cyclin B1 is still unclear. Some evidence exists that phosphorylation of caldesmon causes it to dissociate from actin filaments *in vivo* (Yamashiro et al., 1994). Given that **1.** Cdk1/cyclin B1 phosphorylates substrates required for mitosis and **2.** ABPs have critical roles in cell cycle progression, we hypothesized that FLNa may be an *in vivo* Cdk1/cyclin B1 substrate with a role in mitotic actin remodelling. Therefore we decided to further investigate this interaction *in vitro* and *in vivo*.

A previous member of our lab identified FLNa serines 1436, 1533 and 1630 as *in vitro* phosphorylation sites (Cukier et al., 2007). Mutation of serine 1436 to nonphosphorylatable glycine substantially reduced phosphorylation *in vitro*, whereas single mutations at serine 1533 and 1630 reduced phosphorylation (Cukier et al., 2007). Therefore, phosphorylation of serine 1436 could direct the phosphorylation of serines 1533 and 1630.

Alternatively, serine 1436 may be the only residue that is phosphorylated but the interaction between Cdk1/cyclin B1 and serines 1533 and 1630 are necessary for maximal 1436 phosphorylation (Cukier et al., 2007). To further investigate the functional relevance of Cdk1-phosphorylation of FLNa at serine 1436, we obtained a p-FLNa antibody raised against a FLNa peptide containing phosphorylated serine 1436 (p-FLNa antibody).

Using this p-FLNa antibody, **my first objective is to determine whether or not FLNa phosphorylation by Cdk1/cyclin B1 occurs *in vivo*. My second objective is to identify *in vivo* FLNa phosphorylation sites using quantitative mass spectrometry.**

## 3.3 RESULTS

### 3.3.1 FLNa is phosphorylated in mitosis by Cdk1/cyclin B1

To investigate FLNa phosphorylation in intact cells, we used a p-FLNa antibody that was raised against a FLNa peptide containing phosphorylated serine 1436 (see Material and Methods). This residue, as well as serines 1533 and 1630 were previously identified by our lab as sites phosphorylated *in vitro* by Cdk1/cyclin B1 (Cukier et al., 2007). Immunopurified Cdk1/cyclin B1 (from mitotic HeLa cells) can phosphorylate immunopurified endogenous HeLa FLNa in a dose-dependent manner and generates epitopes recognized by the p-FLNa antibody (Figure 3.1A, left panel). The reaction is also ATP-dependent (Figure 3.1A, right panel). Furthermore, recombinant His-FLNa fragments (Figure 3.1, B and C) and full-length recombinant FLAG-tagged FLNa (Figure 3.1D) are also detected by the p-FLNa antibody after *in vitro* phosphorylation with immunopurified Cdk1/cyclin B1. *In vivo*, the p-FLNa antibody detects a protein that corresponds to the expected size of FLNa (280 kD) from nocodazole-treated (mitotic) but not DMSO-treated (interphase) HeLa cells and is only able to immunoprecipitate FLNa from nocodazole-treated cells (Figure 3.1E). The p-FLNa antibody does not recognize FLNa after lambda phosphatase (serine/threonine phosphatase) treatment of mitotic HeLa extracts (Figure 3.1F, upper panel) showing it specifically detects phosphorylated FLNa.

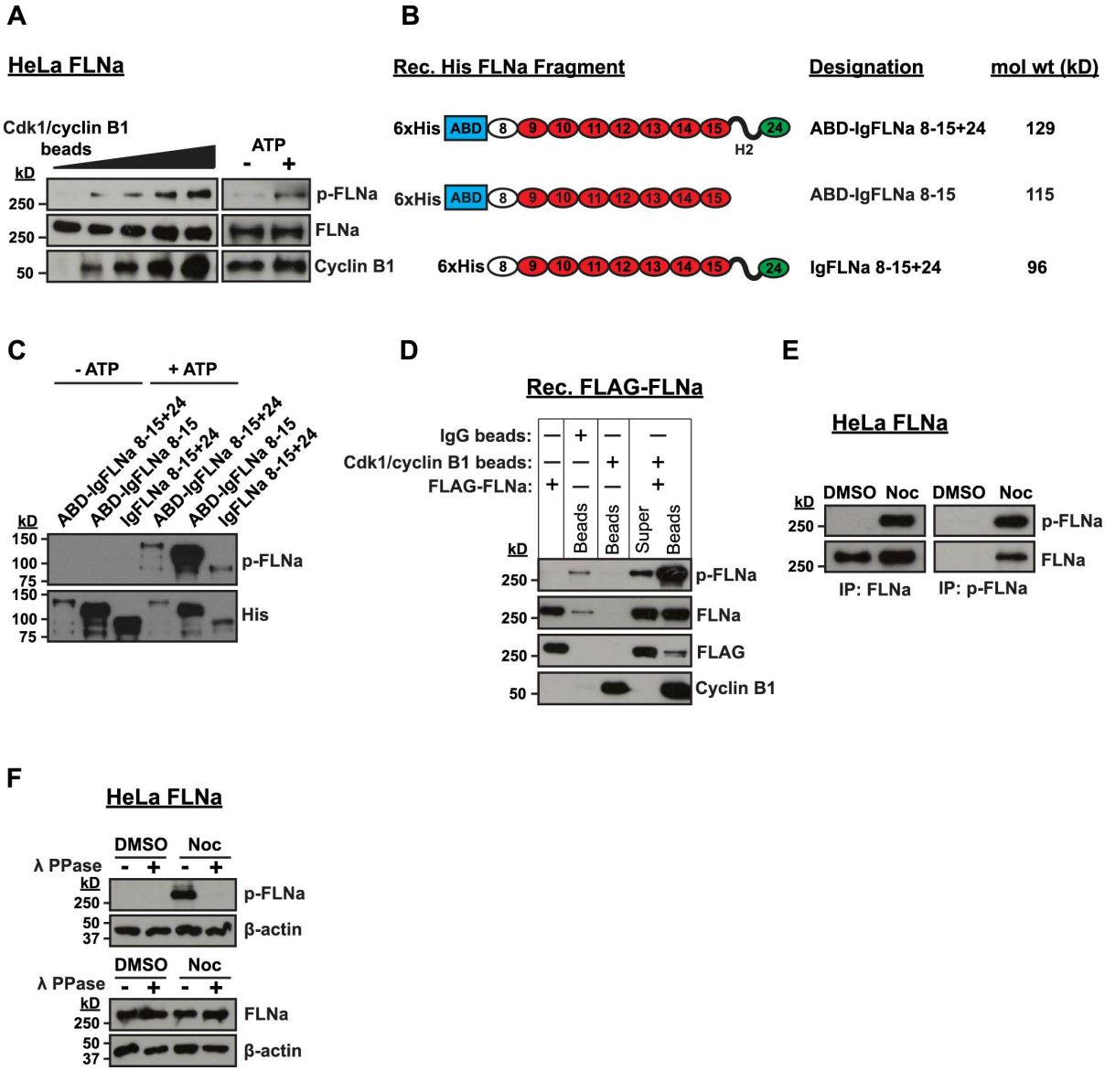
A
HeLa FLNa
Cdk1/cyclin B1 beads
ATP
- +
kD
250
250
50
p-FLNa
FLNa
Cyclin B1
B
Rec. His FLNa Fragment
Designation
mol wt (kD)
6xHis ABD 8 9 10 11 12 13 14 15 24 H2
ABD-IgFLNa 8-15+24
129
6xHis ABD 8 9 10 11 12 13 14 15
ABD-IgFLNa 8-15
115
6xHis 8 9 10 11 12 13 14 15 24
IgFLNa 8-15+24
96
C
- ATP
+ ATP
ABD-IgFLNa 8-15+24
ABD-IgFLNa 8-15
IgFLNa 8-15+24
ABD-IgFLNa 8-15
ABD-IgFLNa 8-15+24
IgFLNa 8-15+24
kD
150
100
75
150
100
75
p-FLNa
His
D
Rec. FLAG-FLNa
IgG beads:
Cdk1/cyclin B1 beads:
FLAG-FLNa:
Beads
Beads
Super
Beads
kD
250
250
250
50
p-FLNa
FLNa
FLAG
Cyclin B1
E
HeLa FLNa
kD
250
250
DMSO Noc DMSO Noc
p-FLNa
FLNa
IP: FLNa
IP: p-FLNa
F
HeLa FLNa
DMSO Noc
λ PPase - + - +
kD
250
50
37
p-FLNa
β-actin
DMSO Noc
λ PPase - + - +
kD
250
50
37
FLNa
β-actin

**Figure 3.1. FLNa is phosphorylated by Cdk1/cyclin B1 in mitosis. (A)** *In vitro*, FLNa is phosphorylated by Cdk1/cyclin B1 in a dose-dependent manner and is ATP-dependent. **(B)** Schematic of recombinant His-FLNa fragments. FLNa repeats are numbered. The secondary F-actin binding segment is located in repeats 9-15 (red). The conserved actin-binding domain (ABD) (blue) is located at the N-terminus and the self-association domain (repeat 24) (green) is located at the C-terminus. H2 represents Hinge region 2. **(C)** Recombinant His-tagged FLNa fragments can be phosphorylated *in vitro* by Cdk1/cyclin in the presence of ATP. **(D)** The p-FLNa antibody detects Cdk1/cyclin B1-mediated phosphorylation of full-length recombinant FLAG-FLNa. **(E)** FLNa immunoprecipitated from nocodazole-arrested HeLa cells, but not DMSO-treated cells, is detected by the p-FLNa antibody. **(F)** p-FLNa detection from mitotic HeLa cell lysate is abrogated upon treatment with lambda phosphatase (λ PPase).

Phosphorylated FLNa increases as cells arrest in mitosis after nocodazole treatment (Figure 3.2A) and decreases as cells are released from mitotic-arrest (Figure 3.2B). Total FLNa levels remain stable. The increase and decrease in p-FLNa correlate with an increase and decrease in cyclin B1, respectively (Figure 3.2, A and B). The decrease in phosphorylated FLNa is slowed when cells are treated with okadaic acid, a protein phosphatase 1 (PP1) and protein phosphatase 2A (PP2A) inhibitor. This suggests FLNa may be dephosphorylated by PP1 or PP2A as cells progress to anaphase and re-enter G1 (Figure 3.2C).

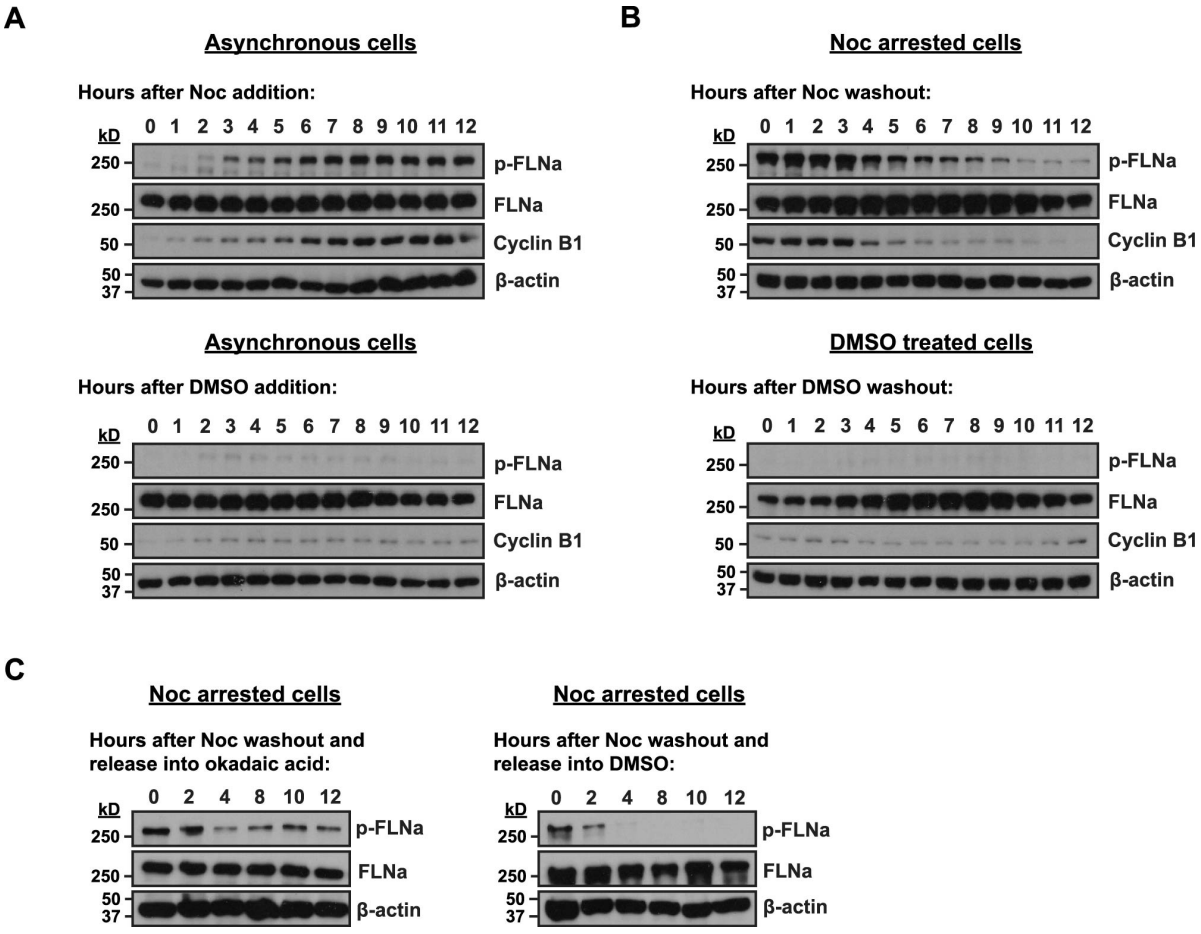
A
Asynchronous cells
Hours after Noc addition:
kD
0 1 2 3 4 5 6 7 8 9 10 11 12
250
p-FLNa
250
FLNa
50
Cyclin B1
50
37
β-actin
Asynchronous cells
Hours after DMSO addition:
kD
0 1 2 3 4 5 6 7 8 9 10 11 12
250
p-FLNa
250
FLNa
50
Cyclin B1
50
37
β-actin
B
Noc arrested cells
Hours after Noc washout:
kD
0 1 2 3 4 5 6 7 8 9 10 11 12
250
p-FLNa
250
FLNa
50
Cyclin B1
50
37
β-actin
DMSO treated cells
Hours after DMSO washout:
kD
0 1 2 3 4 5 6 7 8 9 10 11 12
250
p-FLNa
250
FLNa
50
Cyclin B1
50
37
β-actin
C
Noc arrested cells
Hours after Noc washout and release into okadaic acid:
kD
0 2 4 8 10 12
250
p-FLNa
250
FLNa
50
37
β-actin
Noc arrested cells
Hours after Noc washout and release into DMSO:
kD
0 2 4 8 10 12
250
p-FLNa
250
FLNa
50
37
β-actin

**Figure 3.2. FLNa phosphorylation and dephosphorylation correlate with nocodazole treatment and washout, respectively. (A)** FLNa phosphorylation is nocodazole-dependent and correlates with the expression of cyclin B1. Asynchronous HeLa cells were treated with nocodazole (100 ng/mL) or DMSO for the indicated times and whole cell lysate was probed for FLNa, p-FLNa and cyclin B1. β-actin was probed as a loading control. **(B)** FLNa phosphorylation after nocodazole-treatment decreases as a function of time after nocodazole is removed. The experiment was performed as in part A, except nocodazole was washed out. β-actin was probed as a loading control. **(C)** Okadaic acid inhibits FLNa dephosphorylation in nocodazole-arrested HeLa cells. HeLa cells were nocodazole-arrested for 18 h and then released into okadaic acid (1 μM) for the times indicated. In the presence of okadaic acid, p-FLNa detection persists compared to nocodazole-arrested cells released into DMSO. β-actin was probed as a loading control.

Because Cdk1 phospho-epitopes can be promiscuous (Wu et al., 2010), we next determined whether p-S1436 was the only residue detected by our antibody. To this end, we generated a nonphosphorylatable FLNa-S1436G mutant and transfected it into FLNa-deficient M2 melanoma cells. We found that the p-FLNa antibody still detected a 280 kD band in nocodozole-treated M2 cells (Figure 3.3 A), indicating that the p-FLNa antibody recognizes multiple Cdk1 epitopes on FLNa. Next, we compared p-FLNa levels in mitotic M2 cells expressing FLNa-WT and FLNa-S1436G and found that p-FLNa detection in both cell lines are approximately the same (Figure 3.3B), suggesting p-S1436 may not be a major phosphorylation site *in vivo*.

FLNa is a 280 kD protein and inspection of its amino acid sequence reveals many possible Cdk1/cyclin B1 phosphorylation sites (Table 3.1). Of these, 10 serines are located within stringent Cdk1 phosphorylation consensus sequences (K/R)-(S/T)*-P-x-(K/R) or (S/T)*-P-x-(K/R) and 29 serines/threonines are found within the minimal (S/T)*-P consensus sequence (x represents any amino acid; asterisk indicates site of phosphorylation) (Nigg, 1993). Therefore, it is possible that FLNa is also phosphorylated on one or more of these sites *in vivo*. Taken together, these results suggest that our p-FLNa antibody recognizes multiple Cdk1/cyclin B1-generated epitopes on FLNa.

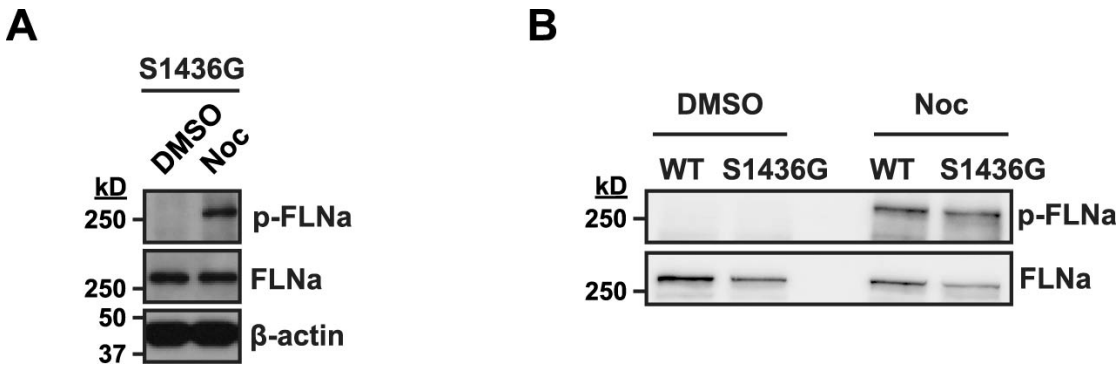
A
S1436G
DMSO
Noc
kD
250
p-FLNa
250
FLNa
50
37
β-actin
B
DMSO
Noc
WT
S1436G
WT
S1436G
kD
250
p-FLNa
250
FLNa

**Figure 3.3. The p-FLNa antibody detects FLNa S1436G in mitotic M2 cells. (A)** The p-FLNa antibody detects mitotic M2 cell expressing FLNa S1436G. **(B)** The p-FLNa antibody detects FLNa-WT and FLNa-S1436 equally in nocodazole-treated (mitotic) M2 cells.

**Table 3.1. Cdk1 phosphorylation consensus sites in FLNa.** 10 serines are located within stringent Cdk1 phosphorylation consensus sequences (K/R)-(S/T)*-P-x-(K/R) or (S/T)*-P-x-(K/R) and 29 serines/threonines are found within the minimal (S/T)*-P consensus sequence.

| **(K/R)-(S/T)*-P-x-(K/R)[1]** | **(S/T)*-P-x-(K/R)[1]** | **(S/T)*-P** | | |
|---|---|---|---|---|
| S1533 | S757 | T167 | S966 | S2025 |
| | S860 | T243 | S1055 | S2120 |
| | S1084 | S368 | T1322 | S2172 |
| | S1148 | S468 | S1338 | S2216 |
| | S1436 | S564 | S1343 | S2311 |
| | S1630 | S657 | S1459 | S2319 |
| | S2406 | T839 | T1682 | S2362 |
| | S2502 | T857 | S1726 | T2480 |
| | S2632 | T938 | S1846 | T2591 |
| | | S959 | S1938 | |

[1] where x represents any amino acid

* site of phosphorylation

### 3.3.2 FLNa is phosphorylated in intact mitotic HeLa cells

Using the p-FLNa antibody, we next examined the localization of endogenous p-FLNa in intact HeLa cells using immunofluorescence confocal microscopy. Consistent with Western blot results (Figure 3.1, Figure 3.2A), p-FLNa was only detected in mitotic cells and not interphase cells (Figure 3.4A). Interestingly, we observed that p-FLNa fluorescence intensity is variable among the different stages of mitosis. Specifically, FLNa phosphorylation is most visible during prophase but nearly undetectable by telophase (Figure 3.4B). This is consistent with FLNa being a Cdk1/cyclin B1 substrate since such substrates are phosphorylated early in mitosis, when Cdk1 is activated, and dephosphorylated during anaphase (Nigg, 1993; Gavet and Pines, 2010). The decline in visible FLNa phosphorylation in anaphase correlates with the loss of p-FLNa signal following nocodazole washout (Figure 3.2B).

A

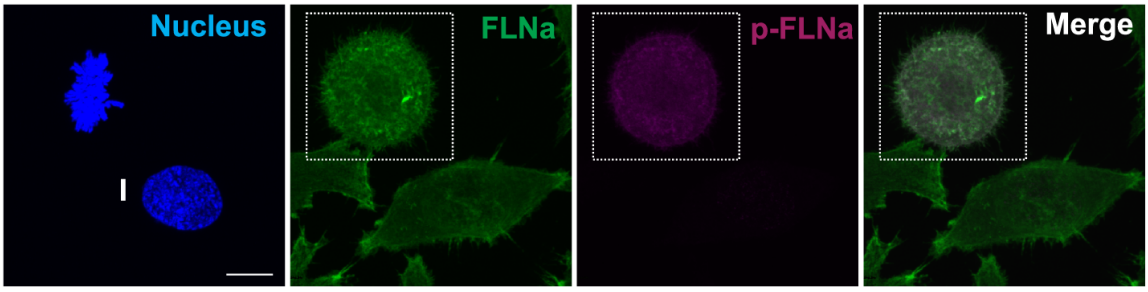
Nucleus
FLNa
p-FLNa
Merge

B

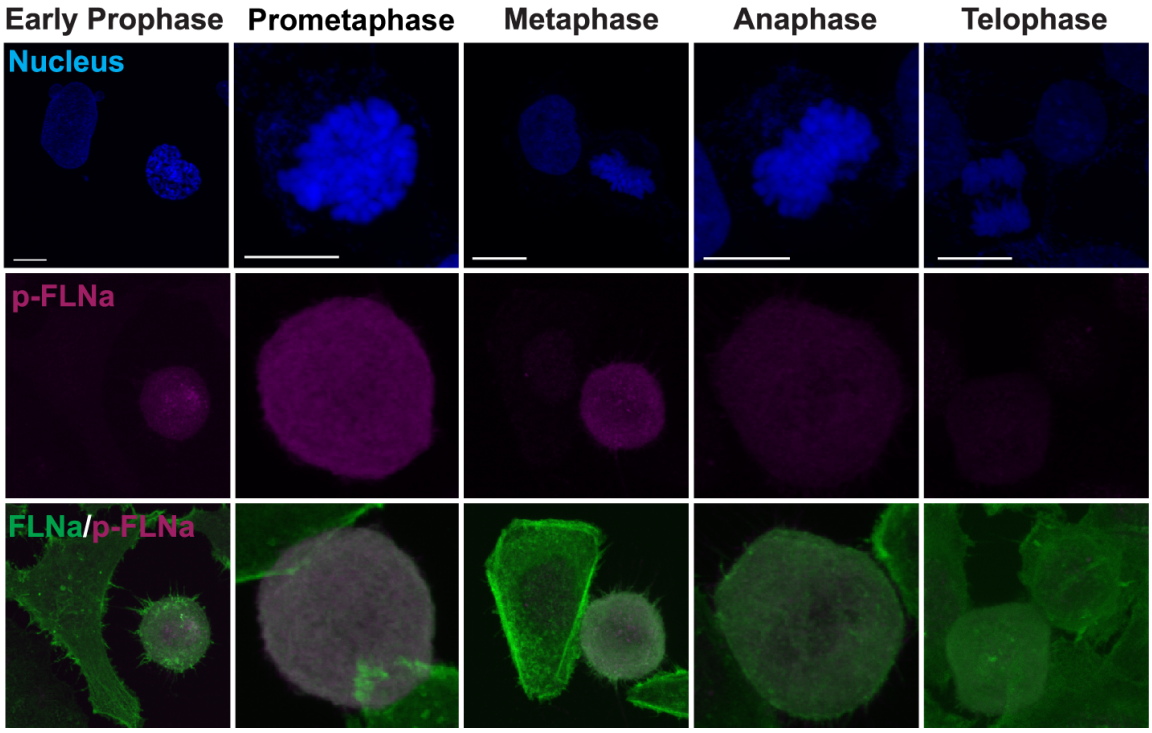
Early Prophase
Prometaphase
Metaphase
Anaphase
Telophase
Nucleus
p-FLNa
FLNa/p-FLNa

**Figure 3.4. FLNa is phosphorylated by Cdk1/cyclin B1 in intact HeLa cells in mitosis.** **(A)** p-FLNa is detectable in mitotic (M) but not interphase (I) HeLa cells. Confocal images are compiled Z-stacks. **(B)** HeLa cells at various stages of mitosis (early prophase, prometaphase, metaphase, anaphase and telophase). FLNa phosphorylation is highest in mitotic prophase and nearly undetectable by telophase. Merge panel shows colocalization of FLNa and p-FLNa (white). Interphase cells are shown next to mitotic cells for comparison of p-FLNa levels. During image acquisition, microscope settings were kept constant so p-FLNa intensity could be compared in different stages of mitosis. Confocal images are compiled Z-stacks. Scale bar, 10 μm. Immunofluorescence images are of fixed cells.

### 3.3.3 The majority of FLNa is phosphorylated in mitosis

To quantify the percentage of FLNa that is phosphorylated in mitosis, p-FLNa was depleted from HeLa cell lysate harvested from nocodazole-arrested cells and the remaining undepleted FLNa, i.e. non-phosphorylated FLNa, was assessed by Western blot (Figure 3.5A). Densitometric analysis of three blots from independent experiments showed that approximately 34% of total FLNa is non-immunoprecipitable by the p-FLNa antibody compared to approximately 81% in a control immunoprecipitation with beads only (Figure 3.5B). Thus, at least 66% (100%-34%) of total cellular FLNa is likely to be phosphorylated in mitosis.

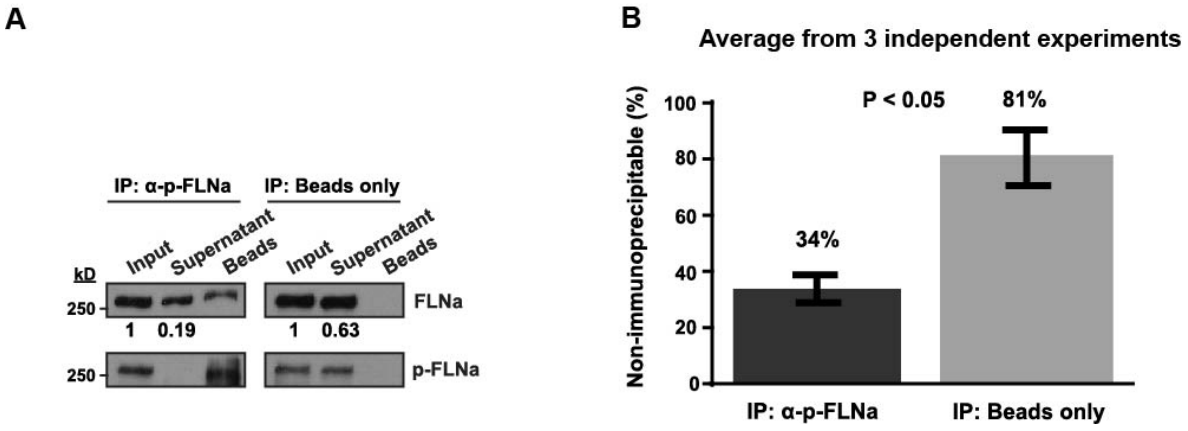
A
IP: α-p-FLNa
IP: Beads only
Input
Supernatant
Beads
Input
Supernatant
Beads
kD
250
1
0.19
1
0.63
FLNa
250
p-FLNa
B
Average from 3 independent experiments
P < 0.05
81%
34%
Non-immunoprecipitable (%)
100
80
60
40
20
0
IP: α-p-FLNa
IP: Beads only

**Figure 3.5. The majority of FLNa is phosphorylated in mitosis. (A)** p-FLNa was depleted from mitotic HeLa cell lysate by immunoprecipitation and supernatant and bead fractions were analyzed by Western blot. As a control, a parallel experiment was performed with beads only. Densitometry values are shown below blots and normalized to the input. A representative Western blot is shown. **(B)** Approximately 34% of FLNa from mitotic HeLa cell lysate is non-immunoprecipitable using α-p-FLNa bound beads and approximately 81% of FLNa from mitotic HeLa cell lysate is non-immunoprecipitable using beads only (control); therefore, approximately 66% is immunoprecipitable (i.e. phosphorylated FLNa). Quantification was performed using ImageJ software and averaged from three independent experiments. Error bars are ± SEM.

### 3.3.4 Quantitative mass spectrometry shows FLNa is phosphorylated on serines 1084, 1459 and 1533 in mitotic cells

We have previously shown that FLNa is an *in vitro* Cdk1/cyclin B1 substrate (Cukier, 2007). Inspection of that FLNa amino acid sequence reveals many possible Cdk1/cyclin B1 phosphorylation sites (Table 3.1). Of these, 10 serines are located within stringent Cdk1 phosphorylation consensus sequences (K/R)-(S/T)*-P-x-(K/R) or (S/T)*-P-x-(K/R) and 29 serines/threonines are found within the minimal (S/T)*-P consensus sequence (Nigg, 1993). Because many FLNa residues are likely phosphorylated during mitosis, we next attempted to comprehensively identify these sites. To this end, we used stable isotope labeling with amino acids in cell culture (SILAC) coupled with liquid chromatography tandem mass spectrometry (LC-MS/MS). Four FLNa phosphorylation sites were identified. Phospho-serines 1084, 1459 and 1533 were enriched in mitotic cells and phospho-serine 2152 was enriched in interphase cells (Table A2). Analysis of the FLNa tryptic peptides shows 68% overall sequence coverage (Figure 3.7) with 33 of 39 Cdk1 phosphorylation consensus sequences present (Tables A3 and A4). FLNa peptides that were not detected include those containing S1148, T167, T243, T839, T1682 and S1846 (Table A4). Serine 2152 has previously been identified as a p90 ribosomal S6 protein kinase (p90RSK) (Jiang and Campbell, 2008) and p21-activated kinase (Pak1) (Vadlamudi et al., 2002) phosphorylation site and is associated with cytoskeletal reorganization. Serines 1084, 1459 and 1533 are found within the secondary F-actin binding segment in FLNa repeats 9-15 (Figure 3.6), a region that has been found to be required for high-avidity F-actin binding (Nakamura et al., 2007).

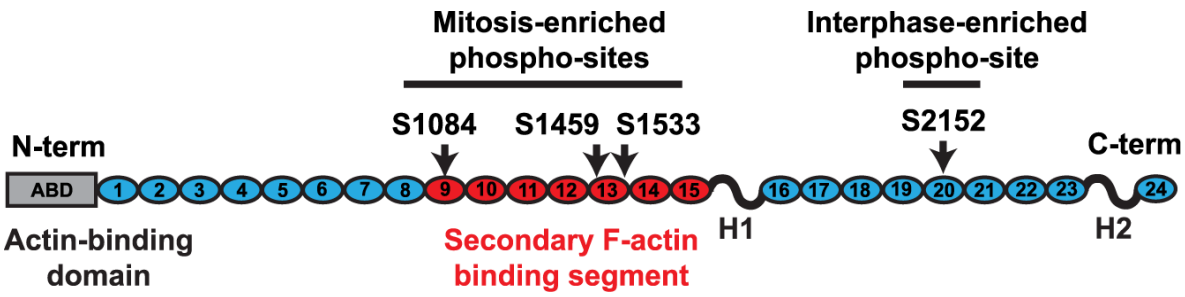
Mitosis-enriched
phospho-sites
Interphase-enriched
phospho-site
S1084
S1459
S1533
S2152
N-term
C-term
ABD
1
2
3
4
5
6
7
8
9
10
11
12
13
14
15
16
17
18
19
20
21
22
23
24
H1
H2
Actin-binding
domain
Secondary F-actin
binding segment

**Figure 3.6. Schematic of FLNa molecule with the location of FLNa phosphorylation sites identified from mass spectrometry.** All mitosis-enriched phosphorylation sites (S1084, S1459 and S1533) are located in a secondary F-actin binding segment (shown in red, repeats 9-15). Phospho-serine 2152 is enriched in interphase cells.

MSSSHSRAGQSAAGAAPGGGVDTRDAEMPATEKDLAEDAPWKKIQQNTFTRWCNEHLKCVSK
RIANLQTDLSDGLRLIALLEVLSQKKMHRKHNQRPTFRQMQLENVSVALEFLDRESIKLVSI
DSKAIVDGNLKLILGLIWTLILHYSISMPMWDEEEDEEAKKQTPKQRLLGWIQNKLPQLPIT
NFSRDWQSGRALGALVDSCAPGLCPDWDSWDASKPVTNAREAMQQADDWLGIPQVITPEEIV
DPNVDEHSVMTYLSQFPKAKLKPGAPLRPKLNPKKARAYGPGIEPTGNMVKKRAEFTVETRS
AGQGEVLVYVEDPAGHQEEAKVTANNDKNRTFSVWYVPEVTGTHKVTVLFAGQHIAKSPFEV
YVDKSQGDASKVTAQGPGLEPSGNIANKTTYFEIFTAGAGTGEVEVVIQDPMGQKGTVEPQL
EARGDSTYRCSYQPTMEGVHTVHVTFAGVPIPRSPYTVTVGQACNPSACRAVGRGLQPKGVR
VKETADFKVYTKGAGSGELKVTVKGPKGEERVKQKDLGDGVYGFEYYPMVPGTYIVTITWGG
QNIGRSPFEVKVGTECGNQKVRAWGPGLEGGVVGKSADFVVEAIGDDVGTLGFSVEGPSQAK
IECDDKGDGSCDVRYWPQEAGEYAVHVLCNSEDIRLSPFMADIRDAPQDFHPDRVKARGPGL
EKTGVAVNKPAEFTVDAKHGGKAPLRVQVQDNEGCPVEALVKDNGNGTYSCSYVPRKPVKHT
AMVSWGGVSIPNSPFRVNVGAGSHPNKVKVYGPGVAKTGLKAHEPTYFTVDCAEAGQGDVSI
GIKCAPGVVGPAEADIDFDIIRNDNDTFTVKYTPRGAGSYTIMVLFADQATPTSPIRVKVEP
SHDASKVKAEGPGLSRTGVELGKPTHFTVNAKAAGKGKLDVQFSGLTKGDAVRDVDIIDHHD
NTYTVKYTPVQQGPVGVNVTYGGDPIPKSPFSVAVSPSLDLSKIKVSGLGEKVDVGKDQEFT
VKSKGAGGQGKVASKIVGPSGAAVPCKVEPGLGADNSVVRFLPREEGPYEVEVTYDGVPVPG
SPFPLEAVAPTKPSKVKAFGPGLQGGSAGSPARFTIDTKGAGTGGLGLTVEGPCEAQLECLD
NGDGTCSVSYVPTEPGDYNINILFADTHIPGSPFKAHVVPCFDASKVKCSGPGLERATAGEV
GQFQVDCSSAGSAELTIEICSEAGLPAEVYIQDHGDGTHTITYIPLCPGAYTVTIKYGGQPV
PNFPSKLQVEPAVDTSGVQCYGPGIEGQGVFREATTEFSVDARALTQTGGPHVKARVANPSG
NLTETYVQDRGDGMYKVEYTPYEEGLHSVDVTYDGSPVPSSPFQVPVTEGCDPSRVRVHGPG
IQSGTTNKPNKFTVETRGAGTGGLGLAVEGPSEAKMSCMDNKDGSCSVEYIPYEAGTYSLNV
TYGGHQVPGSPFKVPVHDVTDASKVKCSGPGLSPGMVRANLPQSFQVDTSKAGVAPLQVKVQ
GPKGLVEPVDVVDNADGTQTVNYVPSREGPYSISVLYGDEEVPRSPFKVKVLPTHDASKVKA
SGPGLNTTGVPASLPVEFTIDAKDAGEGLLAVQITDPEGKPKKTHIQDNHDGTYTVAYVPDV
TGRYTILIKYGGDEIPFSPYRVRAVPTGDASKCTVTGAGIGPTIQIGEETVITVDTKAAGKG
KVTCTVCTPDGSEVDVDVVENEDGTFDIFYTAPQPGKYVICVRFGGEHVPNSPFQVTALAGD
QPSVQPPLRSQQLAPQYTYAQGGQQTWAPERPLVGVNGLDVTSLRPFDLVIPFTIKKGEITG
EVRMPSGKVAQPTITDNKDGTVTVRYAPSEAGLHEMDIRYDNMHIPGSPLQFYVDYVNCGHV
TAYGPGLTHGVVNKPATFTVNTKDAGEGGLSLAIEGPSKAEISCTDNQDGTCSVSYLPVLPG
DYSILVKYNEQHVPGSPFTARVTGDDSMRMSHLKVGSAADIPINISETDLSLLTATVVPPSG
REEPCLLKRLRNGHVGISFVPKETGEHLVHVKKNGQHVASSPIPVVISQSEIGDASRVRVSG
QGLHEGHTFEPAEFIIDTRDAGYGGLSLSIEGPSKVDINTEDLEDGTCR*VTYCPTEPGNYII*
NIKFADQHVPGSPFSVKVTGEGRVKESITRRRRAPSVANVGSHCDLSLKIPEISIQDMTAQV
TSPSGKTHEAEIVEGENHTYCIRFVPAEMGTHTVSVKYKGQHVPGSPFQFTVGPLGEGGAHK
VRAGGPGLERAEAGVPAEFSIWTREAGAGGLAIAVEGPSKAEISFEDRKDGSCGVAYVVQEP
GDYEVSVKFNEEHIPDSPFVVPVASPSGDARRLTVSSLQESGLKVNQPASFAVSLNGAKGAI
DAKVHSPSGALEECYVTEIDQDKYAVRFIPRENGVYLIDVKFNGTHIPGSPFKIRVGEPGHG
GDPGLVSAYGAGLEGGVTGNPAEFVVNTSNAGAGALSVTIDGPSKVKMDCQECPEGYRVTYT
PMAPGSYLISIKYGGPYHIGGSPFKAKVTGPRLVSNHSLHETSSVFVDSLTKATCAPQHGAP
GPGPADASKVVAKGLGLSKAYVGQKSSFTVDCSKAGNNMLLVGVHGPRTPCEEILVKHVGSR
LYSVSYLLKDKGEYTLVVKWGDEHIPGSPYRVVVP

**Figure 3.7. Sequence coverage of FLNa from mass spectrometry.** Peptides detected by mass spectrometry covered 68.4% of FLNa's amino acid sequence. Residues highlighted in grey were covered.

### 3.3.5 FLNa is phosphorylated by Cdk1 on serines 1084, 1459 and 1533

We next determined whether our p-FLNa antibody had reactivity against serines 1084, 1459 and 1533. The p-FLNa antibody recognizes an *in vitro* phosphorylated fragment of FLNa containing FLNa repeats 8-15 (IgFLNa 8-15 WT) (Figure 3.8, A and B), and when the three serines are mutated to nonphosphorylatable alanine residues (IgFLNa 8-15 AAA) it is recognized less well (Figure 3.8B, right). Furthermore, *in vitro* phosphorylation of these FLNa fragments in the presence of γ [$^{32}$P]ATP also confirms that IgFLNa 8-15 AAA is phosphorylated to a lesser extent than IgFLNa 8-15 WT (Figure 3.8C).

To confirm that serines 1084, 1459 and 1533 are phosphorylated *in vivo*, we mutated these sites to alanine in full-length FLNa with a C-terminal GFP tag. FLNa-WT GFP and FLNa-AAA GFP were stably expressed in FLNa-deficient M2 melanoma cells so that the GFP-tagged proteins were the only source of FLNa in the cell. Consistent with our *in vitro* findings (Figure 3.1), p-FLNa is only detectable in mitotic (nocodazole-treated) and not asynchronous (DMSO-treated) cells (Figure 3.8D). Importantly, lower levels of p-FLNa were detected in lysates from FLNa-AAA GFP-expressing cells compared to FLNa-WT GFP-expressing cells (Figure 3.8D, left panel). Unexpectedly, a p-FLNa band was also detected in the GFP EV control in mitotic cells (Figure 3.8D, left panel). However, the p-FLNa antibody has non-specific affinity for a protein approximately the same size as GFP FLNa because immunoprecipitation of FLNa from these cells does not pull down a protein that is recognized very well by the p-FLNa antibody in the GFP EV control (Figure 3.8E). As shown in Figure 3.8D, the immunoprecipitated FLNa-AAA GFP is phosphorylated less than FLNa-WT GFP (Figure 3.8E). Similar results were obtained when GFP FLNa was immunoprecipitated with a GFP antibody (GFP Trap A). The GFP antibody immunoprecipitates FLNa that is detected less well by the p-FLNa antibody in FLNa-AAA

GFP-expressing cell lines compared to FLNa-WT GFP-expressing cell lines (Figure 3.8F). Taken together, the results show that serines 1084, 1459 and 1533 are *bona fide* mitotic phosphorylation sites, although additional phosphorylation sites likely exist.

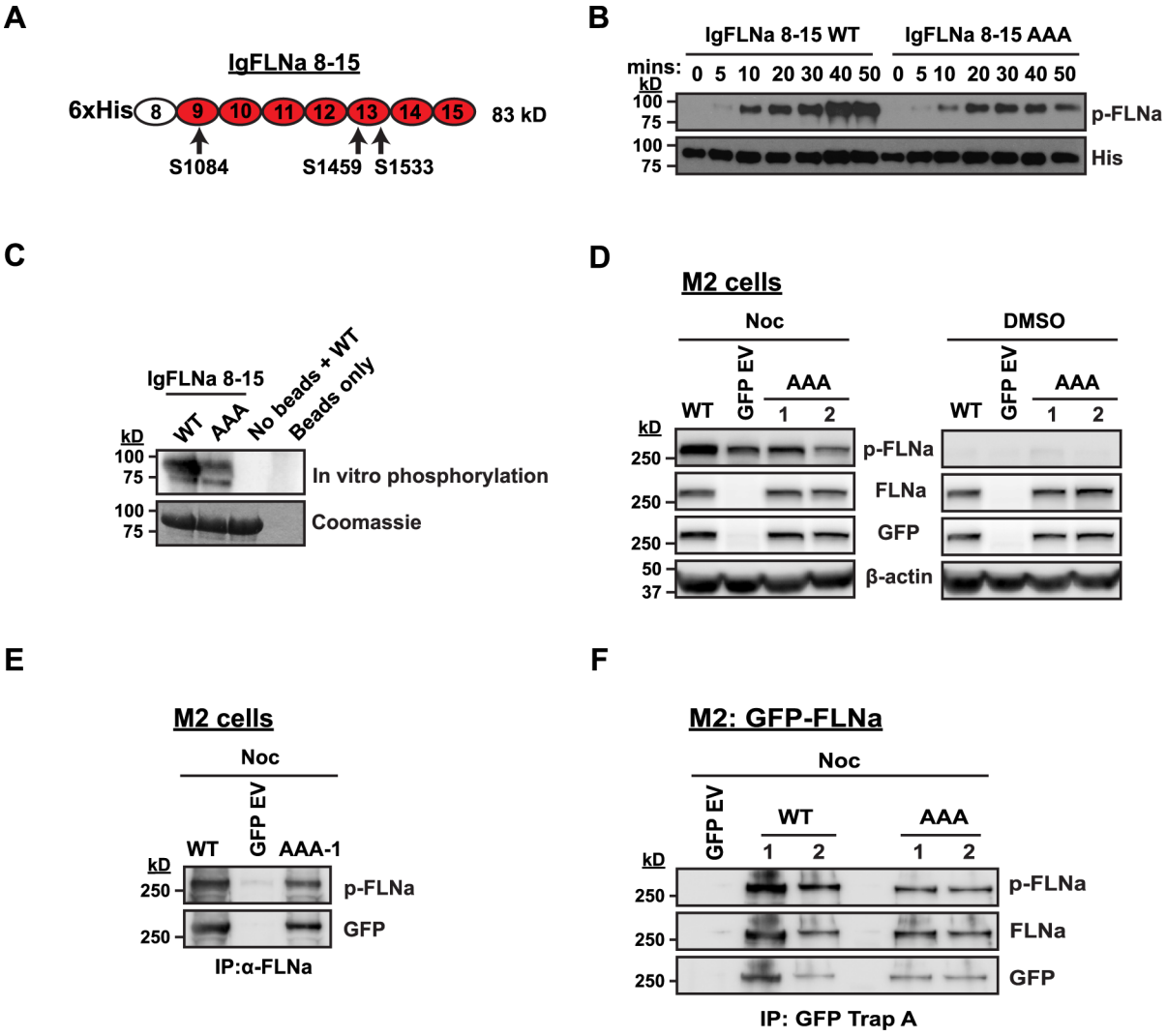
A
IgFLNa 8-15
6xHis
8
9
10
11
12
13
14
15
83 kD
S1084
S1459
S1533
B
IgFLNa 8-15 WT
IgFLNa 8-15 AAA
mins: 0 5 10 20 30 40 50 0 5 10 20 30 40 50
kD
100
75
p-FLNa
His
C
IgFLNa 8-15
WT
AAA
No beads + WT
Beads only
In vitro phosphorylation
Coomassie
D
M2 cells
Noc
DMSO
GFP EV
AAA
WT
1
2
p-FLNa
FLNa
GFP
β-actin
E
M2 cells
Noc
GFP EV
WT
AAA-1
p-FLNa
GFP
IP:α-FLNa
F
M2: GFP-FLNa
Noc
GFP EV
WT
AAA
p-FLNa
FLNa
GFP
IP: GFP Trap A

**Figure 3.8. FLNa is phosphorylated by Cdk1/cyclin B1 on serines 1084, 1459 and 1533 in mitosis. (A)** Schematic of recombinant His-FLNa fragment IgFLNa8-15. The secondary F-actin binding segment is shown in red. **(B)** Timecourse of IgFLNa8-15 (WT AAA) phosphorylation by immunopurified Cdk1/cyclin B1. IgFLNa8-15 AAA detection by the p-FLNa antibody is decreased compared to IgFLNa8-15 WT. **(C)** In vitro phosphorylation with Cdk1/cyclin B1 in the presence of γ [$^{32}$P]ATP shows R8-15 AAA is phosphorylated to a lesser extent than WT. **(D)** FLNa expression levels in M2 cell lines expressing FLNa-WT GFP, FLNa-AAA GFP and GFP EV. In nocodazole-treated cells, p-FLNa detection is lower in AAA cell lines than WT. **(E)** Immunoprecipitation of FLNa-WT GFP and FLNa-AAA GFP from mitotic M2 cells using α-FLNa antibody. FLNa-AAA GFP detection by p-FLNa antibody is lower compared to WT. **(F)** FLNa AAA GFP immunoprecipitated from mitotic M2 cells with a portion of the GFP antibody bound to beads (GFP-Trap A) is detected at a lower level by the p-FLNa antibody.

### 3.3.6 Summary

Using a p-FLNa antibody that was raised against FLNa p-S1436, an *in vitro* phosphorylation site previously identified by our lab, we have shown that FLNa is phosphorylated *in vivo* in mitotic HeLa cells. FLNa serines 1084, 1459 and 1533 were identified as mitosis-enriched phosphorylation sites in HeLa cells using quantitative mass spectrometry. The p-FLNa antibody still detects cells expressing FLNa-AAA GFP, but to a lesser extent than FLNa-WT GFP, suggesting the antibody recognizes multiple Cdk1-generated epitopes *in vivo*, including serines 1084, 1459 and 1533. This suggests that while serines 1084, 1459 and 1533 are *bona fide* sites, other mitotic phosphorylation sites also exist.

## 3.4 DISCUSSION.

### 3.4.1 Cdk1/cyclin B1 phosphorylates FLNa on serines 1084, 1459 and 1533

We have identified serines 1084, 1459 and 1533 as mitosis-enriched phosphorylation sites. p-S2152 was identified as an interphase phosphorylation site. Multiple kinases are activated at or before mitosis. These include Cdk1 and members of the Polo, Aurora and NEK families (Nigg, 2001). It is possible that any of these kinases could be phosphorylating FLNa. However, serines 1084, 1459 and 1533 are found in sequences that perfectly match the Cdk1 phosphorylation consensus sequences (Table 3.1) and their mutation to non-phosphorylatable alanine reduces phosphorylation in vitro (Figure. 3.8, B and C). As such, it is most likely that these serines are phosphorylated by Cdk1/cyclin B1 rather than by other mitotic kinases.

### 3.4.2 Literature on FLNa phospho-sites in mitotic HeLa cells

FLNa p-S1084, p-S1459 and p-S1533 were identified in the present study as *in vivo* phosphorylation sites. FLNa p-S1436, p-S1533 and p-S1630 were previously identified as *in vitro* Cdk1 phosphorylation sites (Cukier et al., 2007). To determine if these were novel sites, we used "PhosphoSitePlus", an online tool that allows you to view all known phosphorylation sites for a specific protein and the references linked to the identification of that site. Almost all of the studies that identified these sites were from phospho-proteome studies using mass spectrometry. Interestingly, one report identified p-S1084 and p-S1459 in a large-scale characterization of HeLa cell nuclear phosphoproteins (Beausoleil et al., 2004). p-S1084, p-S1459 and p-S1533 were identified as mitosis-enriched phosphorylation sites in HeLa cells in a study by Dephoure et al. (2008) and two years later a very similar study by Olsen et al. (2010) identified the same three sites and p-S1630 as well. In another study, phospho-proteome analysis of purified mitotic spindles from HeLa S3 cells again identified

FLNa p-S1084 (Nousiainen et al., 2006). This study localized a total of 736 phosphorylation sites in 260 proteins, including 312 sites in 72 known spindle proteins (Nousiainen et al., 2006). However, in all of the reports, FLNa was not specifically investigated, nor was it mentioned in the text. The only report that had functional data on these sites was from our lab in the paper by Cukier et al. (2007). Therefore, functional relevance of these sites is currently unknown and warrants further investigation. Surprisingly, none of these proteome-wide studies identified p-S1436 using MS and this is consistent with our results.

### 3.4.3 Discrepancy between *in vitro* and *in vivo* FLNa phosphorylation sites in mitosis

We previously identified serines 1436, 1533 and 1630 as in vitro Cdk1/cyclin B1 phosphorylation sites (Cukier et al., 1992). Mitotic M2 cells expressing FLNa-WT and FLNa-S1436G had similar p-FLNa levels (Figure 3.3B). It is possible that mutation of one phosphorylation site is not enough to dramatically reduce p-FLNa antibody binding to an extent it can be seen on a Western blot, however, the lack of published reports on the existence of p-S1436 *in vivo* suggest that S1436 may not be phosphorylated *in vivo*. Our failure to detect serine 1436 and 1630 phosphorylation *in vivo* may be due to their low abundance relative to non-phosphorylated peptides, poor ionizability, and neutral loss of the phosphate at these sites (Boersema et al., 2009). It is possible that p-S1436 and p-S1630 were not detected due to higher susceptibility to phosphatase activity during sample preparation compared to p-S1084, p-S1459 and p-S1533. On the other hand, it is also possible p-S1084, p-S1459 and p-S1533 were phosphorylated after cell lysis, allowing Ser/Thr kinases to inappropriately phosphorylate FLNa. Another possibility is that the spectrum of FLNa residues phosphorylated by Cdk1 *in vitro* may be different in intact mitotic cells.

### 3.4.4 The p-FLNa antibody recognizes multiple mitotic epitopes on FLNa

Using FLNa-AAA mutants (IgFLNa8-15AAA fragment and full-length FLNa-AAA GFP) we showed that the p-FLNa antibody recognizes mitotic FLNa sites in addition to p-S1084, p-S1459 and p-S1533 (Figure 3.8). The ability of our p-FLNa antibody to recognize multiple phospho-residues on FLNa is not surprising since Cdk1 epitopes are highly conserved. Other phospho-antibodies share this property. For example, the widely available monoclonal mpm2 antibody recognizes mitotic Cdk1-generated epitopes on many different proteins and in many different cell types (Kuang and Ashorn, 1993). Furthermore, all of the FLNa repeats (domains) exhibit a canonical immunoglobulin-like domain fold (Page et al., 2011). Combined with the similarity between different Cdk1 phosphorylation consensus sites, different epitopes may be recognized by the p-FLNa antibody. In addition, the antibody was generated from the immunization of a rabbit, a process that generates polyclonal antibodies. Compared to monoclonal antibodies, polyclonal antibodies recognize different antigens and have different affinities for the same epitope (Lipman et al., 2005).

### 3.4.5 The p-FLNa antibody likely has nonspecific binding to p-FLNb

Prior to using the p-FLNa antibody, titrations were performed to determine the optimal concentration (dilution) that resulted in minimal background on Western blots and immunofluorescence. The optimal dilution was determined to be 1:50 000–1:100 000 for Western blots and 1:1 000 for immunofluorescence. The normal dilution range is 1:1000-1:20 000 for Western blots and 1:50-1:200 for immunofluorescence, suggesting the p-FLNa antibody has higher than average nonspecific binding. However, background was only observed in mitotic cell lysate and not interphase cell lysate (data not shown), therefore at high concentrations, the p-FLNa antibody likely recognizes Cdk1-generated epitopes on

multiple proteins in mitosis. In immunofluorescence, background staining was always observed in mitotic FLNa-deficient M2 cells, even when the antibody was titrated (data not shown). Therefore the p-FLNa seems to have some cross-reactivity with phosphorylated FLNb, which is expressed at low levels in M2 cells. This is evident in Figure 3.8D, where a p-FLNa band is observed in mitotic M2 cells (GFP EV). FLNa GFP and FLNb could not be resolved by SDS-PAGE; therefore FLNa GFP was immunoprecipitated using anti-FLNa-beads and GFP Trap A (Figure 3.8, E and F). Both results show a reduction in p-FLNa detection in immunoprecipitated FLNa-AAA GFP compared to FLNa-WT GFP (Figure 3.8, E and F), showing the p-FLNa antibody detects FLNa p-S1084, p-S1459 and p-S1533.

### 3.4.6 We estimate that FLNa is stoichiometrically phosphorylated in mitosis

We found that at least 66% of total cellular FLNa is likely to be phosphorylated in mitosis. (Figure 3.5). However, the actual amount of phosphorylated FLNa in a cell is likely higher because all of the FLNa from the control immunoprecipitation should have been non-immunoprecipitable with the p-FLNa antibody (100%), while only 81% was (Figure 3.5B), therefore there is about 19% error in our control. This error is probably due non-specific binding of FLNa or p-FLNa to beads because FLNa (and cytoskeletal proteins in general) is frequently found as a sepharose-bead contaminant in MS co-immunoprecipitation (Co-IP) experiments (Trinkle-Mulcahy et al., 2008). In this experiment, it is also worthwhile to note that the bead control was not bound to Normal mouse IgG. In other experiments, we have observed that FLNa is less frequently found as a contaminant when cell lysate is incubated with Normal mouse IgG-beads instead of beads alone. Therefore FLNa may be more prone to bind to beads alone than antibody-bound beads. It is possible the Normal mouse IgG blocks sites on sepharose beads that nonspecifically bind FLNa and other contaminants.

We also believe our estimate that 66% of FLNa is phosphorylated is a low due to inherent experimental errors. The cell lysate was obtained from mitotic HeLa cells but a small number of interphase cells were likely harvested as well. In addition, some sites on FLNa may have been dephosphorylated during sample preparation. Because nocodazole arrests cells in prometaphase of mitosis, 66% refers to the percentage of FLNa phosphorylated at prometaphase. Thus, it is possible that *in vivo* much more than 66% of FLNa is phosphorylated during mitosis.

### 3.4.7 p-FLNa is dephosphorylated at the end of mitosis

Using immunofluorescence to observe p-FLNa in various stages of mitosis, we noticed that global p-FLNa intensity was much lower in anaphase and telophase, compared to in prophase (Figure 3.4). The decrease in p-FLNa levels can be due to two reasons: proteolytic degradation or dephosphorylation.

Proteolytic degradation would most likely be mediated by the anaphase-promoting complex (APC), an E3 ubiquitin ligase that targets proteins for proteasomal degradation, since many cell cycle-regulated proteins are degraded through this pathway (Pfleger and Kirschner, 2000; Manchado et al., 2010). However, we eliminated this possibility based on the following evidence. **1.** FLNa does not contain a destruction box (D-box) or a KEN box, both of which are recognition signals for the APC (Yamano et al., 1998; Pfleger and Kirschner, 2000; Glickman and Ciechanover, 2002). **2.** Western blots show that total FLNa levels do not change during the cell cycle (Figure 3.2, A and B). **3.** Treatment of mitotic cells with the 26S proteasome inhibitor, MG132, did not stabilize p-FLNa levels on Western blot (data not shown), suggesting p-FLNa is not degraded by the 26S proteasome.

Based on this evidence, we reasoned that p-FLNa is likely dephosphorylated. Dephosphorylation at anaphase onset is also consistent with Cdk1/cyclin B1 substrates whose phosphorylation-dependent functions are no longer needed when cells exit mitosis. Indeed, treatment of mitotic cells with okadaic acid, a PP1 and PP2A inhibitor, inhibited p-FLNa dephosphorylation as cells exited mitosis and re-entered G1 (Figure 3.2C). This suggests PP1 or PP2A dephosphorylates FLNa either directly or indirectly *in vivo*. PP1 and PP2A are major serine/threonine phosphatases in mammalian cells (Colbran, 2004). PP1 is composed of a catalytic subunit ($PP1_C$) and a regulatory subunit that dictates substrate specificity and subcellular localization (Katayose et al., 2000). PP2A is a heterotrimeric complex composed of a catalytic subunit bound to regulatory subunits A and B. The A-subunit links the catalytic subunit to any number of different B-subunits that dictate substrate recognition and subcellular localization (Katayose et al., 2000). There are greater than 40 known PP1 regulatory subunits and it is estimated that greater than 60 heterotrimeric PP2A complexes can be generated by all the permutations of its subunits (Colbran, 2004). Based on this knowledge, we decided not to pursue the identity of the regulatory subunits that confer FLNa specificity to PP1 and PP2A. Nonetheless, our results suggest that FLNa phosphorylation has a specific function from mitotic onset until anaphase, after which p-FLNa levels decline.

# CHAPTER 4 FILAMIN A PHOSPHORYLATION REGULATES ITS SUBCELLULAR LOCALIZATION AND IS IMPORTANT FOR CELL SEPARATION AND INTERPHASE CELL BEHAVIOUR

## 4.1 ABSTRACT

Prior to mitosis, mammalian cells undergo substantial actin cytoskeleton rearrangement as they detach from the extracellular matrix and become spherical. At the end of mitosis the actin cytoskeleton is also required for cytokinesis and the reassembly of interphase structures as cells spread and reattach to substrate. To understand the processes regulating mitotic cytoskeletal remodelling, we studied how mitotic phosphorylation regulates filamin A (FLNa). Using a p-FLNa antibody that detects cyclin-dependent kinase 1 (Cdk1)-generated epitopes, we find that p-FLNa has decreased cortical actin localization compared to total FLNa in mitotic cells. To investigate the functional role of mitotic FLNa phosphorylation, we mutated serines 1084, 1459 and 1533 to nonphosphorylatable alanine residues and expressed FLNa-S1084A, S1459A, S1533A (FLNa-AAA GFP) in FLNa-deficient human M2 melanoma cells. FLNa-AAA GFP cells have enhanced FLNa-AAA GFP and actin localization at sites of contact between daughter cells, impaired post-mitotic daughter cell separation and defects in cell migration. Therefore, mitotic delocalization of cortical FLNa is important for successful cell division and interphase cell behaviour.

## 4.2 INTRODUCTION

Mitotic cells are more spherical and compact than their interphase counterparts; this is due to substantial actin cytoskeleton rearrangement that occurs during the rounding up process that accompanies mitotic entry. Mitotic cell rounding is a complex process that involves the disassembly of focal adhesion complexes, decreased attachment with the extracellular matrix (ECM), actin cytoskeleton remodelling and increased cortical actin rigidity (Revel et al., 1974; Maddox and Burridge, 2003; Théry and Bornens, 2008). At the end of mitosis, actin remodelling is also required for cytokinesis, and for post-mitotic cell spreading and substrate reattachment. How cells achieve these cell cycle-dependent changes in the cytoskeleton is poorly understood. Actin cytoskeletal changes also facilitate chromosome segregation and positioning of the cytokinetic furrow; however, the mechanisms regulating this process are also largely unknown (Glotzer, 2001; Maddox and Burridge, 2003).

FLNa is involved in many cellular processes, including cell migration (Calderwood et al., 2001; Baldassarre et al., 2009), cell-cell adhesion (Kanters et al., 2008; Griffiths et al., 2010), integrin-mediated adhesion (D'Addario et al., 2001; Tu et al., 2003; Gehler et al., 2009), signal transduction (Glogauer et al., 1998; Gehler et al., 2009) and plasma membrane integrity (Cunningham, 1995; Charras et al., 2005). M2 cells (human melanoma cell line) that are deficient in FLNa have reduced motility and an unstable plasma membrane that leads to the frequent appearance of cell blebs; expression of FLNa rescues these defects (Cunningham, 1995; Charras et al., 2005).

The FLNa protein consists of a high-affinity actin-binding domain (ABD) at its N-terminus, followed by 24 tandem immunoglobulin (Ig)-like repeats, each with an average of

96 amino acids. A secondary F-actin-binding segment in repeats 9-15 is necessary for high avidity F-actin binding (Nakamura et al., 2007).

FLNa function is highly regulated by phosphorylation. In addition to Cdk1/cyclin B1, p21-activated kinase 1 (Pak1) (Vadlamudi et al., 2002), p90 ribosomal S6 protein kinase (p90 RSK) (Woo et al., 2004), cAMP-dependent protein kinase (cAMP-kinase) (Chen and Stracher, 1989; Jay et al., 2000), protein kinase Cα (PKCα) (Tigges et al., 2003) and $Ca^{2+}$/calmodulin-dependent protein kinase II (CaM kinase II) (Ohta and Hartwig, 1995) all phosphorylate FLNa *in vitro*. *In situ* phosphorylation of FLNa by cAMP- kinase increases its resistance to calpain cleavage (Chen and Stracher, 1989) and *in vivo*, Pak1-mediated phosphorylation of FLNa on serine 2152 leads to actin cytoskeletal reorganization and Pak1-dependent membrane ruffling (Vadlamudi et al., 2002). Phosphorylation at S2152 by p90 RSK, a key kinase in the Ras-mitogen-activated protein kinase pathway, is also required for cell migration regulation (Ohta and Hartwig, 1996; Woo et al., 2004). Phosphorylation also appears to regulate FLNa binding to F-actin. Phosphorylation of chicken gizzard filamin and FLNa by CaM kinase II (Ohta and Hartwig, 1995) and Cdk1/cyclin B1 (Cukier et al., 2007), respectively, decreases F-actin gelation *in vitro*.

FLNa S2152 is the most characterized phosphorylation site and is important in cytoskeletal organization. However, FLNa contains many sites for phosphorylation, including 10 Cdk1 phosphorylation consensus sites and 19 minimum (Ser/Thr)-Pro motifs (Chapter 3, Table 3.1). The functional relevance of these phosphorylation sites is unknown.

In chapter 3, we showed that FLNa is phosphorylated by Cdk1/cyclin B1 on serines 1084, 1459 and 1533 *in vivo*. **My next objective is to determine the functional relevance of FLNa phosphorylation by Cdk1/cyclin B1.** In this chapter, we show that phosphorylated

FLNa has decreased subcellular localization to the cortex compared to total FLNa in HeLa cells. However, Cdk1 phosphorylation does not affect the ability of FLNa to bind F-actin *in vitro*, suggesting phosphorylation may indirectly impact FLNa interaction with cortical actin. We further show that inhibition of FLNa phosphorylation on S1084, S1459 and S1533 (FLNa-AAA GFP) leads to impaired post-mitotic daughter cell separation, enhanced FLNa-AAA GFP localization at sites of contact between daughter cells and defects in cell migration.

## 4.3 RESULTS

### 4.3.1 Actin structures are different in interphase and mitotic HeLa cells

When mammalian cells enter mitosis, they detach from the ECM and alter their cell shape. Interphase HeLa cells have a spread-out, slightly elongated morphology that is characterized by distinct actin-containing structures such as focal adhesions, stress fibres (Figure 4.1A, arrow labeled S) and filopodia (Figure 4.1A, arrow labeled F). Mitotic cells, on the other hand, have a spherical morphology that lack stress fibres and focal adhesions. Instead of filopodia, cells display prominent retraction fibres (Figure 4.1B, arrow labeled R), which are remnants of former adhesion sites that resist cell margin regression prior to mitotic onset (Maddox and Burridge, 2003; Théry and Bornens, 2008). In both interphase and mitotic cells, FLNa is found at the cell cortex where it colocalizes with cortical actin (Figure 4.1, A and B, arrows labeled C). These alterations in cell shape and actin structures also occur in FLNa-deficient M2 cells (Figure 4.1C) and suggest actin remodelling occurs when cells enter mitosis.

A

HeLa: Interphase

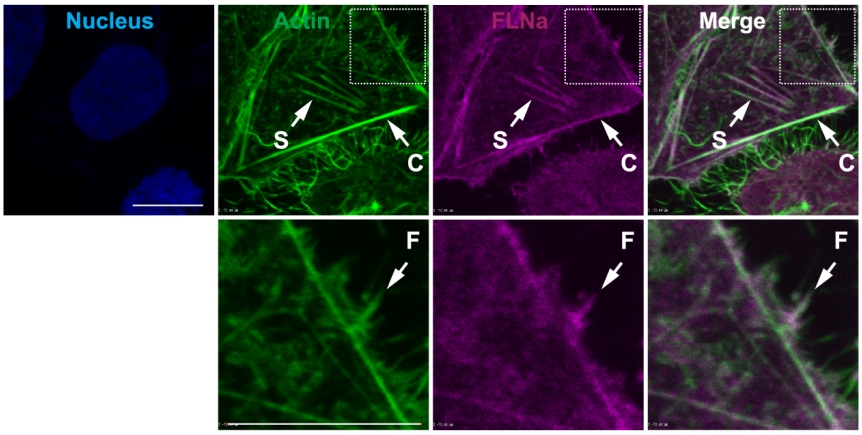


B

HeLa: Mitosis

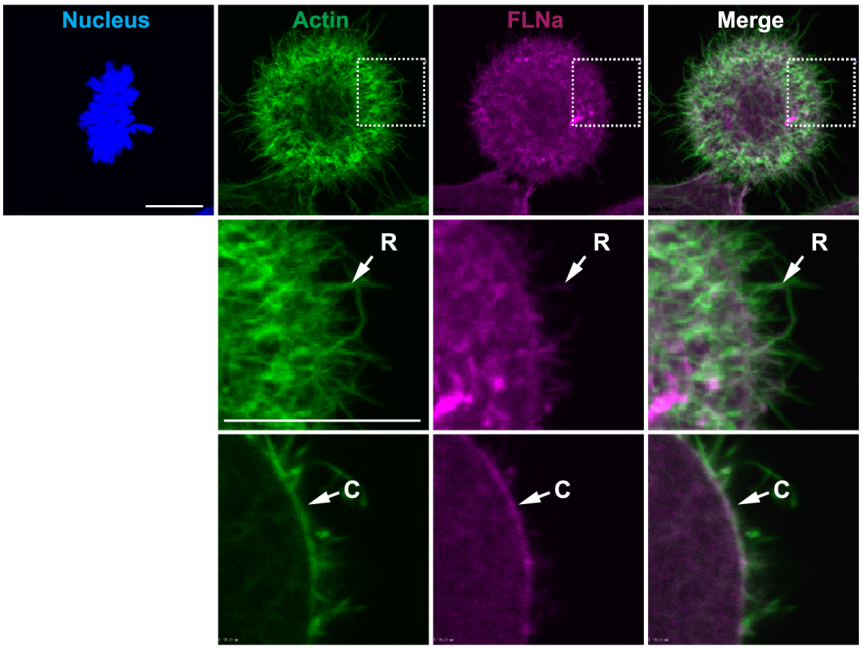


C

M2 cells

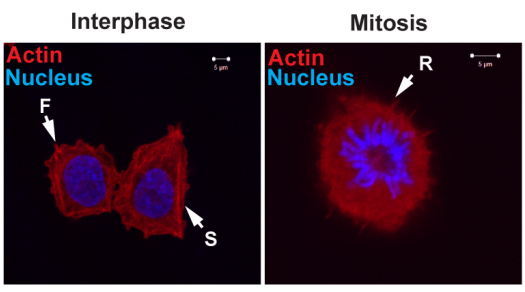

**Figure 4.1. Interphase and mitotic HeLa and M2 cells have distinct actin structures. (A**) In interphase FLNa is localized to the cell cortex (C), base of filopodia (F, enlarged area) and stress fibres (S). Single Z-slices (0.25 μm thick) are shown. **(B)** In mitotic cells, FLNa is localized to the base of retraction fibres (R) and the cell cortex (C). First two rows of images in A and B are compiled Z-stacks. Last row of images in A and B consist of a single Z-slice. Merge panel shows FLNa and actin colocalization in white. Scale bar, 10 μm. Immunofluorescence images are of fixed cells. **(C)** During mitotic entry, M2 cells adopt a rounded morphology. Stress fibers (arrow, S) and filopodia (arrow, F) are prominent in interphase cells. In mitotic cells, retraction fibers (arrow, R) are observed. Scale bar, 5 μm. Immunofluorescence images are of fixed cells. *Note: Jonathan M. Lee performed experiment for panel C; see Contributions of Collaborators*.

### 4.3.2 Effect of FLNa phosphorylation by Cdk1/cyclin B1 on F-actin binding

#### 4.3.2.1 p-FLNa appears to colocalize less with actin

To assess the effect of FLNa phosphorylation on F-actin binding, we first examined the localization of endogenous p-FLNa with actin in fixed mitotic HeLa cells. As a control we observed the localization of total FLNa in both mitotic and interphase cells in the same field of view. As mentioned previously, total FLNa colocalizes with actin structures in both interphase and mitotic cells (Figure 4.1, Figure 4.2, top panel). In confocal images of compiled Z-stacks (all Z-slices combined into one image), p-FLNa is observed in mitotic and not interphase cells; however, it does not appear to colocalize as well with actin in mitotic cells (Figure 4.2, middle panel, merge). Total FLNa in mitotic cells also have decreased colocalization with actin compared to total FLNa with actin in interphase cells (Figure 4.2, top panel, merge). Based on these preliminary observations we hypothesized that mitotic FLNa phosphorylation decreases the ability of FLNa to bind F-actin. Decreased FLNa binding to actin at mitotic entry could allow the actin filament network to undergo actin rearrangement.

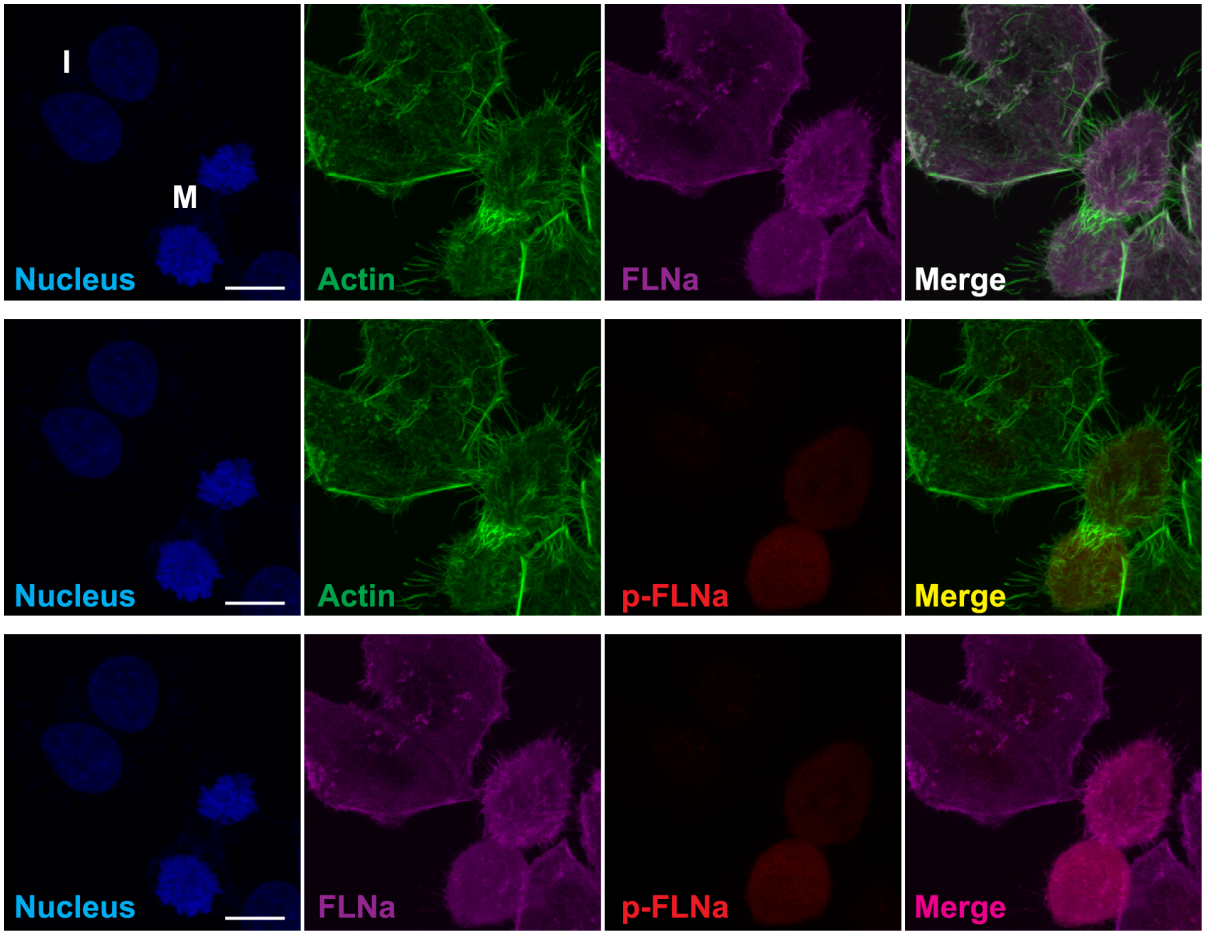
I
M
Nucleus
Actin
FLNa
Merge
Nucleus
Actin
p-FLNa
Merge
Nucleus
FLNa
p-FLNa
Merge

**Figure 4.2. In mitotic HeLa cells, p-FLNa colocalizes less well with actin than total FLNa with actin.** Two interphase (I) and two mitotic (M) cells are shown in the same field of view for comparison. Confocal images are compiled Z-stacks. Scale bar, 10 μm. Immunofluorescence images are of fixed cells.

#### 4.3.2.2 The secondary F-actin-binding segment does not significantly bind F-actin *in vitro*

Serines 1084, 1459 and 1533 are all located within the secondary F-actin-binding segment on FLNa repeats 9-15 (Chapter 3, Figure 3.6). One simple hypothesis is that phosphorylation of serines 1084, 1459 and 1533 affect F-actin interaction with the secondary F-actin binding segment and poor actin binding may contribute to mitotic changes to the cytoskeleton.

In order to test the relative contribution of the ABD and dimerization domain (repeat 24) to F-actin binding we purified the following recombinant His-FLNa fragments: the secondary F-actin-binding segment (IgFLNa 8-15), IgFLNa 8-15 fused to the ABD (ABD-IgFLNa 8-15), IgFLNa 8-15 fused to R24 (IgFLNa 8-15+24) and IgFLNa 8-15 fused to both the ABD and R24 (ABD-IgFLNa 8-15+24) (Figure 4.3A). F-actin cosedimentation assays were performed to assess F-actin binding and changes after *in vitro* phosphorylation with immunopurified Cdk1/cyclin B1. In the absence of phosphorylation, 60% of ABD-IgFLNa 8-15+24 cosediments with F-actin in the pellet fraction (Figure 4.3B), while 45% of the ABD-IgFLNa 8-15 fragment and 14% of the IgFLNa 8-15+24 fragment cosediments with F-actin (Figure 4.3, B and C). Interestingly, there is no significant shift ($p=0.24$) of IgFLNa 8-15 to the pellet fraction in the presence of F-actin compared to protein alone (Figure 4.3E). This shows that IgFLNa 8-15 (WT), by itself, does not bind to F-actin. IgFLNa 8-15AAA (S1084A, S1459A, S1533A) also does not bind F-actin ($p=0.40$) (Figure 4.3F), indicating S1084A, S1459A and S1533A mutations do not affect F-actin binding in the absence of phosphorylation.

A

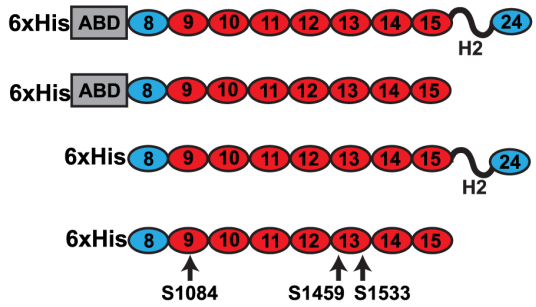


B

ABD-IgFLNa 8-15+24

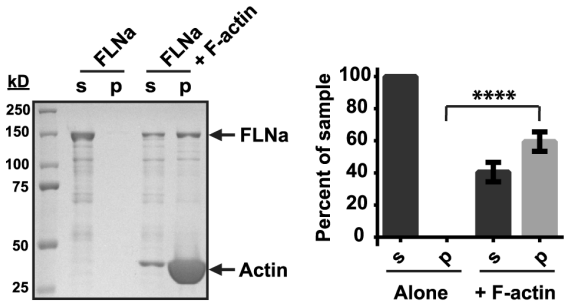


C

ABD-IgFLNa 8-15

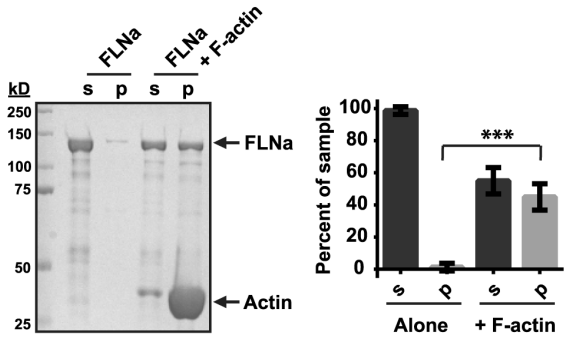


D

IgFLNa 8-15+24

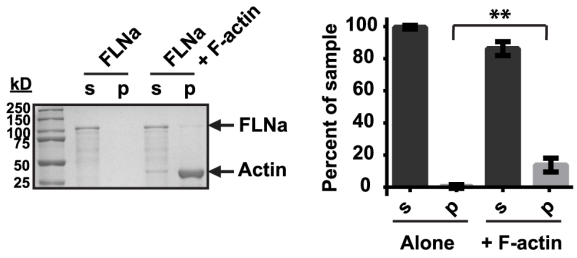


E

IgFLNa 8-15 WT

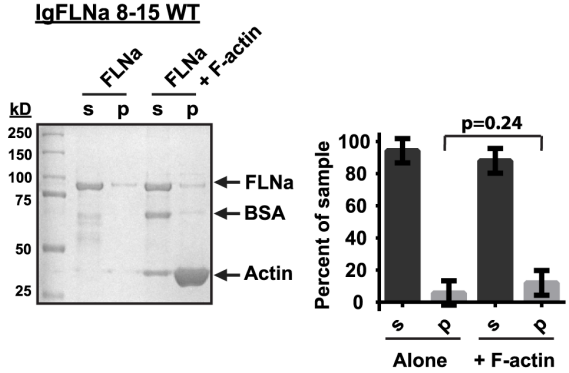


F

IgFLNa 8-15 AAA

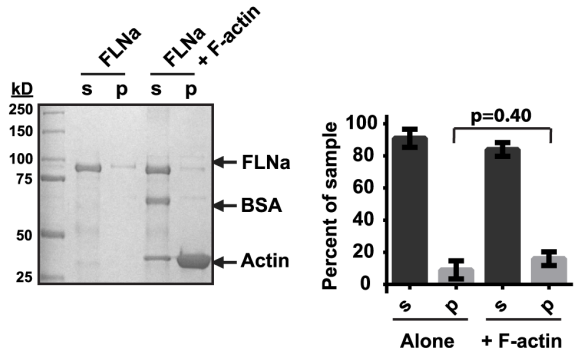

**Figure 4.3. The secondary F-actin-binding segment does not significantly bind F-actin.** **(A)** Schematic of recombinant His-FLNa constructs purified from *E.coli*. **(B-F)** F-actin cosedimentation assays of nonphosphorylated recombinant His-FLNa fragments. SDS-PAGE of supernatant (s) and pellet (p) fractions show the shift of ABD-IgFLNa8-15+24, IgFLNa8-15+24 and ABD-IgFLNa8-15 from the supernatant to the pellet fraction when incubated in the presence of F-actin. Densitometry of gel bands is shown on the right. Representative gels are shown. **** $p<0.0001$, *** $p<0.001$, ** $p<0.01$ (student's t-test, two-tailed). Quantifications of gel bands were calculated from three independent experiments using ImageJ 1.47v software.

#### 4.3.2.3 Phosphorylation of the secondary F-actin binding segment does not affect overall F-actin binding *in vitro*

Next, we tested if Cdk1/cyclin B1 phosphorylation of these fragments alters their binding to F-actin. All four fragments can be phosphorylated by immunopurified Cdk1/cyclin B1 *in vitro* (Figure 4.4A) and we previously showed that IgFLNa 8-15 AAA is phosphorylated less than IgFLNa 8-15 WT (Chapter 3, Figure 3.8B). However, we find that phosphorylation does not significantly affect the ability of any of the fragments to bind F-actin (Figure 4.4, B-E). As shown in Coomassie gels, there is no apparent change in the band of FLNa in the pellet and supernatant fractions in the presence and absence of phosphorylation (Figure 4.4, B-E, gels). Quantification of the shift of FLNa to the pellet fraction in the presence of F-actin shows no statistically significant difference between unphosphorylated and phosphorylated protein (Figure 4.4, B-E, graphs). We conclude, therefore, that Cdk1/cyclin B1 phosphorylation of FLNa on serines 1084, 1459 and 1533 does not substantially affect association with F-actin *in vitro*.

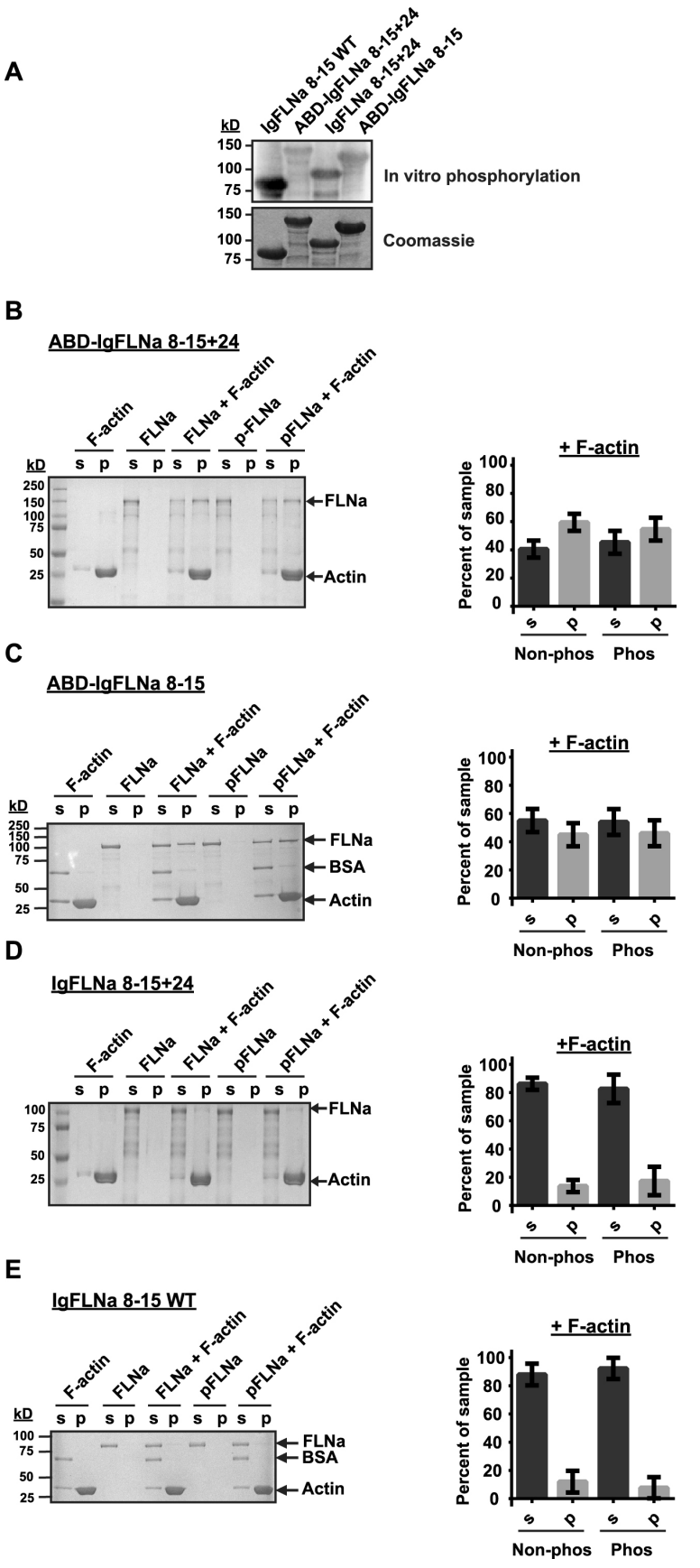
A
IgFLNa 8-15 WT
ABD-IgFLNa 8-15+24
IgFLNa 8-15+24
ABD-IgFLNa 8-15
kD
150
100
75
In vitro phosphorylation
Coomassie
B
ABD-IgFLNa 8-15+24
F-actin
FLNa
FLNa + F-actin
p-FLNa
pFLNa + F-actin
s p
250
150
100
75
50
25
FLNa
Actin
+ F-actin
Percent of sample
Non-phos
Phos
C
ABD-IgFLNa 8-15
BSA
D
IgFLNa 8-15+24
+F-actin
E
IgFLNa 8-15 WT

**Figure 4.4. Cdk1/cyclin B1 phosphorylation of recombinant His-FLNa constructs does not alter F-actin interaction *in vitro*. (A)** *In vitro* phosphorylation of IgFLNa 8-15 WT, ABD-IgFLNa 8-15+24, IgFLNa 8-15+24 and ABD-IgFLNa 8-15 by Cdk1/cyclin B1 in the presence of γ[$^{32}$P]ATP. **(B-E)** F-actin cosedimentation assays of nonphosphorylated (non-phos) and Cdk1-phosphorylated (phos) recombinant His-FLNa fragments in the presence and absence of F-actin. Densitometry of gel bands is shown on the right. Representative gels are shown. Quantifications of gel bands were calculated from three independent experiments and ImageJ 1.47v software. *Note, panel A was prepared by Elizabeth C. Williams; see Contributions of Collaborators*.

#### 4.3.2.4 Phosphorylation of full-length FLNa does not significantly alter F-actin binding *in vitro*

We also examined changes in the ability of full-length FLNa to cosediment with F-actin when phosphorylated by Cdk1/cyclin B1 *in vitro*. Immunopurified endogenous FLNa from asynchronous (interphase) HeLa cells is primarily found in the pellet fraction in a F-actin cosedimentation assay and is not detected by the p-FLNa antibody (Figure 4.5A, middle lanes). When interphase HeLa FLNa is *in vitro* phosphorylated by immunopurified Cdk1/cyclin B1 we observe no changes in the fraction of FLNa in the pellet and supernatant fractions compared to nonphosphorylated FLNa (Figure 4.5A, middle lanes). Furthermore, we observe no changes in the ability of recombinant full-length FLNa to cosediment with F-actin in the presence or absence of Cdk1/cyclin B1 phosphorylation *in vitro* (Figure 4.5B). Increasing the amount of recombinant full-length FLNa used in the assay also did not alter F-actin binding (Figure 4.5B).

**A**

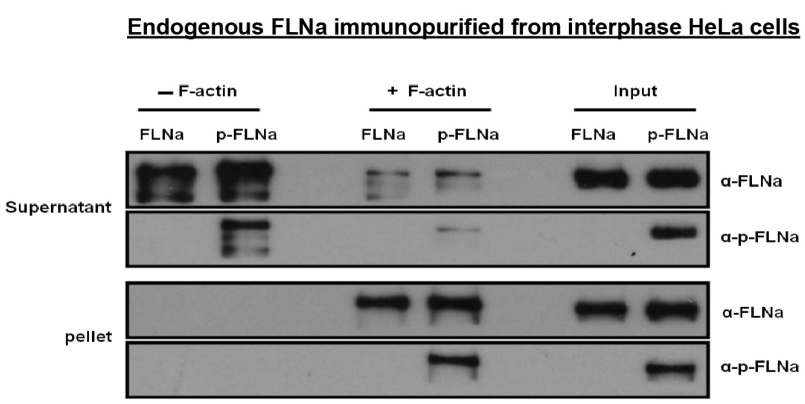
Endogenous FLNa immunopurified from interphase HeLa cells
– F-actin
+ F-actin
Input
FLNa
p-FLNa
FLNa
p-FLNa
FLNa
p-FLNa
Supernatant
α-FLNa
α-p-FLNa
pellet
α-FLNa
α-p-FLNa

**B**

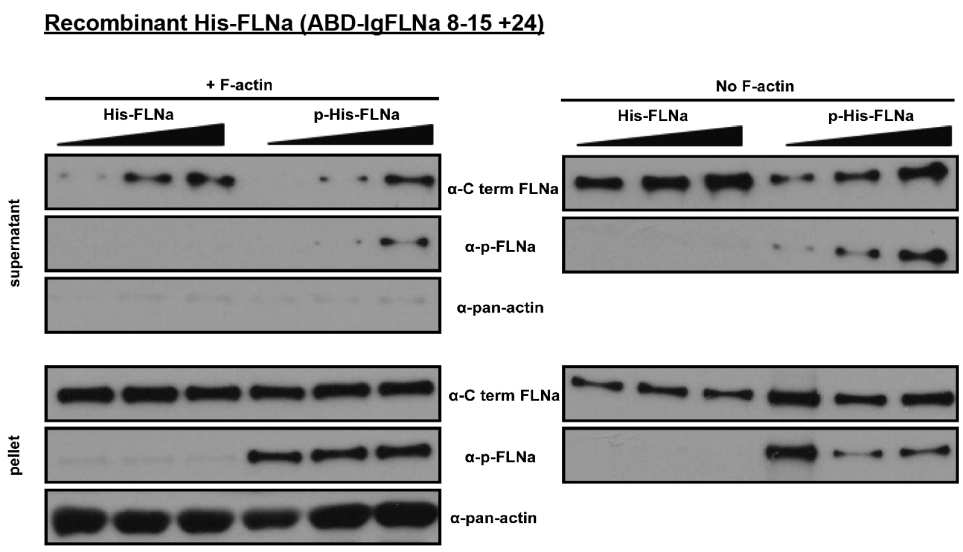
Recombinant His-FLNa (ABD-IgFLNa 8-15 +24)
+ F-actin
No F-actin
His-FLNa
p-His-FLNa
His-FLNa
p-His-FLNa
supernatant
α-C term FLNa
α-p-FLNa
α-pan-actin
pellet
α-C term FLNa
α-p-FLNa
α-pan-actin

**Figure 4.5. Phosphorylation of endogenous FLNa from interphase HeLa cells and recombinant full-length His-FLNa with Cdk1/cyclin B1 does not alter its ability to cosediment with F-actin *in vitro*. (A)** Endogenous interphase FLNa was immunoprecipitated and incubated with Cdk1/cyclin B1-beads or beads alone to obtain phosphorylated and nonphosphorylated FLNa, respectively. **(B)** Furthermore, phosphorylation by Cdk1/cyclin B1 also does not alter the ability of recombinant full-length FLNa to cosediment with F-actin *in vitro*.

### 4.3.3 FLNa-WT GFP and FLNa-AAA GFP localize to prominent actin structures in interphase M2 and HeLa cells.

To determine the functional importance of S1084, S1459 and S1533 phosphorylation on FLNa function *in vivo*, we mutated these sites to nonphosphorylatable alanine residues in full-length FLNa with a C-terminal GFP tag. FLNa-WT GFP and FLNa-AAA GFP were stably expressed in FLNa-deficient M2 melanoma cells so that the GFP-tagged proteins were the only source of FLNa in the cell. As a control, cells were transfected with a FLNa variant that lacks the N-terminal ABD (FLNa-ΔABD GFP) and is defective in F-actin binding. Expression of exogenous protein was confirmed by Western blot (Figure 4.6).

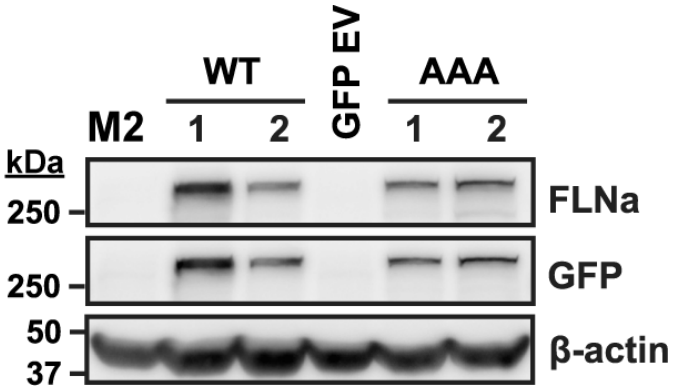
WT
GFP EV
AAA
M2
1
2
1
2
kDa
250
FLNa
250
GFP
50
37
β-actin

**Figure 4.6. Expression of FLNa-WT GFP, FLNa-AAA GFP and GFP (EV) in stable M2 cell lines.** M2 is nontransfected. β-actin was probed as a loading control.

We observed the localization of FLNa-WT GFP and FLNa-AAA GFP in these stable M2 cell lines. FLNa-WT GFP and FLNa-AAA GFP both colocalize with actin at the cortex and the base of filopodia in interphase cells (Figure 4.7A, enlarged areas, white arrows labeled C and F). FLNa-ΔABD GFP retains some localization with cortical actin and filopodia but has altered cytosolic localization compared to FLNa-WT GFP and FLNa-AAA GFP (Figure 4.7A, white arrows labeled C and F). M2 cells expressing GFP EV shows poor localization of GFP with cortical actin (Figure 4.7A, blue arrows labeled C). Because serines 1084, 1459 and 1533 are unphosphorylated during interphase we were not surprised that FLNa-WT GFP and FLNa-AAA GFP localize to similar structures in interphase M2 cells.

To corroborate these observations, FLNa-WT GFP and FLNa-AAA GFP were transiently transfected into HeLa cells. Similar in M2 cells, FLNa-WT GFP and FLNa-AAA GFP show the same localization at the cortex and the base of filopodia (Figure 4.7B, white arrows labeled C and F). FLNa-WT GFP and FLNa-AAA GFP also shows localization on actin stress fibres, which are abundant in HeLa cells (Figure 4.7B, white arrows labeled S). The localization of exogenous FLNa is similar to the localization of endogenous FLNa in interphase HeLa cells (Figure 4.1A). HeLa cells expressing FLNa-ΔABD GFP and GFP EV controls show poor localization with actin (Figure 4.7B, blue arrows). Overall, these results show that FLNa-WT GFP and FLNa-AAA GFP both localize to actin structures in M2 and HeLa cells, as expected.

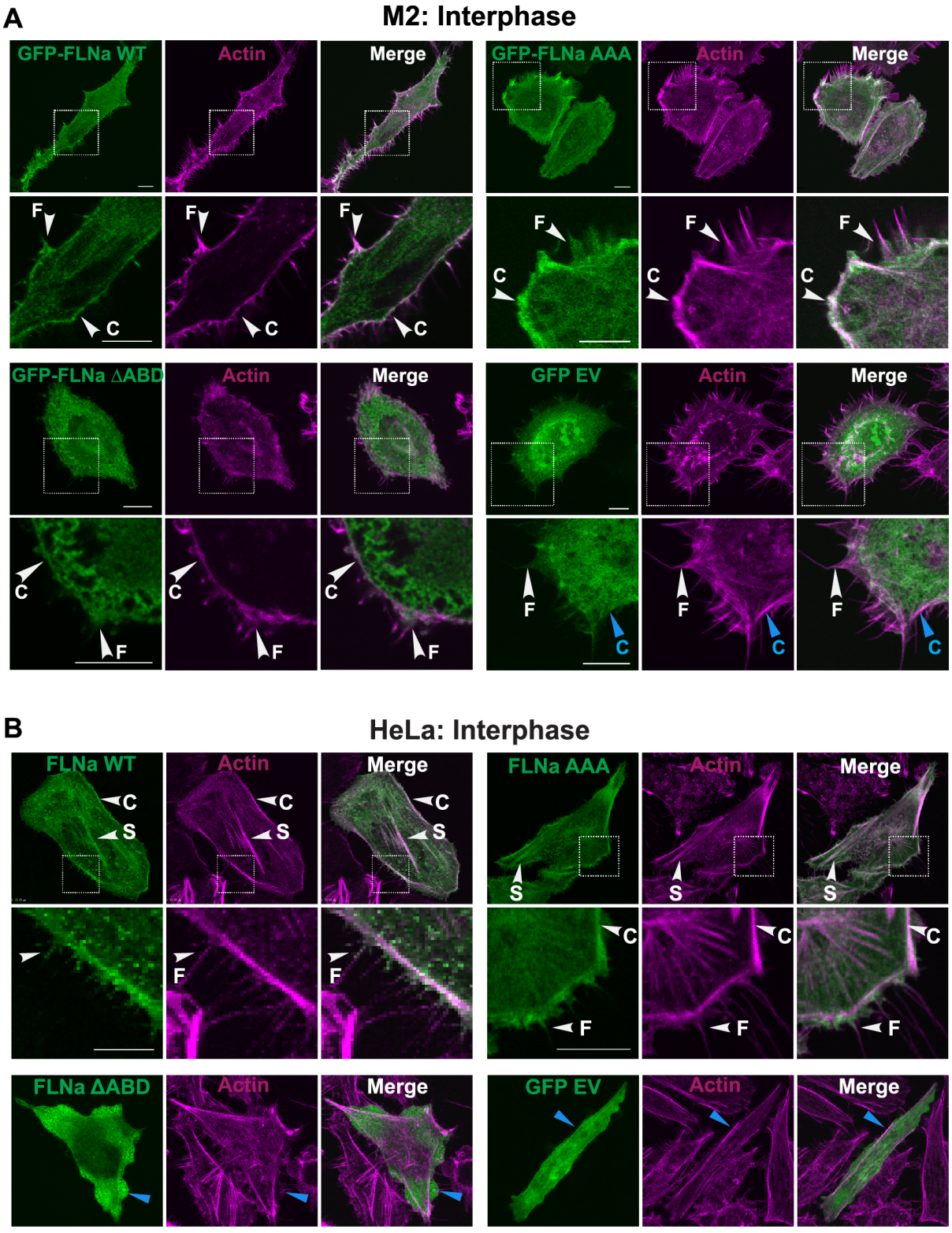
A
M2: Interphase
GFP-FLNa WT
Actin
Merge
GFP-FLNa AAA
GFP-FLNa ΔABD
GFP EV
F
C
B
HeLa: Interphase
FLNa WT
FLNa AAA
FLNa ΔABD
S

**Figure 4.7. FLNa-WT GFP and FLNa-AAA GFP localize to actin structures in interphase M2 and HeLa cells. (A)** In interphase M2 cells, FLNa-WT GFP and FLNa-AAA GFP colocalize with actin at the base of filopodia (white arrows, F) and in the cortex (white arrows, C). M2 cells expressing GFP EV show poor localization with cortical actin (blue arrows and merge panel). FLNa-ΔABD GFP has some localization with actin structures (white arrows, C and F) but has altered cytosolic localization. Confocal images of whole cells are compiled Z-stacks. Enlarged areas are single Z-slices (0.25 μm thick). Scale bar, 10 μm. Immunofluorescence images are of fixed cells. **(B)** In interphase HeLa cells, FLNa-WT GFP and FLNa-AAA GFP colocalize with actin at the base of filopodia (white arrows, F), at the cortex (white arrows, C) and in stress fibres (white arrow, S). HeLa cells expressing FLNa-ΔABD GFP and GFP EV show poor localization with actin (blue arrows). Confocal mages of entire cells are compiled Z-stacks. Enlarged areas are single Z-slices (0.25 μm thick). Scale bar, 10 μm. Immunofluorescence images are of fixed cells.

### 4.3.4 FLNa-WT GFP and FLNa-AAA GFP localize to the cortex in mitotic M2 and HeLa cells

Next we examined the localization of FLNa-WT GFP and FLNa-AAA GFP in mitotic M2 and HeLa cells. We previously showed that FLNa-WT GFP and FLNa-AAA GFP are phosphorylated during mitosis in M2 cells (Chapter 3, Figure 3.8, D-F). In mitotic M2 cells we also find no dramatic differences in the localization of FLNa-AAA GFP and FLNa-WT GFP (Figure 4.8A, enlarged areas). Both FLNa-WT GFP and FLNa-AAA GFP localize at the cortex (Figure 4.8A, white arrows labeled C) and the base of retraction fibres (Figure 4.8A, white arrows labeled R). Again, similar localization patterns for endogenous FLNa in mitotic HeLa cells (Figure 4.1B) and exogenous FLNa (FLNa-WT GFP and FLNa-AAA GFP) were observed in HeLa cells (Figure 4.7B). GFP protein, on its own, does not colocalize with cortical actin in mitotic M2 and HeLa cells (Figure 4.8, A and B, blue arrows). These results are consistent with our *in vitro* F-actin cosedimentation assay results that show Cdk1 phosphorylation of recombinant His-FLNa fragments does not significantly alter F-actin binding (Figure 4.4, B-E).

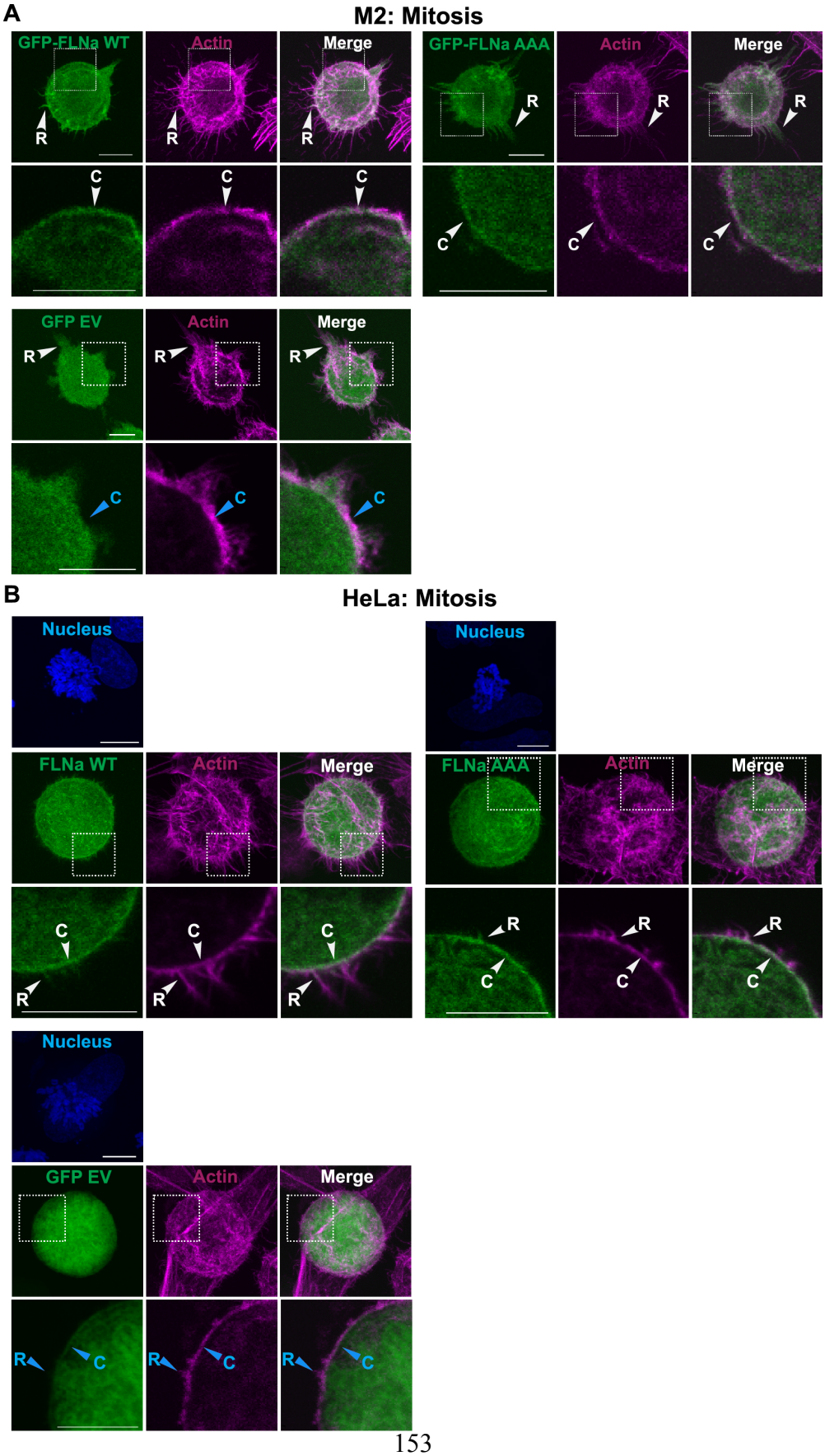
A
M2: Mitosis
GFP-FLNa WT
Actin
Merge
GFP-FLNa AAA
Actin
Merge
R
C
GFP EV
Actin
Merge
B
HeLa: Mitosis
Nucleus
Nucleus
FLNa WT
Actin
Merge
FLNa AAA
Actin
Merge
Nucleus
GFP EV
Actin
Merge

**Figure 4.8. FLNa-WT GFP and FLNa-AAA GFP localize to the cortex in mitotic M2 and HeLa cells. (A)** Mitotic M2 cells expressing FLNa-WT GFP and FLNa-AAA GFP show similar localization of FLNa with actin at the base of retraction fibres (white arrow, R) and the cell cortex (white arrow, C) compared to the GFP EV control which does not localize to the cortex (blue arrow, C). Confocal images of whole cells are compiled Z-stacks. Enlarged areas are single Z-slices (0.25 μm thick). Scale bar, 10 μm. Immunofluorescence images are of fixed cells. **(B)** Mitotic HeLa cells expressing FLNa-WT GFP and FLNa-AAA GFP show similar localization of FLNa with actin at the base of retraction fibres (white arrows, R) and the cell cortex (white arrow, C) compared to the GFP EV control which does not localize to these actin structures (blue arrows, R and C). Confocal mages of entire cells are compiled Z-stacks. Enlarged areas are single Z-slices (0.25 μm thick). Scale bar, 10 μm. Immunofluorescence images are of fixed cells.

### 4.3.5 p-FLNa localization at the cortex decreases as cells progress through mitosis

We next decided to re-examine the localization of endogenous p-FLNa in mitotic HeLa cells in more detail in individual Z-slices of confocal images (thickness of each Z-slice is 0.25 μm). Using the p-FLNa antibody we observed the localization of endogenous p-FLNa relative to total FLNa within stages of mitosis in HeLa cells. In prophase, when p-FLNa levels peak (Chapter 3, Figure 3.4B), FLNa and p-FLNa have the same localization at the cell cortex, in the cytoplasm and at the base of retraction fibres (Figure 4.9A). Quantification of FLNa and p-FLNa fluorescence intensity across a linear segment of the cell shows a similar localization profile with peaks in FLNa and p-FLNa signal intensity at the cell cortex (Figure 4.9A, graph). As discussed in Chapter 3, we believe that FLNa is stoichiometrically phosphorylated. In metaphase and anaphase cells p-FLNa has decreased cortical localization compared to total FLNa (Figure 4.9, B and C, enlarged areas). Relative to prophase p-FLNa intensity, in metaphase and anaphase p-FLNa intensity is decreased by almost half (Figure 4.9, A-C graphs). Note that in metaphase and anaphase images the intensity of the p-FLNa signal was linearly increased post-image acquisition to facilitate visualization; relative levels of p-FLNa fluorescence intensity are shown in Chapter 3, Figure 3.4B. The quantification of p-FLNa signal intensity reflects the non-adjusted intensity. These results suggest that Cdk1-mediated phosphorylation of FLNa causes p-FLNa to dissociate from the cell cortex during mitotic progression.

**A**

Prophase

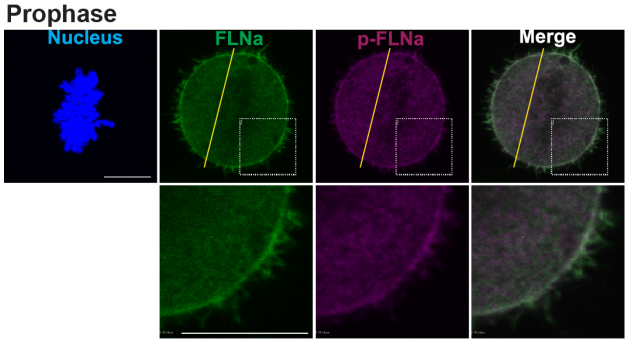


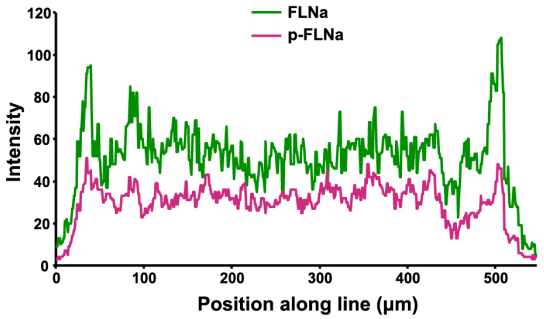


**B**

Metaphase

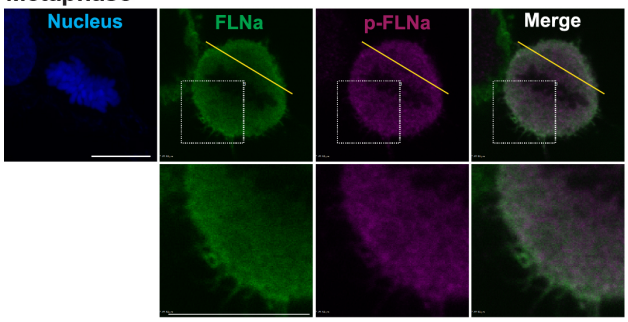


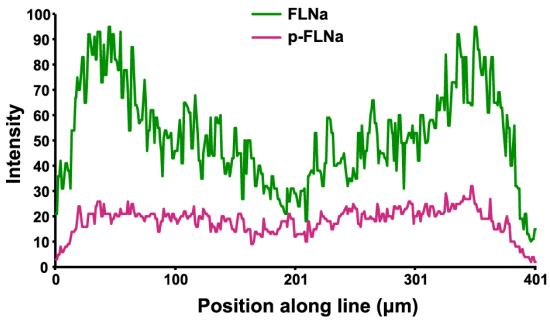


**C**

Anaphase

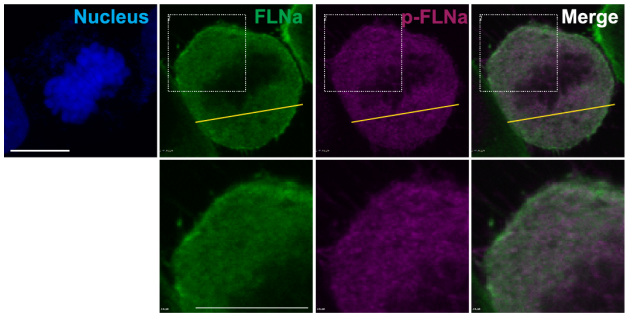


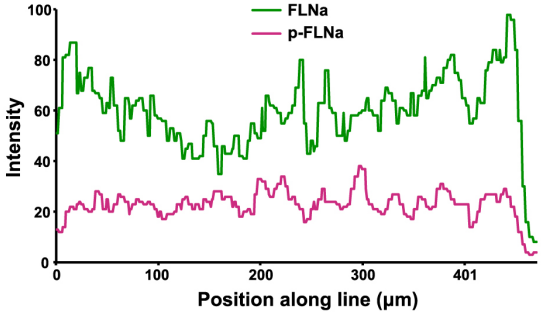

**Figure 4.9. p-FLNa delocalizes from the cortex during mitotic progression in HeLa cells. (A)** FLNa and p-FLNa localization in prophase. **(B)** FLNa and p-FLNa localization in metaphase. **(C)** FLNa and p-FLNa localization in anaphase. Note that in metaphase and anaphase images the intensity of the p-FLNa signal was linearly increased post-image acquisition to facilitate visualization; relative levels of p-FLNa fluorescence intensity are shown in Chapter3, Figure 3.4B. Quantification of fluorescence signal intensity across a linear segment of the cell (yellow line) is shown on the right. For quantification, p-FLNa intensity was not increased. FLNa, green; p-FLNa, magenta. Confocal images are of single Z -slices (each 0.25 μm thick). Scale bar, 10 μm. Immunofluorescence images are of fixed cells.

### 4.3.6 After mitosis, the majority of FLNa-AAA GFP daughter cells fail to separate and FLNa-AAA GFP is enriched at sites of cell-cell contact

Based on our observation that p-FLNa delocalizes from the cortex as cells progress through mitosis, we carefully examined the localization of FLNa-WT GFP and FLNa-AAA GFP in stable M2 cell lines during mitotic progression and cytokinesis. Consistent with the localization of FLNa-WT GFP and FLNa-AAA GFP in fixed M2 interphase cells (Figure 4.7A), time-lapse images show that both FLNa-WT GFP and FLNa-AAA GFP localize to the base of pseudopodia and the cortex during interphase (Figure 4.10A, yellow arrows; Videos 1 and 2). However, we observed that cells expressing FLNa-AAA GFP tend to remain attached after mitosis, while FLNa-WT GFP cells separate. FLNa-WT GFP daughter cells separate in approximately 30 min after the appearance of the cleavage furrow and then begin to elongate (Figure 4.10A; Videos 1 and 3). On the other hand, the majority of FLNa-AAA GFP daughter cells remain attached for at least six hours after the appearance of the cleavage furrow and do not elongate (Figure 4.10A; Videos 2 and 4). Quantification shows that 79% of FLNa-WT GFP cells separate, compared to only 24% of FLNa-AAA GFP cells (Figure 4.10B). Furthermore, we often observe FLNa-AAA GFP enriched at sites of cell-cell contact between daughter cells that do not separate (Figure 4.10A, red arrows).

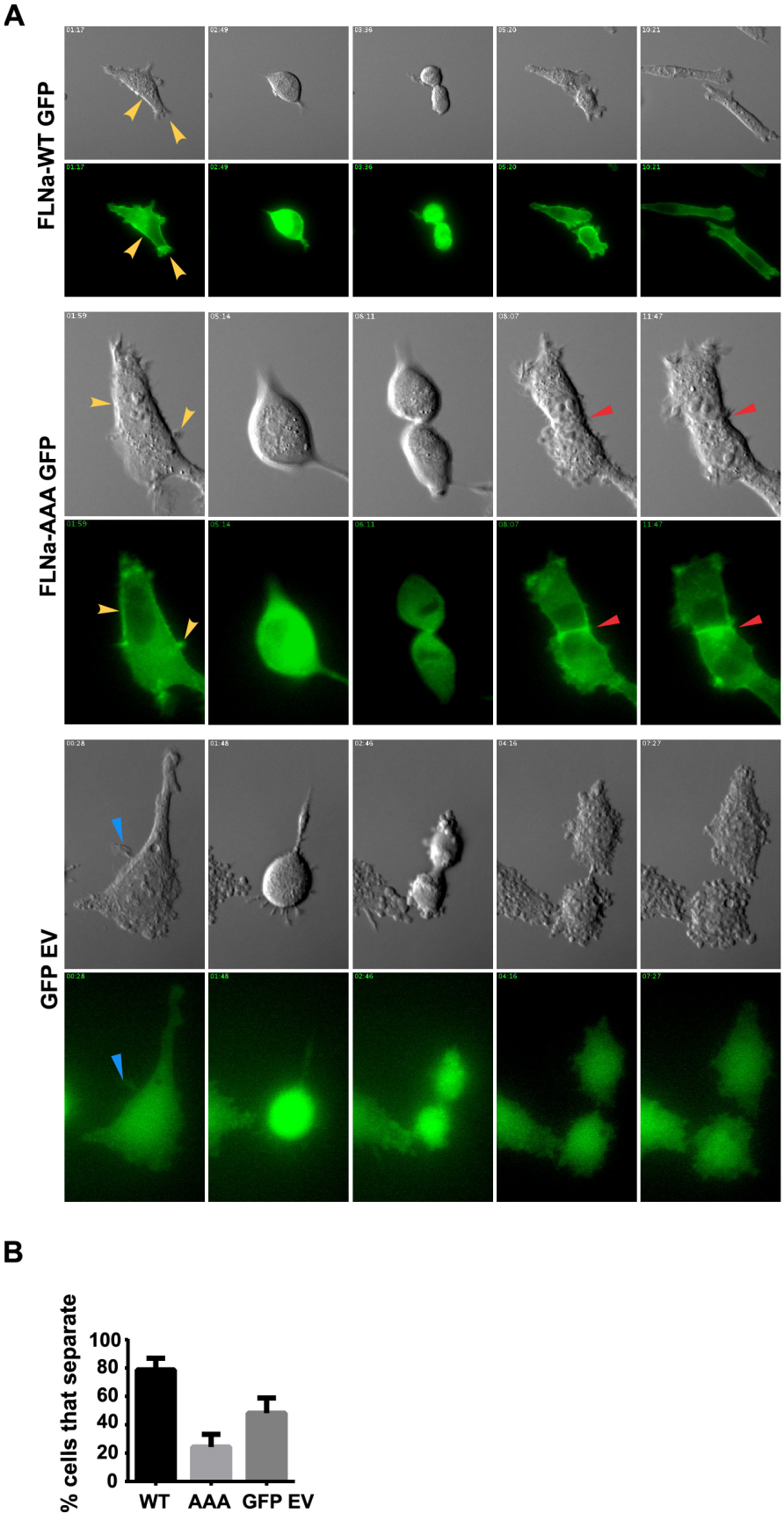
A
FLNa-WT GFP
FLNa-AAA GFP
GFP EV
B
% cells that separate
100
80
60
40
20
0
WT
AAA
GFP EV

**Figure 4.10. FLNa-AAA GFP-expressing M2 cells tend to remain attached after mitosis and FLNa-AAA GFP is enriched at sites of cell-cell contact between daughter cells. (A)** Time-lapse images (differential interference contrast and fluorescence) of cells undergoing mitosis. In interphase (frame 1), FLNa-WT GFP and FLNa-AAA GFP are localized to protrusive actin structures and the cortex (yellow arrows). In GFP EV cells, GFP is diffusely localized (blue arrows). After mitosis, FLNa-AAA GFP is enriched at sites of cell-cell contact between daughter cells that did not separate (red arrows, frames 4 and 5). **(B)** Quantification of the percentage of cells that separate after mitosis. 79%, 24%, and 48% of FLNa-WT GFP, FLNa-AAA GFP and GFP EV-expressing cells separate, respectively. Total cells imaged for FLNa-WT GFP, FLNa-AAA GFP and GFP-expressing cells are 94, 90 and 83, respectively. Confidence intervals for WT, AAA and GFP EV are ± 8.28%, ± 8.87% and ± 10.75%, respectively at 95% confidence. *Note: Jonathan M. Lee performed time-lapse imaging and obtained data for panel B; see Contributions of Collaborators*.

When we image clustered cells with confocal microscopy we also observe enhanced localization of FLNa-AAA GFP and actin at cell-cell contact sites (Figure 4.11A, white arrows). In FLNa-WT GFP cells, however, we do not observe FLNa or actin enriched at sites of cell-cell contact (Figure 4.11A, yellow arrows). In HeLa cells, FLNa-AAA, but not FLNa-WT, is also observed at sites of cell-cell contact in clustered cells (Figure. 4.11B, white arrow). This suggests that the failure of FLNa-AAA GFP to be phosphorylated at mitosis enhances its ability to interact with cortical actin structures where cells contact each other.

**A** M2 cells

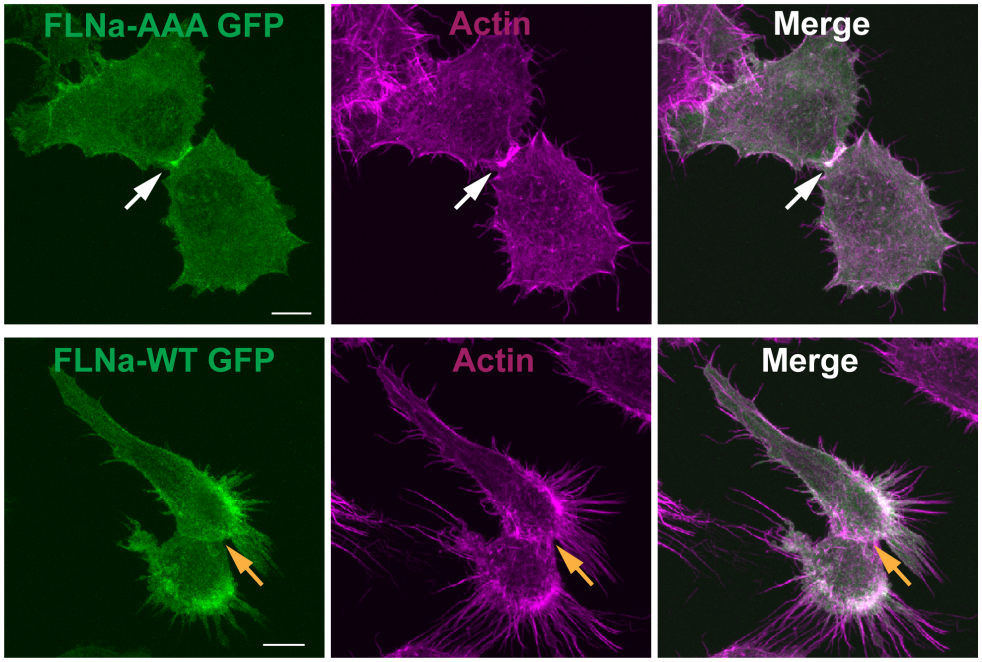


**B** HeLa cells

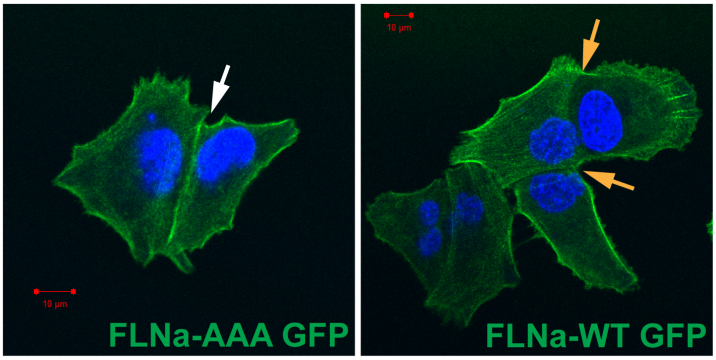

**Figure 4.11. FLNa-AAA GFP is enriched at sites of cell-cell contact in clustered M2 and HeLa cells. (A)** FLNa-AAA GFP and actin are enriched at sites of cell-cell contact in clustered M2 cells (white arrows). FLNa-WT GFP, on the other hand, is not enriched at sites of cell-cell contact in clustered cells (yellow arrows). Confocal images are of compiled Z-stacks. Scale bar, 10 μm. Immunofluorescence images are of fixed cells. **(B)** FLNa-AAA GFP, but not FLNa-WT GFP, is enriched at sites of cell-cell contact in a clustered of HeLa cells. Arrows point to sites of cell-cell contact. The nucleus is shown in blue. Confocal images are compiled Z-stacks. Scale bar, 5 μm. Immunofluorescence images are of fixed cells. *Note: Jonathan M. Lee performed experiment for panel B; see Contributions of Collaborators*.

### 4.3.7 FLNa-AAA GFP cells tend to form clusters and fail to elongate

The propensity for FLNa-AAA GFP-expressing M2 cells to remain attached translates into a cell-clustering phenotype that we often observed during cell culture. To quantify this phenotype we plated M2 cell lines and observed them a day later using phase contrast microscopy (Figure 4.12A). Quantification indicates 70-80% of FLNa-AAA GFP cells are found in clusters of two or more cells, compared to only 10-19% of FLNa-WT GFP cells (Figure 4.12A, graph). Control cell lines (GFP EV and M2 parental) have a cell clustering phenotype that is intermediate between that of FLNa-WT GFP and FLNa-AAA GFP-expressing cell lines (Figure 4.12A, graph). Even after five days post-plating, FLNa-AAA GFP-expressing cells have a cobblestone-like distribution across the cell plate compared to the uniform distribution of FLNa-WT GFP cells (Figure 4.12B) suggesting that the persistent cortical localization of FLNa-AAA GFP results in cell clustering.

In contrast to FLNa-AAA GFP and control cells, FLNa-WT GFP cells have a more elongated morphology and correspondingly fewer cells adopt a cuboidal morphology (Figure 14C). Quantification shows that 19-47% of FLNa-WT GFP-expressing cells are elongated (Figure 4.12C, graph). In contrast, only approximately 2% of FLNa-AAA GFP-expressing cells have an elongated morphology (Figure 4.12C, graph), a phenotype similar to the M2 parental and GFP EV controls, which show 7% and 1% elongated cells, respectively (Figure 4.12C, graph). In addition, FLNa-WT GFP ells extrude significantly more pseudopodia than FLNa-AAA GFP and control cell lines (14-29% for WT, 2-3% for AAA and 3-7% for controls, Figure 4.12C, graph).

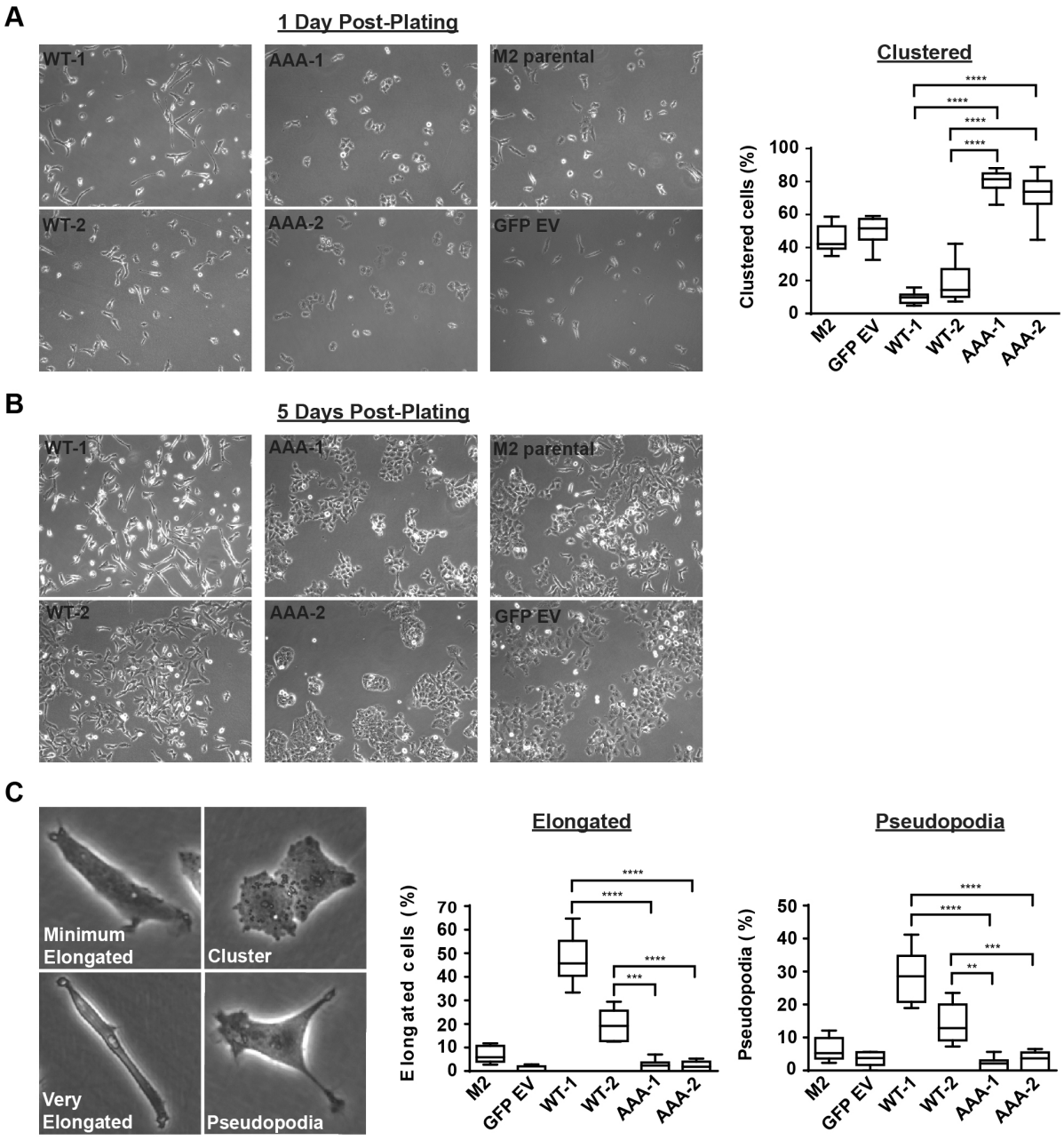
A
1 Day Post-Plating
WT-1
AAA-1
M2 parental
WT-2
AAA-2
GFP EV
Clustered
Clustered cells (%)
M2
GFP EV
WT-1
WT-2
AAA-1
AAA-2
B
5 Days Post-Plating
C
Minimum Elongated
Cluster
Very Elongated
Pseudopodia
Elongated
Elongated cells (%)
Pseudopodia
Pseudopodia (%)

**Figure 4.12. FLNa-AAA GFP cells are more clustered, have fewer pseudopodia and are less elongated than FLNa-WT GFP cells. (A)** FLNa-AAA GFP cells tend to be found in clusters. Phase contrast images are of FLNa-WT GFP, FLNa-AAA GFP and control (M2 parental, GFP EV) cell lines one day after plating. Quantification of cells found in clusters of two or more cells one day after plating. Clustered cells were defined as cells with at least 20% of its diameter in contact with at least one other cell. **(B)** Phase contrast images of FLNa-WT GFP, FLNa-AAA GFP and control M2 cells five days post-plating. **(C)** Representative phenotypes. Elongated, cells with a length at least three times its width; pseudopodia, cells with one or two extensions that are at least three times longer than their filopodia. Quantification of percentage of cells with elongated and pseudopodia phenotypes. FLNa-AAA GFP cells have a less elongated cell shape and fewer pseudopodia compared to FLNa-WT GFP cells. Box and whisker plots show median, quartiles and range of data points. The percent of cells with each phenotype were counted in 10 random fields of view (only fields of views with 40-80 cells were included in the quantification). Cell phenotypes were counted independently of other phenotypes. p-values (two-tailed paired student's t-test) between all WT and AAA cell lines are shown **** $p<0.0001$, *** $p<0.001$, ** $p<0.01$. Total cells counted in all fields of view: M2, 419; GFP EV, 561; WT-1, 441; WT-2, 479; AAA-1, 560; AAA-2, 418.

### 4.3.8 FLNa-AAA GFP cells have impaired migration

M2 cells have a defect in migration that is rescued upon FLNa expression (Cunningham et al., 1992; Flanagan et al., 2001). The changes we observe in cell shape in FLNa-AAA GFP cells suggest that FLNa phosphorylation might play a role in cell migration, so we performed wound closure assays to determine whether S1084A, S1459A and S1533A mutations also affect the ability of FLNa to regulate cell migration. Cells expressing FLNa-WT GFP have complete wound closure after 37.5 h (Figure 4.13; Video 5), while the GFP EV control and M2 parental cells closed 10% and 28% of the wound at this point, respectively (Figure 4.13B; Videos 6 and7). FLNa-AAA GFP-expressing cells have a phenotype intermediate between that of the control and FLNa-WT GFP cell lines with 55% wound closure at 37.5 h (Figure 4.13B; Video 8). FLNa-WT GFP and FLNa-AAA GFP cell lines have similar proliferation rates in an adhesion-based assay (Figure 4.14), indicating that differences in wound closure migration is unlikely to be due to differences in cell proliferation. This result suggests that mitotic phosphorylation of FLNa may be required for proper M2 cell migration.

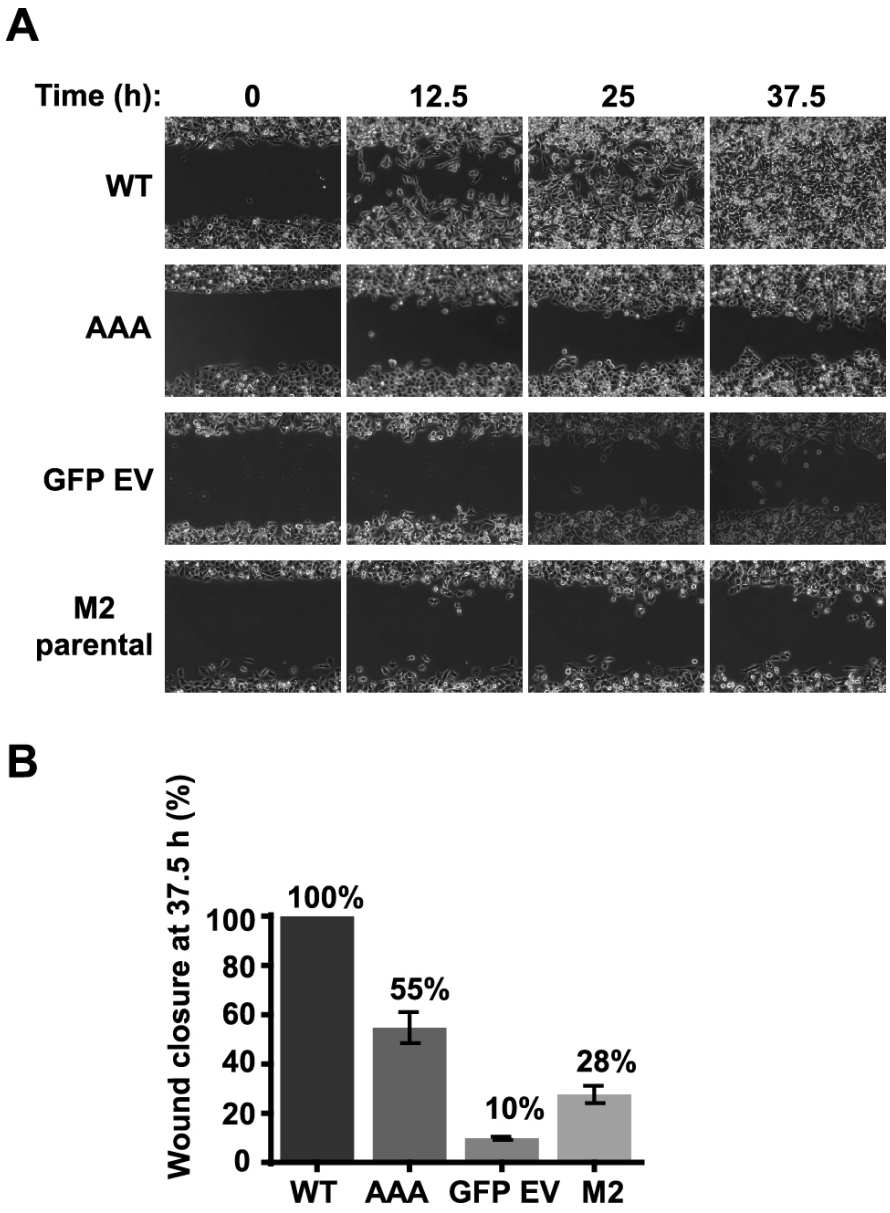
A
Time (h):
0
12.5
25
37.5
WT
AAA
GFP EV
M2
parental
B
Wound closure at 37.5 h (%)
100%
55%
10%
28%
100
80
60
40
20
0
WT
AAA
GFP EV
M2

**Figure 4.13. FLNa-AAA GFP cells have impaired cell migration. (A)** Phase contrast images of wound closure at 0, 12.5, 25 and 37.5 h after creation of the wound. Expression of FLNa-WT GFP restores cell migration defect in M2 cells as shown by complete wound closure by 37.5 h. Expression of FLNa-AAA GFP only partially restores this defect. **(B)** Percentage of wound closure at 37.5 h. Quantification of wound surface area was performed using ImageJ 1.43u. Error bars are mean ± SEM from five different positions along the wound. A representative wound position is shown.

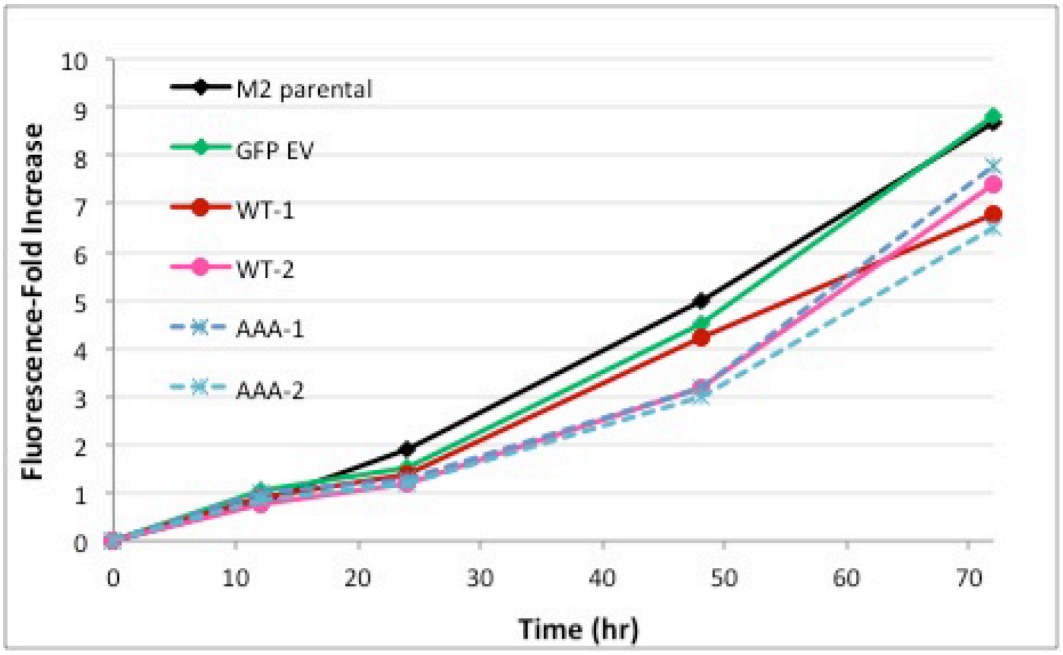
Fluorescence-Fold Increase
Time (hr)
M2 parental
GFP EV
WT-1
WT-2
AAA-1
AAA-2
0
1
2
3
4
5
6
7
8
9
10
0
10
20
30
40
50
60
70

**Figure 4.14. Monoclonal M2 cell lines expressing FLNa-WT and FLNa-AAA have similar proliferation rates.** Graph is representative of three independent experiments. Values across experiments varied due to differences in cell density at time 0. Experiment was performed using CyQUANT Cell Proliferation Assay kit, which is adhesion-based.

### 4.3.9 Identification of putative mitosis-specific FLNa interactors

To fully understand the function of mitotic FLNa phosphorylation we sought to identify proteins that bind specifically with FLNa from mitotic cells and not interphase cells. To this end, we used LC-MS/MS to identify SILAC-labeled proteins that co-immunoprecipitated with FLNa from mitotic (nocodazole-treated) and interphase (DMSO-treated) HeLa cells. Overall, our results show more proteins Co-IP with FLNa from interphase cells than mitotic cells (Figure 4.15B). Proteins enriched in the interphase FLNa Co-IP are shown in Table A5 and proteins enriched in the mitosis FLNa Co-IP are shown in Table A3. Of the 90 known FLNa interactors (Table A1) (Nakamura et al., 2011), 13 proteins were detected by MS, including Cdk1 and F-actin. However, only three of these proteins (14-3-3 epsilon, 14-3-3 zeta/delta and β-1B-glycoprotein, shown in red) are listed in Tables A5 and A6 as interphase or mitotic-FLNa interactors. The remaining 10 proteins were filtered out of these lists because their SILAC ratios suggest they are likely bead or environmental contaminants.

**A**

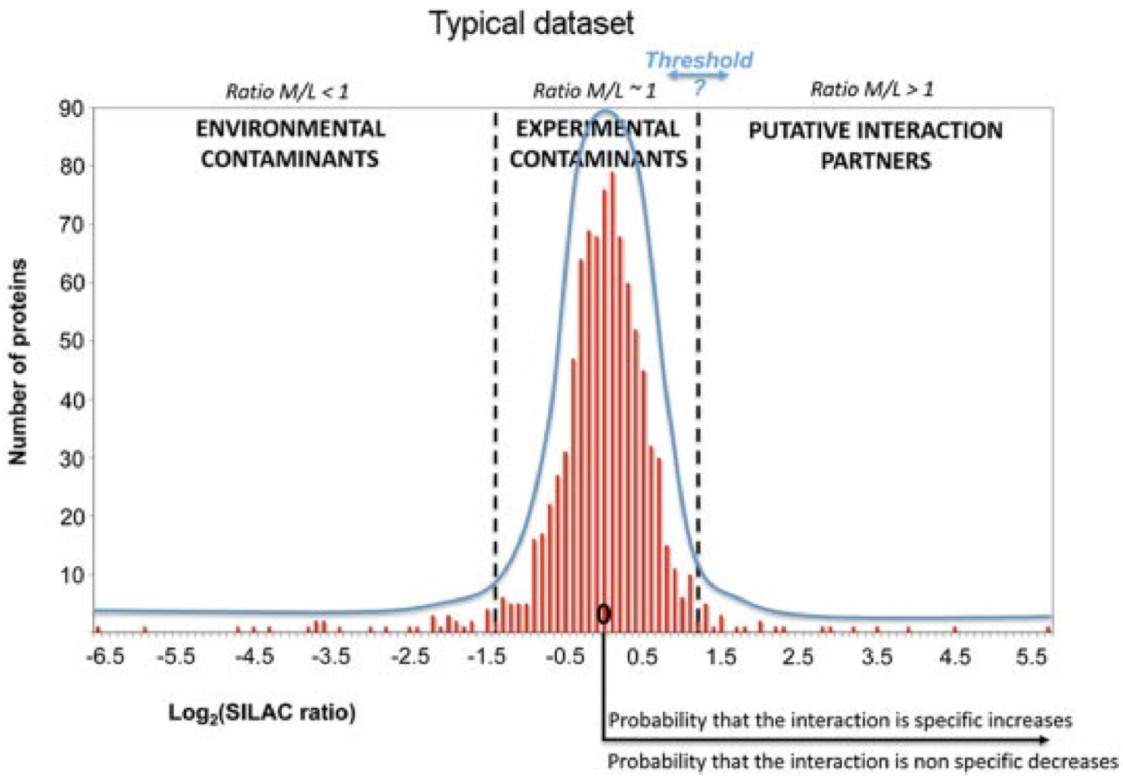
Typical dataset
Threshold
?
Ratio M/L < 1
Ratio M/L ~ 1
Ratio M/L > 1
ENVIRONMENTAL CONTAMINANTS
EXPERIMENTAL CONTAMINANTS
PUTATIVE INTERACTION PARTNERS
Number of proteins
90
80
70
60
50
40
30
20
10
0
-6.5 -5.5 -4.5 -3.5 -2.5 -1.5 -0.5 0.5 1.5 2.5 3.5 4.5 5.5
Log2(SILAC ratio)
Probability that the interaction is specific increases
Probability that the interaction is non specific decreases

**B**

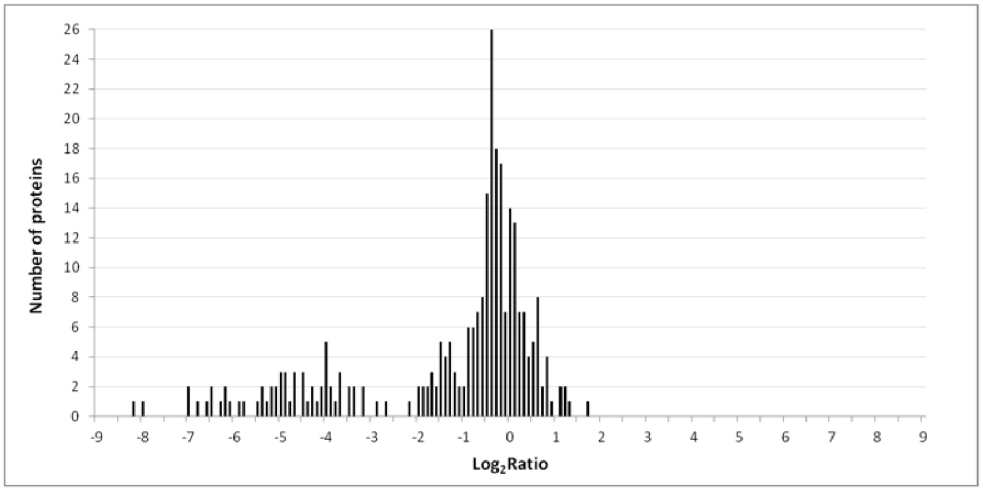
Number of proteins
26
24
22
20
18
16
14
12
10
8
6
4
2
0
-9 -8 -7 -6 -5 -4 -3 -2 -1 0 1 2 3 4 5 6 7 8 9
Log2Ratio

**Figure 4.15. Frequency distribution of $Log_2$ SILAC ratios (noco FLNa IP : DMSO FLNa IP). (A)** Representative frequency distribution of $Log_2$ SILAC ratios. Data are plotted as a histogram with $log_2$ SILAC ratios on the X-axis and number of proteins for a given ratio on the Y-axis. Nonspecific contaminants (environmental and IgG-bead contaminants) reproducibly cluster in a Gaussian (normal) distribution centered at approximately 0. Figure adapted from (Boulon et al., 2010). **(B)** Frequency distribution of $Log_2$ SILAC ratios in experiment described in this thesis. $Log_2$ SILAC ratios > 0 are interphase FLNa-Co-IP enriched proteins. $Log_2$ SILAC ratios <than 0 are mitosis FLNa-Co-IP enriched proteins. An arbitrary cut-off of -3 was chosen for proteins to be considered interphase FLNa-Co-IP enriched and is shown in Table A5. An arbitrary cut-off of +1.5 was chosen for proteins to be considered mitosis FLNa-Co-IP enriched and is shown in Table A6.

To validate the interaction of FLNa with putative binding partners, Western blots of Co-IPs were performed. As a control, we tried to validate the interaction between FLNa and a known binding partner, 14-3-3 (Table A1). Based on our mass spectrometry results, 14-3-3 should interact with FLNa from interphase cells but not mitotic cells (Table A5). However, we find that both mitotic and interphase FLNa Co-IP equally well with 14-3-3 isoforms epsilon, zeta and tau (Figure 4.16, A-E). The same result is obtained from reciprocal Co-IPs using 14-3-3 antibody-bound beads (Figure 4.16, B-F).

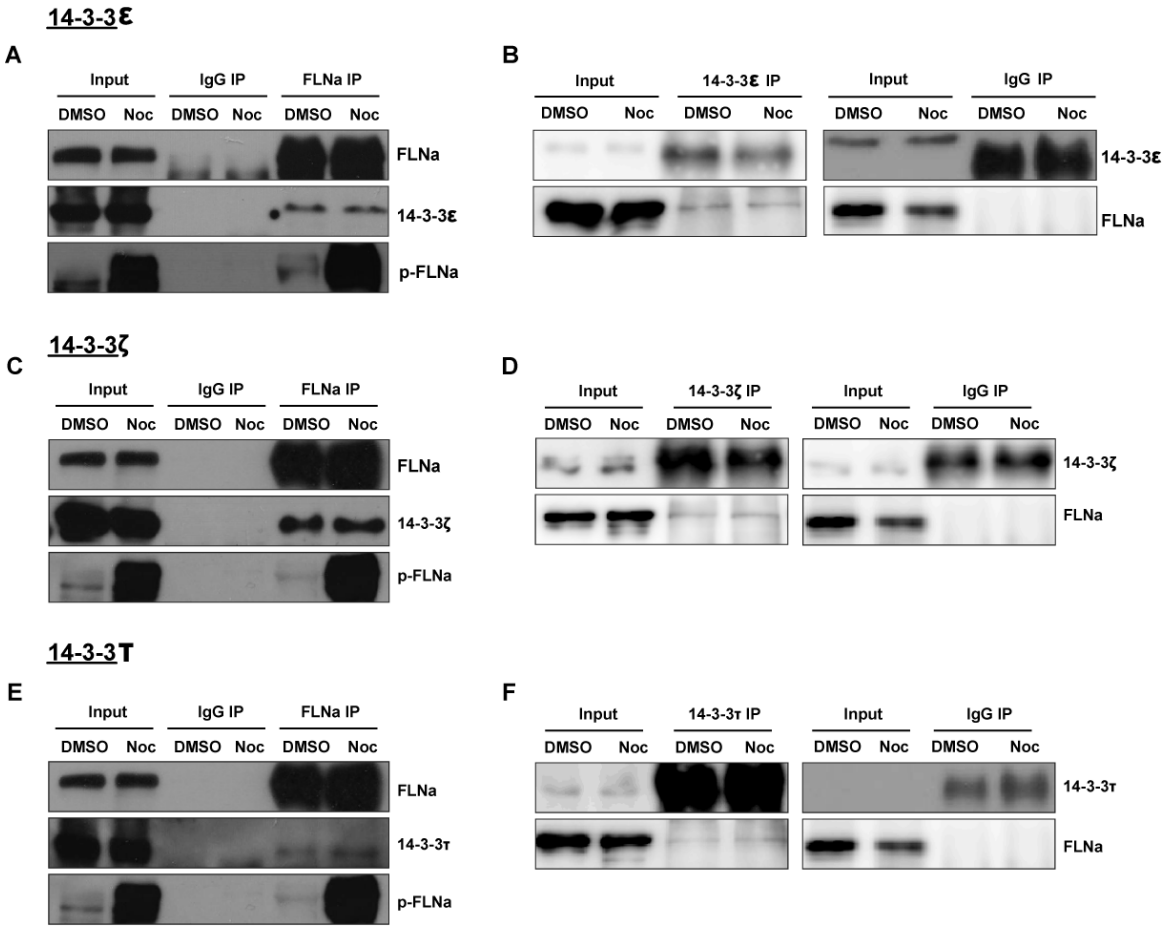
14-3-3ε
A
Input
IgG IP
FLNa IP
DMSO
Noc
FLNa
14-3-3ε
p-FLNa
B
Input
14-3-3ε IP
IgG IP
14-3-3ε
FLNa
14-3-3ζ
C
14-3-3ζ IP
D
14-3-3T
E
14-3-3τ IP
F
14-3-3τ

**Figure 4.16. Mitotic and interphase FLNa interacts with the 14-3-3 family of proteins, isoforms epsilon, zeta and tau. (A)** 14-3-3 epsilon (29 kD) immunoprecipitates with FLNa in both DMSO-treated (interphase) and nocodazole-treated (mitotic) HeLa cells. **(B)** FLNa immunoprecipitates with 14-3-3 epsilon in DMSO and nocodazole-treated cells. **(C)** (A) 14-3-3 zeta (28 kD) immunoprecipitates with FLNa in both DMSO-treated (interphase) and nocodazole-treated (mitotic) HeLa cells. **(D)** FLNa immunoprecipitates with 14-3-3 zeta in DMSO and nocodazole-treated cells. **(E)** 14-3-3 tau immunoprecipitates with FLNa in both DMSO-treated (interphase) and nocodazole-treated (mitotic) HeLa cells. **(F)** FLNa immunoprecipitates with 14-3-3tau in DMSO and nocodazole-treated cells. *Note: Emily Sheppard probed Western blots and Sandy and Emily both performed Co-IPs; see Contributions of Collaborators*.

Our goal was to identify a novel mitosis-specific FLNa interactor, therefore we decided to validate the interaction between FLNa and p16 (Cdk4 inhibitor), one of only three identified putative mitosis-specific FLNa interactors based on our SILAC-MS data (Table A6). Unfortunately, we failed to show an interaction between these two proteins by Western blot (Figure 4.17B).

Next, we tried to validate the putative interaction between interphase FLNa and gelsolin, an F-actin-severing and capping protein. Gelsolin SILAC ratios had a high probability of being a bead or environmental contaminant, however we considered the possibility of it being a real FLNa interactor. Indeed, Western blots show that interphase and mitotic FLNa Co-IP with gelsolin (Figure 4.18). Therefore gelsolin interacts with FLNa directly or indirectly in both mitotic and interphase cells HeLa cells.

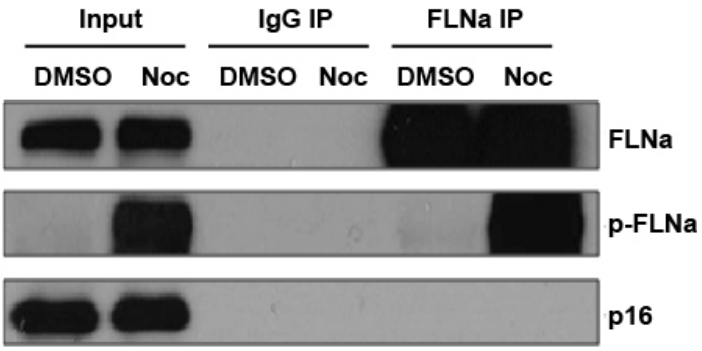
Input
IgG IP
FLNa IP
DMSO
Noc
DMSO
Noc
DMSO
Noc
FLNa
p-FLNa
p16

**Figure 4.17. p16 (Cdk4 inhibitor) does not interact with mitotic or interphase FLNa.** p16 does not immunoprecipitate with FLNa in both DMSO-treated (interphase) and nocodazole-treated (mitotic) HeLa cells. *Note: Emily Sheppard probed Western blots and Sandy and Emily both performed Co-IPs; see Contributions of Collaborators*.

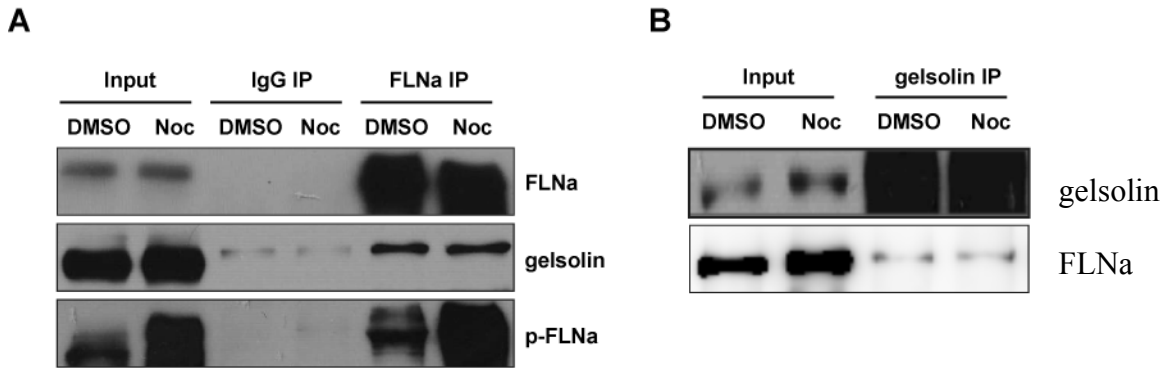
A
Input
IgG IP
FLNa IP
DMSO
Noc
DMSO
Noc
DMSO
Noc
FLNa
gelsolin
p-FLNa
B
Input
gelsolin IP
DMSO
Noc
DMSO
Noc
gelsolin
FLNa

**Figure 4.18. Mitotic and interphase FLNa interacts with gelsolin. (A)** Gelsolin immunoprecipitates with FLNa in both DMSO-treated (interphase) and nocodazole-treated (mitotic) HeLa cells. **(B)** FLNa immunoprecipitates with gelsolin in DMSO and nocodazole-treated cells. *Note: Emily Sheppard probed Western blots and Sandy and Emily both performed Co-IPs; see Contributions of Collaborators*.

### 4.3.10 Summary

Using a p-FLNa antibody that recognizes Cdk1-generated epitopes on FLNa, we find that phosphorylated FLNa has decreased localization to the cell cortex compared to total FLNa during mitotic progression in HeLa cells. Furthermore, FLNa-deficient M2 melanoma cells expressing a nonphosphorylatable FLNa mutant (FLNa-AAA GFP) are impaired in their ability to separate following mitosis and have enhanced FLNa-AAA GFP and actin at sites of cell-cell contact between daughter cells. This alteration in FLNa-AAA GFP localization correlates with fewer pseudopodia, a more cuibodal cell shape and impaired migration in FLNa-AAA GFP-expressing cells compared to FLNa-WT GFP cells. *In vitro* phosphorylation of recombinant FLNa fragments with Cdk1/cyclin B1 does not alter F-actin binding, therefore the defects in FLNa-AAA GFP cells is unlikely to be due to a direct alteration in FLNa-AAA GFP interaction with actin. SILAC analysis of mitotic and interphase-FLNa interactors identified by LC-MS/MS show more proteins Co-IP with FLNa in interphase cells than mitotic cells. The F-actin severing protein gelsolin was identified as a novel FLNa interactor but we were unable to demonstrate that this interaction is specific to mitotic cells.

## 4.4 DISCUSSION

### 4.4.1 Cdk1 phosphorylation of FLNa does not directly affect FLNa binding to F-actin

Since serines 1084, 1459 and 1533 are all found in a secondary F-actin binding segment (FLNa repeats 9-15), we hypothesized that FLNa phosphorylation by Cdk1/cyclin B1 could alter FLNa binding to F-actin and facilitate mitotic actin remodelling. However, *in vitro* F-actin cosedimentation assays showed that Cdk1-phosphorylation of FLNa fragments did not significantly alter their ability to bind F-actin (Figure 4.4, B-E). Furthermore, there were no changes in the ability of full-length endogenous FLNa and recombinant His-FLNa to cosediment with F-actin after *in vitro* phosphorylation with Cdk1/cyclin B1 (Figure 4.5). To investigate the biological significance of phosphorylation on these sites, we mutated all three residues to nonphosphorylatable alanine (FLNa-AAA GFP) and expressed this FLNa mutant in M2 and HeLa cells. Overall, we found that both FLNa-WT GFP and FLNa-AAA GFP have similar localization in mitotic and interphase M2 and HeLa cells (Figures 4.7 and 4.8).

Together these results suggest that phosphorylation does not directly impact FLNa binding with F-actin. It is possible that *in vivo* FLNa phosphorylation alters its interaction with a binding partner other than actin. For example, phosphorylation could enable FLNa interaction with another protein that causes FLNa interaction with F-actin through the secondary F-actin binding segment to become unfavourable. In this case, FLNa may still remain bound to F-actin through its ABD and thus remain colocalized with actin at the cell cortex. This would allow actin filaments to be less constrained and more free to undergo rearrangement.

Phosphorylation of FLNa has been shown to modulate its susceptibility to proteolysis. For example, phosphorylation of S2152 by protein kinase A (PKA) renders the

protein resistant to calpain cleavage at the hinge region (H1) (Chen and Stracher, 1989; Jay et al., 2000; Jay et al., 2004). Phosphorylation-mediated proteolysis of FLNa could be another mechanism for FLNa to dissociate from actin at mitotic onset. This could be mediated by calpain or other unidentified FLNa proteases. Overall, we did not observe FLNa degradation products in mitotic cells but it is possible small fragments were not resolved by SDS-PAGE or detected by FLNa antibody. Prolonged nocodazole arrest activates caspase-mediated apoptosis and we have confirmed that mitotic FLNa degradation products correlate with the activation of caspase-3 (data not shown).

### 4.4.2 Endogenous p-FLNa delocalizes from the cell cortex during mitosis

Initially we observed that FLNa-WT GFP and FLNa-AAA GFP have the same localization in mitotic M2 and HeLa cells (Figure 4.8); however upon re-examination of the localization of endogenous FLNa in mitotic HeLa cells we noticed that p-FLNa delocalizes from the cell cortex during mitotic progression (Figure 4.9). These results suggest that *in vivo* p-FLNa dissociates from the cortex. Therefore, *in vivo* FLNa phosphorylation likely causes FLNa dissociation from F-actin through an indirect mechanism. In light of these findings, we expect inhibition of FLNa phosphorylation (FLNa-AAA GFP) to prevent FLNa delocalization from the cortex. This suggests the localization of FLNa-AAA GFP at the cortex in mitotic M2 and HeLa cells may be a defect (Figure 4.8). Since it is clear that FLNa-AAA GFP-expressing cells have defects in daughter cell separation (Figure 4.10) and migratory capacity (Figure 4.13), we believe FLNa-AAA GFP is functionally different from FLNa-WT GFP at the cortex in mitotic cells and may cause cortical FLNa-AAA GFP persistence. Additional images of FLNa-WT GFP and FLNa-AAA GFP-expressing cells in

different stages of mitosis should be analyzed to determine whether FLNa-AAA GFP mobilization from the cortex is inhibited or delayed.

### 4.4.3 Does FLNa phosphorylation facilitate mitotic cell rounding?

Our hypothesis is that *in vivo* phosphorylation of FLNa by Cdk1/cyclin B1 causes FLNa dissociation from actin filaments to facilitate mitotic actin remodelling. Based on observations of cells undergoing mitosis, the most substantial actin cytoskeleton remodelling occurs during mitotic cell rounding when flat, interphase cells detach from their substrate and become spherical. Accompanying this cell shape change is an increase in cortical actin rigidity (Maddox and Burridge, 2003). Given the critical role of FLNa in cortical actin integrity we reasoned that mitotic FLNa phosphorylation could dissociate FLNa from F-actin. In Figure 4.9A, during prophase (or possibly prometaphase) p-FLNa is observed at the cell cortex and the cell is already fully rounded. This suggests p-FLNa does not dissociate from cortical actin filaments to facilitate mitotic cell rounding. However, as previously mentioned and in light of findings that *in vitro* phosphorylation of FLNa does not alter F-actin binding, we believe it is possible for phosphorylated FLNa to remain localized at the cortex and still allow cortical actin rearrangement, albeit not as dramatic as we initially thought. Furthermore, the localization of p-FLNa at the cortex in cells undergoing mitotic cell rounding may help increase cortical rigidity without altering the affinity of FLNa to F-actin. Mitotic cell rounding is a complex process and likely mediated by the culmination of multiple ABPs acting in concert to alter the dynamics of F-actin and actomyosin.

### 4.4.4 The cell separation defect in FLNa-AAA GFP cells is unlikely due to impaired cytokinesis

In HeLa cells it has been reported that FLNa interacts *in vivo* with PTP-PEST (protein tyrosine phosphatase with a C-terminal PEST motif), a cytoplasmic protein tyrosine phosphatase implicated in the regulation of cytokinesis (Playford et al., 2006). Overexpression of PTP-PEST causes failures in cytokinesis and a multinucleated phenotype that is dependent on FLNa expression (Playford et al., 2006). These results suggest that enhanced FLNa localization to the midbody impairs cytokinetic abscission, likely through interaction with PTP-PEST.

On the other hand, other reports have indicated FLNa recruitment to the midbody is involved in the activation of cytokinesis. Recently, FLNa has been shown to be required for the recruitment of the BRCA2 tumour suppressor to the midbody in HeLa cells where it is involved in maintaining midbody structure and function through the recruitment of cytokinetic and abscission proteins (Yuan and Shen, 2001; Velkova et al., 2010; Mondal et al., 2012). Furthermore, about 20% of FLNa-deficient M2 cells have a multinucleated phenotype and this is presumably due to lack of FLNa (Playford et al., 2006).

In dividing chick embryos, FLNa localizes to the cleavage furrow and midbody. However, the functional importance of this enrichment is unclear (Nunnally et al., 1980). More than 100 proteins have been identified in the regulation of cytokinesis in budding yeast (Huh et al., 2003), *C. elegans*, *Drosophila* and mammalian cells (Echard et al., 2004; Eggert et al., 2004; Skop et al., 2004; Sonnichsen et al., 2005; Zhu et al., 2005). The multiple players implicated in cytokinesis and the seemingly contradictory roles of FLNa in cytokinesis illustrate its complexity.

Our observation that FLNa-deficient control cell lines (GFP EV and M2 parental) have a cell clustering phenotype that is intermediate between that of FLNa-WT GFP and FLNa-AAA GFP-expressing cell lines (Figure 4.12A, graph) suggest a lack of FLNa causes cell clustering. Impaired cytokinesis can lead to multinucleated cells and a clustered cell phenotype. However, we did not notice multinucleated FLNa-AAA GFP or FLNa-WT GFP-expressing cells (data not shown). This suggests both FLNa-WT GFP and FLNa-AAA GFP have the capacity to rescue the cytokinesis defect in M2 cells.

### 4.4.5 Enhanced localization of FLNa-AAA GFP between daughter cells correlates with impaired cell separation and a clustered cell phenotype

We believe the enhanced localization of FLNa-AAA GFP at sites of cell-cell contact between daughter cells (Figures 4.10A) and in clustered M2 and HeLa cells (Figure 4.11) is a consequence of FLNa-AAA GFP persistence at the mitotic cell cortex. The aberrant FLNa-AAA GFP localization at sites of cell-cell contact between daughter cells prevents their separation, leading to the cell clustering phenotype in FLNa-AAA GFP-expressing M2 cells.

### 4.4.6 Persistent cortical FLNa-AAA GFP localization may lead to stronger intercellular adhesion between daughter cells

We believe the accumulation of FLNa-AAA GFP at the cortex in mitotic cells translates to increased intercellular adhesion between daughter cells. At the cortex it has been shown that FLNa interacts with the cytoplasmic domain of intercellular adhesion molecule-1 (ICAM-1) in human endothelial cells and with GFP-tagged ICAM-1 in HeLa cells (Kanters et al., 2008). Cortical FLNa-AAA GFP could become incorporated into intercellular adhesion molecules such as ICAM-1 and lead to stronger adhesion between daughter cells.

### 4.4.7 Enhanced localization of FLNa-AAA GFP between daughter cells correlates with less elongated cells with fewer pseudopodia

FLNa-AAA GFP cells were also significantly less elongated than FLNa-WT GFP cells (Figure 4.12). The persistence of FLNa-AAA GFP at the cell cortex and sites of cell-cell contact between daughter cells may translate to decreased availability of these two proteins to sites of pseudopodial and filopodial extrusion. Dynamic cell processes, such as elongation and migration/locomotion, that require these extensions, may consequently be inhibited in FLNa-AAA GFP-expressing cells. Our observation that FLNa-WT GFP-expressing M2 cells are more elongated and extrude more pseudopodia than control and FLNa-AAA GFP cell lines is consistent with reports that indicate FLNa expression in M2 cells increases pseudopodia protrusion and filopodia extension (Cunningham et al., 1992; Flanagan et al., 2001). The inability of FLNa-AAA GFP to rescue this defect (Figure 4.12C) suggests S1084, S1459A and S1533A mutations result in loss-of-function. However, we do not believe the phenotype in FLNa-AAA GFP cells is due to loss-of FLNa function. Instead, we believe it is a consequence of enhanced FLNa-AAA GFP localization at the cortex and sites of daughter cell contact, limiting its availability to interphase actin structures.

### 4.4.8 FLNa-AAA GFP cells have defects in cell migration

Wound healing assays suggest that the changes in FLNa-AAA GFP localization and the resultant morphological differences between FLNa-WT GFP and FLNa-AAA GFP-expressing cells causes defects in migration (Figure 4.13). Specifically we believe that defects in cell separation prevent FLNa-AAA GFP daughter cells from moving away from each and migrating. Another possibility is that the aberrant localization of FLNa-AAA GFP at sites of cell-cell contact between daughter cells prevents FLNa-AAA GFP redistribution to other regions of the cell that require FLNa for cell migration, for example in focal adhesions,

stress fibres and lamellipodia. This idea is supported by the fact that FLNa-AAA GFP cells have a migration phenotype that is intermediate between that of FLNa-WT GFP and M2 parental/GFP EV cells (Figure 4.13). Therefore expression of FLNa-AAA GFP can only partially rescue the migration defect in M2 cells.

However, we have not ruled out the possibility that the cell migration defect is independent of mitotic FLNa phosphorylation. Although S1084, S1459 and S1533 were not identified as interphase-enriched FLNa phosphorylation sites, this is not conclusive evidence that these sites are not potentially phosphorylated by a non-Cdk1 kinase during interphase.

We do not believe S1084A, S1459A and S1533A cause FLNa loss-of-function because FLNa-AAA GFP still colocalizes with actin structures in interphase cells and can partially rescue the migration defect in M2 cells.

### 4.4.9 Compensation between filamin isoforms

There is high homology among filamin isoforms (Stossel *et al.*, 2001), and the literature suggests they can compensate for each other (Baldassarre *et al.*, 2009). For example, FLNa-knockout mouse embryonic fibroblasts (MEFs) show minimal motility defects (Feng et al., 2006), however, when both FLNa and FLNb are depleted, defects in early cell spreading and migration emerge (Lynch et al., 2011). FLNb-/- MEFs, on the other hand, appear similar to controls (Lynch et al., 2011). The difference in the severity of FLNa-/- and FLNb-/- phenotypes is likely attributed to the fact that FLNa typically comprises 60% of expressed FLNs in fibrosarcoma cells (Baldassarre et al., 2009), indicating that FLNa has a greater impact on filamin levels and this explains the more severe defects observed in FLNa-/- MEFs (Lynch et al., 2011).

In light of this, it is possible that the subtle defects observed in FLNa-AAA GFP cells may be due to compensation by FLNb, which is expressed at low levels in M2 cells. Ultrastructural studies on the cortical actin network in M2 cells show that actin filaments are longer and the network is more rigid than in FLNa-repleted cells (Flanagan et al., 2001). Cortical actin crosslinks in M2 cells are presumably strengthened by non-FLNa ABPs (Flanagan et al., 2001) and FLNb would be an obvious candidate. Based on our model that mitotic FLNa phosphorylation is involved in FLNa mobilization and defects in FLNa-AAA GFP are due to its persistence at the cortex, FLNb could compensate for the lack of FLNa at other sites that require FLNa for cell elongation, filopodial extension and cell migration. Thus, it would be interesting to observe the effects of FLNa-AAA GFP expression on FLNb-depleted M2 cells.

### 4.4.10 Phosphorylation on other Cdk1 sites

In this study, the effect of FLNa phosphorylation on serines 1084, 1459 and 1533 was investigated. However, we showed in Chapter 3 that other Cdk1/cyclin B1 sites are phosphorylated *in vivo* and have yet to be identified. A comprehensive identification of all Cdk1 phosphorylation sites will be necessary to understand the biological significance of mitotic FLNa phosphorylation. Of particular interest are serines 1436 and 1630, which were identified as *in vitro* sites (Cukier et al., 2007) and are also found in the secondary F-actin binding segment.

### 4.4.11 Unintended consequences of mutating phospho-sites

Creating nonphosphorylatable or phosphomimetic mutants is a common technique used to determine the biological significance of protein phosphorylation on specific sites (Li et al., 1995; Zachariae et al., 1998; Jaspersen et al., 1999; Rudner and Murray, 2000). However,

mutating phosphorylation sites can have unintended consequences on protein function that are phosphorylation-independent (Rudner and Murray, 2000). For example, mutation of a putative phosphorylation site could alter protein conformation and thus the interaction of binding partners to nearby sites. Ideally, both phosphomimetic and the corresponding nonphosphorylatable mutant should be investigated to ensure their effects are complementary. Furthermore, the kinase responsible for phosphorylation should also be inactivated as a control and its phenotype should mimick that of the nonphosphorylatable mutant. Unfortunately, this approach is only limited to well-characterized kinases whose substrate specificity is known, otherwise off-target effects could occur.

### 4.4.12 Model for mitotic FLNa phosphorylation

Based on our results, we propose a model for the function of mitotic FLNa phosphorylation on S1084, S1459 and S1533. This model is presented in Figure 4.19. During interphase, nonphosphorylated FLNa is localized to actin structures including stress fibres and the cortex (Figure 4.19, step 1). At mitotic onset, activation of Cdk1 leads to the phosphorylation of FLNa at serines 1084, 1459 and 1533 and likely other sites. p-FLNa remains at the cortex as the cell rounds up and increases its cortical rigidity. At prophase, when the cell is rounded, FLNa is stoichiometrically phosphorylated and at this point FLNa and p-FLNa have the same localization at the cortex and cytoplasm (Figure 4.19, step 2). At metaphase, p-FLNa has decreased localization at the cell cortex relative to total FLNa. Total FLNa is still observed at the cortex. We believe a subset of FLNa always remains at the cortex to maintain cortical rigidity. The cortex-liberated p-FLNa plays an as yet, unidentified role during mitosis. It may be involved in mediating cytokinetic abscission and/or regulating the formation, function, and integrity of the mitotic spindle (Figure 4.19, step 3). By anaphase, no p-FLNa is

observed at the cortex and the remaining p-FLNa has cytoplasmic localization. (Figure 4.19, step 4). At the conclusion of mitosis, FLNa is fully dephosphorylated, daughter cells separate and FLNa re-establishes its interaction with interphase actin structures (Figure 4.19, step 5).

In the case of FLNa-AAA GFP cells, where Cdk1 phosphorylation on serines 1084, 1459 and 1533 is prevented, FLNa-AAA GFP does not delocalize from the cortex during mitosis. We believe the persistent FLNa-AAA GFP cortical localization leads to the incorporation of FLNa-AAA GFP into intercellular adhesions through interaction with ICAM-1. This would strengthen adhesions between daughter cells and impair their separation. Impaired cell separation leads to a cell clustering phenotype and defects in cell migration. This also correlates with defects in cell elongation and pseudopodia extension.

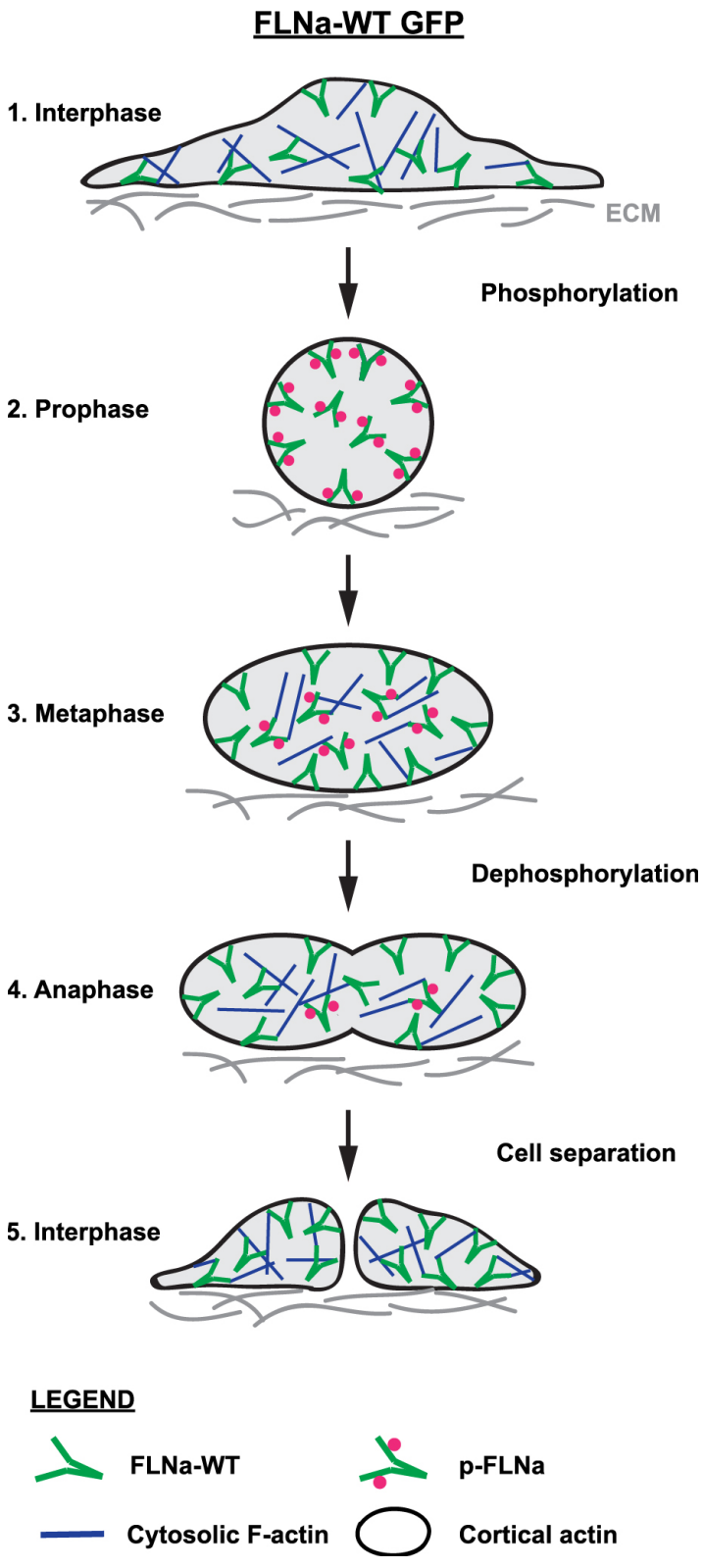
FLNa-WT GFP
1. Interphase
ECM
Phosphorylation
2. Prophase
3. Metaphase
Dephosphorylation
4. Anaphase
Cell separation
5. Interphase
LEGEND
FLNa-WT
p-FLNa
Cytosolic F-actin
Cortical actin

**Figure 4.19. Proposed model for the role of mitotic FLNa phosphorylation in cortical FLNa mobilization.** In interphase (step 1), nonphosphorylated FLNa is localized to interphase actin structures and the cell cortex. Upon mitotic entry, FLNa is phosphorylated by Cdk1/cyclin B1 and remains localized at the cell cortex (step 2). As mitosis proceeds, p-FLNa has decreased localization at the cell cortex compared to total FLNa and has diffuse cytosolic localization (step 3). At anaphase, p-FLNa is dephosphorylated and p-FLNa fluorescence intensity is noticeably diminished (step 4). At the end of mitosis, FLNa is fully dephosphorylated and relocalizes to the cell cortex and interphase actin structures (step 5).

### 4.4.13 FLNa interacts with more proteins in interphase than mitosis

Using SILAC LC-MS/MS we found that a greater number of proteins Co-IP with interphase FLNa than mitotic FLNa (Figure 4.15B). This is consistent with our hypothesis that FLNa dissociates from F-actin during mitosis. This would likely involve the dissociation of other interphase FLNa interactors that use FLNa as a scaffold for mediating signaling events in interphase processes such as cell migration and spreading. Unfortunately we were unable to validate the interaction of FLNa with putative mitosis- or interphase-specific interactors. We did, however, identify gelsolin as a novel FLNa interactor (Figure 4.18). Proteins of the gelsolin family have severing and capping activities that are activated by $Ca^{2+}$ binding (Janmey et al., 1985; Lin et al., 2000). The biological significance of this interaction would be an interesting avenue to explore.

# CONCLUSIONS

Actin cytoskeletal remodelling occurs when mammalian cells undergo mitosis; however, the mechanisms regulating this process are largely unknown. We previously identified the F-actin crosslinking protein FLNa as an *in vitro* Cdk1/cyclin B1 substrate and hypothesized that *in vivo* phosphorylation of FLNa by Cdk1/cyclin causes FLNa dissociation from actin filaments to facilitate mitotic actin remodelling. My objectives were to **1.** Determine whether or not FLNa is phosphorylated *in vivo* by Cdk1/cyclin B1; **2.** Identify *in vivo* FLNa phosphorylation sites by quantitative mass spectrometry; and **3.** Determine the functional relevance of FLNa phosphorylation by Cdk1/cyclin B1. The main findings/conclusions from our research are listed:

**1**. FLNa is phosphorylated by Cdk1/cyclin B1 *in vivo* on serines 1084, 1459 and 1533, although other sites are phosphorylated as well.

**2.** Cdk1/cyclin B1 phosphorylation of FLNa does not directly affect its binding to F-actin *in vitro*.

**3.** In HeLa cells, p-FLNa delocalizes from the cell cortex during mitotic progression, and we believe phosphorylation mediates the indirect dissociation of p-FLNa from actin filaments. During prophase/prometaphase, the cell is already rounded; therefore p-FLNa does not appear to have a major role in the rearrangement of actin filaments during mitotic cell rounding.

**4.** Enhanced localization of FLNa-AAA GFP at sites of cell-cell contact between daughter cells correlates with impaired daughter cell separation, a clustered phenotype, decreased cell elongation, fewer filopodia and a cell migration defect. All of these phenotypes are likely consequences of impaired daughter cell separation.

**5.** Impaired daughter cell separation is likely due to increased intercellular adhesion due to the persistence of FLNa-AAA GFP at the cortex.

**6.** More proteins Co-IP with FLNa from interphase cells than mitotic cells.

# REFERENCES


Agnew, B.J., Minamide, L.S., and Bamburg, J.R. (1995). Reactivation of Phosphorylated Actin Depolymerizing Factor and Identification of the Regulatory Site. J. Biol. Chem. *270*, 17582-17587.

Agromayor, M., and Martin-Serrano, J. (2013). Knowing when to cut and run: mechanisms that control cytokinetic abscission. Trends Cell Biol. *23*, 433-441.

Aguda, A.H., Sakwe, A.M., Rask, L., and Robinson, R.C. (2007). Expression, crystallization and preliminary crystallographic data analysis of filamin A repeats 14-16. Acta Crystallogr. Sect. F Struct. Biol. Cryst. Commun. *63*, 291-293.

Atherton-Fessler, S., Parker, L.L., Geahlen, R.L., and Piwnica-Worms, H. (1993). Mechanisms of p34cdc2 regulation. Mol. Cell. Biol. *13*, 1675-1685.

Athman, R., Louvard, D., and Robine, S. (2002). III. How is villin involved in the actin cytoskeleton dynamics in intestinal cells? American Journal of Physiology - Gastrointestinal and Liver Physiology *283*, G496-G502.

Ayscough, K.R. (1998). In vivo functions of actin-binding proteins. Curr. Opin. Cell Biol. *10*, 102-111.

Baldassarre, M., Razinia, Z., Burande, C.F., Lamsoul, I., Lutz, P.G., and Calderwood, D.A. (2009). Filamins regulate cell spreading and initiation of cell migration. PLoS One *4*.

Baluška, F., Menzel, D., and Barlow, P.W. (2006). Cytokinesis in plant and animal cells: Endosomes 'shut the door'. Dev. Biol. *294*, 1-10.

Bañuelos, S., Saraste, M., and Carugo, K.D. (1998). Structural comparisons of calponin homology domains: implications for actin binding. Structure *6*, 1419-1431.

Bartles, J.R. (2000). Parallel actin bundles and their multiple actin-bundling proteins. Curr. Opin. Cell Biol. *12*, 72-78.

Bazzoni, G., and Dejana, E. (2004). Endothelial Cell-to-Cell Junctions: Molecular Organization and Role in Vascular Homeostasis. Physiol. Rev. *84*, 869-901.

Beausoleil, S.A., Jedrychowski, M., Schwartz, D., Elias, J.E., Villén, J., Li, J., Cohn, M.A., Cantley, L.C., and Gygi, S.P. (2004). Large-scale characterization of HeLa cell nuclear phosphoproteins. Proc. Natl. Acad. Sci. U. S. A. *101*, 12130-12135.

Bechtel, P.J. (1979). Identification of a high molecular weight actin-binding protein in skeletal muscle. J. Biol. Chem. *254*, 1755-1758.

Behrendt, B. (2002). FAP52 - a new partner for filamin in actin cytoskeleton organization. Trends Cell Biol. *12*, 213.

Bellanger, J.M., Astier, C., Sardet, C., Ohta, Y., Stossel, T.P., and Debant, A. (2000). The Rac1- and RhoG-specific GEF domain of Trio targets filamin to remodel cytoskeletal actin. Nat. Cell Biol. *2*, 888-892.

Belmont, L.D., Hyman, A.A., Sawin, K.E., and Mitchison, T.J. (1990). Real-time visualization of cell cycle-dependent changes in microtubule dynamics in cytoplasmic extracts. Cell *62*, 579-589.

Bentley, A.M., Normand, G., Hoyt, J., and King, R.W. (2007). Distinct Sequence Elements of Cyclin B1 Promote Localization to Chromatin, Centrosomes, and Kinetochores during Mitosis. Mol. Biol. Cell *18*, 4847-4858.

Berry, F.B., O'Neill, M.A., Coca-Prados, M., and Walter, M.A. (2005). FOXC1 transcriptional regulatory activity is impaired by PBX1 in a filamin A-mediated manner. Mol. Cell. Biol. *25*, 1415-1424.

Birkenfeld, J., Nalbant, P., Bohl, B.P., Pertz, O., Hahn, K.M., and Bokoch, G.M. (2007). GEF-H1 Modulates Localized RhoA Activation during Cytokinesis under the Control of Mitotic Kinases. Dev. Cell *12*, 699-712.

Blangy, A., Lane, H.A., d'Hérin, P., Harper, M., Kress, M., and Nigg, E.A. (1995). Phosphorylation by p34cdc2 regulates spindle association of human Eg5, a kinesin-related motor essential for bipolar spindle formation in vivo. Cell *83*, 1159-1169.

Blaser, H., Reichman-Fried, M., Castanon, I., Dumstrei, K., Marlow, Florence L., Kawakami, K., Solnica-Krezel, L., Heisenberg, C.-P., and Raz, E. (2006). Migration of Zebrafish Primordial Germ Cells: A Role for Myosin Contraction and Cytoplasmic Flow. Dev. Cell *11*, 613-627.

Blethrow, J.D., Glavy, J.S., Morgan, D.O., and Shokat, K.M. (2008). Covalent capture of kinase-specific phosphopeptides reveals Cdk1-cyclin B substrates. Proc. Natl. Acad. Sci. *105*, 1442-1447.

Bobkov, A.A., Muhlrad, A., Kokabi, K., Vorobiev, S., Almo, S.C., and Reisler, E. (2002). Structural Effects of Cofilin on Longitudinal Contacts in F-actin. J. Mol. Biol. *323*, 739-750.

Boersema, P.J., Mohammed, S., and Heck, A.J.R. (2009). Phosphopeptide fragmentation and analysis by mass spectrometry, J. Mass Spectrom. *44*, 861-878.

Boulon, S., Ahmad, Y., Trinkle-Mulcahy, L., Verheggen, C., Cobley, A., Gregor, P., Bertrand, E., Whitehorn, M., and Lamond, A.I. (2010). Establishment of a Protein Frequency Library and Its Application in the Reliable Identification of Specific Protein Interaction Partners. Mol. Cell. Proteomics *9*, 861-879.

Bradford, M.M. (1976). A rapid and sensitive method for the quantitation of microgram quantities of protein utilizing the principle of protein-dye binding. Anal. Biochem. *72*, 248-254.

Bray, D., and White, J. (1988). Cortical flow in animal cells. Science *239*, 883-888.
Bresnick, A.R., Janmey, P.A., and Condeelis, J. (1991). Evidence that a 27-residue sequence is the actin-binding site of ABP-120. J. Biol. Chem. *266*, 12989-12993.

Bretscher, A. (1986). Caldesmon: Thin filament regulatory proteins of smooth- and non-muscle cells. Nature *321*, 726-727.

Bretscher, A., Edwards, K., and Fehon, R.G. (2002). ERM proteins and merlin: integrators at the cell cortex. Nat. Rev. Mol. Cell Biol. *3*, 586-599.

Brotschi, E.A., Hartwig, J.H., and Stossel, T.P. (1978). The gelation of actin by actin-binding protein. J. Biol. Chem. *253*, 8988-8993.

Browne, K.A., Johnstone, R.W., Jans, D.A., and Trapani, J.A. (2000). Filamin (280-kDa actin-binding protein) is a caspase substrate and is also cleaved directly by the cytotoxic T lymphocyte protease granzyme B during apoptosis. J. Biol. Chem. *275*, 39262-39266.

Buckley, I.K. (1981). Fine-Structural and Related Aspects of Nonmuscle-Cell Motility. In Cell Muscle Motil., R. Dowben, and J. Shay, eds. (Springer US), pp. 135-203.

Burbank, K.S., and Mitchison, T.J. (2006). Microtubule dynamic instability. Curr. Biol. *16*, R516-R517.

Burridge, K., and Connell, L. (1983). A new protein of adhesion plaques and ruffling membranes. J. Cell Biol. *97*, 359-367.

Burton, K., and Taylor, D.L. (1997). Traction forces of cytokinesis measured with optically modified elastic substrata. Nature *385*, 450-454.

Byers, H.R., Etoh, T., Doherty, J. R., Sober, A.J., and Mihm, M.C. (1991). Cell migration and actin organization in cultured human primary, recurrent cutaneous and metastatic melanoma. Am. J. Path. 139, 423-435.

Byers, H.R., and Fujiwara, K. (1982). Stress fibers in cells in situ: immunofluorescence visualization with antiactin, antimyosin, and anti-alpha-actinin. J. Cell Biol. *93*, 804-811.

Byfield, F.J., Wen, Q., Levental, I., Nordstrom, K., Arratia, P.E., Miller, R.T., and Janmey, P.A. (2009). Absence of filamin A prevents cells from responding to stiffness gradients on gels coated with collagen but not fibronectin. Biophys. J. *96*, 5095-5102.

Calderwood, D.A., Huttenlocher, A., Kiosses, W.B., Rose, D.M., Woodside, D.G., Schwartz, M.A., and Ginsberg, M.H. (2001). Increased filamin binding to β-integrin cytoplasmic domains inhibits cell migration. Nat. Cell Biol. *3*, 1060-1068.

Cao, L.G., and Wang, Y.L. (1990). Mechanism of the formation of contractile ring in dividing cultured animal cells. II. Cortical movement of microinjected actin filaments. J. Cell Biol. *111*, 1905-1911.

Carreno, S., Kouranti, I., Glusman, E.S., Fuller, M.T., Echard, A., and Payre, F. (2008). Moesin and its activating kinase Slik are required for cortical stability and microtubule organization in mitotic cells. J. Cell Biol. *180*, 739-746.

Charras, G.T. (2008). A short history of blebbing. J. Microsc. *231*, 466-478.

Charras, G.T., Coughlin, M., Mitchison, T.J., and Mahadevan, L. (2008). Life and Times of a Cellular Bleb. Biophys. J. *94*, 1836-1853.

Charras, G.T., Hu, C.-K., Coughlin, M., and Mitchison, T.J. (2006). Reassembly of contractile actin cortex in cell blebs. J. Cell Biol. *175*, 477-490.

Charras, G.T., Yarrow, J.C., Horton, M.A., Mahadevan, L., and Mitchison, T.J. (2005). Non-equilibration of hydrostatic pressure in blebbing cells. Nature *435*, 365-369.

Chen, H.S., Kolahi, K.S., and Mofrad, M.R. (2009). Phosphorylation facilitates the integrin binding of filamin under force. Biophys. J. *97*, 3095-3104.

Chen, M., and Stracher, A. (1989). In situ phosphorylation of platelet actin-binding protein by cAMP-dependent protein kinase stabilizes it against proteolysis by calpain. J. Biol. Chem. *264*, 14282-14289.

Clute, P., and Pines, J. (1999). Temporal and spatial control of cyclin B1 destruction in metaphase. Nat. Cell Biol. *1*, 82-87.

Colbran, R.J. (2004). Protein Phosphatases and Calcium/Calmodulin-Dependent Protein Kinase II-Dependent Synaptic Plasticity. J. Neurosci. *24*, 8404-8409.

Condeelis, J., Geosits, S., and Vahey, M. (1982). Isolation of a new actin-binding protein from dictyostelium discoideum. Cell Motil. *2*, 273-285.

Condeelis, J., Salisbury, J., and Fujiwara, K. (1981). A new protein that gels F actin in the cell cortex of Dictyostelium discoideum. Nature *292*, 161-162.

Cortese, J.D., Schwab, B., Frieden, C., and Elson, E.L. (1989). Actin polymerization induces a shape change in actin-containing vesicles. Proc. Natl. Acad. Sci. *86*, 5773-5777.

Cox, D., Condeelis, J., Wessels, D., Soll, D., Kern, H., and Knecht, D.A. (1992). Targeted disruption of the ABP-120 gene leads to cells with altered motility. J. Cell Biol. *116*, 943-955.

Cox, D., Ridsdale, J.A., Condeelis, J., and Hartwig, J. (1995). Genetic deletion of ABP-120 alters the three-dimensional organization of actin filaments in Dictyostelium pseudopods. J. Cell Biol. *128*, 819-835.

Cox, D., Wessels, D., Soll, D.R., Hartwig, J., and Condeelis, J. (1996). Re-expression of ABP-120 rescues cytoskeletal, motility, and phagocytosis defects of ABP-120-Dictyostelium mutants. Mol. Biol. Cell *7*, 803-823.

Cramer, L.P., and Mitchison, T.J. (1997). Investigation of the mechanism of retraction of the cell margin and rearward flow of nodules during mitotic cell rounding. Mol. Biol. Cell *8*, 109-119.

Cramer, L.P., Siebert, M., and Mitchison, T.J. (1997). Identification of Novel Graded Polarity Actin Filament Bundles in Locomoting Heart Fibroblasts: Implications for the Generation of Motile Force. J. Cell Biol. *136*, 1287-1305.

Cukier, I.H., Li, Y., and Lee, J.M. (2007). Cyclin B1/Cdk1 binds and phosphorylates Filamin A and regulates its ability to cross-link actin. FEBS Lett. *581*, 1661-1672.

Cunningham, C., Gorlin, J., Kwiatkowski, D., Hartwig, J., Janmey, P., Byers, H., and Stossel, T. (1992). Actin-binding protein requirement for cortical stability and efficient locomotion. Science *255*, 325-327.

Cunningham, C.C. (1995). Actin polymerization and intracellular solvent flow in cell surface blebbing. J. Cell Biol. *129*, 1589-1599.

D'Addario, M., Arora, P.D., Fan, J., Ganss, B., Ellen, R.P., and McCulloch, C.A. (2001). Cytoprotection against mechanical forces delivered through $\beta_1$ integrins requires induction of filamin A. J. Biol. Chem. *276*, 31969-31977.

Dabrowska, R., Goch, A., Osinska, H., Szpacenko, A., and Sosinski, J. (1985). Dual effect of filamin on actomyosin ATPase activity. J. Muscle Res. Cell Motil. *6*, 29-42.

Dalkilic, I., Schienda, J., Thompson, T.G., and Kunkel, L.M. (2006). Loss of FilaminC (FLNc) Results in Severe Defects in Myogenesis and Myotube Structure. Mol. Cell. Biol. *26*, 6522-6534.

DeMaso, C.R., Kovacevic, I., Uzun, A., and Cram, E.J. (2011). Structural and Functional Evaluation of *C. elegans* Filamins FLN-1 and FLN-2. PLoS One *6*, e22428.

Dephoure, N., Zhou, C., Villén, J., Beausoleil, S.A., Bakalarski, C.E., Elledge, S.J., and Gygi, S.P. (2008). A quantitative atlas of mitotic phosphorylation. Proc. Natl. Acad. Sci. *105*, 10762-10767.

DeWard, A.D., and Alberts, A.S. (2009). Ubiquitin-mediated Degradation of the Formin mDia2 upon Completion of Cell Division. J. Biol. Chem. *284*, 20061-20069.
Dipasquale, A. (1975). Locomotion of epithelial cells: Factors involved in extension of the leading edge. Exp. Cell Res. *95*, 425-439.

Dominguez, R., and Holmes, K.C. (2011). Actin Structure and Function. Ann. Rev. Biophys. *40*, 169-186.

Echard, A., Hickson, G.R.X., Foley, E., and O'Farrell, P.H. (2004). Terminal Cytokinesis Events Uncovered after an RNAi Screen. Curr. Biol. *14*, 1685-1693.

Eggert, U.S., Kiger, A., Richter, C., Perlman, Z., Perrimon, N., Mitchison, T.J., and Field, C.M. (2004). Parallel Chemical Genetic and Genome-Wide RNAi Screens Identify Cytokinesis Inhibitors and Targets. PLoS Biol. *2*, 2136-2143.

Ekşioğlu, Y.Z., Scheffer, I.E., Cardenas, P., Knoll, J., DiMario, F., Ramsby, G., Berg, M., Kamuro, K., Berkovic, S.F., Duyk, G.M.*, et al.* (1996). Periventricular Heterotopia: An X-Linked Dominant Epilepsy Locus Causing Aberrant Cerebral Cortical Development. Neuron *16*, 77-87.

Endicott, J.A., Nurse, P., and Johnson, L.N. (1994). Mutational analysis supports a structural model for the cell cycle protein kinase p34. Protein Eng. *7*, 243-253.

Ezratty, E.J., Bertaux, C., Marcantonio, E.E., and Gundersen, G.G. (2009). Clathrin mediates integrin endocytosis for focal adhesion disassembly in migrating cells. J. Cell Biol. *187*, 733-747.

Fackler, O.T., and Grosse, R. (2008). Cell motility through plasma membrane blebbing. J. Cell Biol. *181*, 879-884.

Farrington-Rock, C., Kirilova, V., Dillard-Telm, L., Borowsky, A.D., Chalk, S., Rock, M.J., Cohn, D.H., and Krakow, D. (2008). Disruption of the Flnb gene in mice phenocopies the human disease spondylocarpotarsal synostosis syndrome. Hum. Mol. Genet. *17*, 631-641.

Feng, Y., Chen, M.H., Moskowitz, I.P., Mendonza, A.M., Vidali, L., Nakamura, F., Kwiatkowski, D.J., and Walsh, C.A. (2006). Filamin A (FLNA) is required for cell-cell contact in vascular development and cardiac morphogenesis. Proc. Natl. Acad. Sci. U. S. A. *103*, 19836-19841.

Finger, F.P., and White, J.G. (2002). Fusion and Fission: Membrane Trafficking in Animal Cytokinesis. Cell *108*, 727-730.

Fishkind, D.J., Cao, L.G., and Wang, Y.L. (1991). Microinjection of the catalytic fragment of myosin light chain kinase into dividing cells: effects on mitosis and cytokinesis. J. Cell Biol. *114*, 967-975.

Flanagan, L.A., Chou, J., Falet, H., Neujahr, R., Hartwig, J.H., and Stossel, T.P. (2001). Filamin A, the Arp2/3 complex, and the morphology and function of cortical actin filaments in human melanoma cells. J. Cell Biol. *155*, 511-517.

Foley (2010). Expansion of the Spectrum of *FLNA* Mutations Associated with Melnick-Needles Syndrome. Molecular syndromology *1*, 121–126.

Fox, J.W., Lamperti, E.D., Eksioglu, Y.Z., Hong, S.E., Feng, Y., Graham, D.A., Scheffer, I.E., Dobyns, W.B., Hirsch, B.A., Radtke, R.A.*, et al.* (1998). Mutations in filamin 1 prevent migration of cerebral cortical neurons in human periventricular heterotopia. Neuron *21*, 1315-1325.

Friedl, P., and Wolf, K. (2003). Tumour-cell invasion and migration: diversity and escape mechanisms. Nat. Rev. Cancer *3*, 362-374.

Gachet, Y., Tournier, S., Millar, J.B.A., and Hyams, J.S. (2001). A MAP kinase-dependent actin checkpoint ensures proper spindle orientation in fission yeast. Nature *412*, 352-355.

Gadde, S., and Heald, R. (2004). Mechanisms and Molecules of the Mitotic Spindle. Curr. Biol. *14*, R797-R805.

Galkin, Vitold E., Orlova, A., and Egelman, Edward H. (2012). Actin Filaments as Tension Sensors. Curr. Biol. *22*, R96-R101.

Galkin, V.E., Orlova, A., VanLoock, M.S., Shvetsov, A., Reisler, E., and Egelman, E.H. (2003). ADF/cofilin use an intrinsic mode of F-actin instability to disrupt actin filaments. J. Cell Biol. *163*, 1057-1066.

Gardel, M.L., Nakamura, F., Hartwig, J.H., Crocker, J.C., Stossel, T.P., and Weitz, D.A. (2006). Prestressed F-actin networks cross-linked by hinged filamins replicate mechanical properties of cells. Proc. Natl. Acad. Sci. U. S. A. *103*, 1762-1767.

Gardel, M.L., Sabass, B., Ji, L., Danuser, G., Schwarz, U.S., and Waterman, C.M. (2008). Traction stress in focal adhesions correlates biphasically with actin retrograde flow speed. J. Cell Biol. *183*, 999-1005.

Gardel, M.L., Shin, J.H., MacKintosh, F.C., Mahadevan, L., Matsudaira, P., and Weitz, D.A. (2004). Elastic Behavior of Cross-Linked and Bundled Actin Networks. Science *304*, 1301-1305.

Gardner, M.K., Zanic, M., and Howard, J. (2013). Microtubule catastrophe and rescue. Curr. Opin. Cell Biol. *25*, 14-22.

Gargiulo, A., Auricchio, R., Barone, M.V., Cotugno, G., Reardon, W., Milla, P.J., Ballabio, A., Ciccodicola, A., and Auricchio, A. (2007). Filamin A is mutated in X-linked chronic idiopathic intestinal pseudo-obstruction with central nervous system involvement. Am. J. Hum. Genet. *80*, 751-758.

Gavet, O., and Pines, J. (2010). Progressive Activation of CyclinB1-Cdk1 Coordinates Entry to Mitosis. Dev. Cell *18*, 533-543.

Gehler, S., Baldassarre, M., Lad, Y., Leight, J.L., Wozniak, M.A., Riching, K.M., Eliceiri, K.W., Weaver, V.M., Calderwood, D.A., and Keely, P.J. (2009). Filamin A-β1 integrin complex tunes epithelial cell response to matrix tension. Mol. Biol. Cell *20*, 3224-3238.

Glickman, M.H., and Ciechanover, A. (2002). The Ubiquitin-Proteasome Proteolytic Pathway: Destruction for the Sake of Construction. Physiol. Rev. *82*, 373-428.

Glogauer, M., Arora, P., Chou, D., Janmey, P.A., Downey, G.P., and McCulloch, C.A.G. (1998). The Role of Actin-binding Protein 280 in Integrin-dependent Mechanoprotection. J. Biol. Chem. *273*, 1689-1698.

Glotzer, M. (2001). Animal cell cytokinesis. Annu. Rev. Cell Dev. Biol. *17*, 351-386.

Glotzer, M. (2009). The 3Ms of central spindle assembly: microtubules, motors and MAPs. Nat. Rev. Mol. Cell Biol. *10*, 9-20.

Glotzer, M., Murray, A.W., and Kirschner, M.W. (1991). Cyclin is degraded by the ubiquitin pathway. Nature *349*, 132-138.

Goldmann, W.H. (2002). p56(lck) Controls phosphorylation of filamin (ABP-280) and regulates focal adhesion kinase (pp125(FAK)). Cell Biol. Int. *26*, 567-571.

Gomer, R.H., and Lazarides, E. (1981). The synthesis and deployment of filamin in chicken skeletal muscle. Cell *23*, 524-532.

Gomer, R.H., and Lazarides, E. (1983). Switching of filamin polypeptides during myogenesis in vitro. J. Cell Biol. *96*, 321-329.

Goparaju, S.K., Jolly, P.S., Watterson, K.R., Bektas, M., Alvarez, S., Sarkar, S., Mel, L., Ishii, I., Chun, J., Milstien, S.*, et al.* (2005). The S1P2 Receptor Negatively Regulates Platelet-Derived Growth Factor-Induced Motility and Proliferation. Mol. Cell. Biol. *25*, 4237-4249.

Gorlin, J.B., Yamin, R., Egan, S., Stewart, M., Stossel, T.P., Kwiatkowski, D.J., and Hartwig, J.H. (1990). Human endothelial actin-binding protein (ABP-280, nonmuscle filamin): a molecular leaf spring. J. Cell Biol. *111*, 1089-1105.

Griffiths, G.S., Grundl, M., Allen, J.S., and Matter, M.L. (2010). R-Ras interacts with filamin a to maintain endothelial barrier function. J. Cell. Physiol. *226*, 2287-2296.

Gromley, A., Yeaman, C., Rosa, J., Redick, S., Chen, C.-T., Mirabelle, S., Guha, M., Sillibourne, J., and Doxsey, S.J. (2005). Centriolin Anchoring of Exocyst and SNARE Complexes at the Midbody Is Required for Secretory-Vesicle-Mediated Abscission. Cell *123*, 75-87.

Großhans, J., Wenzl, C., Herz, H.-M., Bartoszewski, S., Schnorrer, F., Vogt, N., Schwarz, H., and Müller, H.-A. (2005). RhoGEF2 and the formin Dia control the formation of the furrow canal by directed actin assembly during Drosophila cellularisation. Development *132*, 1009-1020.

Hagting, A., Karlsson, C., Clute, P., Jackman, M., and Pines, J. (1998). MPF localization is controlled by nuclear export. EMBO J. *17*, 4127-4138.

Hall, A. (1998). Rho GTPases and the Actin Cytoskeleton. Science *279*, 509-514.
Hanson, J., and Lowy, J. (1963). The structure of F-actin and of actin filaments isolated from muscle. J. Mol. Biol. *6*, 46-IN45.

Hansson, M.D., Rzeznicka, K., Rosenbäck, M., Hansson, M., and Sirijovski, N. (2008). PCR-mediated deletion of plasmid DNA. Anal. Biochem. *375*, 373-375.

Hart, A.W., Morgan, J.E., Schneider, J., West, K., McKie, L., Bhattacharya, S., Jackson, I.J., and Cross, S.H. (2006). Cardiac malformations and midline skeletal defects in mice lacking filamin A. Hum. Mol. Genet. *15*, 2457-2467.

Hartwig, J., and Shevlin, P. (1986). The architecture of actin filaments and the ultrastructural location of actin-binding protein in the periphery of lunch macrophages. J. Cell Biol. *103*, 1007-1020.

Hartwig, J.H., and Stossel, T.P. (1975). Isolation and properties of actin, myosin, and a new actinbinding protein in rabbit alveolar macrophages. J. Biol. Chem. *250*, 5696-5705.

Harvey, S.L., Charlet, A., Haas, W., Gygi, S.P., and Kellogg, D.R. (2005). Cdk1-Dependent Regulation of the Mitotic Inhibitor Wee1. Cell *122*, 407-420.

Harvey, S.L., and Kellogg, D.R. (2003). Conservation of Mechanisms Controlling Entry into Mitosis: Budding Yeast Wee1 Delays Entry into Mitosis and Is Required for Cell Size Control. Curr. Biol. *13*, 264-275.

Heath, J.P. (1983). Behaviour and structure of the leading lamella in moving fibroblasts. I. Occurrence and centripetal movement of arc-shaped microfilament bundles beneath the dorsal cell surface. J. Cell Sci. *60*, 331-354.

Helfman, D.M., Levy, E.T., Berthier, C., Shtutman, M., Riveline, D., Grosheva, I., Lachish-Zalait, A., Elbaum, M., and Bershadsky, A.D. (1999). Caldesmon Inhibits Nonmuscle Cell Contractility and Interferes with the Formation of Focal Adhesions. Mol. Biol. Cell *10*, 3097-3112.

Heng, Y.W., and Koh, C.G. (2010). Actin cytoskeleton dynamics and the cell division cycle. Int. J. Biochem. Cell Biol. *42*, 1622-1633.

Herman, I.M. (1993). Actin isoforms. Curr. Opin. Cell Biol. *5*, 48-55.
Hock, R.S., Sanger, J.M., and Sanger, J.W. (1989). Talin dynamics in living microinjected nonmuscle cells. Cell Motil. Cytoskeleton *14*, 271-287.

Horiuchi, K.Y., Miyata, H., and Chacko, S. (1986). Modulation of smooth muscle actomyosin ATPase by thin filament associated proteins. Biochem. Biophys. Res. Commun. *136*, 962-968.

Hosoya, N., Hosoya, H., Yamashiro, S., Mohri, H., and Matsumura, F. (1993). Localization of caldesmon and its dephosphorylation during cell division. J. Cell Biol. *121*, 1075-1082.

Hotulainen, P., and Lappalainen, P. (2006). Stress fibers are generated by two distinct actin assembly mechanisms in motile cells. J. Cell Biol. *173*, 383-394.

Hu, K., Ji, L., Applegate, K.T., Danuser, G., and Waterman-Storer, C.M. (2007). Differential Transmission of Actin Motion Within Focal Adhesions. Science *315*, 111-115.

Huh, W.-K., Falvo, J.V., Gerke, L.C., Carroll, A.S., Howson, R.W., Weissman, J.S., and O'Shea, E.K. (2003). Global analysis of protein localization in budding yeast. Nature *425*, 686-691.

Ishiguro, J., and Kobayashi, W. (1996). An actin point-mutation neighboring the 'hydrophobic plug' causes defects in the maintenance of cell polaroty and septum organization in the fission yeast Schizosaccharomyces pombe. FEBS Lett. *392*, 237-241.

Ishikawa, R., Yamashiro, S., and Matsumura, F. (1989a). Annealing of gelsolin-severed actin fragments by tropomyosin in the presence of Ca2+. Potentiation of the annealing process by caldesmon. J. Biol. Chem. *264*, 16764-16770.

Ishikawa, R., Yamashiro, S., and Matsumura, F. (1989b). Differential modulation of actin-severing activity of gelsolin by multiple isoforms of cultured rat cell tropomyosin. Potentiation of protective ability of tropomyosins by 83-kDa nonmuscle caldesmon. J. Biol. Chem. *264*, 7490-7497.

Jackman, M., Lindon, C., Nigg, E.A., and Pines, J. (2003). Active cyclin B1-Cdk1 first appears on centrosomes in prophase. Nat. Cell Biol. *5*, 143-148.

Janmey, P.A., Chaponnier, C., Lind, S.E., Zaner, K.S., Stossel, T.P., and Yin, H.L. (1985). Interactions of gelsolin and gelsolin-actin complexes with actin. Effects of calcium on actin nucleation, filament severing, and end blocking. Biochemistry *24*, 3714-3723.

Janmey, P.A., and Stossel, T.P. (1987). Modulation of gelsolin function by phosphatidylinositol 4,5-bisphosphate. Nature *325*, 362-364.

Jaspersen, S.L., Charles, J.F., and Morgan, D.O. (1999). Inhibitory phosphorylation of the APC regulator Hct1 is controlled by the kinase Cdc28 and the phosphatase Cdc14. Curr. Biol. *9*, 227-236.

Jay, D., Garcia, E.J., and de la Luz Ibarra, M. (2004). In situ determination of a PKA phosphorylation site in the C-terminal region of filamin. Mol. Cell. Biochem. *260*, 49-53.

Jay, D., García, E.J., Lara, J.E., Medina, M.A., and de la Luz Ibarra, M. (2000). Determination of a cAMP-Dependent Protein Kinase Phosphorylation Site in the C-Terminal Region of Human Endothelial Actin-Binding Protein. Arch. Biochem. Biophys. *377*, 80-84.

Jefferies, J.L., Taylor, M.D., Rossano, J., Belmont, J.W., and Craigen, W.J. (2010). Novel cardiac findings in periventricular nodular heterotopia. American Journal of Medical Genetics Part A *152A*, 165-168.

Jiang, P., and Campbell, I.D. (2008). Integrin binding immunoglobulin type filamin domains have variable stability. Biochemistry *47*, 11055-11061.

Kamijo, K., Ohara, N., Abe, M., Uchimura, T., Hosoya, H., Lee, J.-S., and Miki, T. (2006). Dissecting the Role of Rho-mediated Signaling in Contractile Ring Formation. Mol. Biol. Cell *17*, 43-55.

Kanters, E., van Rijssel, J., Hensbergen, P.J., Hondius, D., Mul, F.P.J., Deelder, A.M., Sonnenberg, A., van Buul, J.D., and Hordijk, P.L. (2008). Filamin B Mediates ICAM-1-driven Leukocyte Transendothelial Migration. J. Biol. Chem. *283*, 31830-31839.

Kasza, K.E., Nakamura, F., Hu, S., Kollmannsberger, P., Bonakdar, N., Fabry, B., Stossel, T.P., Wang, N., and Weitz, D.A. (2009). Filamin A is essential for active cell stiffening but not passive stiffening under external force. Biophys. J. *96*, 4326-4335.

Katayose, Y., Li, M., Al-Murrani, S.W.K., Shenolikar, S., and Damuni, Z. (2000). Protein Phosphatase 2A Inhibitors, I1 PP2A and I2 PP2A, Associate with and Modify the Substrate Specificity of Protein Phosphatase 1. J. Biol. Chem. *275*, 9209-9214.

Kaverina, I., Krylyshkina, O., and Small, J.V. (2002). Int. J. Biochem. Cell Biol. *34*, *746-761*.

Kawamoto, S., and Hidaka, H. (1984). Ca2+-Activated, phospholipid-dependent protein kinase catalyzes the phosphorylation of actin-binding proteins. Biochem. Biophys. Res. Commun. *118*, 736-742.

Kelly, T.J., and Brown, G.W. (2000). REGULATION OF CHROMOSOME REPLICATION. Annu. Rev. Biochem. *69*, 829-880.

Khatau, S.B., Hale, C.M., Stewart-Hutchinson, P.J., Patel, M.S., Stewart, C.L., Searson, P.C., Hodzic, D., and Wirtz, D. (2009). A perinuclear actin cap regulates nuclear shape. Proc. Natl. Acad. Sci. *106*, 19017-19022.

Kim, E.J., Park, J.S., and Um, S.J. (2007). Filamin A negatively regulates the transcriptional activity of p73alpha in the cytoplasm. Biochem. Biophys. Res. Commun. *362*, 1101-1106.

Kim, H., Sengupta, A., Glogauer, M., and McCulloch, C.A. (2008). Filamin A regulates cell spreading and survival via beta1 integrins. Exp. Cell Res. *314*, 834-846.

Kimura, K., Ito, M., Amano, M., Chihara, K., Fukata, Y., Nakafuku, M., Yamamori, B., Feng, J., Nakano, T., Okawa, K.*, et al.* (1996). Regulation of Myosin Phosphatase by Rho and Rho-Associated Kinase (Rho-Kinase). Science *273*, 245-248.

Klaile, E., Muller, M.M., Kannicht, C., Singer, B.B., and Lucka, L. (2005). CEACAM1 functionally interacts with filamin A and exerts a dual role in the regulation of cell migration. J. Cell Sci. *118*, 5513-5524.

Kovacevic, I., and Cram, E.J. (2010). FLN-1/Filamin is required for maintenance of actin and exit of fertilized oocytes from the spermatheca in C. elegans. Dev. Biol. *347*, 247-257.

Kovacevic, I., Orozco, J.M., and Cram, E.J. (2013). Filamin and Phospholipase C-ε Are Required for Calcium Signaling in the *Caenorhabditis elegans* Spermatheca. PLoS Genet *9*, e1003510.

Kovar, D.R., Kuhn, J.R., Tichy, A.L., and Pollard, T.D. (2003). The fission yeast cytokinesis formin Cdc12p is a barbed end actin filament capping protein gated by profilin. J. Cell Biol. *161*, 875-887.

Kuang, J., and Ashorn, C.L. (1993). At least two kinases phosphorylate the MPM-2 epitope during Xenopus oocyte maturation. J. Cell Biol. *123*, 859-868.

Kume, T., Deng, K., and Hogan, B.L. (2000). Murine forkhead/winged helix genes Foxc1 (Mf1) and Foxc2 (Mfh1) are required for the early organogenesis of the kidney and urinary tract. Development *127*, 1387-1395.

Kunda, P., Pelling, A.E., Liu, T., and Baum, B. (2008). Moesin Controls Cortical Rigidity, Cell Rounding, and Spindle Morphogenesis during Mitosis. Curr. Biol. *18*, 91-101.

Kwiatkowski, D.J., and Yin, H.L. (1987). Molecular biology of gelsolin, a calcium-regulated actin filament severing protein. Biorheology *24*, 643-647.

Lad, Y., Kiema, T., Jiang, P., Pentikainen, O.T., Coles, C.H., Campbell, I.D., Calderwood, D.A., and Ylanne, J. (2007). Structure of three tandem filamin domains reveals auto-inhibition of ligand binding. EMBO J. *26*, 3993-4004.

Larsson, N., Marklund, U., Gradin, H.M., Brattsand, G., and Gullberg, M. (1997). Control of microtubule dynamics by oncoprotein 18: dissection of the regulatory role of multisite phosphorylation during mitosis. Mol. Cell. Biol. *17*, 5530-5539.

Lauffenburger, D.A., and Horwitz, A.F. (1996). Cell Migration: A Physically Integrated Molecular Process. Cell *84*, 359-369.

Lee, K., and Song, K. (2007). Actin Dysfunction Activates ERK1/2 and Delays Entry into Mitosis in Mammalian Cells. Cell Cycle *6*, 1486-1494.

Lee, Y.-J., and Keng, P. (2005). Studying the effects of actin cytoskeletal destabilization on cell cycle by cofilin overexpression. Mol. Biotechnol. *31*, 1-10.

Leung, R., Wang, Y., Cuddy, K., Sun, C., Magalhaes, J., Grynpas, M., and Glogauer, M. (2009). Filamin A Regulates Monocyte Migration Through Rho Small GTPases During Osteoclastogenesis. J. Bone Miner. Res.

Lew, D.J. (2003). The morphogenesis checkpoint: how yeast cells watch their figures. Curr. Opin. Cell Biol. *15*, 648-653.

Li, F., and Higgs, H.N. (2003). The Mouse Formin mDia1 Is a Potent Actin Nucleation Factor Regulated by Autoinhibition. Curr. Biol. *13*, 1335-1340.

Li, J., Meyer, A.N., and Donoghue, D.J. (1995). Requirement for phosphorylation of cyclin B1 for Xenopus oocyte maturation. Mol. Biol. Cell *6*, 1111-1124.

Li, M.G., Serr, M., Edwards, K., Ludmann, S., Yamamoto, D., Tilney, L.G., Field, C.M., and Hays, T.S. (1999). Filamin is required for ring canal assembly and actin organization during Drosophila oogenesis. J. Cell Biol. *146*, 1061-1074.

Li, R. (2007). Cytokinesis in development and disease: variations on a common theme. Cell. Mol. Life Sci. *64*, 3044-3058.

Lianga, N., Williams, E.C., Kennedy, E.K., Doré, C., Pilon, S., Girard, S.L., Deneault, J.-S., and Rudner, A.D. (2013). A Wee1 checkpoint inhibits anaphase onset. J. Cell Biol. *201*, 843-862.

Lin, K.-M., Mejillano, M., and Yin, H.L. (2000). Ca2+ Regulation of Gelsolin by Its C-terminal Tail. J. Biol. Chem. *275*, 27746-27752.

Lipman, N.S., Jackson, L.R., Trudel, L.J., and Weis-Garcia, F. (2005). Monoclonal Versus Polyclonal Antibodies: Distinguishing Characteristics, Applications, and Information Resources. ILAR Journal *46*, 258-268.

Liu, Y., Wada, R., Yamashita, T., Mi, Y., Deng, C.-X., Hobson, J.P., Rosenfeldt, H.M., Nava, V.E., Chae, S.-S., Lee, M.-J.*, et al.* (2000). Edg-1, the G protein–coupled receptor for sphingosine-1-phosphate, is essential for vascular maturation. J. Clin. Invest. *106*, 951-961.

Lodish, H., Berk, A., Zipursky, S., Matsudaira, P., Baltimore, D., and Darnell, J. (2000). Intermediate Filaments Section 19.6. In Molecular Cell Biology 4th Edition (New York: W.H. Freeman).

Loo, D.T., Kanner, S.B., and Aruffo, A. (1998). Filamin binds to the cytoplasmic domain of the beta1-integrin. Identification of amino acids responsible for this interaction. J. Biol. Chem. *273*, 23304-23312.

Loy, C.J., Sim, K.S., and Yong, E.L. (2003). Filamin-A fragment localizes to the nucleus to regulate androgen receptor and coactivator functions. Proc. Natl. Acad. Sci. U. S. A. *100*, 4562-4567.

Lu, J., Lian, G., Lenkinski, R., De Grand, A., Vaid, R.R., Bryce, T., Stasenko, M., Boskey, A., Walsh, C., and Sheen, V. (2007). Filamin B mutations cause chondrocyte defects in skeletal development. Hum. Mol. Genet. *16*, 1661-1675.

Lueck, A., Brown, D., and Kwiatkowski, D.J. (1998). The actin-binding proteins adseverin and gelsolin are both highly expressed but differentially localized in kidney and intestine. J. Cell Sci. *111*, 3633-3643.

Lynch, C.D., Gauthier, N.C., Biais, N., Lazar, A.M., Roca-Cusachs, P., Yu, C.-H., and Sheetz, M.P. (2011). Filamin depletion blocks endoplasmic spreading and destabilizes force-bearing adhesions. Mol. Biol. Cell *22*, 1263-1273.

Maceyka, M., Alvarez, S.E., Milstien, S., and Spiegel, S. (2008). Filamin A links sphingosine kinase 1 and sphingosine-1-phosphate receptor 1 at lamellipodia to orchestrate cell migration. Mol. Cell. Biol. *28*, 5687-5697.

Maddox, A.S., and Burridge, K. (2003). RhoA is required for cortical retraction and rigidity during mitotic cell rounding. J. Cell Biol. *160*, 255-265.

Maestrini, E., Patrosso, C., Mancini, M., Rivella, S., Rocchi, M., Repetto, M., Villa, A., Frattini, A., Zoppè, M., Vezzoni, P.*, et al.* (1993). Mapping of two genes encoding isoforms of the actin binding protein ABP-280, a dystrophin like protein, to Xq28 and to chromosome 7. Hum. Mol. Genet. *2*, 761-766.

Manchado, E., Eguren, M., and Malumbres, M. (2010). The anaphase-promoting complex/cyclosome (APC/C): cell-cycle-dependent and-independent functions. Biochem. Soc. Trans. *38*, 65-71.

Marti, A., Luo, Z., Cunningham, C., Ohta, Y., Hartwig, J., Stossel, T.P., Kyriakis, J.M., and Avruch, J. (1997). Actin-biding Protein-280 Binds the Stress-activated Protein Kinase (SAPK) Activator SEK-1 and Is Required for Tumor Necrosis Factor-Î± Activation of SAPK in Melanoma Cells. J. Biol. Chem. *272*, 2620-2628.

Massague, J. (2004). G1 cell-cycle control and cancer. Nature *432*, 298-306.
Matheson, J., Yu, X., Fielding, A., and Gould, G. (2005). Membrane traffic in cytokinesis. Biochem. Soc. Trans. *33*, 1290-1294.

Matloubian, M., Lo, C.G., Cinamon, G., Lesneski, M.J., Xu, Y., Brinkmann, V., Allende, M.L., Proia, R.L., and Cyster, J.G. (2004). Lymphocyte egress from thymus and peripheral lymphoid organs is dependent on S1P receptor 1. Nature *427*, 355-360.

Matsudaira, P. (1991). Modular organization of actin crosslinking proteins. Trends Biochem. Sci. *16*, 87-92.

Matsumura, F. (2005). Regulation of myosin II during cytokinesis in higher eukaryotes. Trends Cell Biol. *15*, 371-377.

Matzke, R., Jacobson, K., and Radmacher, M. (2001). Direct, high-resolution measurement of furrow stiffening during division of adherent cells. Nat. Cell Biol. *3*, 607-610.

McGough, A. (1998). F-actin-binding proteins. Curr. Opin. Struct. Biol. *8*, 166-176.

McGough, A., Pope, B., Chiu, W., and Weeds, A. (1997). Cofilin Changes the Twist of F-Actin: Implications for Actin Filament Dynamics and Cellular Function. J. Cell Biol. *138*, 771-781.

McGough, A.M., Staiger, C.J., Min, J.-K., and Simonetti, K.D. (2003). The gelsolin family of actin regulatory proteins: modular structures, versatile functions. FEBS Lett. *552*, 75-81.

McMillan, J.N., Sia, R.A.L., and Lew, D.J. (1998). A Morphogenesis Checkpoint Monitors the Actin Cytoskeleton in Yeast. J. Cell Biol. *142*, 1487-1499.

McMillan, J.N., Theesfeld, C.L., Harrison, J.C., Bardes, E.S.G., and Lew, D.J. (2002). Determinants of Swe1p Degradation in Saccharomyces cerevisiae. Mol. Biol. Cell *13*, 3560-3575.

Meyer, S.C., Sanan, D.A., and Fox, J.E.B. (1998). Role of Actin-binding Protein in Insertion of Adhesion Receptors into the Membrane. J. Biol. Chem. *273*, 3013-3020.

Mills, J.C., Stone, N.L., Erhardt, J., and Pittman, R.N. (1998). Apoptotic Membrane Blebbing Is Regulated by Myosin Light Chain Phosphorylation. J. Cell Biol. *140*, 627-636.

Minoshima, Y., Kawashima, T., Hirose, K., Tonozuka, Y., Kawajiri, A., Bao, Y.C., Deng, X., Tatsuka, M., Narumiya, S., May Jr, W.S.*, et al.* (2003). Phosphorylation by Aurora B converts MgcRacGAP to a RhoGAP during cytokinesis. Dev. Cell *4*, 549-560.

Mitchison, J.M., and Swann, M.M. (1955). The Mechanical Properties of the Cell Surface: III. The Sea-Urchin Egg from Fertilization to Cleavage. J. Exp. Biol. *32*, 734-750.

Mitchison, T.J., and Cramer, L.P. (1996). Actin-Based Cell Motility and Cell Locomotion. Cell *84*, 371-379.

Mondal, G., Rowley, M., Guidugli, L., Wu, J., Pankratz, V.S., and Couch, F.J. (2012). BRCA2 Localization to the Midbody by Filamin A Regulates CEP55 Signaling and Completion of Cytokinesis. Dev. Cell *23*, 137-152.

Moore, J.D., Yang, J., Truant, R., and Kornbluth, S. (1999). Nuclear Import of Cdk/Cyclin Complexes: Identification of Distinct Mechanisms for Import of Cdk2/Cyclin E and Cdc2/Cyclin B1. J. Cell Biol. *144*, 213-224.

Moores, C.A., Keep, N.H., and Kendrick-Jones, J. (2000). Structure of the utrophin actin-binding domain bound to F-actin reveals binding by an induced fit mechanism. J. Mol. Biol. *297*, 465-480.

Mooseker, M.S., Bonder, E.M., Conzelman, K.A., Fishkind, D.J., Howe, C.L., and Keller, T.C. (1984). Brush border cytoskeleton and integration of cellular functions. J. Cell Biol. *99*, 104s-112s.

Morgan, D.O. (1995). Principles of CDK regulation. Nature *374*, 131-134.

Morgan, D.O. (1997). CYCLIN-DEPENDENT KINASES: Engines, Clocks, and Microprocessors. Annu. Rev. Cell Dev. Biol. *13*, 261-291.

Morgan, D.O., and De Bondt, H.L. (1994). Protein kinase regulation: insights from crystal structure analysis. Curr. Opin. Cell Biol. *6*, 239-246.

Morgan, T., Lockerbie, R., Minamide, L., Browning, M., and Bamburg, J. (1993). Isolation and characterization of a regulated form of actin depolymerizing factor. J. Cell Biol. *122*, 623-633.

Moulding, D.A., Blundell, M.P., Spiller, D.G., White, M.R.H., Cory, G.O., Calle, Y., Kempski, H., Sinclair, J., Ancliff, P.J., Kinnon, C.*, et al.* (2007). Unregulated actin polymerization by WASp causes defects of mitosis and cytokinesis in X-linked neutropenia. J. Exp. Med. *204*, 2213-2224.

Mullins, R.D., Heuser, J.A., and Pollard, T.D. (1998). The interaction of Arp2/3 complex with actin: Nucleation, high affinity pointed end capping, and formation of branching networks of filaments. Proc. Natl. Acad. Sci. *95*, 6181-6186.

Murray, A.W. (2004). Recycling the Cell Cycle: Cyclins Revisited. Cell *116*, 221-234.

Murthy, K., and Wadsworth, P. (2005). Myosin-II-Dependent Localization and Dynamics of F-Actin during Cytokinesis. Curr. Biol. *15*, 724-731.

Nagano, T., Morikubo, S., and Sato, M. (2004). Filamin A and FILIP (Filamin A-Interacting Protein) regulate cell polarity and motility in neocortical subventricular and intermediate zones during radial migration. J. Neurosci. *24*, 9648-9657.

Nakamura, F., Osborn, T.M., Hartemink, C.A., Hartwig, J.H., and Stossel, T.P. (2007). Structural basis of filamin A functions. J. Cell Biol. *179*, 1011-1025.

Nakamura, F., Stossel, T.P., and Hartwig, J.H. (2011). The filamins: Organizers of cell structure and function. Cell Adhesion & Migration *5*, 160-169.

Naumanen, P., Lappalainen, P., and Hotulainen, P. (2008). Mechanisms of actin stress fibre assembly. J. Microsc. *231*, 446-454.

Niederman, R., Amrein, P.C., and Hartwig, J. (1983). Three-dimensional structure of actin filaments and of an actin gel made with actin-binding protein. J. Cell Biol. *96*, 1400-1413.

Niessen, C.M. (2007). Tight Junctions/Adherens Junctions: Basic Structure and Function. J. Invest. Dermatol. *127*, 2525-2532.

Nigg, E.A. (1993). Cellular substrates of p34cdc2 and its companion cyclin-dependent kinases. Trends Cell Biol. *3*, 296-301.

Nigg, E.A. (1995). Cyclin-dependent protein kinases: Key regulators of the eukaryotic cell cycle. Bioessays *17*, 471-480.

Nigg, E.A. (2001). Mitotic kinases as regulators of cell division and its checkpoints. Nat. Rev. Mol. Cell Biol. *2*, 21-32.

Nikki, M., Merilainen, J., and Lehto, V.P. (2002). FAP52 regulates actin organization via binding to filamin. J. Biol. Chem. *277*, 11432-11440.

Nishimura, Y., and Yonemura, S. (2006). Centralspindlin regulates ECT2 and RhoA accumulation at the equatorial cortex during cytokinesis. J. Cell Sci. *119*, 104-114.

Northrop, J., Weber, A., Mooseker, M.S., Franzini-Armstrong, C., Bishop, M.F., Dubyak, G.R., Tucker, M., and Walsh, T.P. (1986). Different calcium dependence of the capping and cutting activities of villin. J. Biol. Chem. *261*, 9274-9281.

Nousiainen, M., Silljé, H.H.W., Sauer, G., Nigg, E.A., and Körner, R. (2006). Phosphoproteome analysis of the human mitotic spindle. Proc. Natl. Acad. Sci. *103*, 5391-5396.

Nunnally, M.H., D'Angelo, J.M., and Craig, S.W. (1980). Filamin concentration in cleavage furrow and midbody region: frequency of occurrence compared with that of alpha-actinin and myosin. J. Cell Biol. *87*, 219-226.

Nurse, P. (1990). Universal control mechanism regulating onset of M-phase. Nature *344*, 503-508.

O'Connell, M.P., Fiori, J.L., Baugher, K.M., Indig, F.E., French, A.D., Camilli, T.C., Frank, B.P., Earley, R., Hoek, K.S., Hasskamp, J.H.*, et al.* (2009). Wnt5A activates the calpain-mediated cleavage of filamin A. J. Invest. Dermatol. *129*, 1782-1789.

O'Connor, C. (2008). Cell Division: Stages of Mitosis. Nature Education *1*, 188.
Ohta, Y., and Hartwig, J.H. (1995). Actin filament cross-linking by chicken gizzard filamin is regulated by phosphorylation in vitro. Biochemistry *34*, 6745-6754.

Ohta, Y., and Hartwig, J.H. (1996). Phosphorylation of Actin-binding Protein 280 by Growth Factors Is Mediated by p90 Ribosomal Protein S6 Kinase. J. Biol. Chem. *271*, 11858-11864.

Ohta, Y., Suzuki, N., Nakamura, S., Hartwig, J.H., and Stossel, T.P. (1999). The small GTPase RalA targets filamin to induce filopodia. Proc. Natl. Acad. Sci. U. S. A. *96*, 2122-2128.

Okita, J.R., Pidard, D., Newman, P.J., Montgomery, R.R., and Kunicki, T.J. (1985). On the association of glycoprotein Ib and actin-binding protein in human platelets. J. Cell Biol. *100*, 317-321.

Olsen, J.V., Vermeulen, M., Santamaria, A., Kumar, C., Miller, M.L., Jensen, L.J., Gnad, F., Cox, J., Jensen, T.S., Nigg, E.A.*, et al.* (2010). Quantitative Phosphoproteomics Reveals Widespread Full Phosphorylation Site Occupancy During Mitosis. Sci. Signal. *3*, 1-15.

Ott, I., Fischer, E.G., Miyagi, Y., Mueller, B.M., and Ruf, W. (1998). A Role for Tissue Factor in Cell Adhesion and Migration Mediated by Interaction with Actin-binding Protein 280. J. Cell Biol. *140*, 1241-1253.

Page, R.C., Clark, J.G., and Misra, S. (2011). Structure of filamin A immunoglobulin-like repeat 10 from Homo sapiens. Acta Crystallographica Section F *67*, 871-876.

Pavalko, F.M., Otey, C.A., and Burridge, K. (1989). Identification of a filamin isoform enriched at the ends of stress fibers in chicken embryo fibroblasts. J. Cell Sci. *94 ( Pt 1)*, 109-118.

Pelham, R.J., and Chang, F. (2002). Actin dynamics in the contractile ring during cytokinesis in fission yeast. Nature *419*, 82-86.

Pellegrin, S., and Mellor, H. (2007). Actin stress fibres. J. Cell Sci. *120*, 3491-3499.

Pentikäinen, U., and Ylänne, J. (2009). The regulation mechanism for the auto-inhibition of binding of human filamin A to integrin. J. Mol. Biol. *393*, 644-657.

Peter, M., Nakagawa, J., Dorée, M., Labbé, J.C., and Nigg, E.A. (1990). In vitro disassembly of the nuclear lamina and M phase-specific phosphorylation of lamins by cdc2 kinase. Cell *61*, 591-602.

Pfleger, C.M., and Kirschner, M.W. (2000). The KEN box: an APC recognition signal distinct from the D box targeted by Cdh1. Genes Dev. *14*, 655-665.

Piaggio, G., Farina, A., Perrotti, D., Manni, I., Fuschi, P., Sacchi, A., and Gaetano, C. (1995). Structure and Growth-Dependent Regulation of the Human Cyclin B1 Promoter. Exp. Cell Res. *216*, 396-402.

Piekny, A., Werner, M., and Glotzer, M. (2005). Cytokinesis: welcome to the Rho zone. Trends Cell Biol. *15*, 651-658.

Pines, J. (1995). Cyclins and cyclin-dependent kinases: a biochemical view. Biochem. J. *308*, 697-711.

Pines, J., and Hunter, T. (1989). Isolation of a human cyclin cDNA: Evidence for cyclin mRNA and protein regulation in the cell cycle and for interaction with p34cdc2. Cell *58*, 833-846.

Pines, J., and Hunter, T. (1991). Human cyclins A and B1 are differentially located in the cell and undergo cell cycle-dependent nuclear transport. J. Cell Biol. *115*, 1-17.

Playford, M.P., Lyons, P.D., Sastry, S.K., and Schaller, M.D. (2006). Identification of a Filamin Docking Site on PTP-PEST. J Biol Chem *281*, 34104-34112.

Polesello, C., Delon, I., Valenti, P., Ferrer, P., and Payre, F. (2002). Dmoesin controls actin-based cell shape and polarity during Drosophila melanogaster oogenesis. Nat. Cell Biol. *4*, 782-789.

Pollard, T.D. (2010). Mechanics of cytokinesis in eukaryotes. Curr. Opin. Cell Biol. *22*, 50-56.

Pollard, T.D., and Borisy, G.G. (2003). Cellular Motility Driven by Assembly and Disassembly of Actin Filaments. Cell *112*, 453-465.

Ponti, A., Machacek, M., Gupton, S.L., Waterman-Storer, C.M., and Danuser, G. (2004). Two Distinct Actin Networks Drive the Protrusion of Migrating Cells. Science *305*, 1782-1786.

Popowicz, G.M., Müller, R., Noegel, A.A., Schleicher, M., Huber, R., and Holak, T.A. (2004). Molecular structure of the rod domain of dictyostelium filamin. J. Mol. Biol. *342*, 1637-1646.

Popowicz, G.M., Schleicher, M., Noegel, A.A., and Holak, T.A. (2006). Filamins: promiscuous organizers of the cytoskeleton. Trends Biochem. Sci. *31*, 411-419.

Potter, D.A., Tirnauer, J.S., Janssen, R., Croall, D.E., Hughes, C.N., Fiacco, K.A., Mier, J.W., Maki, M., and Herman, I.M. (1998). Calpain Regulates Actin Remodeling during Cell Spreading. J. Cell Biol. *141*, 647-662.

Prasanth, S.G., Méndez, J., Prasanth, K.V., and Stillman, B. (2004). Dynamics of pre-replication complex proteins during the cell division cycle. Philos. Trans. R. Soc. Lond. B Biol. Sci. *359*, 7-16.

Pring, M., Evangelista, M., Boone, C., Yang, C., and Zigmond, S.H. (2002). Mechanism of Formin-Induced Nucleation of Actin Filaments. Biochemistry *42*, 486-496.

Pruyne, D., Evangelista, M., Yang, C., Bi, E., Zigmond, S., Bretscher, A., and Boone, C. (2002). Role of Formins in Actin Assembly: Nucleation and Barbed-End Association. Science *297*, 612-615.

Razinia, Z., Mäkelä, T., Ylänne, J., and Calderwood, D.A. (2012). Filamins in Mechanosensing and Signaling. Ann. Rev. Biophys. *41*, 227-246.

Reinstein, E., Frentz, S., Morgan, T., Garcia-Minaur, S., Leventer, R.J., McGillivray, G., Pariani, M., van der Steen, A., Pope, M., Holder-Espinasse, M*., et al.* (2012). Vascular and connective tissue anomalies associated with X-linked periventricular heterotopia due to mutations in Filamin A. Eur. J. Hum. Genet.

Reshetnikova, G., Barkan, R., Popov, B., Nikolsky, N., and Chang, L.-S. (2000). Disruption of the Actin Cytoskeleton Leads to Inhibition of Mitogen-Induced Cyclin E Expression, Cdk2 Phosphorylation, and Nuclear Accumulation of the Retinoblastoma Protein-Related p107 Protein. Exp. Cell Res. *259*, 35-53.

Revel, J.P., Hoch, P., and Ho, D. (1974). Adhesion of culture cells to their substratum. Exp. Cell Res. *84*, 207-218.

Revenu, C., Athman, R., Robine, S., and Louvard, D. (2004). The co-workers of actin filaments: from cell structures to signals. Nat. Rev. Mol. Cell Biol. *5*, 635-646.

Ridley, Anne J. (2011). Life at the Leading Edge. Cell *145*, 1012-1022.

Ridley, A.J., and Hall, A. (1992). The small GTP-binding protein rho regulates the assembly of focal adhesions and actin stress fibers in response to growth factors. Cell *70*, 389-399.

Robertson, S.P. (2005). Filamin A: phenotypic diversity. Curr. Opin. Genet. Dev. *15*, 301-307.

Robertson, S.P., Jenkins, Z.A., Morgan, T., Adès, L., Aftimos, S., Boute, O., Fiskerstrand, T., Garcia-Miñaur, S., Grix, A., Green, A.*, et al.* (2006). Frontometaphyseal dysplasia: Mutations in FLNA and phenotypic diversity. American Journal of Medical Genetics Part A *140A*, 1726-1736.

Robertson, S.P., Twigg, S.R., Sutherland-Smith, A.J., Biancalana, V., Gorlin, R.J., Horn, D., Kenwrick, S.J., Kim, C.A., Morava, E., Newbury-Ecob, R.*, et al.* (2003). Localized mutations in the gene encoding the cytoskeletal protein filamin A cause diverse malformations in humans. Nat. Genet. *33*, 487-491.

Rudner, A.D., and Murray, A.W. (2000). Phosphorylation by Cdc28 Activates the Cdc20-Dependent Activity of the Anaphase-Promoting Complex. J. Cell Biol. *149*, 1377-1390.

Rupeš, I. (2002). Checking cell size in yeast. Trends Genet. *18*, 479-485.

Safer, D., Elzinga, M., and Nachmias, V.T. (1991). Thymosin beta 4 and Fx, an actin-sequestering peptide, are indistinguishable. J. Biol. Chem. *266*, 4029-4032.

Salbreux, G., Charras, G., and Paluch, E. (2012). Actin cortex mechanics and cellular morphogenesis. Cell *22*, 536-545.

Sanchez, T., Thangada, S., Wu, M.-T., Kontos, C.D., Wu, D., Wu, H., and Hla, T. (2005). PTEN as an effector in the signaling of antimigratory G protein-coupled receptor. Proc. Natl. Acad. Sci. U. S. A. *102*, 4312-4317.

Sanger, J.M., Mittal, B., Pochapin, M.B., and Sanger, J.W. (1987). Stress fiber and cleavage furrow formation in living cells microinjected with fluorescently labeled α-actinin. Cell Motil. Cytoskeleton *7*, 209-220.

Sasaki, A., Masuda, Y., Ohta, Y., Ikeda, K., and Watanabe, K. (2001). Filamin associates with Smads and regulates transforming growth factor-beta signaling. J. Biol. Chem. *276*, 17871-17877.

Schafer, D.A., and Cooper, J.A. (1995). Control of Actin Assembly at Filament Ends. Annu. Rev. Cell Dev. Biol. *11*, 497-518.

Schiel, J.A., and Prekeris, R. (2010). Making the Final Cut-Mechanisms Mediating the Abscission Step of Cytokinesis. TheScientificWorldJOURNAL *10*, 1424-1434.

Schliwa, M., and van Blerkom, J. (1981). Structural interaction of cytoskeletal components. J. Cell Biol. *90*, 222-235.

Schlüter, K., Jockusch, B.M., and Rothkegel, M. (1997). Profilins as regulators of actin dynamics. Biochimica et Biophysica Acta (BBA) - Molecular Cell Research *1359*, 97-109.

Schollmeyer, J., Rao, G., and White, J. (1978). An actin-binding protein in human platelets. Interactions with alpha-actinin on gelatin of actin and the influence of cytochalasin B. Am. J. Pathol. *93*, 433-446.

Schroeder, T. (1990). The Contractile Ring and Furrowing in Dividing Cells. Ann. NY Acad. Sci. *582*, 78-87.

Segal, M., and Bloom, K. (2001). Control of spindle polarity and orientation in Saccharomyces cerevisiae. Trends Cell Biol. *11*, 160-166.

Sharma, C.P., Ezzell, R.M., and Arnaout, M.A. (1995). Direct interaction of filamin (ABP-280) with the beta 2-integrin subunit CD18. J. Immunol. *154*, 3461-3470.

Sharma, C.P., and Goldmann, W.H. (2004). Phosphorylation of actin-binding protein (ABP-280; filamin) by tyrosine kinase p56lck modulates actin filament cross-linking. Cell Biol. Int. *28*, 935-941.

Sheen, V.L., Dixon, P.H., Fox, J.W., Hong, S.E., Kinton, L., Sisodiya, S.M., Duncan, J.S., Dubeau, F., Scheffer, I.E., Schachter, S.C*., et al.* (2001). Mutations in the X-linked filamin 1 gene cause periventricular nodular heterotopia in males as well as in females. Hum. Mol. Genet. *10*, 1775-1783.

Skop, A.R., Liu, H., Yates, J., Meyer, B.J., and Heald, R. (2004). Dissection of the Mammalian Midbody Proteome Reveals Conserved Cytokinesis Mechanisms. Science *305*, 61-66.

Small, J.V. (1994). Lamellipodia architecture: actin filament turnover and the lateral flow of actin filaments during motility. Semin. Cell Biol. *5*, 157-163.

Small, J.V., Rottner, K., Kaverina, I., and Anderson, K.I. (1998). Assembling an actin cytoskeleton for cell attachment and movement. Biochimica et Biophysica Acta (BBA) - Molecular Cell Research *1404*, 271-281.

Smits, V.A.J., and Medema, R.H. (2001). Checking out the G2/M transition. Biochimica et Biophysica Acta (BBA) - Gene Structure and Expression *1519*, 1-12.

Sohn, R.H., and Goldschmidt-Clermont, P.J. (1994). Profilin: At the crossroads of signal transduction and the actin cytoskeleton. Bioessays *16*, 465-472.

Sokol, N.S., and Cooley, L. (1999). Drosophila filamin encoded by the cheerio locus is a component of ovarian ring canals. Curr. Biol. *9*, 1221-1230.

Sokol, N.S., and Cooley, L. (2003). Drosophila filamin is required for follicle cell motility during oogenesis. Dev. Biol. *260*, 260-272.

Somers, W.G., and Saint, R. (2003). A RhoGEF and Rho Family GTPase-Activating Protein Complex Links the Contractile Ring to Cortical Microtubules at the Onset of Cytokinesis. Dev. Cell *4*, 29-39.

Sonnichsen, B., Koski, L.B., Walsh, A., Marschall, P., Neumann, B., Brehm, M., Alleaume, A.-M., Artelt, J., Bettencourt, P., Cassin, E.*, et al.* (2005). Full-genome RNAi profiling of early embryogenesis in Caenorhabditis elegans. Nature *434*, 462-469.

Stewart, M.P., Jonne, H., Yusuke, T., Subramanian, P.R., Daniel, J.M., and Anthony, A.H. (2011). Hydrostatic pressure and the actomyosin cortex drive mitotic cell rounding. Nature *469*, 226-230.

Stossel, T.P. (1984). Contribution of actin to the structure of the cytoplasmic matrix. J. Cell Biol. *99*, 15s-21s.

Stossel, T.P., Condeelis, J., Cooley, L., Hartwig, J.H., Noegel, A., Schleicher, M., and Shapiro, S.S. (2001). Filamins as integrators of cell mechanics and signalling. Nat. Rev. Mol. Cell Biol. *2*, 138-145.

Stossel, T.P., Fenteany, G., and Hartwig, J.H. (2006). Cell surface actin remodeling. J. Cell Sci. *119*, 3261-3264.

Sugimoto, N., Takuwa, N., Okamoto, H., Sakurada, S., and Takuwa, Y. (2003). Inhibitory and Stimulatory Regulation of Rac and Cell Motility by the G12/13-Rho and Gi Pathways Integrated Downstream of a Single G Protein-Coupled Sphingosine-1-Phosphate Receptor Isoform. Mol. Cell. Biol. *23*, 1534-1545.

Svitkina, T.M., Bulanova, E.A., Chaga, O.Y., Vignjevic, D.M., Kojima, S.-i., Vasiliev, J.M., and Borisy, G.G. (2003). Mechanism of filopodia initiation by reorganization of a dendritic network. J. Cell Biol. *160*, 409-421.

Svitkina, T.M., Verkhovsky, A.B., McQuade, K.M., and Borisy, G.G. (1997). Analysis of the Actin–Myosin II System in Fish Epidermal Keratocytes: Mechanism of Cell Body Translocation. J. Cell Biol. *139*, 397-415.

Tachikawa, M., Nakagawa, H., Terasaki, A.G., Mori, H., and Ohashi, K. (1997). A 260-kDa filamin/ABP-related protein in chicken gizzard smooth muscle cells is a new component of the dense plaques and dense bodies of smooth muscle. J. Biochem. *122*, 314-321.

Takafuta, T., Wu, G., Murphy, G.F., and Shapiro, S.S. (1998). Human beta-filamin is a new protein that interacts with the cytoplasmic tail of glycoprotein Ibalpha. J. Biol. Chem. *273*, 17531-17538.

Terasima, T., and Tolmach, L.J. (1963). Growth and nucleic acid synthesis in synchronously dividing populations of HeLa cells. Exp. Cell Res. *30*, 344-362.

Théry, M., and Bornens, M. (2008). Get round and stiff for mitosis. HFSP Journal *2*, 65-71.

Thompson, T.G., Chan, Y.M., Hack, A.A., Brosius, M., Rajala, M., Lidov, H.G., McNally, E.M., Watkins, S., and Kunkel, L.M. (2000). Filamin 2 (FLN2): A muscle-specific sarcoglycan interacting protein. J. Cell Biol. *148*, 115-126.

Tigges, U., Koch, B., Wissing, J., Jockusch, B.M., and Ziegler, W.H. (2003). The F-actin cross-linking and focal adhesion protein filamin A is a ligand and in vivo substrate for protein kinase C alpha. J. Biol. Chem. *278*, 23561-23569.

Tilney, L.G., and Tilney, M.S. (1984). Observations on how actin filaments become organized in cells. J. Cell Biol. *99*, 76s-82s.
Tojkander, S., Gateva, G., and Lappalainen, P. (2012). Actin stress fibers – assembly, dynamics and biological roles. J. Cell Sci. *125*, 1855-1864.

Tolliday, N., VerPlank, L., and Li, R. (2002). Rho1 Directs Formin-Mediated Actin Ring Assembly during Budding Yeast Cytokinesis. Curr. Biol. *12*, 1864-1870.

Totsukawa, G., Yamakita, Y., Yamashiro, S., Hartshorne, D.J., Sasaki, Y., and Matsumura, F. (2000). Distinct Roles of Rock (Rho-Kinase) and Mlck in Spatial Regulation of Mlc Phosphorylation for Assembly of Stress Fibers and Focal Adhesions in 3t3 Fibroblasts. J. Cell Biol. *150*, 797-806.

Toyoshima, F., Moriguchi, T., Wada, A., Fukuda, M., and Nishida, E. (1998). Nuclear export of cyclin B1 and its possible role in the DNA damage induced G2 checkpoint. EMBO J. *17*, 2728-2735.

Trapani, J.A., Jans, D.A., Jans, P.J., Smyth, M.J., Browne, K.A., and Sutton, V.R. (1998). Efficient Nuclear Targeting of Granzyme B and the Nuclear Consequences of Apoptosis Induced by Granzyme B and Perforin Are Caspase-dependent, but Cell Death Is Caspase-independent. J. Biol. Chem. *273*, 27934-27938.

Trinkle-Mulcahy, L., Boulon, S., Lam, Y.W., Urcia, R., Boisvert, F.M., Vandermoere, F., Morrice, N.A., Swift, S., Rothbauer, U., Leonhardt, H.*, et al.* (2008). Identifying specific protein interaction partners using quantitative mass spectrometry and bead proteomes. J. Cell Biol. *183*, 223-239.

Tu, Y., Wu, S., Shi, X., Chen, K., and Wu, C. (2003). Migfilin and Mig-2 link focal adhesions to filamin and the actin cytoskeleton and function in cell shape modulation. Cell *113*, 37-47.

Ueda, K., Ohta, Y., and Hosoya, H. (2003). The carboxy-terminal pleckstrin homology domain of ROCK interacts with filamin-A. Biochem. Biophys. Res. Commun. *301*, 886-890.
Ueda, M., Oho, C., Takisawa, H., and Ogihara, S. (1992). Interaction of the low-molecular-mass, guanine-nucleotide-binding protein with the actin-binding protein and its modulation by the cAMP-dependent protein kinase in bovine platelets. Eur. J. Biochem. *203*, 347-352.

Vadlamudi, R.K., Li, F., Adam, L., Nguyen, D., Ohta, Y., Stossel, T.P., and Kumar, R. (2002). Filamin is essential in actin cytoskeletal assembly mediated by p21-activated kinase 1. Nat. Cell Biol. *4*, 681-690.

Vagnarelli, P. (2012). Mitotic chromosome condensation in vertebrates. Exp. Cell Res. *318*, 1435-1441.

Van der Flier, A. (2001). Structural and functional aspects of filamins. Biochim. Biophys. Acta *1538*, 99-117.

van der Ven, P.F., Obermann, W.M., Lemke, B., Gautel, M., Weber, K., and Furst, D.O. (2000). Characterization of muscle filamin isoforms suggests a possible role of gamma-filamin/ABP-L in sarcomeric Z-disc formation. Cell Motil. Cytoskeleton *45*, 149-162.

Vargas, M., Sansonetti, P., and Guillén, N. (1996). Identification and cellular localization of the actin-binding protein ABP-120 from Entamoeba histolytica. Mol. Microbiol. *22*, 849-857.

Velkova, A., Carvalho, M.A., Johnson, J.O., Tavtigian, S.V., and Monteiro, A.N.A. (2010). Identification of Filamin A as a BRCA1-interacting protein required for efficient DNA repair. Cell Cycle *9*, 1421-1433.

Vial, D., and McKeown-Longo, P.J. (2012). EGF Regulates alpha5beta1 Integrin Activation State in Human Cancer Cell Lines Through the p90RSK-Dependent Phosphorylation of Filamin A. J. Biol. Chem. *287*, 40371-40380.

Wallach, D., Davies, P.J., and Pastan, I. (1978a). Cyclic AMP-dependent phosphorylation of filamin in mammalian smooth muscle. J. Biol. Chem. *253*, 4739-4745.

Wallach, D., Davies, P.J., and Pastan, I. (1978b). Purification of mammalian filamin. Similarity to high molecular weight actin-binding protein in macrophages, platelets, fibroblasts, and other tissues. J. Biol. Chem. *253*, 3228-3235.

Wang, K., Ash, J.F., and Singer, S.J. (1975). Filamin, a new high-molecular-weight protein found in smooth muscle and non-muscle cells. Proc. Natl. Acad. Sci. U. S. A. *72*, 4483-4486.

Watanabe, T., Yoshida, N., and Satake, M. (2005). Biological Implications of Filamin A-Bound PEBP2β /CBFβ Retention in the Cytoplasm. Critical Reviews™ in Eukaryotic Gene Expression *15*, 197-206.

Weber, A., Pennise, C.R., Babcock, G.G., and Fowler, V.M. (1994). Tropomodulin caps the pointed ends of actin filaments. J. Cell Biol. *127*, 1627-1635.
Wegner, A., and Isenberg, G. (1983). 12-fold difference between the critical monomer concentrations of the two ends of actin filaments in physiological salt conditions. Proc. Natl. Acad. Sci. *80*, 4922-4925.

Wehrle-Haller, B., and Imhof, B.A. (2002). The inner lives of focal adhesions. Trends Cell Biol. *12*, 382-389.

Wickstead, B., and Gull, K. (2011). The evolution of the cytoskeleton. J. Cell Biol. *194*, 513-525.

Wojnacki, J., Quassollo, G., Marzolo, M.P., and Cáceres, A. (2014). Rho GTPases at the crossroad of signaling networks in mammals: Impact of Rho-GTPases on microtubule organization and dynamics. Small GTPases *5*, 0-1.

Wong, A., Pollard, T., and Herman, I. (1983). Actin filament stress fibers in vascular endothelial cells in vivo. Science *219*, 867-869.

Woo, M.S., Ohta, Y., Rabinovitz, I., Stossel, T.P., and Blenis, J. (2004). Ribosomal S6 kinase (RSK) regulates phosphorylation of filamin A on an important regulatory site. Mol. Cell. Biol. *24*, 3025-3035.

Wu, C.F., Wang, R., Liang, Q., Liang, J., Li, W., Jung, S.Y., Qin, J., Lin, S.H., and Kuang, J. (2010). Dissecting the M Phase–specific Phosphorylation of Serine–Proline or Threonine–Proline Motifs. Mol. Biol. Cell *21*, 1470-1481.

Wurtz, J.-M., Bourguet, W., Renaud, J.-P., Vivat, V., Chambon, P., Moras, D., and Gronemeyer, H. (1996). A canonical structure for the ligand-binding domain of nuclear receptors. Nat. Struct. Mol. Biol. *3*, 87-94.

Xian, W., and Janmey, P.A. (2002). Dissecting the Gelsolin–Polyphosphoinositide Interaction and Engineering of a Polyphosphoinositide-sensitive Gelsolin C-terminal Half Protein. J. Mol. Biol. *322*, 755-771.

Yamakita, Y., Totsukawa, G., Yamashiro, S., Fry, D., Zhang, X., Hanks, S.K., and Matsumura, F. (1999). Dissociation of FAK/p130CAS/c-Src Complex during Mitosis: Role of Mitosis-specific Serine Phosphorylation of FAK. J. Cell Biol. *144*, 315-324.

Yamamoto, M., Hilgemann, D.H., Feng, S., Bito, H., Ishihara, H., Shibasaki, Y., and Yin, H.L. (2001). Phosphatidylinositol 4,5-Bisphosphate Induces Actin Stress-Fiber Formation and Inhibits Membrane Ruffling in Cv1 Cells. J. Cell Biol. *152*, 867-876.

Yamano, H., Tsurumi, C., Gannon, J., and Hunt, T. (1998). The role of the destruction box and its neighbouring lysine residues in cyclin B for anaphase ubiquitin dependent proteolysis in fission yeast: defining the D box receptor. The EMBO Journal *17*, 5670-5678.

Yamashiro, S., Chern, H., Yamakita, Y., and Matsumura, F. (2001). Mutant Caldesmon Lacking cdc2 Phosphorylation Sites Delays M-Phase Entry and Inhibits Cytokinesis. Mol. Biol. Cell *12*, 239-250.

Yamashiro, S., and Matsumura, F. (1991). Mitosis-specific phosphorylation of caldesmon: Possible molecular mechanism of cell rounding during mitosis. Bioessays *13*, 563-568.

Yamashiro, S., Yamakita, Y., Hosoya, H., and Matsumura, F. (1991). Phosphorylation of non-muscle caldesmon by p34cdc2 kinase during mitosis. Nature *349*, 169-172.

Yamashiro, S., Yamakita, Y., Ishikawa, R., and Matsumura, F. (1990). Mitosis-specific phosphorylation causes 83K non-muscle caldesmon to dissociate from microfilaments. Nature *344*, 675-678.

Yamashiro, S., Yoshida, K., Yamakita, Y., and Matsumura, F. (1994). Caldesmon: Possible Functions in Microfilament Reorganization During Mitosis and Cell Transformation. In Actin, J. Estes, and P. Higgins, eds. (Springer US), pp. 113-122.

Yoneda, M., and Dan, K. (1972). Tension at the Surface of the Dividing Sea-Urchin Egg. J. Exp. Biol. *57*, 575-587.

Yoshida, K., and Soldati, T. (2006). Dissection of amoeboid movement into two mechanically distinct modes. J. Cell Sci. *119*, 3833-3844.

Yoshida, N., Ogata, T., Tanabe, K., Li, S., Nakazato, M., Kohu, K., Takafuta, T., Shapiro, S., Ohta, Y., Satake, M*., et al.* (2005). Filamin A-bound PEBP2beta/CBFbeta is retained in the cytoplasm and prevented from functioning as a partner of the Runx1 transcription factor. Mol. Cell. Biol. *25*, 1003-1012.

Yuan, Y., and Shen, Z. (2001). Interaction with BRCA2 suggests a role for filamin-1 (hsFLNa) in DNA damage response. J. Biol. Chem. *276*, 48318-48324.

Yüce, Ö., Piekny, A., and Glotzer, M. (2005). An ECT2–centralspindlin complex regulates the localization and function of RhoA. J. Cell Biol. *170*, 571-582.

Yue, J., Huhn, S., and Shen, Z. (2013). Complex roles of filamin-A mediated cytoskeleton network in cancer progression. Cell and Bioscience *3*, 1-12.

Zachariae, W., Schwab, M., Nasmyth, K., and Seufert, W. (1998). Control of Cyclin Ubiquitination by CDK-Regulated Binding of Hct1 to the Anaphase Promoting Complex. Science *282*, 1721-1724.

Zheng, L., Baek, H.J., Karsenty, G., and Justice, M.J. (2007). Filamin B represses chondrocyte hypertrophy in a Runx2/Smad3-dependent manner. J. Cell Biol. *178*, 121-128.

Zhong, Z., Yeow, W.-S., Zou, C., Wassell, R., Wang, C., Pestell, R.G., Quong, J.N., and Quong, A.A. (2010). Cyclin D1/Cyclin-Dependent Kinase 4 Interacts with Filamin A and Affects the Migration and Invasion Potential of Breast Cancer Cells. Cancer Res. *70*, 2105-2114.

Zhou, A.-X., Hartwig, J.H., and Akyürek, L.M. (2010). Filamins in cell signaling, transcription and organ development. Trends Cell Biol. *20*, 113-123.

Zhou, X., Tian, F., Sandzen, J., Cao, R., Flaberg, E., Szekely, L., Cao, Y., Ohlsson, C., Bergo, M.O., Boren, J.*, et al.* (2007). Filamin B deficiency in mice results in skeletal malformations and impaired microvascular development. Proc. Natl. Acad. Sci. U. S. A. *104*, 3919-3924.

Zhu, C., Zhao, J., Bibikova, M., Leverson, J.D., Bossy-Wetzel, E., Fan, J.-B., Abraham, R.T., and Jiang, W. (2005). Functional Analysis of Human Microtubule-based Motor Proteins, the Kinesins and Dyneins, in Mitosis/Cytokinesis Using RNA Interference. Mol. Biol. Cell *16*, 3187-3199.

Zhuang, Q., Rosenberg, S., Lawrence, J., and Stracher, A. (1984). Role of actin binding protein phosphorylation in platelet cytoskeleton assembly. Biochem. Biophys. Res. Commun. *118*, 508-513.

Zigmond, S.H. (2004). Formin-induced nucleation of actin filaments. Curr. Opin. Cell Biol. *16*, 99-105.

# CONTRIBUTIONS OF COLLABORATORS

## COLLABORATOR 1

**Name:** Jonathan M. Lee
**Position:** Principal Investigator
**Relationship to Sandy Szeto:** Thesis supervisor

**Affiliations:**
Department of Biochemistry, Microbiology and Immunology, Faculty of Medicine, University of Ottawa, Roger Guindon Hall, 451 Smyth Road, Ottawa, ON K1H 8M5 Canada.

**Description of Contribution**
Performed time-lapse microscopy of M2 cells expressing FLNa-WT GFP, FLNa-AAA GFP and GFP EV undergoing mitosis (Figure 4.10A). Provided raw data for quantification of the number of cells that separate post-mitotically (4.10B). See Material and Methods, section 2.15. Performed experiments and imaging for Figures 4.1C and Figure 4.11B.

**Figures**
Figure 4.1C
Figure 4.10
Figure 4.11B
Videos 1-4

**COLLABORATOR 2**

**Name:** Elizabeth C. Williams
**Position:** Ph.D. student in Dr. Adam D. Rudner's lab
**Relationship to Sandy Szeto:** Colleague, Adam D. Rudner is a member of Sandy Szeto's Thesis Advisory Committee

**Affiliations:**
Department of Biochemistry, Microbiology and Immunology and Ottawa Institute of Systems Biology, Faculty of Medicine, University of Ottawa, Roger Guindon Hall, 451 Smyth Road, Ottawa, ON K1H 8M5 Canada.

**Description of Contribution**
Performed *in vitro* phosphorylation reactions with radioactive ATP. See Materials and Methods, section 2.9.2.

**Figures**
Figure 3.8C
Figure 4.4A

**COLLABORATOR 3**

**Name:** Emily Sheppard
**Position:** 4th year undergraduate Biology Honours Project student
**Relationship to Sandy Szeto:** Honour's project student

**Affiliations (while Honour's student):**
Department of Biochemistry, Microbiology and Immunology, Faculty of Medicine, University of Ottawa, Roger Guindon Hall, 451 Smyth Road, Ottawa, ON K1H 8M5 Canada.

**Description of Contribution**
Helped Sandy Szeto perform Co-IP experiments and probed Western Blots. See Materials and Methods, section 2.7.3.

**Figures**
Figure 4.16
Figure 4.17
Figure 4.18

# APPENDIX

## VIDEOS

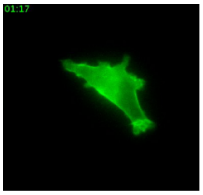


**Video 1. Localization of FLNa-WT GFP in M2 cells undergoing mitosis.** M2 cells were stably transfected with FLNa-WT GFP (green). Time-lapse images (fluorescent) were acquired on an Olympus VivaView FL incubator microscope. Frames were taken every three minutes for 24 h.

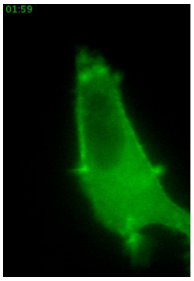


**Video 2. Localization of FLNa-AAA GFP in M2 cells undergoing mitosis.** M2 cells were stably transfected with FLNa-AAA GFP (green). Time-lapse images (fluorescent) were acquired on an Olympus VivaView FL incubator microscope. Frames were taken every three minutes for 24 h.

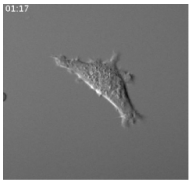


**Video 3. FLNa-WT GFP-expressing M2 cells undergoing mitosis.** M2 cells were stably transfected with FLNa-WT GFP. Time-lapse images (differential interference contrast) were acquired on an Olympus VivaView FL incubator microscope. Frames were taken every three minutes for 24 h

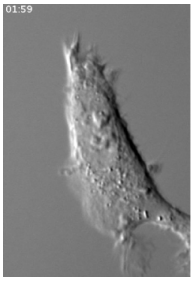


**Video 4. FLNa-AAA GFP-expressing M2 cells undergoing mitosis.** M2 cells were stably transfected with FLNa-AAA GFP. Time-lapse images (differential interference contrast) were acquired on an Olympus VivaView FL incubator microscope. Frames were taken every three minutes for 24 h.

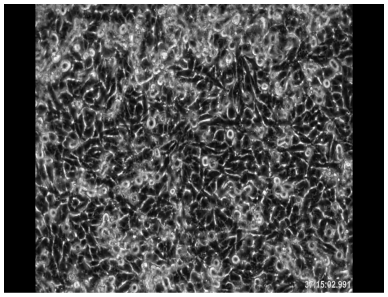

**Video 5. Wound closure assay of FLNa-WT GFP-expressing M2 cells.** M2 cells were stably transfected with FLNa-WT GFP. Time-lapse images (phase contrast) were acquired on a Zeiss LSM 5 Pascal/AxioVert 200 inverted confocal microscope. Frames were taken every 15 min for approximately 48 h.

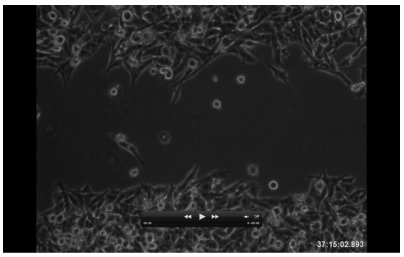

**Video 6. Wound closure assay of GFP EV-expressing M2 cells.** M2 cells were stably transfected with GFP EV. Time-lapse images (phase contrast) were acquired on a Zeiss LSM 5 Pascal/AxioVert 200 inverted confocal microscope. Frames were taken every 15 min for approximately 48 h.

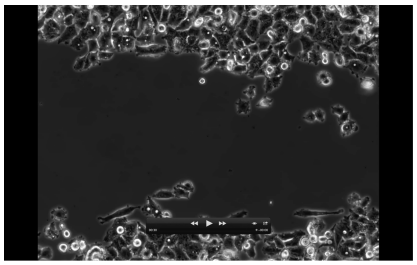

**Video 7. Wound closure assay of nontransfected M2 cells.** Time-lapse images (phase contrast) were acquired on a Zeiss LSM 5 Pascal/AxioVert 200 inverted confocal microscope. Frames were taken every 15 min for approximately 48 h.

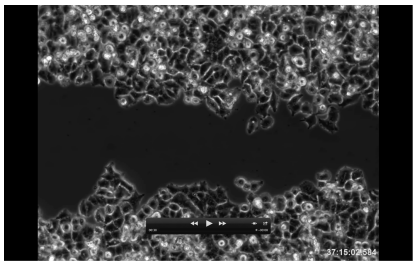

**Video 8. Wound closure assay of FLNa-AAA GFP-expressing M2 cells.** M2 cells were stably transfected with FLNa-AAA GFP. Time-lapse images (phase contrast) were acquired on a Zeiss LSM 5 Pascal/AxioVert 200 inverted confocal microscope. Frames were taken every 15 min for approximately 48 h.

# TABLES

**Table A1: FLNa interactors to date.** Proteins shown in red were detected by mass spectrometry in this study. Table adapted from (Nakamura et al., 2011).

| Protein | Category |
|---|---|
| F-actin | cytoskeleton |
| Vimentin | cytoskeleton |
| Supervillin | cytoskeleton |
| CFTR | Ion channel |
| Kv4.2 $K^+$ channel | Ion channel |
| Large conductance $Ca^{2+}$-activated $K^+$ channels | Ion channel |
| Kir2.1 | Ion channel |
| HCN1 | Ion channel |
| Acetylcholine receptors | Ion channel |
| Polycystin2 | Ion channel |
| Syk | kinase |
| Sphingosine kinase 1 | kinase |
| ROCK | kinase |
| Mytotilin | Muscle development |
| FATZ (Myozenin-1/Calsarein-2) | Muscle development |
| Calsarein-2 (Myozenin-3) | Muscle development |
| N-RAP | Muscle development |
| KY protein | Muscle development |
| Xin | Muscle development |
| Myopodin | Muscle development |
| CAP | Muscle development |
| Titin | Muscle development |
| gamma-delta sarcoglycans | Muscle development |
| IGFN1 | Muscle development |
| RasGAP | Muscle development |
| Caveolin-1 | Other |
| Heptatitis B virus core protein | Other |
| Decorin | Other |
| cvHsp | Other |
| Nephorocystin | Other |
| Presenilins | Other |
| Pdlim2 | Other |
| ASB2 (ankyrin repeat-containing protein with a suppressor of cytokine signaling box 2) | Other |
| [14C] carboplatin | Other |
| Naloxone, naltrexone, PTI-609 | Other |
| FIP | Other |

| | |
|---|---|
| Micelle of mixed DMPC, DMPG, PC and PS | Other |
| 3-sulfate galactosyl ceramide | Other |
| Calmodulin | Other |
| Pro-Prion | Other |
| FAP52(PASCIN2/Syndapin II) | Other |
| ECSM2 | Other |
| FILIP | Other |
| Migfilin (FBLP-1) | Other |
| FILIP-1L(downregulated in ovarian cancer 1) | Other |
| IKAP (ELP1) | Other |
| p311 | Other |
| Protein kinase A (PKA) | phosphorylation |
| P21-activated kinase 1 (PAK1) | phosphorylation |
| Ribosomal S6 Kinase (RSK) | phosphorylation |
| SHIP-2 | phosphorylation |
| Calcineurin | phosphorylation |
| Cyclin-dependent kinase 1 (Cdk1)/Cyclin B1 | phosphorylation |
| Cyclin D1/Cdk4 | phosphorylation |
| PKB-α | phosphorylation |
| PKC-α | phosphorylation |
| PKC-theta | phosphorylation |
| PKC-epsilon | phosphorylation |
| Ror2 | phosphorylation |
| PTP-PEST | phosphorylation |
| p56lck | phosphorylation |
| CaM kinaseII | phosphorylation |
| Tc-mip | phosphorylation |
| 14-3-3 | phosphorylation |
| TRAF2 | phosphorylation |
| Lnk | phosphorylation |
| CD4 | phosphorylation |
| CD28 | phosphorylation |
| Fc gamma R | phosphorylation |
| Epithin | Proteolysis |
| PMSA | Proteolysis |
| mu Calpain | Proteolysis |
| Furin | Proteolysis |
| Caspase | Proteolysis |
| Granzyme B | Proteolysis |
| Dopamine D2, 3 R | Receptors |
| metabotropic Glu R (4a, 5a/b, 7a/b, 8a) | Receptors |
| $Ca^{2+}$-sensing R | Receptors |
| mu opioid R | Receptors |

| | |
|---|---|
| Insulin R | Receptors |
| Calcitonin R | Receptors |
| P2Y2 nucleotide R | Receptors |
| chemokine (C-C motif) receptor 2B (CCR2B) | Receptors |
| LL5b | signaling |
| SEK1 (MKK4) | signaling |
| MEKK1 (MAPKKK1) | signaling |
| MKK4 (SEK1/MEK4/MAPKK)/7b, gamma | signaling |
| JNK1 (SAPK/MAPK) | signaling |
| b-arrestin | signaling |
| R-Ras | small GTP-binding proteins and their regulators |
| Trio | small GTP-binding proteins and their regulators |
| FilGAP | small GTP-binding proteins and their regulators |
| Rho | small GTP-binding proteins and their regulators |
| Rac | small GTP-binding proteins and their regulators |
| Cdc42 | small GTP-binding proteins and their regulators |
| RalA | small GTP-binding proteins and their regulators |
| Lbc | small GTP-binding proteins and their regulators |
| P190RhoGAP | small GTP-binding proteins and their regulators |
| Vav-2 | small GTP-binding proteins and their regulators |
| Androgen Receptor | Transcription |
| FOXC1 | Transcription |
| FEBP2b/CBFb | Transcription |
| p73α | Transcription |
| Smad1~6 | Transcription |
| BRCA1,2 | Transcription |
| Glycoprotein 1bα (CD42b) | transmembrane protein |
| ICAM-1 | transmembrane protein |
| Integrin b | transmembrane protein |
| Tissue Factor | transmembrane protein |
| CEACAM1 (CD66a) | transmembrane protein |

**Table A2: FLNa phospho-sites detected by LC-MS/MS.** Ratio (Mitosis FLNa IP: Interphase FLNa IP) >1 indicates enrichment in mitotic cells (nocodazole-treated) and <1 indicates enrichment in interphase cells (DMSO-treated). Two independent experiments were performed and each sample was analyzed twice (four sets of data). The data is compiled from all four data sets. In instances where one peptide contains more than one possible phosphorylation site, the phospho-site corresponds to the site with the higher probability of being the phosphorylated.

| Phospho site | PEP | Score | Phospho (STY) Probabilities | Ratio (Mitosis FLNa IP:Interphase FLNa IP) |
|---|---|---|---|---|
| 1084 | 0.002 | 156.57 | AFGPGLQGGS(0.008)AGS(0.992)PAR | 13.162 |
| 1084 | 0.000 | 172.57 | AFGPGIQGGS(0.001)AGS(0.999)PAR | 8.947 |
| 1084 | 0.000 | 172.57 | AFGPGIQGGSAGS(1)PAR | 11.523 |
| 1084 | 0.000 | 152.34 | AFGPGIQGGS(0.001)AGS(0.999)PAR | 8.488 |
| 1459 | 0.474 | 95.27 | CSGPGLS(1)PGMVR | 2.074 |
| 1459 | 0.103 | 132.50 | CSGPGIS(1)PGMVR | n/a |
| 1533 | 0.000 | 152.00 | EGPYSISVIYGDEEVPRS(1)PFK | 15.424 |
| 2152 | 0.005 | 146.86 | RAPS(1)VANVGSHCDLSLK | 0.590 |
| 2152 | 0.000 | 162.26 | RAPS(1)VANVGSHCDISIK | 0.764 |
| 2152 | 0.000 | 151.39 | RAPS(0.993)VANVGSHCDIS(0.007)IK | 0.773 |
| 2152 | 0.000 | 218.12 | RAPS(0.99)VANVGSHCDIS(0.01)IK | 0.789 |

**Table A3. FLNa peptides detected by LC-MS/MS.** Ratio (Mitosis FLNa IP: Interphase FLNa IP) >1 indicates enrichment in mitotic cells (nocodazole-treated) and <1 indicates enrichment in interphase cells (DMSO-treated). Two independent experiments were performed and each sample was analyzed twice (four sets of data). The data is compiled from all four data sets but duplicate peptides are not shown. The phosphorylated residue is underlined. The peptides cover 68.4% of the FLNa sequence.

| FLNa site | Sequence | PEP | Score | Ratio (Mitosis FLNa IP:Interphase FLNa IP) | Intensity |
|---|---|---|---|---|---|
| p-S1084 | AFGPGLQGGSAGSPAR | 0.00 | 206.49 | 3.02 | 36785000000 |
| p-S1459 | CSGPGLSPGMVR | 0.00 | 192.5 | 1.2 | 3687700000 |
| p-S1533 | EGPYSISVLYGDEEVPRSPFK | 0.00 | 152 | | 194560000 |
| p-S2152 | APSVANVGSHCDLSLK | 0.00 | 186.05 | 0.88 | 4864700000 |
| p-S2152 | RAPSVANVGSHCDLSLK | 0.02 | 134.93 | 0.89 | 6753200000 |
| S1055 | EEGPYEVEVTYDGVPVPGSPFPLEAVAPTKPSK | 0.00 | 252.51 | 1.26 | 133530000 |
| S1436 | DGSCSVEYIPYEAGTYSLNVTYGGHQVPGSPFK | 0.00 | 116.2 | | 569860000 |
| S1630 | YGGDEIPFSPYR | 0.00 | 171.62 | | 3355700000 |
| S1726 | FGGEHVPNSPFQVTALAGDQPSVQPPLR | 0.00 | 205.43 | 0.58 | 569750000000 |
| S1938 | YNEQHVPGSPFTAR | 0.00 | 152.16 | | 3151900000 |
| S2025 | NGQHVASSPIPVVISQSEIGDASR | 0.00 | 231.93 | | 679440000 |
| S2025 | KNGQHVASSPIPVVISQSEIGDASR | 0.00 | 153.11 | 0.71 | 380710000 |
| S2025 | NGQHVASSPIPVVISQSEIGDASRVR | 0.00 | 118.37 | | 1093800000 |
| S2120 | FADQHVPGSPFSVKVTGEGR | 0.00 | 237.3 | | 2397000000 |
| S2120 | FADQHVPGSPFSVK | 0.00 | 161.48 | | 2783900000 |
| S2120 | VTYCPTEPGNYIINIKFADQHVPGSPFSVK | 0.15 | 121.77 | 0.62 | 16981000 |

| | | | | | |
|---|---|---|---|---|---|
| S2172 | IPEISIQDMTAQVTSPSGK | 0.00 | 239.55 | | 1577200000 |
| S2216 | YKGQHVPGSPFQFTVGPLGEGGAHK | 0.00 | 177 | 0.82 | 11770000000 |
| S2216 | GQHVPGSPFQFTVGPLGEGGAHK | 0.00 | 171.98 | 0.8 | 25019000000 |
| S2311, S2319 | FNEEHIPDSPFVVPVASPSGDAR | 0.00 | 184.56 | | 3488500000 |
| S2362 | VHSPSGALEECYVTEIDQDK | 0.00 | 259.29 | 1.05 | 2114100000 |
| S2362 | VHSPSGALEECYVTEIDQDKYAVR | 0.00 | 158.17 | 0.96 | 62175000000 |
| S2406 | FNGTHIPGSPFK | 0.00 | 158.3 | | 2279100000 |
| S2502 | YGGPYHIGGSPFK | 0.00 | 199.08 | | 6579600000 |
| S2632 | WGDEHIPGSPYR | 0.00 | 147.91 | | 1972900000 |
| S368 | SPFEVYVDK | 0.00 | 204.19 | | 1453900000 |
| S368 | SPFEVYVDKSQGDASK | 0.04 | 137.62 | 1.01 | 292600000 |
| S468 | SPYTVTVGQACNPSACR | 0.00 | 233.4 | | 1331600000 |
| S564 | SPFEVK | 0.15 | 110.24 | | 31305000 |
| S657 | LSPFMADIR | 0.01 | 154.49 | 1.88 | 1.06E+11 |
| S757 | HTAMVSWGGVSIPNSPFR | 0.00 | 224.55 | | 2681300000 |
| S959, S966 | SPFSVAVSPSLDLSK | 0.00 | 204.48 | 3.58 | 40040000000 |
| T1322, S1338, S1343 | VEYTPYEEGLHSVDVTYDGSPVPSSPFQVPVTEGCDPSR | 0.00 | 143.07 | 0.51 | 1820800000 |
| T2480 | VTYTPMAPGSYLISIK | 0.00 | 183.89 | 0.8 | 41039000000 |
| T2591 | TPCEEILVK | 0.02 | 130.75 | 0.71 | 671120000 |
| T857, S860 | GAGSYTIMVLFADQATPTSPIR | 0.00 | 293.2 | 0.81 | 27863000000 |
| T938 | YTPVQQGPVGVNVTYGGDPIPK | 0.00 | 192.62 | | 593860000 |
| | QMQLENVSVALEFLDR | 0.00 | 428.06 | 1.03 | 366710000 |
| | THEAEIVEGENHTYCIR | 0.00 | 322.23 | | 3909200000 |
| | VANPSGNLTETYVQDR | 0.00 | 303.3 | 2.13 | 1.93E+11 |
| | LIALLEVLSQK | 0.00 | 293.18 | 1.17 | 744410000 |
| | DAGEGLLAVQITDPEGKPK | 0.00 | 292.66 | 0.84 | 43941000000 |

| | | | | | |
|---|---|---|---|---|---|
| | SADFVVEAIGDDVGTLGFSVEGPSQAK | 0.00 | 291.08 | 3.4 | 4727300000 |
| | LVSNHSLHETSSVFVDSLTK | 0.00 | 281.09 | | 3944000000 |
| | LVSNHSLHETSSVFVDSLTK | 0.00 | 272.24 | 1.04 | 68725000000 |
| | VQVQDNEGCPVEALVK | 0.00 | 268.9 | 2.76 | 559440000 |
| | VAQPTITDNKDGTVTVR | 0.00 | 268.59 | | 1367700000 |
| | DVDIIDHHDNTYTVK | 0.00 | 265.22 | | 4934000000 |
| | DAGEGGLSLAIEGPSK | 0.00 | 257.8 | 0.87 | 120460000000 |
| | VTAQGPGLEPSGNIANK | 0.00 | 255.91 | 1.33 | 355520000000 |
| | VNQPASFAVSLNGAK | 0.00 | 255.85 | 0.94 | 236950000000 |
| | GLVEPVDVVDNADGTQTVNYVPSR | 0.00 | 253.95 | 0.76 | 410220000000 |
| | ANLPQSFQVDTSK | 0.00 | 253.54 | 0.99 | 562630000000 |
| | THIQDNHDGTYTVAYVPDVTGR | 0.00 | 243.41 | | 3222100000 |
| | KTHIQDNHDGTYTVAYVPDVTGR | 0.00 | 241.38 | | 125310000000 |
| | LTVSSLQESGLK | 0.00 | 240.85 | 0.99 | 352880000000 |
| | LPQLPITNFSR | 0.00 | 239.93 | 1.28 | 4.22E+11 |
| | TGVAVNKPAEFTVDAK | 0.00 | 233.97 | | 6052000000 |
| | EAGAGGLAIAVEGPSK | 0.00 | 233.24 | 0.88 | 192120000000 |
| | DAGYGGLSLSIEGPSK | 0.00 | 232.5 | 0.66 | 3865300000 |
| | CAPGVVGPAEADIDFDIIR | 0.00 | 230.26 | | 1537100000 |
| | LQVEPAVDTSGVQCYGPGIEGQGVFR | 0.00 | 224.57 | 2.42 | 168700000000 |
| | VDINTEDLEDGTCRVTYCPTEPGNYIINIK | 0.00 | 222.69 | 0.9 | 6023600 |
| | LIALLEVLSQK | 0.00 | 222 | | 3473400000 |
| | TGVELGKPTHFTV | 0.00 | 218.68 | 3.72 | 6685400000 |

| | | | | | |
|---|---|---|---|---|---|
| | NAK | | | | 0 |
| | VDINTEDLEDGTCR | 0.00 | 218.11 | 0.97 | 3740700000 |
| | IANLQTDLSDGLR | 0.00 | 216.68 | 1.55 | 78026000000 |
| | LPQLPITNFSR | 0.00 | 215.06 | | 5893700000 |
| | EGPYSISVLYGDEEVPR | 0.00 | 212.87 | 0.76 | 89139000000 |
| | LDVQFSGLTK | 0.00 | 208.63 | 2.09 | 24219000000 |
| | YWPQEAGEYAVHVLCNSEDIR | 0.00 | 207.43 | 1.03 | 43797000000 |
| | SAGQGEVLVYVEDPAGHQEEAK | 0.00 | 206.64 | 1.13 | 35960000000 |
| | VTYCPTEPGNYIINIK | 0.00 | 204.35 | | 834170000 |
| | DAEMPATEKDLAEDAPWK | 0.00 | 200.77 | 0.84 | 1617200000 |
| | LQVEPAVDTSGVQCYGPGIEGQGVFR | 0.00 | 198.84 | | 7362500000 |
| | VSGQGLHEGHTFEPAEFIIDTR | 0.00 | 198.49 | 0.9 | 34240000000 |
| | VGSAADIPINISETDLSLLTATVVPPSGR | 0.00 | 196.28 | 0.66 | 65411000000 |
| | AHEPTYFTVDCAEAGQGDVSIGIK | 0.00 | 193.85 | | 1586100000 |
| | KDGSCGVAYVVQEPGDYEVSVK | 0.00 | 192.25 | | 268580000 |
| | VDVGKDQEFTVK | 0.00 | 191.79 | | 3543900000 |
| | ENGVYLIDVK | 0.00 | 190.96 | 0.96 | 17623000000 |
| | LLGWIQNK | 0.00 | 186.43 | | 2933600000 |
| | ALGALVDSCAPGLCPDWDSWDASKPVTNAR | 0.00 | 186.13 | 1.15 | 20174000000 |
| | AWGPGLEGGVVGK | 0.00 | 184.24 | 1.26 | 66426000000 |
| | VTVLFAGQHIAK | 0.00 | 183.99 | 2.41 | 74849000000 |
| | AEAGVPAEFSIWTR | 0.00 | 183.66 | | 2233000000 |
| | LLGWIQNK | 0.00 | 183.2 | 1.45 | 767320000 |
| | QMQLENVSVALEFLDRESIK | 0.00 | 180.17 | 1.21 | 119910000 |

| | | | | | |
|---|---|---|---|---|---|
| | YGGQPVPNFPSK | 0.00 | 176.6 | | 1760600000 |
| | PFDLVIPFTIK | 0.00 | 174.48 | 0.76 | 2777700 |
| | NGHVGISFVPK | 0.00 | 172.94 | | 593710000 |
| | GKLDVQFSGLTK | 0.00 | 172.88 | 1.2 | 5236000000 |
| | LIALLEVLSQKK | 0.00 | 172.27 | 2.27 | 9472600000 |
| | ASGPGLNTTGVPASLPVEFTIDAK | 0.00 | 171.47 | 0.85 | 6856000000 |
| | FVPAEMGTHTVSVK | 0.00 | 171.32 | | 2524100000 |
| | AYGPGIEPTGNMVK | 0.00 | 170.47 | | 2276200000 |
| | RLTVSSLQESGLK | 0.00 | 168.61 | 1.01 | 17484000000 |
| | IECDDKGDGSCDVR | 0.00 | 167.71 | 1.1 | 95751000 |
| | KGEITGEVR | 0.02 | 166.09 | 1.04 | 255950000 |
| | YAPSEAGLHEMDIR | 0.00 | 164.48 | 0.88 | 71268000000 |
| | TFSVWYVPEVTGTHK | 0.00 | 162.31 | | 2677100000 |
| | ALGALVDSCAPGLCPDWDSWDASK | 0.00 | 161.08 | 4.62 | 143810000 |
| | DGSCGVAYVVQEPGDYEVSVK | 0.00 | 160.64 | | 956080000 |
| | DKGEYTLVVK | 0.04 | 159.83 | 0.97 | 4874000000 |
| | DLAEDAPWKK | 0.01 | 157.61 | 1.3 | 182890000 |
| | GAGSGELKVTVK | 0.00 | 156.58 | 0.96 | 31564000 |
| | RAEFTVETR | 0.01 | 153.24 | 1.18 | 3394000000 |
| | AGNNMLLVGVHGPR | 0.00 | 150.46 | 0.88 | 289190000000 |
| | VRVSGQGLHEGHTFEPAEFIIDTR | 0.00 | 149.44 | 0.95 | 6583800000 |
| | AEISFEDR | 0.01 | 147.52 | | 291580000 |
| | GAGTGGLGLAVEGPSEAK | 0.00 | 143.97 | 2.36 | 1.22E+11 |
| | RIANLQTDLSDGLR | 0.00 | 139.48 | 2.56 | 2979300000 |
| | PLVGVNGLDVTSLRPFDLVIPFTIK | 0.00 | 137.69 | 0.73 | 4697700000 |
| | CTVTVSIGGHGLGAGIGPTIQIGEETVITVDTK | 0.06 | 137.41 | 0.91 | 4350800 |
| | LYSVSYLLK | 0.01 | 136.8 | 1.01 | 469420000000 |
| | IQQNTFTR | 0.42 | 135.84 | | 161980000 |

| | | | | | |
|---|---|---|---|---|---|
| | DAEMPATEKDLAEDAPWKK | 0.07 | 135.23 | 1.26 | 2117400000 |
| | VEPGLGADNSVVR | 0.01 | 134.49 | 3.88 | 873680000 0 |
| | AEFTVETR | 0.00 | 133.6 | | 37605000 |
| | AGQSAAGAAPGGGVDTR | 0.01 | 131.24 | | 3458300 |
| | VKVEPSHDASK | 0.00 | 130.98 | | 277840 |
| | SSFTVDCSK | 0.02 | 130.56 | 0.95 | 32029000 |
| | DLAEDAPWK | 0.02 | 129.95 | 1.64 | 58207000 |
| | CAPGVVGPAEADIDFDIIRNDNDTFTVK | 0.03 | 127.87 | 0.94 | 7433800 |
| | DAGEGLLAVQITDPEGK | 0.03 | 124.2 | 0.84 | 195900000 |
| | ATCAPQHGAPGPGPADASK | 0.01 | 122.75 | | 7007600 |
| | AGVAPLQVK | 0.03 | 121.29 | | 992070000 |
| | VPVHDVTDASK | 0.02 | 119.27 | | 24777000 |
| | MDCQECPEGYR | 0.10 | 118.9 | | 4717800 |
| | GTVEPQLEAR | 0.02 | 114.97 | 4.14 | 74109000 |
| | EATTEFSVDAR | 0.02 | 114.5 | | 243700000 |
| | LYSVSYLLK | 0.04 | 114.5 | | 2020600000 |
| | YTILIK | 0.06 | 113.82 | | 445170000 |
| | CSYQPTMEGVHTVHVTFAGVPIPR | 0.02 | 110.56 | | 494500000 |
| | AHVVPCFDASK | 0.47 | 106.36 | | 23696000 |
| | NDNDTFTVK | 0.06 | 104.2 | | 5923100 |
| | VGSAADIPINISETDLSLLTATVVPPSGREEPCLLK | 0.00 | 102.28 | 0.67 | 209280000 |
| | AEISFEDRK | 2.52 | 101.54 | | 16016000 |
| | ALTQTGGPHVK | 0.21 | 96.17 | 0.93 | 61242000 |
| | DNGNGTYSCSYVPR | 1.31 | 94.69 | | 124830000 |
| | VNVGAGSHPNK | 0.24 | 92.54 | 3.57 | 12747000 |
| | CSGPGLER | 0.49 | 89.3 | 1.59 | 17092000 |
| | EEPCLLK | 0.89 | 86.09 | | 39194000 |
| | VLPTHDASK | 0.47 | 83.01 | 0.93 | 22756000 |
| | ETADFK | 3.70 | 79.03 | | 11742000 |
| | GEITGEVR | 3.89 | 78.5 | | 3669100 |
| | VSGLGEK | 0.98 | 76.59 | | 3240300 |
| | VYGPGVAK | 0.59 | 74.74 | | 3058100 |
| | DAPQDFHPDR | 3.66 | 71.22 | | 2334700 |
| | ETGEHLVHVK | 0.93 | 68.02 | 1.31 | 9551100 |
| | VAQPTITDNK | 1.09 | 62.82 | 0.88 | 13415000 |

| | | | | | |
|---|---|---|---|---|---|
| | PTHFTVNAK | 1.07 | 62.55 | 1.01 | 4838600 |
| | AVPTGDASK | 1.38 | 50.88 | | 5217900 |

**Table A4. Sequence coverage of FLNa from mass spectrometry includes 33 out of the 39 Cdk1 phosphorylation consensus sequences.** Percent sequence coverage of FLNa from mass spectrometry was 68.4%. Sites shown in red are on FLNa sequences that were not covered (S1148, T167, T243, T839, T1682, S1846). Sites in bold are mitosis-enriched phosphorylation sites (Serines 1084, 1459 and 1533).

| (K/R)-(S/T)*-P-x-(K/R) | (S/T)*-P-x-(K/R) | (S/T)*-P | | |
|---|---|---|---|---|
| **S1533** | S757 | T167 | S966 | S2025 |
| | S860 | T243 | S1055 | S2120 |
| | **S1084** | S368 | T1322 | S2172 |
| | S1148 | S468 | S1338 | S2216 |
| | S1436 | S564 | S1343 | S2311 |
| | S1630 | S657 | **S1459** | S2319 |
| | S2406 | T839 | T1682 | S2362 |
| | S2502 | T857 | S1726 | T2480 |
| | S2632 | T938 | S1846 | T2591 |
| | | S959 | S1938 | |

* site of phosphorylation

**Table A5: Interphase FLNa IP-enriched proteins.** Proteins with LogRatios < -3 were considered to be enriched in the interphase FLNa IP. Proteins with PEP <0.01 was chosen as the cut-off. Only proteins that are non-bead or environmental contaminants are included (positive *DMSO FLNa IP: Noco IgG IP* ratio or positive *Noco FLNa IP: Noco IgG IP* ratio). Proteins are listed alphabetically. Proteins shown in red are known FLNa interactors.

| Protein Name | Uniprot | PEP | $Log_2$Ratio |
|---|---|---|---|
| 11S regulator complex subunit alpha | Q06323 | 2.16E-03 | -4.10 |
| 14-3-3 protein epsilon | P62258 | 5.87E-27 | -4.01 |
| 14-3-3 protein zeta/delta | P63104 | 4.02E-69 | -3.26 |
| 26 kDa prosomal protein | P28070 | 2.43E-05 | -4.92 |
| 27 kDa prosomal protein | P60900 | 5.04E-11 | -6.60 |
| 30 kDa prosomal protein | P25786 | 1.05E-06 | -5.01 |
| Alpha-1-antichymotrypsin | P01011 | 8.12E-04 | -5.96 |
| Alpha-globin | P69905 | 1.46E-15 | -7.04 |
| Barrier-to-autointegration factor | O75531 | 2.80E-06 | -3.45 |
| Beta-1B-glycoprotein | P02790 | 7.00E-03 | -5.51 |
| C3 and PZP-like alpha-2-macroglobulin domain-containing protein 6 | P20742 | 1.68E-04 | -4.39 |
| cDNA FLJ61136, highly similar to Ras-related protein Rab-11A | B4DMN1 | 5.21E-05 | -3.22 |
| cDNA FLJ76262, highly similar to Homo sapiens I factor (complement) (IF), mRNA | A8K3L0 | 1.97E-06 | -5.02 |
| Ceruloplasmin | P00450 | 6.94E-07 | -6.27 |
| COP9 homolog | Q99627 | 5.46E-05 | -8.00 |
| Delta-aminolevulinic acid dehydratase | P13716 | 2.80E-04 | -6.69 |
| Epididymal secretory glutathione peroxidase | O75715 | 1.53E-03 | -6.24 |
| Extracellular glutathione peroxidase | P22352 | 1.26E-05 | -4.52 |
| Fructose-bisphosphate aldolase A | P04075 | 4.05E-78 | -5.41 |
| Haptoglobin | P00738 | 1.84E-07 | -6.32 |
| Ig kappa chain V-I region Lay | P01605 | 9.56E-13 | -4.90 |
| Inter-alpha (Globulin) inhibitor H4 (Plasma Kallikrein-sensitive glycoprotein) | B2RMS9 | 6.73E-03 | -3.71 |
| Inter-alpha-trypsin inhibitor heavy chain H3 | Q06033 | 1.53E-06 | -4.14 |
| Macropain epsilon chain | P28074 | 1.68E-24 | -5.00 |
| Macropain subunit C3 | P25787 | 3.56E-33 | -5.27 |
| Macropain subunit C5 | P20618 | 2.41E-35 | -4.04 |
| Macropain subunit C7-I | P49721 | 6.30E-09 | -5.88 |
| Macropain subunit C8 | P25788 | 3.76E-35 | -5.34 |
| Macropain zeta chain | P28066 | 5.37E-46 | -4.01 |
| Microfibrillar protein 2 | Q9NP29 | 6.85E-16 | -3.50 |
| N-alpha-acetyltransferase 38, NatC auxiliary subunit | O95777 | 5.92E-13 | -3.88 |
| Nucleoside diphosphate kinase | Q32Q12 | 9.95E-70 | -4.72 |
| Proteasome chain 13 | P49720 | 3.06E-30 | -6.90 |
| Proteasome subunit alpha type-7 | O14818 | 1.77E-03 | -4.05 |

| | | | |
|---|---|---|---|
| Putative uncharacterized protein | Q8TCD0 | 2.99E-04 | -4.37 |
| Putative uncharacterized protein ARPC4 | C9JWM7 | 2.48E-05 | -3.58 |
| Putative uncharacterized protein FGG | C9JC84 | 3.99E-64 | -4.60 |
| Single-chain Fv | Q65ZC9 | 4.15E-06 | -5.13 |
| Transaldolase | P37837 | 1.56E-04 | -3.76 |
| Translin | Q15631 | 1.45E-10 | -5.18 |
| Triosephosphate isomerase | Q53HE2 | 7.77E-09 | -3.95 |
| U6 snRNA-associated Sm-like protein LSm3 | P62310 | 1.67E-07 | -6.10 |

**Table A6: Mitosis FLNa IP-enriched proteins.** Proteins with LogRatios >1.5 were considered to be enriched in the mitotic FLNa IP. Proteins with PEP <0.01 was chosen as the cut-off. Only proteins that are non-bead or environmental contaminants are included (positive *DMSO FLNa IP: Noco IgG IP* ratio or positive *Noco FLNa IP: Noco IgG IP* ratio). Proteins are listed alphabetically.

| Protein Name | Uniprot | PEP | $Log_2$Ratio |
|---|---|---|---|
| Importin-4 | Q8TEX9 | 5.42E-03 | 1.05 |
| DNase IV | P39748 | 3.69E-06 | 1.20 |
| Cyclin-dependent kinase 4 inhibitor A | P42771 | 7.33E-04 | 1.67 |

## COPYRIGHT PERMISSIONS

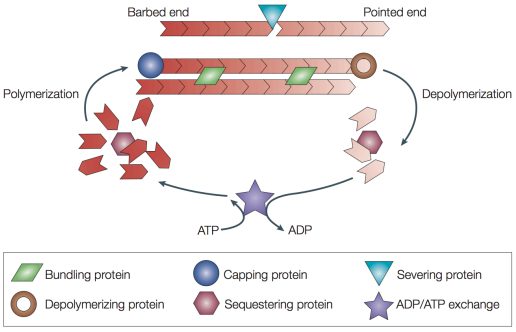


**Figure 1.1. Actin dynamics.** Actin polymerization occurs at the barbed end and actin depolymerization occurs at the pointed end. F-actin treadmilling occurs when there is a net addition of actin monomers at the barbed end and a net loss of actin monomers at the pointed end. The substrate for polymerization is ATP-bound G-actin, which is thermodynamically favoured under physiological conditions. *In vivo*, numerous actin-binding proteins have activities that include bundling, capping, severing, depolymerizing, sequestering and ATPase activities. Figure from (Revenu et al., 2004).

**Revenu, C., Athman, R., Robine, S., and Louvard, D. (2004). The co-workers of actin filaments: from cell structures to signals. Nat. Rev. Mol. Cell Biol. *5*, 635-646.**

## NATURE PUBLISHING GROUP LICENSE

## TERMS AND CONDITIONS

Jul 27, 2014

This is a License Agreement between Sandy Szeto ("You") and Nature Publishing Group ("Nature Publishing Group") provided by Copyright Clearance Center ("CCC"). The license consists of your order details, the terms and conditions provided by Nature Publishing Group, and the payment terms and conditions.

**All payments must be made in full to CCC. For payment instructions, please see information listed at the bottom of this form.**

License Number: 3436910508901

License date: Jul 27, 2014

Licensed content publisher: Nature Publishing Group

Licensed content publication: Nature Reviews Molecular Cell Biology

Licensed content title: The co-workers of actin filaments: from cell structures to signals

Licensed content author: Céline Revenu, Rafika Athman, Sylvie Robine, Daniel Louvard

Licensed content date: Aug 1, 2004

Volume number: 5

Issue number: 8

Type of Use: reuse in a dissertation / thesis

Requestor type: academic/educational

Format: electronic

Portion: figures/tables/illustrations

Number of figures/tables/illustrations: 2

High-res required: no

Figures: Box 1 | Actin filaments: structure and dynamics (figure) Box 2 | Molecular features implicated in actin crosslinking and bundling (figure)

Author of this NPG article: no

Your reference number: None

Title of your thesis / dissertation: Mitotic filamin A phosphorylation regulates filamin A localization and is important for daughter cell separation

Expected completion date: Oct 2014

Estimated size (number of pages): 250

Total: 0.00 USD

Terms and Conditions

Terms and Conditions for Permissions

Nature Publishing Group hereby grants you a non-exclusive license to reproduce this material for this purpose, and for no other use,subject to the conditions below:

1. NPG warrants that it has, to the best of its knowledge, the rights to license reuse of this material. However, you should ensure that the material you are requesting is original to Nature Publishing Group and does not carry the copyright of another entity (as credited in the published version). If the credit line on any part of the material you have requested indicates that it was reprinted or adapted by NPG with permission from another source, then you should also seek permission from that source to reuse the material.

2. Permission granted free of charge for material in print is also usually granted for any electronic version of that work, provided that the material is incidental to the work as a whole and that the electronic version is essentially equivalent to, or substitutes for, the print version.Where print permission has been granted for a fee, separate permission must be obtained for any additional, electronic re-use (unless, as in the case of a full paper, this has already been accounted for during your initial request in the calculation of a print run).NB: In all cases, web-based use of full-text articles must be authorized separately through the 'Use on a Web Site' option when requesting permission.

3. Permission granted for a first edition does not apply to second and subsequent editions and for editions in other languages (except for signatories to the STM Permissions Guidelines, or where the first edition permission was granted for free).

4. Nature Publishing Group's permission must be acknowledged next to the figure, table or abstract in print. In electronic form, this acknowledgement must be visible at the same time as the figure/table/abstract, and must be hyperlinked to the journal's homepage.

5. The credit line should read:
   Reprinted by permission from Macmillan Publishers Ltd: [JOURNAL NAME] (reference citation), copyright (year of publication)
   For AOP papers, the credit line should read:
   Reprinted by permission from Macmillan Publishers Ltd: [JOURNAL NAME], advance online publication, day month year (doi: 10.1038/sj.[JOURNAL ACRONYM].XXXXX)

   **Note: For republication from the *British Journal of Cancer,* the following credit lines apply.**
   Reprinted by permission from Macmillan Publishers Ltd on behalf of Cancer Research UK: [JOURNAL NAME] (reference citation), copyright (year of publication)For AOP papers, the credit line should read:
   Reprinted by permission from Macmillan Publishers Ltd on behalf of Cancer Research UK: [JOURNAL NAME], advance online publication, day month year (doi: 10.1038/sj.[JOURNAL ACRONYM].XXXXX)

6. Adaptations of single figures do not require NPG approval. However, the adaptation should be credited as follows:

   Adapted by permission from Macmillan Publishers Ltd: [JOURNAL NAME] (reference citation), copyright (year of publication)

   **Note: For adaptation from the *British Journal of Cancer,* the following credit line applies.**
   Adapted by permission from Macmillan Publishers Ltd on behalf of Cancer Research UK: [JOURNAL NAME] (reference citation), copyright (year of publication)

7. Translations of 401 words up to a whole article require NPG approval. Please visithttp://www.macmillanmedicalcommunications.com for more information.Translations of up to a 400 words do not require NPG approval. The translation should be credited as follows:

   Translated by permission from Macmillan Publishers Ltd: [JOURNAL NAME] (reference citation), copyright (year of publication).

   **Note: For translation from the *British Journal of Cancer,* the following credit line applies.**
   Translated by permission from Macmillan Publishers Ltd on behalf of Cancer Research UK: [JOURNAL NAME] (reference citation), copyright (year of publication)

We are certain that all parties will benefit from this agreement and wish you the best in the use of this material.

Thank you.

Special Terms:

v1.1

**You will be invoiced within 48 hours of this transaction date. You may pay your invoice by credit card upon receipt of the invoice for this transaction. Please follow instructions provided at that time.**

**To pay for this transaction now; please remit a copy of this document along with your payment. Payment should be in the form of a check or money order referencing your account number and this invoice number RLNK501362262.**

**Make payments to "COPYRIGHT CLEARANCE CENTER" and send to:**

**Copyright Clearance Center**

**Dept 001**

**P.O. Box 843006**

**Boston, MA 02284-3006**

**Please disregard electronic and mailed copies if you remit payment in advance.**

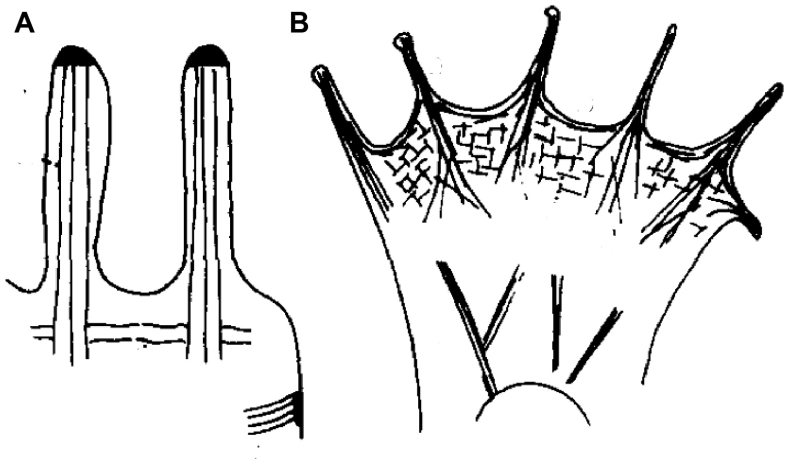


**Figure 1.2. Schematic of the two main types of actin configurations in cells. (A)** Microvilli showing parallel, unbranched bundles of actin filaments. **(B)** Highly branched, orthogonal networks found in the lamellipodia of motile cells. Filopodia microspikes containing F-actin bundles originate from the lamellae containing orthogonal F-actin networks. Figure adapted from (Stossel, 1984).

**Stossel, T.P. (1984). Contribution of actin to the structure of the cytoplasmic matrix. J. Cell Biol. *99*, 15s-21s.**

It is the mission of The Rockefeller University Press to promote widespread reuse and distribution of the articles and data we publish. In this spirit, authors retain copyright to their own work and can reuse it for any purpose as long as proper attribution is provided. Third parties may use our published materials under a Creative Commons Attribution-Noncommercial-Share Alike 3.0 Unported License six months after publication. Within the first six months, the same conditions for reuse apply, except we prohibit the creation of mirror sites. Commercial reuse must be requested as described below and will incur a fee.

We encourage you to read more about our permission policies and the Creative Commons License terms:

- You wrote it; you own it! (Hill and Rossner, 2008)
- RUP Copyright Policy

## Requesting Permission Licensing

Please read below to determine if you must obtain permission for your specific reuse.

### Original author reuse (commercial and noncommercial)

Ownership of copyright remains with RUP authors, who may reuse their own material forany purpose, including commercial profit, as long as they provide proper attribution. The permission does not extend to the institution.

- Note that our preferred citation style is as follows:
- ©AUTHOR et al., YEAR. Originally published in *JOURNAL NAME*. doi:########.
- If an article does not carry a doi, our preferred citation style is as follows:
- ©AUTHOR et al., YEAR. Originally published in *JOURNAL NAME*. VOL:PP–PP.

### Noncommercial third-party reuse

Third parties may reuse our content for noncommercial purposes without specific permission as long as they provide proper attribution (see citation preferences provided above). Within the first 6 months after publication, the creation of mirror sites is prohibited.

## Commercial third-party reuse

Commercial publishers, profit-based companies, as well as third-party authors publishing in a commercial journal or book must obtain permission to reuse RUP material. In most cases, this permission will incur a fee. Uses include, for example, use of a figure in a commercial journal article or book, posting of images on a manufacturer's website, inclusion of content in marketing materials, etc. The RUP acknowledges that text or data mining by commercial entities for their internal research purposes is allowed without further permission from RUP. Commercial entities may develop indexing or search services—available to the public for free or for a fee—based on text or data mining without further permission from RUP, but they may reproduce only snippets of text up to 156 characters in length, or thumbnails of images up to 72 pixels in the long direction, as part of such a service.

## How to obtain permission

Permission for commercial reuse can be obtained by emailing the following information to Suzanne O'Donnell, Permissions Director, at permissions@rockefeller.edu:

- Your name, institution, and title
- Your complete mailing address, email address, phone number, and fax number
- A description of the content you wish to reuse:
- Journal or book title
- Article title
- Authors' names
- Volume number, issue date, page numbers (provide all that apply)
- Specific figure numbers or portion of text (or supply a photocopy)
- Include the following information about your intended reuse:
- Type of work in which our material will be used (e.g., book, journal, newsletter, etc.)
- Title of work in which RUP material will appear
- Title of article/chapter (if applicable)
- Author(s)/editor(s)
- Expected publication date
- Publishing company
- Retail price (for books only)
- Print run (for books only)
- Indicate if there will be ancillaries published simultaneous to the print (DVD, website, CD-ROM, etc.). Will ancillaries be sold separately?
- Intended audience for the work
- If you wish to reprint the material online, please include the following:
- Your website's URL
- Website's sponsoring organization/company
- Description of the purpose and nature of your website
- Description of the website's visitors (customers, scholars, professors, etc.)
- Whether the site is open to the public or access is restricted

## Educational use

No permission is required to reuse RUP material for noncommercial purposes in course packs, classroom handouts, or electronic classroom presentations. If the educational material will be offered for sale, please follow the instructions above for Commercial third-party reuse.

## Reprints

Commercial reprints are available by special order. Please contact Suzanne O'Donnell atpermissions@rockefeller.edu to request pricing information. Please supply the full article citation (author, year, vol, pp) and the number of reprints you would like to order.

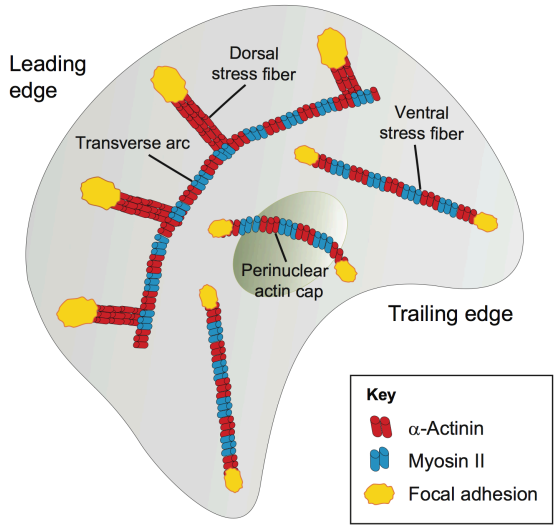


**Figure 1.3. Different types of stress fibres in cultured motile cells.** Dorsal stress fibres are anchored to focal adhesions at their distal end. Transverse arcs are curved actomyosin bundles near the cell center and typically connected to focal adhesions through interaction with dorsal stress fibres. Ventral stress fibres are anchored to focal adhesions at both ends. Perinuclear actin cap bundles resemble ventral stress fibres but are located above the nucleus. Figure from (Tojkander et al., 2012).

**Tojkander, S., Gateva, G., and Lappalainen, P. (2012). Actin stress fibers – assembly, dynamics and biological roles. J. Cell Sci. *125*, 1855-1864.**

**Order Details**

## Journal of cell science

- **Order detail ID:**65668632
- **Order License Id:**3436930573811
- **ISSN:**1477-9137
- **Publication Type:**e-Journal
- **Volume:**
- **Issue:**
- **Start page:**
- **Publisher:**COMPANY OF BIOLOGISTS LTD.
- **Author/Editor:**Company of Biologists
- **Permission Status:** **Granted**
- **Permission type:**Republish or display content
- **Type of use:**Republish in a thesis/dissertation
- Hide details

| | |
|---|---|
| **Requestor type** | Academic institution |
| **Format** | Electronic |
| **Portion** | cartoon |
| **Number of cartoons** | 1 |
| **Title or numeric reference of the portion(s)** | Chapter 1: Introduction<br>Figure 1.3. |
| **Title of the article or chapter the portion is from** | N/A |
| **Editor of portion(s)** | N/A |
| **Author of portion(s)** | N/A |
| **Volume of serial or monograph** | N/A |
| **Page range of portion** | 11 |
| **Publication date of portion** | Oct 2014 |
| **Rights for** | Main product |
| **Duration of use** | Life of current edition |
| **Creation of copies for the disabled** | no |

| | |
|---|---|
| **With minor editing privileges** | no |
| **For distribution to** | Worldwide |
| **In the following language(s)** | Original language of publication |
| **With incidental promotional use** | no |
| **Lifetime unit quantity of new product** | Up to 499 |
| **Made available in the following markets** | researchers |
| **The requesting person/organization** | Sandy Szeto |
| **Order reference number** | None |
| **Author/Editor** | Sandy Szeto |
| **The standard identifier** | sszet028 |
| **Title** | Mitotic filamin A phosphorylation regulates filamin A localization and is important for daughter cell separation |
| **Publisher** | University of Ottawa |
| **Expected publication date** | Oct 2014 |
| **Estimated size (pages)** | 250 |

**Note:** This item will be invoiced or charged separately through CCC's **RightsLink** service. More info**$ 0.00**

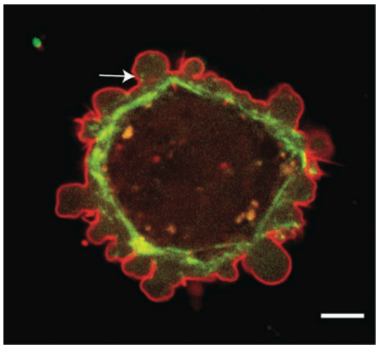

**Figure 1.4. FLNa-deficient M2 cell undergoing blebbing.** Cells were transfected with Myosin regulatory light-chain GFP and with PH- PLCδ-mRFP and imaged with a spinning disk confocal microscope. Myosin regulatory light chain (in green) is localized to the cell cortex and present in distinct foci (arrow) in retracting blebs. The cell membrane is shown in red using the pleckstrin homology (PH) domain of phospholipase C (PLC)δ. Scale bar, 5μm. Figure from (Charras, 2008).

**Charras, G.T. (2008). A short history of blebbing. J. Microsc. *231*, 466-478.**

## JOHN WILEY AND SONS LICENSE

## TERMS AND CONDITIONS

Jul 27, 2014

This is a License Agreement between Sandy Szeto ("You") and John Wiley and Sons ("John Wiley and Sons") provided by Copyright Clearance Center ("CCC"). The license consists of your order details, the terms and conditions provided by John Wiley and Sons, and the payment terms and conditions.

**All payments must be made in full to CCC. For payment instructions, please see information listed at the bottom of this form.**

License Number: 3436930918933

License date: Jul 27, 2014

Licensed content publisher: John Wiley and Sons

Licensed content publication: Journal of Microscopy

Licensed content title: A short history of blebbing

Licensed copyright line: © 2008 The Author Journal compilation © 2008 The Royal Microscopical Society

Licensed content author: G.T. CHARRAS

Licensed content date: Aug 28, 2008

Start page: 466

End page: 478

Type of use: Dissertation/Thesis

Requestor type: University/Academic

Format: Electronic

Portion: Figure/table

Number of figures/tables:1

Original Wiley figure/table number(s): Figure 6

Will you be translating?: No

Title of your thesis / dissertation: Mitotic filamin A phosphorylation regulates filamin A localization and is important for daughter cell separation

Expected completion date: Oct 2014

Expected size (number of pages): 250

Total: 0.00 USD

Terms and Conditions

**TERMS AND CONDITIONS**

This copyrighted material is owned by or exclusively licensed to John Wiley & Sons, Inc. or one of its group companies (each a"Wiley Company") or handled on behalf of a society with which a Wiley Company has exclusive publishing rights in relation to a particular work (collectively "WILEY"). By clicking accept in connection with completing this licensing transaction, you agree that the following terms and conditions apply to this transaction (along with the billing and payment terms and conditions established by the Copyright Clearance Center Inc., ("CCC's Billing and Payment terms and conditions"), at the time that you opened your Rightslink account (these are available at any time at http://myaccount.copyright.com).

**Terms and Conditions**

- The materials you have requested permission to reproduce or reuse (the "Wiley Materials") are protected by copyright.
- You are hereby granted a personal, non-exclusive, non-sub licensable (on a stand-alone basis), non-transferable, worldwide, limited license to reproduce the Wiley Materials for the purpose specified in the licensing process. This license is for a one-time use only and limited to any maximum distribution number specified in the license. The first instance of republication or reuse granted by this licence must be completed within two years of the date of the grant of this licence (although copies prepared before the end date may be distributed thereafter). The Wiley Materials shall not be used in any other manner or for any other purpose, beyond what is granted in the license. Permission is granted subject to an appropriate acknowledgement given to the author, title of the material/book/journal and the publisher. You shall also duplicate the copyright notice that appears in the Wiley publication in your use of the Wiley Material. Permission is also granted on the understanding that nowhere in the text is a previously published source acknowledged for all or part of this Wiley Material. Any third party content is expressly excluded from this permission.
- With respect to the Wiley Materials, all rights are reserved. Except as expressly granted by the terms of the license, no part of the Wiley Materials may be copied, modified, adapted (except for minor reformatting required by the new Publication), translated, reproduced, transferred or distributed, in any form or by any means, and no derivative works may be made based on the Wiley Materials without the prior permission of the respective copyright owner. You may not alter, remove or suppress in any manner any copyright, trademark or other notices displayed by the Wiley Materials. You may not license, rent, sell, loan, lease, pledge, offer as security, transfer or assign the Wiley Materials on a stand-alone basis, or any of the rights granted to you hereunder to any other person.
- The Wiley Materials and all of the intellectual property rights therein shall at all times remain the exclusive property of John Wiley & Sons Inc, the Wiley Companies, or their respective licensors, and your interest therein is only that of having possession of and the right to reproduce the Wiley Materials pursuant to Section 2 herein during the continuance of this Agreement. You agree that you own no

right, title or interest in or to the Wiley Materials or any of the intellectual property rights therein. You shall have no rights hereunder other than the license as provided for above in Section 2. No right, license or interest to any trademark, trade name, service mark or other branding ("Marks") of WILEY or its licensors is granted hereunder, and you agree that you shall not assert any such right, license or interest with respect thereto.

- NEITHER WILEY NOR ITS LICENSORS MAKES ANY WARRANTY OR REPRESENTATION OF ANY KIND TO YOU OR ANY THIRD PARTY, EXPRESS, IMPLIED OR STATUTORY, WITH RESPECT TO THE MATERIALS OR THE ACCURACY OF ANY INFORMATION CONTAINED IN THE MATERIALS, INCLUDING, WITHOUT LIMITATION, ANY IMPLIED WARRANTY OF MERCHANTABILITY, ACCURACY, SATISFACTORY QUALITY, FITNESS FOR A PARTICULAR PURPOSE, USABILITY, INTEGRATION OR NON-INFRINGEMENT AND ALL SUCH WARRANTIES ARE HEREBY EXCLUDED BY WILEY AND ITS LICENSORS AND WAIVED BY YOU

- WILEY shall have the right to terminate this Agreement immediately upon breach of this Agreement by you.
- You shall indemnify, defend and hold harmless WILEY, its Licensors and their respective directors, officers, agents and employees, from and against any actual or threatened claims, demands, causes of action or proceedings arising from any breach of this Agreement by you.

- IN NO EVENT SHALL WILEY OR ITS LICENSORS BE LIABLE TO YOU OR ANY OTHER PARTY OR ANY OTHER PERSON OR ENTITY FOR ANY SPECIAL, CONSEQUENTIAL, INCIDENTAL, INDIRECT, EXEMPLARY OR PUNITIVE DAMAGES, HOWEVER CAUSED, ARISING OUT OF OR IN CONNECTION WITH THE DOWNLOADING, PROVISIONING, VIEWING OR USE OF THE MATERIALS REGARDLESS OF THE FORM OF ACTION, WHETHER FOR BREACH OF CONTRACT, BREACH OF WARRANTY, TORT, NEGLIGENCE, INFRINGEMENT OR OTHERWISE (INCLUDING, WITHOUT LIMITATION, DAMAGES BASED ON LOSS OF PROFITS, DATA, FILES, USE, BUSINESS OPPORTUNITY OR CLAIMS OF THIRD PARTIES), AND WHETHER OR NOT THE PARTY HAS BEEN ADVISED OF THE POSSIBILITY OF SUCH DAMAGES. THIS LIMITATION SHALL APPLY NOTWITHSTANDING ANY FAILURE OF ESSENTIAL PURPOSE OF ANY LIMITED REMEDY PROVIDED HEREIN.

- Should any provision of this Agreement be held by a court of competent jurisdiction to be illegal, invalid, or unenforceable, that provision shall be deemed amended to achieve as nearly as possible the same economic effect as the original provision, and the legality, validity and enforceability of the remaining provisions of this Agreement shall not be affected or impaired thereby.

- The failure of either party to enforce any term or condition of this Agreement shall not constitute a waiver of either party's right to enforce each and every term and condition of this Agreement. No breach under this agreement shall be deemed waived or excused by either party unless such waiver or consent is in writing signed by the party granting such waiver or consent. The waiver by or consent of a party to a breach of any provision of this Agreement shall not operate or be construed as a waiver of or consent to any other or subsequent breach by such other party.

- This Agreement may not be assigned (including by operation of law or otherwise) by you without WILEY's prior written consent.

- Any fee required for this permission shall be non-refundable after thirty (30) days from receipt by the CCC.

- These terms and conditions together with CCC's Billing and Payment terms and conditions (which are incorporated herein) form the entire agreement between you and WILEY concerning this licensing transaction and (in the absence of fraud) supersedes all prior agreements and representations of the

parties, oral or written. This Agreement may not be amended except in writing signed by both parties. This Agreement shall be binding upon and inure to the benefit of the parties' successors, legal representatives, and authorized assigns.

- In the event of any conflict between your obligations established by these terms and conditions and those established by CCC's Billing and Payment terms and conditions, these terms and conditions shall prevail.

- WILEY expressly reserves all rights not specifically granted in the combination of (i) the license details provided by you and accepted in the course of this licensing transaction, (ii) these terms and conditions and (iii) CCC's Billing and Payment terms and conditions.

- This Agreement will be void if the Type of Use, Format, Circulation, or Requestor Type was misrepresented during the licensing process.

- This Agreement shall be governed by and construed in accordance with the laws of the State of New York, USA, without regards to such state's conflict of law rules. Any legal action, suit or proceeding arising out of or relating to these Terms and Conditions or the breach thereof shall be instituted in a court of competent jurisdiction in New York County in the State of New York in the United States of America and each party hereby consents and submits to the personal jurisdiction of such court, waives any objection to venue in such court and consents to service of process by registered or certified mail, return receipt requested, at the last known address of such party.

**WILEY OPEN ACCESS TERMS AND CONDITIONS**

Wiley Publishes Open Access Articles in fully Open Access Journals and in Subscription journals offering Online Open. Although most of the fully Open Access journals publish open access articles under the terms of the Creative Commons Attribution (CC BY) License only, the subscription journals and a few of the Open Access Journals offer a choice of Creative Commons Licenses:: Creative Commons Attribution (CC-BY) license Creative Commons Attribution Non-Commercial (CC-BY-NC) license and Creative Commons Attribution Non-Commercial-NoDerivs (CC-BY-NC-ND) License. The license type is clearly identified on the article.

Copyright in any research article in a journal published as Open Access under a Creative Commons License is retained by the author(s). Authors grant Wiley a license to publish the article and identify itself as the original publisher. Authors also grant any third party the right to use the article freely as long as its integrity is maintained and its original authors, citation details and publisher are identified as follows: [Title of Article/Author/Journal Title and Volume/Issue. Copyright (c) [year] [copyright owner as specified in the Journal]. Links to the final article on Wiley's website are encouraged where applicable.

**The Creative Commons Attribution License**

the author not to have the work altered in such a way that the author's reputation or integrity may be impugned).

- Where content in the article is identified as belonging to a third party, it is the obligation of the user to ensure that any reuse complies with the copyright policies of the owner of that content.

- If article content is copied, downloaded or otherwise reused for non-commercial research and education purposes, a link to the appropriate bibliographic citation (authors, journal, article title, volume, issue, page numbers, DOI and the link to the definitive published version on **Wiley Online Library**) should be maintained. Copyright notices and disclaimers must not be deleted.

- Any translations, for which a prior translation agreement with Wiley has not been agreed, must prominently display the statement: "This is an unofficial translation of an article that appeared in a Wiley publication. The publisher has not endorsed this translation."

**Use by commercial "for-profit" organisations**

Use of Wiley Open Access articles for commercial, promotional, or marketing purposes requires further explicit permission from Wiley and will be subject to a fee. Commercial purposes include:

- Copying or downloading of articles, or linking to such articles for further redistribution, sale or licensing;

- Copying, downloading or posting by a site or service that incorporates advertising with such content;

- The inclusion or incorporation of article content in other works or services (other than normal quotations with an appropriate citation) that is then available for sale or licensing, for a fee (for example, a compilation produced for marketing purposes, inclusion in a sales pack)

- Use of article content (other than normal quotations with appropriate citation) by for-profit organisations for promotional purposes

- Linking to article content in e-mails redistributed for promotional, marketing or educational purposes;

- Use for the purposes of monetary reward by means of sale, resale, licence, loan, transfer or other form of commercial exploitation such as marketing products

- Print reprints of Wiley Open Access articles can be purchased from:corporatesales@wiley.com

Further details can be found on Wiley Online Libraryhttp://olabout.wiley.com/WileyCDA/Section/id-410895.html

Other Terms and Conditions:

**v1.9**

**You will be invoiced within 48 hours of this transaction date. You may pay your invoice by credit card upon receipt of the invoice for this transaction. Please follow instructions provided at that time.**

**To pay for this transaction now; please remit a copy of this document along with your payment. Payment should be in the form of a check or money order referencing your account number and this invoice number RLNK501362278.**

**Make payments to "COPYRIGHT CLEARANCE CENTER" and send to:**

**Copyright Clearance Center**

**Dept 001**

**P.O. Box 843006**

**Boston, MA 02284-3006**

**Please disregard electronic and mailed copies if you remit payment in advance.**

**Questions? customercare@copyright.com or +1-855-239-3415 (toll free in the US) or +1-978-646-2777.**

**Gratis licenses (referencing $0 in the Total field) are free. Please retain this printable license for your reference. No payment is required.**

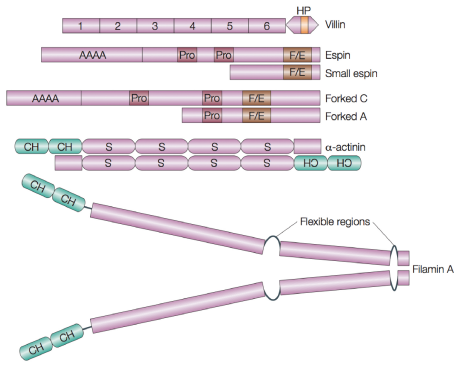


**Figure 1.5. Structural organization of actin-crosslinking proteins.** Filamin crosslinks F-actin into high-angle orthogonal networks. Villin binds actin monomers on repeat 1 and 4-6 and actin filaments on repeats 2-3 and the villin headpiece (HP) on the C-terminus. The KKEK motif is essential for filament binding (shown in yellow). The forked/espin homology domain (F/E) contains two actin-binding domains (ABDs) to mediate filament bundling. Pro and AAAA designate proline-rich regions and amino-terminal ankyrin repeats, respectively. In α-actinin and filamin A pairs of calponin-homology (CH) form the ABD. α-actinin forms an anti-parallel homodimer and filamin A forms a parallel homodimer to mediate its crosslinking activities. Figure adapted from (Revenu et al., 2004).

**Revenu, C., Athman, R., Robine, S., and Louvard, D. (2004). The co-workers of actin filaments: from cell structures to signals. Nat. Rev. Mol. Cell Biol. *5*, 635-646.**

## NATURE PUBLISHING GROUP LICENSE

## TERMS AND CONDITIONS

Jul 27, 2014

This is a License Agreement between Sandy Szeto ("You") and Nature Publishing Group ("Nature Publishing Group") provided by Copyright Clearance Center ("CCC"). The license consists of your order details, the terms and conditions provided by Nature Publishing Group, and the payment terms and conditions.

**All payments must be made in full to CCC. For payment instructions, please see information listed at the bottom of this form.**

License Number: 3436910508901

License date: Jul 27, 2014

Licensed content publisher: Nature Publishing Group

Licensed content publication: Nature Reviews Molecular Cell Biology

Licensed content title: The co-workers of actin filaments: from cell structures to signals

Licensed content author: Céline Revenu, Rafika Athman, Sylvie Robine, Daniel Louvard

Licensed content date: Aug 1, 2004

Volume number: 5

Issue number: 8

Type of Use: reuse in a dissertation / thesis

Requestor type: academic/educational

Format: electronic

Portion: figures/tables/illustrations

Number of figures/tables/illustrations: 2

High-res required: no

Figures: Box 1 | Actin filaments: structure and dynamics (figure) Box 2 | Molecular features implicated in actin crosslinking and bundling (figure)

Author of this NPG article: no

Your reference number: None

Title of your thesis / dissertation: Mitotic filamin A phosphorylation regulates filamin A localization and is important for daughter cell separation

Expected completion date: Oct 2014

Estimated size (number of pages): 250

Total: 0.00 USD

Terms and Conditions

Terms and Conditions for Permissions

Nature Publishing Group hereby grants you a non-exclusive license to reproduce this material for this purpose, and for no other use,subject to the conditions below:

1. NPG warrants that it has, to the best of its knowledge, the rights to license reuse of this material. However, you should ensure that the material you are requesting is original to Nature Publishing Group and does not carry the copyright of another entity (as credited in the published version). If the credit line on any part of the material you have requested indicates that it was reprinted or adapted by NPG with permission from another source, then you should also seek permission from that source to reuse the material.

2. Permission granted free of charge for material in print is also usually granted for any electronic version of that work, provided that the material is incidental to the work as a whole and that the electronic version is essentially equivalent to, or substitutes for, the print version.Where print permission has been granted for a fee, separate permission must be obtained for any additional, electronic re-use (unless, as in the case of a full paper, this has already been accounted for during your initial request in the calculation of a print run).NB: In all cases, web-based use of full-text articles must be authorized separately through the 'Use on a Web Site' option when requesting permission.

3. Permission granted for a first edition does not apply to second and subsequent editions and for editions in other languages (except for signatories to the STM Permissions Guidelines, or where the first edition permission was granted for free).

4. Nature Publishing Group's permission must be acknowledged next to the figure, table or abstract in print. In electronic form, this acknowledgement must be visible at the same time as the figure/table/abstract, and must be hyperlinked to the journal's homepage.

5. The credit line should read:
   Reprinted by permission from Macmillan Publishers Ltd: [JOURNAL NAME] (reference citation), copyright (year of publication)
   For AOP papers, the credit line should read:
   Reprinted by permission from Macmillan Publishers Ltd: [JOURNAL NAME], advance online publication, day month year (doi: 10.1038/sj.[JOURNAL ACRONYM].XXXXX)

   **Note: For republication from the *British Journal of Cancer,* the following credit lines apply.**
   Reprinted by permission from Macmillan Publishers Ltd on behalf of Cancer Research UK: [JOURNAL NAME] (reference citation), copyright (year of publication)For AOP papers, the credit line should read:
   Reprinted by permission from Macmillan Publishers Ltd on behalf of Cancer Research UK: [JOURNAL NAME], advance online publication, day month year (doi: 10.1038/sj.[JOURNAL ACRONYM].XXXXX)

6. Adaptations of single figures do not require NPG approval. However, the adaptation should be credited as follows:

   Adapted by permission from Macmillan Publishers Ltd: [JOURNAL NAME] (reference citation), copyright (year of publication)

   **Note: For adaptation from the *British Journal of Cancer,* the following credit line applies.**
   Adapted by permission from Macmillan Publishers Ltd on behalf of Cancer Research UK: [JOURNAL NAME] (reference citation), copyright (year of publication)

7. Translations of 401 words up to a whole article require NPG approval. Please visithttp://www.macmillanmedicalcommunications.com for more information.Translations of up to a 400 words do not require NPG approval. The translation should be credited as follows:

   Translated by permission from Macmillan Publishers Ltd: [JOURNAL NAME] (reference citation), copyright (year of publication).

   **Note: For translation from the *British Journal of Cancer,* the following credit line applies.**
   Translated by permission from Macmillan Publishers Ltd on behalf of Cancer Research UK: [JOURNAL NAME] (reference citation), copyright (year of publication)

We are certain that all parties will benefit from this agreement and wish you the best in the use of this material.

Thank you.

Special Terms:

v1.1

**You will be invoiced within 48 hours of this transaction date. You may pay your invoice by credit card upon receipt of the invoice for this transaction. Please follow instructions provided at that time.**

**To pay for this transaction now; please remit a copy of this document along with your payment. Payment should be in the form of a check or money order referencing your account number and this invoice number RLNK501362262.**

**Make payments to "COPYRIGHT CLEARANCE CENTER" and send to:**

**Copyright Clearance Center**

**Dept 001**

**P.O. Box 843006**

**Boston, MA 02284-3006**

**Please disregard electronic and mailed copies if you remit payment in advance.**

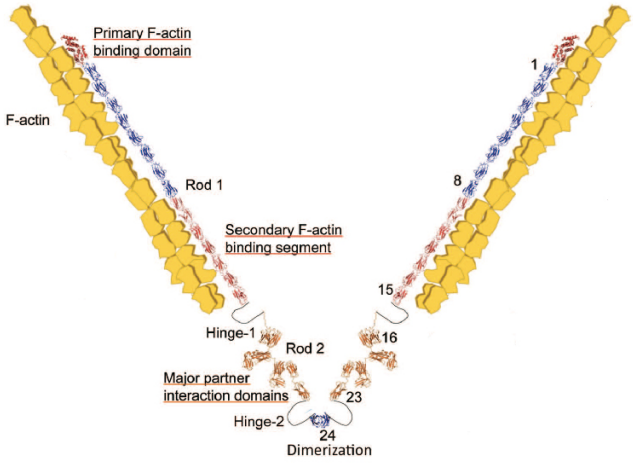


**Figure 1.6. Schematic representation of filamin A molecule and its interaction with actin filaments.** Self-association of two filamin A monomers is mediated by IgFLNa domain 24 at the C-terminus. The primary actin-binding domain (ABD) is located at the N-terminus and a secondary F-actin binding segment is located in IgFLNa domains 8-15. Two flexible hinge regions are located between domains 15 and 16 (H1) and 23 and 24 (H2). Figure adapted from (Nakamura et al., 2011).

**Nakamura, F., Stossel, T.P., and Hartwig, J.H. (2011). The filamins: Organizers of cell structure and function. Cell Adhesion & Migration *5*, 160-169.**

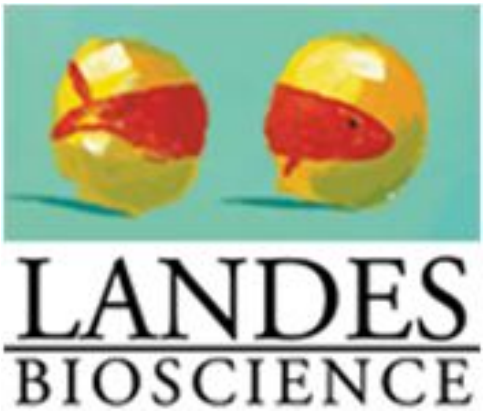

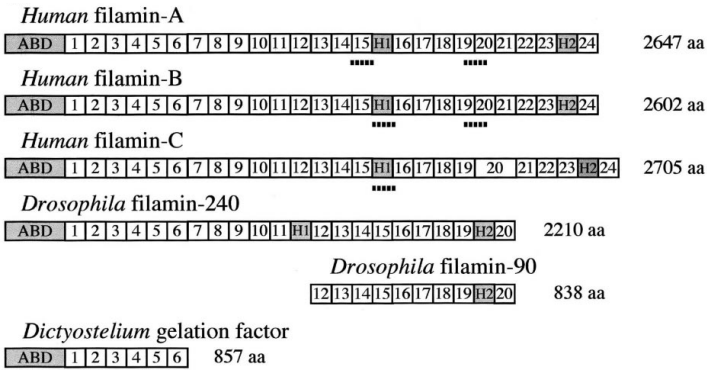


**Figure 1.7. Schematic representation of the domain composition of human, *Drosophila* and *Dictyostelium* filamins.** There are three human filamin isoforms, FLNa, FLNb and FLNc. The actin-binding domain (ABD), hinge 1 (H1) and hinge 2 (H2) are shown in grey. Dotted lines indicate sites of alternative splicing. Figure from (Van der Flier, 2001).

**Van der Flier, A. (2001). Structural and functional aspects of filamins. Biochim. Biophys. Acta *1538*, 99-117.**

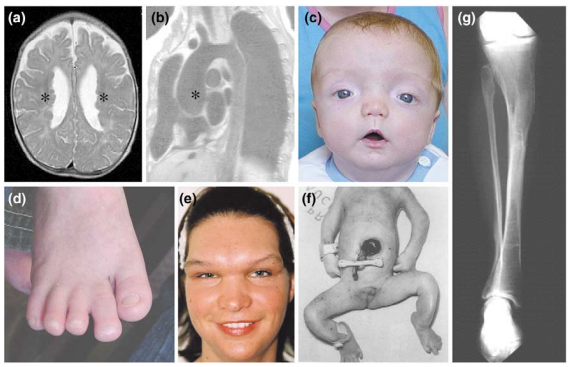


**Figure 1.8. Phenotypes associated with mutations in FLNA. (A)** Magnetic resonance image (MRI) of the brain of a female with periventricular nodular heterotopia (PH). The asterisks indicate nodules of heterotopic neurons lining the lateral ventricular margins. **(B)** MRI showing aortic dilatation (asterisk) in an individual with PH-Ehlers-Danlos syndrome. **(C)** Facial features of a male infant with otopalatodigital syndrome type 1 (OPD1). Note the widely spaced eyes. **(D)** Foot of the subject pictured in panel C showing partial syndactyly of toes and a foreshortened great toe. **(E)** Female carrier with frontometaphyseal dysplasia (FMD) with marked prominence of the supraorbital region. **(F)** Male with otopalatodigital syndrome type 2 (OPD2) with omphalocoele (sac containing the intestines in the midline) and bowed lower limbs. **(G)** Bowing of the tibia and fibula in a female with Melnick Needles syndrome (MNS). Figure from (Robertson, 2005).

**Robertson, S.P. (2005). Filamin A: phenotypic diversity. Curr. Opin. Genet. Dev. *15*, 301-307.**

## ELSEVIER LICENSE

## TERMS AND CONDITIONS

Jul 27, 2014

This is a License Agreement between Sandy Szeto ("You") and Elsevier ("Elsevier") provided by Copyright Clearance Center ("CCC"). The license consists of your order details, the terms and conditions provided by Elsevier, and the payment terms and conditions.

**All payments must be made in full to CCC. For payment instructions, please see information listed at the bottom of this form.**

Supplier

Elsevier Limited

The Boulevard,Langford Lane

Kidlington,Oxford,OX5 1GB,UK

Registered Company Number

1982084

Customer name

Sandy Szeto

License number

3436951253612

License date

Jul 27, 2014

Licensed content publisher

Elsevier

Licensed content publication

Current Opinion in Genetics & Development

Licensed content title

Filamin A: phenotypic diversity

Licensed content author

Veronica van Heyningen,David FitzPatrick,Stephen P Robertson

Licensed content date

June 2005

Licensed content volume number

15

Licensed content issue number

3

Number of pages

7

Start Page

301

End Page

307

Type of Use

reuse in a thesis/dissertation

Portion

figures/tables/illustrations

Number of figures/tables/illustrations

1

Format

electronic

Are you the author of this Elsevier article?

No

Will you be translating?

No

Title of your thesis/dissertation

Mitotic filamin A phosphorylation regulates filamin A localization and is important for daughter cell separation

Expected completion date

Oct 2014

Estimated size (number of pages)

250

Elsevier VAT number

GB 494 6272 12

Permissions price

0.00 USD

VAT/Local Sales Tax

0.00 USD / 0.00 GBP

Total

0.00 USD

Terms and Conditions

**INTRODUCTION**

1. The publisher for this copyrighted material is Elsevier. By clicking "accept" in connection with completing this licensing transaction, you agree that the following terms and conditions apply to this transaction (along with the Billing and Payment terms and conditions established by Copyright Clearance Center, Inc. ("CCC"), at the time that you opened your Rightslink account and that are available at any time at http://myaccount.copyright.com).

**GENERAL TERMS**

2. Elsevier hereby grants you permission to reproduce the aforementioned material subject to the terms and conditions indicated.

3. Acknowledgement: If any part of the material to be used (for example, figures) has appeared in our publication with credit or acknowledgement to another source, permission must also be sought from that source. If such permission is not obtained then that material may not be included in your publication/copies. Suitable acknowledgement to the source must be made, either as a footnote or in a reference list at the end of your publication, as follows:

"Reprinted from Publication title, Vol /edition number, Author(s), Title of article / title of chapter, Pages No., Copyright (Year), with permission from Elsevier [OR APPLICABLE SOCIETY COPYRIGHT OWNER]."

Also Lancet special credit - "Reprinted from The Lancet, Vol. number, Author(s), Title of article, Pages No., Copyright (Year), with permission from Elsevier."

4. Reproduction of this material is confined to the purpose and/or media for which permission is hereby given.

5. Altering/Modifying Material: Not Permitted. However figures and illustrations may be altered/adapted minimally to serve your work. Any other abbreviations, additions, deletions and/or any other alterations shall be made only with prior written authorization of Elsevier Ltd. (Please contact Elsevier at permissions@elsevier.com)

6. If the permission fee for the requested use of our material is waived in this instance, please be advised that your future requests for Elsevier materials may attract a fee.

7. Reservation of Rights: Publisher reserves all rights not specifically granted in the combination of (i) the license details provided by you and accepted in the course of this licensing transaction, (ii) these terms and conditions and (iii) CCC's Billing and Payment terms and conditions.

8. License Contingent Upon Payment: While you may exercise the rights licensed immediately upon issuance of the license at the end of the licensing process for the transaction, provided that you have disclosed complete and accurate details of your proposed use, no license is finally effective unless and until full payment is received from you (either by publisher or by CCC) as provided in CCC's Billing and Payment terms and conditions. If full payment is not received on a timely basis, then any license preliminarily granted shall be deemed automatically revoked and shall be void as if never granted. Further, in the event that you breach any of these terms and conditions or any of CCC's Billing and Payment terms and conditions, the license is automatically revoked and shall be void as if never granted. Use of materials as described in a revoked license, as well as any use of the materials beyond the scope of an unrevoked license, may constitute copyright infringement and publisher reserves the right to take any and all action to protect its copyright in the materials.

9. Warranties: Publisher makes no representations or warranties with respect to the licensed material.

10. Indemnity: You hereby indemnify and agree to hold harmless publisher and CCC, and their respective officers, directors, employees and agents, from and against any and all claims arising out of your use of the licensed material other than as specifically authorized pursuant to this license.

11. No Transfer of License: This license is personal to you and may not be sublicensed, assigned, or transferred by you to any other person without publisher's written permission.

12. No Amendment Except in Writing: This license may not be amended except in a writing signed by both parties (or, in the case of publisher, by CCC on publisher's behalf).

13. Objection to Contrary Terms: Publisher hereby objects to any terms contained in any purchase order, acknowledgment, check endorsement or other writing prepared by you, which terms are inconsistent with these terms and conditions or CCC's Billing and Payment terms and conditions. These terms and conditions, together with CCC's Billing and Payment terms and conditions (which are incorporated herein), comprise the entire agreement between you and publisher (and CCC) concerning this licensing transaction. In the event of any conflict between your obligations established by these terms and conditions and those established by CCC's Billing and Payment terms and conditions, these terms and conditions shall control.

14. Revocation: Elsevier or Copyright Clearance Center may deny the permissions described in this License at their sole discretion, for any reason or no reason, with a full refund payable to you. Notice of such denial will be made using the contact information provided by you. Failure to receive such notice will not alter or invalidate the denial. In no event will Elsevier or Copyright Clearance Center be responsible or liable for any costs, expenses or damage incurred by you as a result of a denial of your permission request, other than a refund of the amount(s) paid by you to Elsevier and/or Copyright Clearance Center for denied permissions.

**LIMITED LICENSE**

The following terms and conditions apply only to specific license types:

15. **Translation**: This permission is granted for non-exclusive world **English** rights only unless your license was granted for translation rights. If you licensed translation rights you may only translate this content into the languages you requested. A professional translator must perform all translations and reproduce the content word for word preserving the integrity of the article. If this license is to re-use 1 or 2 figures then permission is granted for non-exclusive world rights in all languages.

16. **Posting licensed content on any Website**: The following terms and conditions apply as follows: Licensing material from an Elsevier journal: All content posted to the web site must maintain the copyright information line on the bottom of each image; A hyper-text must be included to the Homepage of the journal from which you are licensing athttp://www.sciencedirect.com/science/journal/xxxxx or the Elsevier homepage for books athttp://www.elsevier.com; Central Storage: This license does not include permission for a scanned version of the material to be stored in a central repository such as that provided by Heron/XanEdu.

Licensing material from an Elsevier book: A hyper-text link must be included to the Elsevier homepage at http://www.elsevier.com . All content posted to the web site must maintain the copyright information line on the bottom of each image.

**Posting licensed content on Electronic reserve**: In addition to the above the following clauses are applicable: The web site must be password-protected and made available only to bona fide students registered on a relevant course. This permission is granted for 1 year only. You may obtain a new license for future website posting.

**For journal authors:** the following clauses are applicable in addition to the above: Permission granted is limited to the author accepted manuscript version* of your paper.

***Accepted Author Manuscript (AAM) Definition:** An accepted author manuscript (AAM) is the author's version of the manuscript of an article that has been accepted for publication and which may include any author-incorporated changes suggested through the processes of submission processing, peer review, and editor-author communications. AAMs do not include other publisher value-added contributions such as copy-editing, formatting, technical enhancements and (if relevant) pagination.

You are not allowed to download and post the published journal article (whether PDF or HTML, proof or final version), nor may you scan the printed edition to create an electronic version. A hyper-text must be included to the Homepage of the journal from which you are licensing at http://www.sciencedirect.com/science/journal/xxxxx. As part of our normal production process, you will receive an e-mail notice when your article appears on Elsevier's online service ScienceDirect (www.sciencedirect.com). That e-mail will include the article's Digital Object Identifier (DOI). This number provides the electronic link to the published article and should be included in the posting of your personal version. We ask that you wait until you receive this e-mail and have the DOI to do any posting.

**Posting to a repository:** Authors may post their AAM immediately to their employer's institutional repository for internal use only and may make their manuscript publically available after the journal-specific embargo period has ended.

Please also refer to Elsevier's Article Posting Policy for further information.

18. **For book authors** the following clauses are applicable in addition to the above: Authors are permitted to place a brief summary of their work online only.. You are not allowed to download and post the published

electronic version of your chapter, nor may you scan the printed edition to create an electronic version. **Posting to a repository:** Authors are permitted to post a summary of their chapter only in their institution's repository.

20. **Thesis/Dissertation**: If your license is for use in a thesis/dissertation your thesis may be submitted to your institution in either print or electronic form. Should your thesis be published commercially, please reapply for permission. These requirements include permission for the Library and Archives of Canada to supply single copies, on demand, of the complete thesis and include permission for UMI to supply single copies, on demand, of the complete thesis. Should your thesis be published commercially, please reapply for permission.

**Elsevier Open Access Terms and Conditions**

Elsevier publishes Open Access articles in both its Open Access journals and via its Open Access articles option in subscription journals.

Authors publishing in an Open Access journal or who choose to make their article Open Access in an Elsevier subscription journal select one of the following Creative Commons user licenses, which define how a reader may reuse their work: Creative Commons Attribution License (CC BY), Creative Commons Attribution – Non Commercial - ShareAlike (CC BY NC SA) and Creative Commons Attribution – Non Commercial – No Derivatives (CC BY NC ND)

**Terms & Conditions applicable to all Elsevier Open Access articles:**

Any reuse of the article must not represent the author as endorsing the adaptation of the article nor should the article be modified in such a way as to damage the author's honour or reputation.

The author(s) must be appropriately credited.

If any part of the material to be used (for example, figures) has appeared in our publication with credit or acknowledgement to another source it is the responsibility of the user to ensure their reuse complies with the terms and conditions determined by the rights holder.

**Additional Terms & Conditions applicable to each Creative Commons user license:**

**CC BY:** You may distribute and copy the article, create extracts, abstracts, and other revised versions, adaptations or derivative works of or from an article (such as a translation), to include in a collective work (such as an anthology), to text or data mine the article, including for commercial purposes without permission from Elsevier

**CC BY NC SA:** For non-commercial purposes you may distribute and copy the article, create extracts, abstracts and other revised versions, adaptations or derivative works of or from an article (such as a translation), to include in a collective work (such as an anthology), to text and data mine the article and license new adaptations or creations under identical terms without permission from Elsevier

**CC BY NC ND:** For non-commercial purposes you may distribute and copy the article and include it in a collective work (such as an anthology), provided you do not alter or modify the article, without permission from Elsevier

Any commercial reuse of Open Access articles published with a CC BY NC SA or CC BY NC ND license requires permission from Elsevier and will be subject to a fee.

Commercial reuse includes:

- Promotional purposes (advertising or marketing)
- Commercial exploitation ( e.g. a product for sale or loan)
- Systematic distribution (for a fee or free of charge)

Please refer to Elsevier's Open Access Policy for further information.

21. **Other Conditions**:

v1.6

**You will be invoiced within 48 hours of this transaction date. You may pay your invoice by credit card upon receipt of the invoice for this transaction. Please follow instructions provided at that time.**

**To pay for this transaction now; please remit a copy of this document along with your payment. Payment should be in the form of a check or money order referencing your account number and this invoice number RLNK501362291.**

**Make payments to "COPYRIGHT CLEARANCE CENTER" and send to:**

**Copyright Clearance Center**

**Dept 001**

**P.O. Box 843006**

**Boston, MA 02284-3006**

**Please disregard electronic and mailed copies if you remit payment in advance.**

**Questions? customercare@copyright.com or +1-855-239-3415 (toll free in the US) or +1-978-646-2777.**

**Gratis licenses (referencing $0 in the Total field) are free. Please retain this printable license for your reference. No payment is required.**

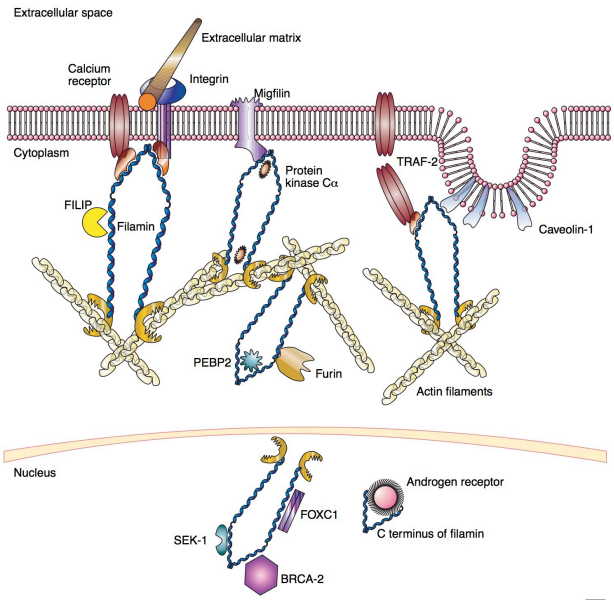


**Figure 1.9. Filamin A functions.** In the cytoplasm, filamin A can crosslink F-actin, anchor transmembrane proteins, act as a scaffold for signaling complexes and link membrane receptors to the actin cytoskeleton. In the nucleus, filamin A has been implicated in transcription regulation. Both full-length and a 100 kD calpain-mediated cleavage fragment of filamin A have been found in the nucleus. Figure from (Popowicz et al., 2006).

**Popowicz, G.M., Schleicher, M., Noegel, A.A., and Holak, T.A. (2006). Filamins: promiscuous organizers of the cytoskeleton. Trends Biochem. Sci. *31*, 411-419.**

## ELSEVIER LICENSE

## TERMS AND CONDITIONS

Jul 27, 2014

This is a License Agreement between Sandy Szeto ("You") and Elsevier ("Elsevier") provided by Copyright Clearance Center ("CCC"). The license consists of your order details, the terms and conditions provided by Elsevier, and the payment terms and conditions.

**All payments must be made in full to CCC. For payment instructions, please see information listed at the bottom of this form.**

Supplier

Elsevier Limited

The Boulevard,Langford Lane

Kidlington,Oxford,OX5 1GB,UK

Registered Company Number: 1982084

Customer name: Sandy Szeto

License number: 3436951384863

License date: Jul 27, 2014

Licensed content publisher: Elsevier

Licensed content publication: Trends in Biochemical Sciences

Licensed content title: Filamins: promiscuous organizers of the cytoskeleton

Licensed content author: Grzegorz M. Popowicz,Michael Schleicher,Angelika A. Noegel,Tad A. Holak

Licensed content date: July 2006

Licensed content volume number: 31

Licensed content issue number: 7

Number of pages: 9

Start Page: 411

End Page: 419

Type of Use: reuse in a thesis/dissertation

Intended publisher of new work: other

Portion: figures/tables/illustrations

Number of figures/tables/illustrations: 1

Format: electronic

Are you the author of this Elsevier article?:No

Will you be translating?: No

Title of your thesis/dissertation: Mitotic filamin A phosphorylation regulates filamin A localization and is important for daughter cell separation

Expected completion date: Oct 2014

Estimated size (number of pages): 250

Elsevier VAT number: GB 494 6272 12

Permissions price: 0.00 USD

VAT/Local Sales Tax: 0.00 USD / 0.00 GBP

Total: 0.00 USD

Terms and Conditions

**INTRODUCTION**

1. The publisher for this copyrighted material is Elsevier. By clicking "accept" in connection with completing this licensing transaction, you agree that the following terms and conditions apply to this transaction (along with the Billing and Payment terms and conditions established by Copyright Clearance Center, Inc. ("CCC"), at the time that you opened your Rightslink account and that are available at any time at http://myaccount.copyright.com).

**GENERAL TERMS**

2. Elsevier hereby grants you permission to reproduce the aforementioned material subject to the terms and conditions indicated.

3. Acknowledgement: If any part of the material to be used (for example, figures) has appeared in our publication with credit or acknowledgement to another source, permission must also be sought from that source. If such permission is not obtained then that material may not be included in your publication/copies. Suitable acknowledgement to the source must be made, either as a footnote or in a reference list at the end of your publication, as follows:

"Reprinted from Publication title, Vol /edition number, Author(s), Title of article / title of chapter, Pages No., Copyright (Year), with permission from Elsevier [OR APPLICABLE SOCIETY COPYRIGHT OWNER]." Also Lancet special credit - "Reprinted from The Lancet, Vol. number, Author(s), Title of article, Pages No., Copyright (Year), with permission from Elsevier."

4. Reproduction of this material is confined to the purpose and/or media for which permission is hereby given.

5. Altering/Modifying Material: Not Permitted. However figures and illustrations may be altered/adapted minimally to serve your work. Any other abbreviations, additions, deletions and/or any other alterations shall be made only with prior written authorization of Elsevier Ltd. (Please contact Elsevier at permissions@elsevier.com)

6. If the permission fee for the requested use of our material is waived in this instance, please be advised that your future requests for Elsevier materials may attract a fee.

7. Reservation of Rights: Publisher reserves all rights not specifically granted in the combination of (i) the license details provided by you and accepted in the course of this licensing transaction, (ii) these terms and conditions and (iii) CCC's Billing and Payment terms and conditions.

8. License Contingent Upon Payment: While you may exercise the rights licensed immediately upon issuance of the license at the end of the licensing process for the transaction, provided that you have disclosed complete and accurate details of your proposed use, no license is finally effective unless and until full payment is received from you (either by publisher or by CCC) as provided in CCC's Billing and Payment terms and conditions. If full payment is not received on a timely basis, then any license preliminarily granted shall be deemed automatically revoked and shall be void as if never granted. Further, in the event that you breach any of these terms and conditions or any of CCC's Billing and Payment terms and conditions, the license is automatically revoked and shall be void as if never granted. Use of materials as described in a revoked license, as well as any use of the materials beyond the scope of an unrevoked license, may constitute copyright infringement and publisher reserves the right to take any and all action to protect its copyright in the materials.

9. Warranties: Publisher makes no representations or warranties with respect to the licensed material.

10. Indemnity: You hereby indemnify and agree to hold harmless publisher and CCC, and their respective officers, directors, employees and agents, from and against any and all claims arising out of your use of the licensed material other than as specifically authorized pursuant to this license.

11. No Transfer of License: This license is personal to you and may not be sublicensed, assigned, or transferred by you to any other person without publisher's written permission.

12. No Amendment Except in Writing: This license may not be amended except in a writing signed by both parties (or, in the case of publisher, by CCC on publisher's behalf).

13. Objection to Contrary Terms: Publisher hereby objects to any terms contained in any purchase order, acknowledgment, check endorsement or other writing prepared by you, which terms are inconsistent with these terms and conditions or CCC's Billing and Payment terms and conditions. These terms and conditions, together with CCC's Billing and Payment terms and conditions (which are incorporated herein), comprise the entire agreement between you and publisher (and CCC) concerning this licensing transaction. In the event of any conflict between your obligations established by these terms and conditions and those established by CCC's Billing and Payment terms and conditions, these terms and conditions shall control.

14. Revocation: Elsevier or Copyright Clearance Center may deny the permissions described in this License at their sole discretion, for any reason or no reason, with a full refund payable to you. Notice of such denial will be made using the contact information provided by you. Failure to receive such notice will not alter or invalidate the denial. In no event will Elsevier or Copyright Clearance Center be responsible or liable for any costs, expenses or damage incurred by you as a result of a denial of your permission request, other than a refund of the amount(s) paid by you to Elsevier and/or Copyright Clearance Center for denied permissions.

**LIMITED LICENSE**

The following terms and conditions apply only to specific license types:

15. **Translation**: This permission is granted for non-exclusive world **English** rights only unless your license was granted for translation rights. If you licensed translation rights you may only translate this content into the languages you requested. A professional translator must perform all translations and reproduce the content word for word preserving the integrity of the article. If this license is to re-use 1 or 2 figures then permission is granted for non-exclusive world rights in all languages.

16. **Posting licensed content on any Website**: The following terms and conditions apply as follows: Licensing material from an Elsevier journal: All content posted to the web site must maintain the copyright information line on the bottom of each image; A hyper-text must be included to the Homepage of the journal from which you are licensing athttp://www.sciencedirect.com/science/journal/xxxxx or the Elsevier homepage for books

athttp://www.elsevier.com; Central Storage: This license does not include permission for a scanned version of the material to be stored in a central repository such as that provided by Heron/XanEdu.

Licensing material from an Elsevier book: A hyper-text link must be included to the Elsevier homepage at http://www.elsevier.com . All content posted to the web site must maintain the copyright information line on the bottom of each image.

**Posting licensed content on Electronic reserve**: In addition to the above the following clauses are applicable: The web site must be password-protected and made available only to bona fide students registered on a relevant course. This permission is granted for 1 year only. You may obtain a new license for future website posting.

**For journal authors:** the following clauses are applicable in addition to the above: Permission granted is limited to the author accepted manuscript version* of your paper.

***Accepted Author Manuscript (AAM) Definition:** An accepted author manuscript (AAM) is the author's version of the manuscript of an article that has been accepted for publication and which may include any author-incorporated changes suggested through the processes of submission processing, peer review, and editor-author communications. AAMs do not include other publisher value-added contributions such as copy-editing, formatting, technical enhancements and (if relevant) pagination.

You are not allowed to download and post the published journal article (whether PDF or HTML, proof or final version), nor may you scan the printed edition to create an electronic version. A hyper-text must be included to the Homepage of the journal from which you are licensing at http://www.sciencedirect.com/science/journal/xxxxx. As part of our normal production process, you will receive an e-mail notice when your article appears on Elsevier's online service ScienceDirect (www.sciencedirect.com). That e-mail will include the article's Digital Object Identifier (DOI). This number provides the electronic link to the published article and should be included in the posting of your personal version. We ask that you wait until you receive this e-mail and have the DOI to do any posting.

**Posting to a repository:** Authors may post their AAM immediately to their employer's institutional repository for internal use only and may make their manuscript publically available after the journal-specific embargo period has ended.

Please also refer to Elsevier's Article Posting Policy for further information.

18. **For book authors** the following clauses are applicable in addition to the above: Authors are permitted to place a brief summary of their work online only.. You are not allowed to download and post the published electronic version of your chapter, nor may you scan the printed edition to create an electronic version. **Posting to a repository:** Authors are permitted to post a summary of their chapter only in their institution's repository.

20. **Thesis/Dissertation**: If your license is for use in a thesis/dissertation your thesis may be submitted to your institution in either print or electronic form. Should your thesis be published commercially, please reapply for permission. These requirements include permission for the Library and Archives of Canada to supply single copies, on demand, of the complete thesis and include permission for UMI to supply single copies, on demand, of the complete thesis. Should your thesis be published commercially, please reapply for permission.

**Elsevier Open Access Terms and Conditions**

Elsevier publishes Open Access articles in both its Open Access journals and via its Open Access articles option in subscription journals.

Authors publishing in an Open Access journal or who choose to make their article Open Access in an Elsevier subscription journal select one of the following Creative Commons user licenses, which define how a reader may reuse their work: Creative Commons Attribution License (CC BY), Creative Commons Attribution – Non Commercial - ShareAlike (CC BY NC SA) and Creative Commons Attribution – Non Commercial – No Derivatives (CC BY NC ND)

**Terms & Conditions applicable to all Elsevier Open Access articles:**

Any reuse of the article must not represent the author as endorsing the adaptation of the article nor should the article be modified in such a way as to damage the author's honour or reputation.

The author(s) must be appropriately credited.

If any part of the material to be used (for example, figures) has appeared in our publication with credit or acknowledgement to another source it is the responsibility of the user to ensure their reuse complies with the terms and conditions determined by the rights holder.

**Additional Terms & Conditions applicable to each Creative Commons user license:**

**CC BY:** You may distribute and copy the article, create extracts, abstracts, and other revised versions, adaptations or derivative works of or from an article (such as a translation), to include in a collective work

(such as an anthology), to text or data mine the article, including for commercial purposes without permission from Elsevier

**CC BY NC SA:** For non-commercial purposes you may distribute and copy the article, create extracts, abstracts and other revised versions, adaptations or derivative works of or from an article (such as a translation), to include in a collective work (such as an anthology), to text and data mine the article and license new adaptations or creations under identical terms without permission from Elsevier

**CC BY NC ND:** For non-commercial purposes you may distribute and copy the article and include it in a collective work (such as an anthology), provided you do not alter or modify the article, without permission from Elsevier

Any commercial reuse of Open Access articles published with a CC BY NC SA or CC BY NC ND license requires permission from Elsevier and will be subject to a fee.

Commercial reuse includes:

- Promotional purposes (advertising or marketing)
- Commercial exploitation ( e.g. a product for sale or loan)
- Systematic distribution (for a fee or free of charge)

Please refer to Elsevier's Open Access Policy for further information.

21. **Other Conditions**:

v1.6

**You will be invoiced within 48 hours of this transaction date. You may pay your invoice by credit card upon receipt of the invoice for this transaction. Please follow instructions provided at that time.**

**To pay for this transaction now; please remit a copy of this document along with your payment. Payment should be in the form of a check or money order referencing your account number and this invoice number RLNK501362294.**

**Make payments to "COPYRIGHT CLEARANCE CENTER" and send to:**

**Copyright Clearance Center**

**Dept 001**

**P.O. Box 843006**

**Boston, MA 02284-3006**

**Please disregard electronic and mailed copies if you remit payment in advance.**

**Questions? customercare@copyright.com or +1-855-239-3415 (toll free in the US) or +1-978-646-2777.**

**Gratis licenses (referencing $0 in the Total field) are free. Please retain this printable license for your reference. No payment is required.**

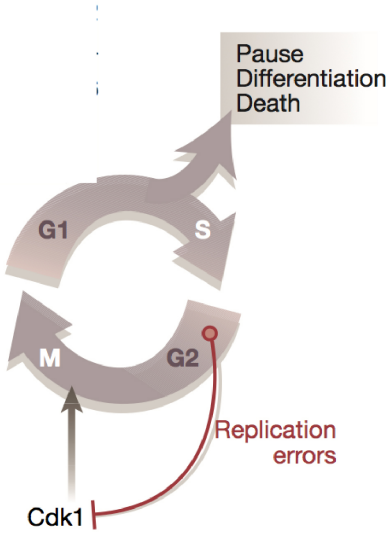


**Figure 1.10. Cell cycle and assignment of Cdk activity to particular cell transitions.** The cell cycle includes a gap period (G1 phase) during which the activity of various Cdks is controlled by positive (growth, survival and mitogenic) and negative (apoptotic and cytostatic; genotoxic, metabolic, oncogenic and oxidative stress) signals. During S-phase DNA replication occurs. Another gap period (G2 phase) is devoted to mending replication errors, which if present, inhibit Cdk1 and thus mitotic entry. Figure adapted from (Massague, 2004)**.**

**Massague, J. (2004). G1 cell-cycle control and cancer. Nature *432*, 298-306.**

## NATURE PUBLISHING GROUP LICENSE

## TERMS AND CONDITIONS

Jul 27, 2014

This is a License Agreement between Sandy Szeto ("You") and Nature Publishing Group ("Nature Publishing Group") provided by Copyright Clearance Center ("CCC"). The license consists of your order details, the terms and conditions provided by Nature Publishing Group, and the payment terms and conditions.

**All payments must be made in full to CCC. For payment instructions, please see information listed at the bottom of this form.**

License Number: 3436911106343

License date: Jul 27, 2014

Licensed content publisher: Nature Publishing Group

Licensed content publication: Nature

Licensed content title: G1 cell-cycle control and cancer

Licensed content author: Joan Massague

Licensed content date: Nov 17, 2004

Volume number: 432

Issue number: 7015

Type of Use: reuse in a dissertation / thesis

Requestor type: academic/educational

Format: electronic

Portion: figures/tables/illustrations

Number of figures/tables/illustrations: 1

High-res required: no

Figures: Figure 1 Simple and complex cell cycles (part b only)

Author of this NPG article: no

Your reference number: None

Title of your thesis / dissertation: Mitotic filamin A phosphorylation regulates filamin A localization and is important for daughter cell separation

Expected completion date: Oct 2014

Estimated size (number of pages): 250

Total: 0.00 USD

Terms and Conditions

Terms and Conditions for Permissions

Nature Publishing Group hereby grants you a non-exclusive license to reproduce this material for this purpose, and for no other use,subject to the conditions below:

1. NPG warrants that it has, to the best of its knowledge, the rights to license reuse of this material. However, you should ensure that the material you are requesting is original to Nature Publishing Group and does not carry the copyright of another entity (as credited in the published version). If the credit line on any part of the material you have requested indicates that it was reprinted or adapted by NPG with permission from another source, then you should also seek permission from that source to reuse the material.

2. Permission granted free of charge for material in print is also usually granted for any electronic version of that work, provided that the material is incidental to the work as a whole and that the electronic version is essentially equivalent to, or substitutes for, the print version.Where print permission has been granted for a fee, separate permission must be obtained for any additional, electronic re-use (unless, as in the case of a full paper, this has already been accounted for during your initial request in the calculation of a print run).NB: In all cases, web-based use of full-text articles must be authorized separately through the 'Use on a Web Site' option when requesting permission.

3. Permission granted for a first edition does not apply to second and subsequent editions and for editions in other languages (except for signatories to the STM Permissions Guidelines, or where the first edition permission was granted for free).

4. Nature Publishing Group's permission must be acknowledged next to the figure, table or abstract in print. In electronic form, this acknowledgement must be visible at the same time as the figure/table/abstract, and must be hyperlinked to the journal's homepage.

5. The credit line should read:
   Reprinted by permission from Macmillan Publishers Ltd: [JOURNAL NAME] (reference citation), copyright (year of publication)
   For AOP papers, the credit line should read:
   Reprinted by permission from Macmillan Publishers Ltd: [JOURNAL NAME], advance online publication, day month year (doi: 10.1038/sj.[JOURNAL ACRONYM].XXXXX)

   **Note: For republication from the *British Journal of Cancer,* the following credit lines apply.**
   Reprinted by permission from Macmillan Publishers Ltd on behalf of Cancer Research UK: [JOURNAL NAME] (reference citation), copyright (year of publication)For AOP papers, the credit line should read:
   Reprinted by permission from Macmillan Publishers Ltd on behalf of Cancer Research UK: [JOURNAL NAME], advance online publication, day month year (doi: 10.1038/sj.[JOURNAL ACRONYM].XXXXX)

6. Adaptations of single figures do not require NPG approval. However, the adaptation should be credited as follows:

Adapted by permission from Macmillan Publishers Ltd: [JOURNAL NAME] (reference citation), copyright (year of publication)

**Note: For adaptation from the *British Journal of Cancer,* the following credit line applies.**
Adapted by permission from Macmillan Publishers Ltd on behalf of Cancer Research UK: [JOURNAL NAME] (reference citation), copyright (year of publication)

7. Translations of 401 words up to a whole article require NPG approval. Please visithttp://www.macmillanmedicalcommunications.com for more information.Translations of up to a 400 words do not require NPG approval. The translation should be credited as follows:

   Translated by permission from Macmillan Publishers Ltd: [JOURNAL NAME] (reference citation), copyright (year of publication).

   **Note: For translation from the *British Journal of Cancer,* the following credit line applies.**
   Translated by permission from Macmillan Publishers Ltd on behalf of Cancer Research UK: [JOURNAL NAME] (reference citation), copyright (year of publication)

We are certain that all parties will benefit from this agreement and wish you the best in the use of this material.

Thank you.

Special Terms:

v1.1

**You will be invoiced within 48 hours of this transaction date. You may pay your invoice by credit card upon receipt of the invoice for this transaction. Please follow instructions provided at that time.**

**To pay for this transaction now; please remit a copy of this document along with your payment. Payment should be in the form of a check or money order referencing your account number and this invoice number RLNK501362267.**

**Make payments to "COPYRIGHT CLEARANCE CENTER" and send to:**

**Copyright Clearance Center**

**Dept 001**

**P.O. Box 843006**

**Boston, MA 02284-3006**

**Please disregard electronic and mailed copies if you remit payment in advance.**

**Questions? customercare@copyright.com or +1-855-239-3415 (toll free in the US) or +1-978-646-2777.**

**Gratis licenses (referencing $0 in the Total field) are free. Please retain this printable license for your reference. No payment is required.**

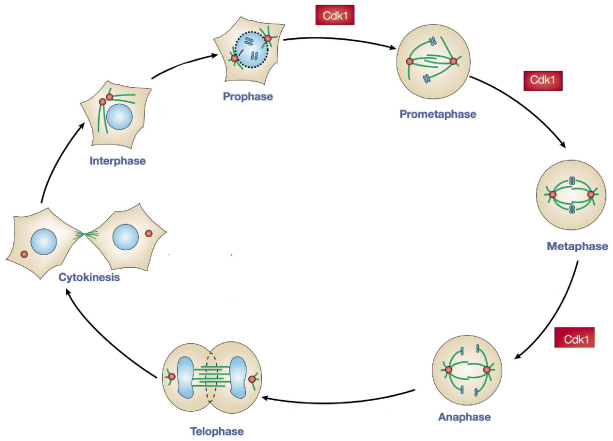


**Figure 1.11. Stages of mitosis.** ***Prophase:*** chromosome condensation and nuclear envelope breakdown occur. ***Prometaphase:*** microtubules are captured by kinetochores. ***Metaphase:*** chromosomes align at the "metaphase plate". ***Anaphase:*** a loss of sister chromatid cohesion allows sister chromatids to be pulled towards the poles. This is mediated by both the shortening of kinetochore microtubules (anaphase A) and the separation of spindle poles as they move toward the cortex (anaphase B). ***Telophase:*** sister chromatids reach the poles, chromosomes begin to decondense and the nuclear membrane reassembles. ***Cytokinesis:*** formation of an actomyosin-based contractile ring "pinches off" the membrane to generate two daughter cells. Legend: Blue: nucleus, chromatin and chromosomes; Green: microtubules; Red: centrosome, mitotic spindle. Figure adapted from (Nigg, 2001).

**Nigg, E.A. (2001). Mitotic kinases as regulators of cell division and its checkpoints. Nat. Rev. Mol. Cell Biol. *2*, 21-32.**

## NATURE PUBLISHING GROUP LICENSE

## TERMS AND CONDITIONS

Jul 27, 2014

This is a License Agreement between Sandy Szeto ("You") and Nature Publishing Group ("Nature Publishing Group") provided by Copyright Clearance Center ("CCC"). The license consists of your order details, the terms and conditions provided by Nature Publishing Group, and the payment terms and conditions.

**All payments must be made in full to CCC. For payment instructions, please see information listed at the bottom of this form.**

License Number: 3436910888992

License date: Jul 27, 2014

Licensed content publisher: Nature Publishing Group

Licensed content publication: Nature Reviews Molecular Cell Biology

Licensed content title: Cell division: Mitotic kinases as regulators of cell division and its checkpoints

Licensed content author: Erich A. Nigg

Licensed content date: Jan 1, 2001

Volume number: 2

Issue number: 1

Type of Use: reuse in a dissertation / thesis

Requestor type: academic/educational

Format: electronic

Portion: figures/tables/illustrations

Number of figures/tables/illustrations: 1

Figures: Box 1 | A primer on the chronology of M-phase events (Figure)

Author of this NPG article: no

Your reference number: None

Title of your thesis / dissertation: Mitotic filamin A phosphorylation regulates filamin A localization and is important for daughter cell separation

Expected completion date: Oct 2014

Estimated size (number of pages): 250

Total: 0.00 USD

Terms and Conditions

Terms and Conditions for Permissions

Nature Publishing Group hereby grants you a non-exclusive license to reproduce this material for this purpose, and for no other use,subject to the conditions below:

1. NPG warrants that it has, to the best of its knowledge, the rights to license reuse of this material. However, you should ensure that the material you are requesting is original to Nature Publishing Group and does not carry the copyright of another entity (as credited in the published version). If the credit line on any part of the material you have requested indicates that it was reprinted or adapted by NPG with permission from another source, then you should also seek permission from that source to reuse the material.

2. Permission granted free of charge for material in print is also usually granted for any electronic version of that work, provided that the material is incidental to the work as a whole and that the electronic version is essentially equivalent to, or substitutes for, the print version.Where print permission has been granted for a fee, separate permission must be obtained for any additional, electronic re-use (unless, as in the case of a full paper, this has already been accounted for during your initial request in the calculation of a print run).NB: In all cases, web-based use of full-text articles must be authorized separately through the 'Use on a Web Site' option when requesting permission.

3. Permission granted for a first edition does not apply to second and subsequent editions and for editions in other languages (except for signatories to the STM Permissions Guidelines, or where the first edition permission was granted for free).

4. Nature Publishing Group's permission must be acknowledged next to the figure, table or abstract in print. In electronic form, this acknowledgement must be visible at the same time as the figure/table/abstract, and must be hyperlinked to the journal's homepage.

5. The credit line should read:
   Reprinted by permission from Macmillan Publishers Ltd: [JOURNAL NAME] (reference citation), copyright (year of publication)
   For AOP papers, the credit line should read:
   Reprinted by permission from Macmillan Publishers Ltd: [JOURNAL NAME], advance online publication, day month year (doi: 10.1038/sj.[JOURNAL ACRONYM].XXXXX)

   **Note: For republication from the *British Journal of Cancer,* the following credit lines apply.**
   Reprinted by permission from Macmillan Publishers Ltd on behalf of Cancer Research UK: [JOURNAL NAME] (reference citation), copyright (year of publication)For AOP papers, the credit line should read:
   Reprinted by permission from Macmillan Publishers Ltd on behalf of Cancer Research UK: [JOURNAL NAME], advance online publication, day month year (doi: 10.1038/sj.[JOURNAL ACRONYM].XXXXX)

6. Adaptations of single figures do not require NPG approval. However, the adaptation should be credited as follows:

Adapted by permission from Macmillan Publishers Ltd: [JOURNAL NAME] (reference citation), copyright (year of publication)

**Note: For adaptation from the *British Journal of Cancer,* the following credit line applies.**
Adapted by permission from Macmillan Publishers Ltd on behalf of Cancer Research UK: [JOURNAL NAME] (reference citation), copyright (year of publication)

7. Translations of 401 words up to a whole article require NPG approval. Please visithttp://www.macmillanmedicalcommunications.com for more information.Translations of up to a 400 words do not require NPG approval. The translation should be credited as follows:

   Translated by permission from Macmillan Publishers Ltd: [JOURNAL NAME] (reference citation), copyright (year of publication).

   **Note: For translation from the *British Journal of Cancer,* the following credit line applies.**
   Translated by permission from Macmillan Publishers Ltd on behalf of Cancer Research UK: [JOURNAL NAME] (reference citation), copyright (year of publication)

We are certain that all parties will benefit from this agreement and wish you the best in the use of this material.

Thank you.

Special Terms:

v1.1

**You will be invoiced within 48 hours of this transaction date. You may pay your invoice by credit card upon receipt of the invoice for this transaction. Please follow instructions provided at that time.**

**To pay for this transaction now; please remit a copy of this document along with your payment. Payment should be in the form of a check or money order referencing your account number and this invoice number RLNK501362264.**

**Make payments to "COPYRIGHT CLEARANCE CENTER" and send to:**

**Copyright Clearance Center**

**Dept 001**

**P.O. Box 843006**

**Boston, MA 02284-3006**

**Please disregard electronic and mailed copies if you remit payment in advance.**

**Questions? customercare@copyright.com or +1-855-239-3415 (toll free in the US) or +1-978-646-2777.**

**Gratis licenses (referencing $0 in the Total field) are free. Please retain this printable license for your reference. No payment is required.**

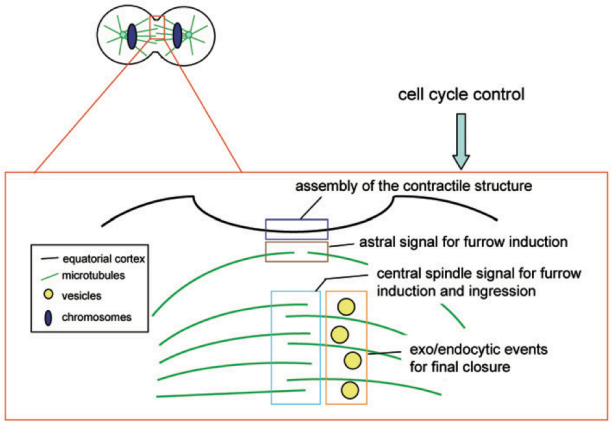


**Figure 1.12. Key events in animal cell cytokinesis.** Cytokinesis requires highly coordinated events at the equatorial region of the cell (red box), including spatial positioning of the cleavage furrow by astral microtubules (brown box) and central spindle (light blue box) associated complexes, assembly and activation of the actomysoin contractile ring (dark blue box) to drive furrow ingression, and targeted exocytosis and endocytosis (orange box) to deposit membrane and complete final closure. Many of these events are directly controlled by cell cycle regulators to ensure temporal coordination with chromosome segregation. Figure from (Li, 2007).

**Li, R. (2007). Cytokinesis in development and disease: variations on a common theme. Cell. Mol. Life Sci. *64*, 3044-3058.**

## SPRINGER LICENSE

## TERMS AND CONDITIONS

Jul 27, 2014

This is a License Agreement between Sandy Szeto ("You") and Springer ("Springer") provided by Copyright Clearance Center ("CCC"). The license consists of your order details, the terms and conditions provided by Springer, and the payment terms and conditions.

**All payments must be made in full to CCC. For payment instructions, please see information listed at the bottom of this form.**

License Number: 3436960014074

License date: Jul 27, 2014

Licensed content publisher: Springer

Licensed content publication: Cellular and Molecular Life Sciences

Licensed content title: Cytokinesis in development and disease: variations on a common theme

Licensed content author: R. Li

Licensed content date: Jan 1, 2007

Volume number: 64

Issue number: 23

Type of Use: Thesis/Dissertation

Portion: Figures

Author of this Springer article: No

Order reference number: None

Original figure numbers: Figure 1

Title of your thesis / dissertation: Mitotic filamin A phosphorylation regulates filamin A localization and is important for daughter cell separation

Expected completion date: Oct 2014

Estimated size(pages): 250

Total: 0.00 USD

Terms and Conditions

Introduction

The publisher for this copyrighted material is Springer Science + Business Media. By clicking "accept" in connection with completing this licensing transaction, you agree that the following terms and conditions apply to this transaction (along with the Billing and Payment terms and conditions established by Copyright Clearance Center, Inc. ("CCC"), at the time that you opened your Rightslink account and that are available at any time athttp://myaccount.copyright.com).

Limited License

With reference to your request to reprint in your thesis material on which Springer Science and Business Media control the copyright, permission is granted, free of charge, for the use indicated in your enquiry.

Licenses are for one-time use only with a maximum distribution equal to the number that you identified in the licensing process.

This License includes use in an electronic form, provided its password protected or on the university's intranet or repository, including UMI (according to the definition at the Sherpa website: http://www.sherpa.ac.uk/romeo/). For any other electronic use, please contact Springer at (permissions.dordrecht@springer.com or permissions.heidelberg@springer.com).

The material can only be used for the purpose of defending your thesis limited to university-use only. If the thesis is going to be published, permission needs to be re-obtained (selecting "book/textbook" as the type of use).

Although Springer holds copyright to the material and is entitled to negotiate on rights, this license is only valid, subject to a courtesy information to the author (address is given with the article/chapter) and provided it concerns original material which does not carry references to other sources (if material in question appears with credit to another source, authorization from that source is required as well).

Permission free of charge on this occasion does not prejudice any rights we might have to charge for reproduction of our copyrighted material in the future.

Altering/Modifying Material: Not Permitted

You may not alter or modify the material in any manner. Abbreviations, additions, deletions and/or any other alterations shall be made only with prior written authorization of the author(s) and/or Springer Science +

Business Media. (Please contact Springer at (permissions.dordrecht@springer.com or permissions.heidelberg@springer.com)

Reservation of Rights

Springer Science + Business Media reserves all rights not specifically granted in the combination of (i) the license details provided by you and accepted in the course of this licensing transaction, (ii) these terms and conditions and (iii) CCC's Billing and Payment terms and conditions.

Copyright Notice:Disclaimer

You must include the following copyright and permission notice in connection with any reproduction of the licensed material: "Springer and the original publisher /journal title, volume, year of publication, page, chapter/article title, name(s) of author(s), figure number(s), original copyright notice) is given to the publication in which the material was originally published, by adding; with kind permission from Springer Science and Business Media"

Warranties: None

Example 1: Springer Science + Business Media makes no representations or warranties with respect to the licensed material.

Example 2: Springer Science + Business Media makes no representations or warranties with respect to the licensed material and adopts on its own behalf the limitations and disclaimers established by CCC on its behalf in its Billing and Payment terms and conditions for this licensing transaction.

Indemnity

You hereby indemnify and agree to hold harmless Springer Science + Business Media and CCC, and their respective officers, directors, employees and agents, from and against any and all claims arising out of your use of the licensed material other than as specifically authorized pursuant to this license.

No Transfer of License

This license is personal to you and may not be sublicensed, assigned, or transferred by you to any other person without Springer Science + Business Media's written permission.

No Amendment Except in Writing

This license may not be amended except in a writing signed by both parties (or, in the case of Springer Science + Business Media, by CCC on Springer Science + Business Media's behalf).

Objection to Contrary Terms

Springer Science + Business Media hereby objects to any terms contained in any purchase order, acknowledgment, check endorsement or other writing prepared by you, which terms are inconsistent with these terms and conditions or CCC's Billing and Payment terms and conditions. These terms and conditions, together with CCC's Billing and Payment terms and conditions (which are incorporated herein), comprise the entire agreement between you and Springer Science + Business Media (and CCC) concerning this licensing transaction. In the event of any conflict between your obligations established by these terms and conditions and those established by CCC's Billing and Payment terms and conditions, these terms and conditions shall control.

Jurisdiction

All disputes that may arise in connection with this present License, or the breach thereof, shall be settled exclusively by arbitration, to be held in The Netherlands, in accordance with Dutch law, and to be conducted under the Rules of the 'Netherlands Arbitrage Instituut' (Netherlands Institute of Arbitration).***OR:***

**All disputes that may arise in connection with this present License, or the breach thereof, shall be settled exclusively by arbitration, to be held in the Federal Republic of Germany, in accordance with German law.**

**Other terms and conditions:**

**v1.3**

**You will be invoiced within 48 hours of this transaction date. You may pay your invoice by credit card upon receipt of the invoice for this transaction. Please follow instructions provided at that time.**

**To pay for this transaction now; please remit a copy of this document along with your payment. Payment should be in the form of a check or money order referencing your account number and this invoice number RLNK501362295.**

**Make payments to "COPYRIGHT CLEARANCE CENTER" and send to:**

**Copyright Clearance Center**

**Dept 001**

**P.O. Box 843006**

**Boston, MA 02284-3006**

**Please disregard electronic and mailed copies if you remit payment in advance.**

**Questions? customercare@copyright.com or +1-855-239-3415 (toll free in the US) or +1-978-646-2777.**

**Gratis licenses (referencing $0 in the Total field) are free. Please retain this printable license for your reference. No payment is required.**

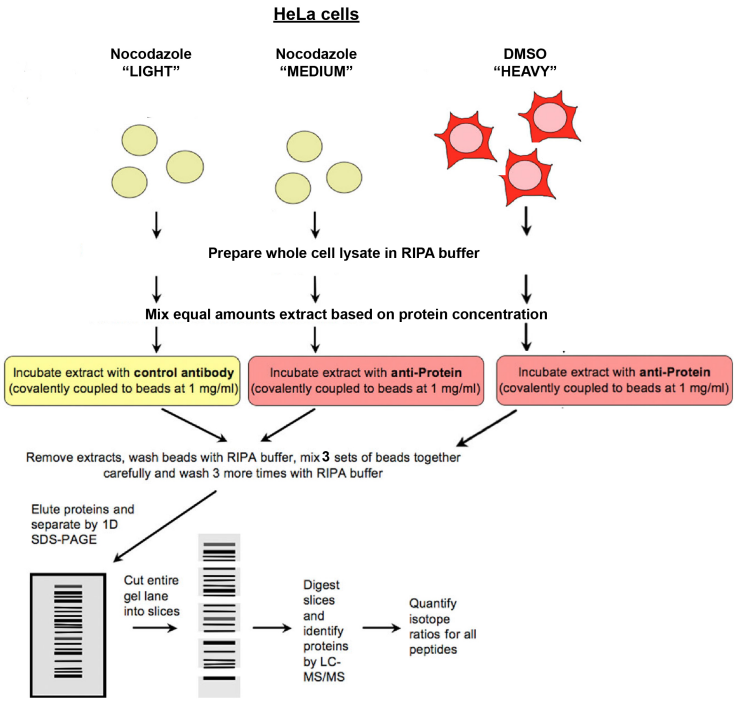


**Figure 2.2. Workflow for SILAC LC-MS/MS based analysis of mitotic and interphase-specific FLNa interactors in HeLa cells.** HeLa cells are grown in light, medium and heavy SILAC media for 5-6 passages. Light and medium cells are treated with nocodazole and immunoprecipitated with Normal mouse IgG beads and anti-FLNa-beads, respectively. Heavy cells are immunoprecipitated with anti-FLNa-beads. Beads are mixed, eluted and separated by SDS-PAGE. Proteins are digested and analyzed by LC-MS/MS. SILAC analysis is performed. Figure adapted from (Trinkle-Mulcahy et al., 2008).

**Trinkle-Mulcahy, L., Boulon, S., Lam, Y.W., Urcia, R., Boisvert, F.M., Vandermoere, F., Morrice, N.A., Swift, S., Rothbauer, U., Leonhardt, H., *et al.* (2008). Identifying specific protein interaction partners using quantitative mass spectrometry and bead proteomes. J. Cell Biol. *183*, 223-239.**

It is the mission of The Rockefeller University Press to promote widespread reuse and distribution of the articles and data we publish. In this spirit, authors retain copyright to their own work and can reuse it for any purpose as long as proper attribution is provided. Third parties may use our published materials under a Creative Commons Attribution-Noncommercial-Share Alike 3.0 Unported License six months after publication. Within the first six months, the same conditions for reuse apply, except we prohibit the creation of mirror sites. Commercial reuse must be requested as described below and will incur a fee.

We encourage you to read more about our permission policies and the Creative Commons License terms:

- You wrote it; you own it! (Hill and Rossner, 2008)
- RUP Copyright Policy

# Requesting Permission Licensing

Please read below to determine if you must obtain permission for your specific reuse.

## Original author reuse (commercial and noncommercial)

Ownership of copyright remains with RUP authors, who may reuse their own material forany purpose, including commercial profit, as long as they provide proper attribution. The permission does not extend to the institution.

- Note that our preferred citation style is as follows:
- ©AUTHOR et al., YEAR. Originally published in *JOURNAL NAME*. doi:########.
- If an article does not carry a doi, our preferred citation style is as follows:
- ©AUTHOR et al., YEAR. Originally published in *JOURNAL NAME*. VOL:PP–PP.

## Noncommercial third-party reuse

Third parties may reuse our content for noncommercial purposes without specific permission as long as they provide proper attribution (see citation preferences provided above). Within the first 6 months after publication, the creation of mirror sites is prohibited.

## Commercial third-party reuse

Commercial publishers, profit-based companies, as well as third-party authors publishing in a commercial journal or book must obtain permission to reuse RUP material. In most cases, this permission will incur a fee. Uses include, for example, use of a figure in a commercial journal article or book, posting of images on a manufacturer's website, inclusion of content in marketing materials, etc. The RUP acknowledges that text or data mining by commercial entities for their internal research purposes is allowed without further permission from RUP. Commercial entities may develop indexing or search services—available to the public for free or for a fee—based on text or data mining without further permission from RUP, but they may reproduce only snippets of text up to 156 characters in length, or thumbnails of images up to 72 pixels in the long direction, as part of such a service.

## How to obtain permission

Permission for commercial reuse can be obtained by emailing the following information to Suzanne O'Donnell, Permissions Director, at permissions@rockefeller.edu:

- Your name, institution, and title
- Your complete mailing address, email address, phone number, and fax number
- A description of the content you wish to reuse:
- Journal or book title
- Article title
- Authors' names
- Volume number, issue date, page numbers (provide all that apply)
- Specific figure numbers or portion of text (or supply a photocopy)
- Include the following information about your intended reuse:
- Type of work in which our material will be used (e.g., book, journal, newsletter, etc.)
- Title of work in which RUP material will appear
- Title of article/chapter (if applicable)
- Author(s)/editor(s)
- Expected publication date
- Publishing company
- Retail price (for books only)
- Print run (for books only)
- Indicate if there will be ancillaries published simultaneous to the print (DVD, website, CD-ROM, etc.). Will ancillaries be sold separately?
- Intended audience for the work
- If you wish to reprint the material online, please include the following:
- Your website's URL
- Website's sponsoring organization/company
- Description of the purpose and nature of your website
- Description of the website's visitors (customers, scholars, professors, etc.)
- Whether the site is open to the public or access is restricted

## Educational use

No permission is required to reuse RUP material for noncommercial purposes in course packs, classroom handouts, or electronic classroom presentations. If the educational material will be offered for sale, please follow the instructions above for Commercial third-party reuse.

## Reprints

Commercial reprints are available by special order. Please contact Suzanne O'Donnell atpermissions@rockefeller.edu to request pricing information. Please supply the full article citation (author, year, vol, pp) and the number of reprints you would like to order.

# CURRICULUM VITAE

## EDUCATION

**2008-2014** **Ph.D., Biochemistry**
*University of Ottawa*, Faculty of Medicine, Ottawa ON

**2003-2007** **B.Sc,. Biochemistry, Honours (with Co-op)**
*University of Guelph*, Guelph ON

## WORK EXPERIENCE

**2009 - 2014** **Teaching Assistant & Laboratory Demonstrator**
*University of Ottawa*, Ottawa ON

- Supervised groups of 18 students in 3-hour labs
- Marked laboratory reports and provided feedback
- Evaluated students' laboratory performance
- Demonstrated analytical techniques in pre-lab presentation
- Maintained Excel spreadsheet of student's marks
- Explained purpose of experiment and theory behind analytical techniques

**May - Aug, 2007** **Research Assistant, Microbiology Lab**
*University of Guelph*, Guelph ON

- Purified putative recombinant bacterial toxins
- Tested toxins for activity associated with virulence
- Results used to understand mechanism of action of bacteria that cause Cholera and Diphtheria
- Presented results in poster and PowerPoint presentations
- Acquired skills in SDS-PAGE, Western blot and protein purification
- Learned bacterial cell culture, aseptic technique and plasmid purification
- 4 month co-op term

**Jan - Aug, 2006** **Sensory Technician - R&D Department**
*Iovate Health Sciences Inc*., Mississauga, ON

- Performed QC testing on sports nutrition products
- Analyzed results using Compusense and Excel software
- Results used to monitor product quality and determine shelf life
- Performed sensory tests on in-house participants from various departments
- Developed strategies to increase participation
- 8 month co-op term

**Jan - Apr, 2005** **Research Assistant, Biochemistry Lab**
*University of Guelph*, Guelph ON

- Investigated the existence of lipid rafts in eukaryotic cell membrane
- Acquired skills in pipetting, ultracentrifugation and spectrophotometry
- Learned mammalian cell culture
- Presented results in poster and PowerPoint presentations
- 4 month co-op term

**Jan - Apr, 2002** **Technician, Physics Lab**
*Carleton University*, Ottawa, ON

- Performed QC tests on a component of the Large Hadron Collider
- Learned about the Higgs Boson
- Worked in clean-room
- 4 month co-op term

## VOLUNTEER ACTIVITIES

| | |
|---|---|
| 2013-current | Gutsy Walk Volunteer, Crohn's and Colitis Canada |
| 2011-2013 | Let's Talk Science Outreach Program Volunteer |
| 2010-2012 | University of Ottawa departmental newsletter contributor |
| 2009 | Ottawa Hospital General Campus Volunteer |
| 2008 | Ottawa Tulip Festival Volunteer |

## SCIENTIFIC CONTRIBUTIONS

**Manuscript (submitted):**
Szeto, S., Williams, E., Rudner, A. and Lee, J.M. 2014. Mitotic phosphorylation of filamin A by Cdk1 regulates filamin A subcellular localization and post-mitotic cell separation. Experimental Cell Research.

**Attended Gordon Research Conference: 'Fibronectin, Integrins and Related Molecules' in Italy,** Presented poster "Control of actin remodelling by Cdk1 phosphorylation of filamin A"